

**THE DEVELOPMENT OF TUMOUR - SPECIFIC ASSAYS FOR CELLULAR
RESPONSE TO ANTHRACYCLINE DRUGS USING LASER CYTOMETRY**

Louise J Reeve B.Sc.

Department of Surgery
University of Leicester
Clinical Sciences Wing, Glenfield Hospital

Submitted for the degree of Ph. D. to
The Faculty of Medicine and Therapeutics
University of Leicester
September 1999

UMI Number: U536147

All rights reserved

INFORMATION TO ALL USERS

The quality of this reproduction is dependent upon the quality of the copy submitted.

In the unlikely event that the author did not send a complete manuscript and there are missing pages, these will be noted. Also, if material had to be removed, a note will indicate the deletion.



UMI U536147

Published by ProQuest LLC 2013. Copyright in the Dissertation held by the Author.
Microform Edition © ProQuest LLC.

All rights reserved. This work is protected against
unauthorized copying under Title 17, United States Code.



ProQuest LLC
789 East Eisenhower Parkway
P.O. Box 1346
Ann Arbor, MI 48106-1346

Declaration

The work presented in this thesis is original and unless otherwise noted in the text or references was contacted solely by the author in the Department of Surgery, University of Leicester, during the period from September 1995 to September 1999.

Louise J Reeve

Acknowledgements

I would like to thank Mr David A. Rew as my first supervisor, source of the original project concept and for overall guidance for my time of study at Leicester University.

I would also like to thank Dr Alison H. Goodall as second supervisor, whom has been a huge source of never ending help and encouragement. An extra special thank you, to Miss Davinder Kaur and Dr George D. Wilson for the collaborative work. Other academic and technical support was gratefully received from Dr Gerrit Woltmann, Mr Ed Luther, Mr Peter Carleen, Dr Doug Burger, Prof. Laurence Patterson, Dr Roger James, Dr Nick Brindle, Miss Joanne Carter, Dr Ian Brotherick, Dr Rosemary Walker, Dr Alan Cooper, Ms Rachel Carter, Dr Julian O'Neill, Dr Martin Myers, Dr Time Gant and all in the Histopathology Department at Glenfield NHS Trust.

Many colleagues, past and present at the clinical sciences have contributed to my ability to produce this thesis. I would like to thank them all especially Rich, Taff, Clare, Rachel, Debbie, Paul, Fiona, Liz, Kai and Neil.

I would also like to show my appreciation to Trent Regional Health authority and the Surgery Department, Leicester University for my funding.

To date from this work one paper has been published-
Rew DA, Reeve LR and Wilson GD. (1998) Comparison of flow and laser cytometry for the assay of cell proliferation in human solid tumours. *Cytometry*, **33**; 355 – 361.

Finally, to thanks Rich and my family, to whom I dedicate this thesis.

Abstract

THE DEVELOPMENT OF TUMOUR-SPECIFIC ASSAYS FOR CELLULAR RESPONSE TO ANTHRACYCLINE DRUGS USING LASER CYTOMETRY

Louise J Reeve

Adjunctive chemotherapy for breast cancer is confounded by varying degrees of drug resistance in individual tumours. This could be overcome by patient-specific assays using laser cytometry to measure drug uptake in viable cells.

Preliminary studies confirmed the spectroscopic, fluorometric and DNA binding characteristics of commonly used anthracyclines and demonstrated that the emission and excitation λ_{\max} for doxorubicin made it suitable for laser cytometric detection.

Flow cytometric (FCM) measurement of doxorubicin ($0.1-100 \mu\text{mol.L}^{-1}$) uptake into drug-sensitive and resistant human breast tumour cell lines (MCF-7/S and MCF-7/R) demonstrated dose- and time-dependent uptake in MCF-7/S but not MCF-7/R cells over 4-144 hours.

By 72h the drug had a cytostatic effect upon the MCF-7/S cells and a loss of population was seen, although viability and apoptosis (Annexin V-FITC binding) were no different from control (untreated) cells. Growth and viability of MCF-7/R cells were unaffected by doxorubicin.

Comparisons of viability probes found that the green fluorescent dye sytox was the most suitable for measuring cell viability simultaneously with doxorubicin uptake. Studies using laser scanning cytometry (LSC) showed light scatter computation was suited to single colour quantification, while fluorescence computation was ideal for two colour fluorescence detection. Comparisons between FCM and LSC of doxorubicin and calcein-AM uptake by MCF-7 cells, and BrdUrd uptake into human tumour nuclei, showed good correlation.

LSC was used to visualise uptake by MCF-7/S cells, of doxorubicin covalently coupled to albumin capsules (CytocapsTM $0 - 2 \mu\text{mol.L}^{-1}$). Maximum binding of CytocapsTM was seen at 24h and they entered the cells by 48h. CytocapsTM caused cells to become cytostatic by 72h and exhibited apoptosis by 96h.

Disruption of primary human breast tumours and FNAs using mechanical and enzymatic techniques yielded low numbers of viable cells.

In this study a model assay, using cell lines has been established to detect doxorubicin uptake in viable tumour cells, using LSC relocation to identify cells.

Table of Contents

Declaration	I
Acknowledgements	II
Abstract	III
Table of contents	IV
List of figures	V
List of tables	VI

INTRODUCTION

1	<u>Aims</u>	1
1.1	<u>Breast cancer</u>	2
1.1.1	Normal breast tissue structure and growth	2
1.2	<u>Types of breast cancer</u>	3
1.3	<u>Therapeutic approaches to breast cancer</u>	3
1.3.1	Chemotherapy for breast cancer	3
1.3.2	Mechanisms of action of chemotherapeutic drugs	5
1.3.3	The anthracycline family	6
1.3.3.1	DNA intercalation	7
1.3.3.2	Topoisomerase II inhibition	9
1.3.3.3	Free radical formation and cell membrane interactions	10
1.3.4	Resistance to anthracycline chemotherapy	12
1.3.5	Clinical formulations and use of anthracyclines	15
1.3.5.1	Clinical limitations to anthracycline use	15
1.4	<u>Research models for human primary breast tumours</u>	16
1.4.1	Drug sensitivity assays	17
1.4.1.1	Tumour cell growth assays	18
1.4.1.2	Fluorescence microscopy assays	19
1.4.1.3	Confocal assays	19
1.4.1.4	Laser scanning microscopy assays	20
1.4.1.5	Flow cytometry assays	20
1.4.1.6	Other anthracycline assays	22
1.5	<u>Laser scanning cytometry (LSC)</u>	22
1.6	<u>Viability determination</u>	25
1.6.1	The MTT assay	25
1.6.2	Trypan blue exclusion	25
1.6.3	Propidium iodide (PI)	26
1.6.4	Fluorescein diacetate (FDA)	26
1.6.5	Calcein acetoxymethyl ester (calcein AM)	26
1.6.6	Sytox	27
1.7	<u>Apoptosis</u>	27
1.8	<u>Aim of the studies</u>	28

MATERIALS AND METHODS

2	<u>Materials and methods</u>	
2.1	<u>Selection and handling of cytotoxic drugs</u>	30
2.1.1	Study of the physical characteristics of fluorescent anthracycline compounds	30
2.1.1.1	Absorbance measurements	30
2.1.1.2	Fluorescence spectroscopy	31
2.1.2	Study of the DNA binding characteristics of drugs	31
2.1.2.1	Isosbestic point determination	31
2.1.2.2.	Calculation of DNA binding coefficients of cytotoxic drugs (Scatchard plot analysis)	31
2.2	<u>Cell studies</u>	32
2.2.1	Culture of cell lines	32
2.2.1.1	Passaging cell lines	32
2.2.1.2	Freezing, thawing and storage of cell lines	33
2.2.1.3	Trypan blue exclusion assay	33
2.2.1.4	Production of non-viable cells	33
2.2.2	Cytotoxic free drug uptake studies	34
2.2.3	Cytotoxic CytocapsTM uptake studies	34
2.2.4	The MTT assay	35
2.2.4.1	MTT formazan titration	35
2.2.4.2	Standard MTT assay	35
2.2.5	Standard curves	35
2.2.5.1	Growth curves of MCF-7/S and MDA MB 231 cell lines	36
2.2.5.2	Cytotoxic studies using MCF-7/S and MDA MB 231 cell lines	36
2.3	<u>Cytometric studies</u>	36
2.3.1	Viability markers	36
2.3.1.1	Propidium iodide (PI)	36
2.3.1.2	Fluorescein diacetate (FDA)	37
2.3.1.3	Preliminary calcein AM experiments	37
2.3.1.4	Standard calcein AM assay	37
2.3.1.5	Preliminary sytox experiments	38
2.3.1.6	Standard sytox assay	38
2.3.2	Measurement of apoptosis	38
2.3.2.1	Annexin V - FITC binding	38
2.3.3	Flow cytometry - FACScan	38
2.3.3.1	Instrumentation and settings	38
2.3.3.2	Analysis of data	39
2.3.3.3	DNA analysis of human dissociated nuclei	40
2.3.4	Laser scanning cytometry (LSC)	40
2.3.4.1	Sample preparation and positioning using the LSC	40
2.3.4.2	Cytocentrifuge preparations - cell lines	41
2.3.4.3	Cytocentrifuge preparations - human tumour nuclei	41
2.3.4.4	Chamber slides for analysis on the LSC	41
2.3.4.5	Relocation and image capturing using the LSC	42
2.3.5	Cytometric measurement of DNA content in cells	43
2.3.6	Manipulations of fresh primary human tumours	43

2.3.6.1	Disaggregation of tumour	44
2.3.6.2	Mechanical disaggregation	44
2.3.6.3	Enzymatic disaggregation	45
2.3.6.4	Viability of disrupted tumour suspensions	45
2.3.6.5	Histological staining of disrupted tumour cells	45
2.3.6.6	Papanicolaou staining procedure	45
2.3.6.7	Haemotoxylin and eosin staining procedure	45
2.3.7	Fine needle aspirate (FNA) samples	46
2.3.7.1	Processing of FNAs	46
2.3.8	Studies of BrdUrd uptake into nuclei of primary human tumours	47
2.3.8.1	Sample preparation and staining	47
2.3.9	Statistical analysis	48

RESULTS

3.1	<u>Characteristics of drugs</u>	49
3.1.1	Physical characteristics of drugs	49
3.1.1.1	Absorbance	49
3.1.1.2	Spectrophotometric titrations	49
3.1.1.3	Extinction coefficient derivation	49
3.1.1.4	Fluorescence	50
3.1.2	DNA binding characteristics of drugs	54
3.1.2.1	Isosbestic point determination	55
3.1.2.2	Spectral titration	55
3.1.3	Discussion	62
3.2	<u>Characterisation of cell line models -MTT assay</u>	65
3.2.1	MTT formazan calibration	65
3.2.2	Standard curves for the MTT assay	65
3.2.3	Growth curves	68
3.2.4	Discussion	71
3.3	<u>Cell viability studies</u>	74
3.3.1	Propidium iodide (PI)	74
3.3.2	Fluorescein diacetate (FDA)	74
3.3.3	Calcein AM	74
3.3.4	Sytox	85
3.3.5	Discussion	88
3.4	<u>Anthracycline uptake and consequent viability of MCF-7/S and MCF-7/R cells</u>	95
3.4.1	Mitoxantrone uptake of MCF-7/S cells	95
3.4.2	Doxorubicin uptake and consequent viability	98
3.4.2.1	Flow cytometry	98
3.4.2.2	Laser scanning cytometry	103
	Chamber slide preparations	103
	Cytocentrifuge preparations	103
3.4.3	Time course of doxorubicin uptake	109

3.4.4	Cytotoxicity of doxorubicin and mitoxantrone	128
3.4.5	Discussion	130
3.5	<u>Uptake of doxorubicin loaded microcapsules Cytocaps™ by MCF-7/S cells</u>	135
3.5.1	Cytocaps™ time course	135
3.5.2	LSC analysis	143
3.5.3	Discussion	150
3.6	<u>Human breast carcinoma manipulations</u>	152
3.6.1	Cytocentrifuge preparations of disrupted tumour cells	152
3.6.2	Cell yield and viability of disrupted tumour cells using mechanical and enzymatic disaggregation	159
3.6.3	Fine needle aspiration (FNA) samples	160
3.6.3.1	Presentation of cell suspensions to the LSC	160
3.6.3.2	Human breast tumour FNA assay	163
3.6.4	Discussion	166
3.7	<u>Human tumour proliferation</u>	172
3.7.1	Comparison of flow and laser scanning cytometry for a bivariate assay using a cell proliferation in human solid tumours as a model	172
3.7.1.1	Flow and laser scanning cytometry	172
3.7.2	Statistical analysis	172
3.7.3	Correlation between LSC and FCM	173
3.7.4	Discussion	176

DISCUSSION

4.1	<u>Technical discussion</u>	180
4.1.1	The investigation of the mechanism of the binding of drug to DNA	180
4.1.2	Cell lines: MCF-7/S and MCF-7/R	180
4.1.3	Instrumentation - FCM and LSC	182
4.1.4	Sample preparation for the LSC	183
4.1.5	Colour compensation	184
4.1.6	Gates/regions	185
4.1.4	Human tumour studies	186
4.2	<u>Biological discussion</u>	186
4.2.1	Response of MCF-7/S and MCF-7/R cells to doxorubicin treatment	186
4.2.2	Optimisation and limitations	188
4.2.2.1	Viable human tumour cells	191
4.2.2.2	Drug uptake and cell killing	191
4.2.2.3	Cytocaps™	191
4.2.3	Future work	192

	APPENDICES	
<u><i>Reagent recipes</i></u>		194
<u><i>Abbreviations</i></u>		196
	REFERENCES	
<u><i>References</i></u>		201

List of figures

Introduction

- 1.1 **Chemical structure of doxorubicin.** 8
- 1.2 **An illustration of the free radical generation caused by intracellular doxorubicin.** 12
- 1.3 **Schematic representation of the laser scanning cytometer (LSC).** 23

Materials and Methods

- 2.1 **Construction of a chamber slide.** 42

Results

Characteristics of drugs

- 3.1 **UV/Visible absorbance spectrum of doxorubicin, mitoxantrone and ethidium bromide.** 51
- 3.2 **Absorbance of doxorubicin, mitoxantrone and ethidium bromide at 488 nm and λ max. of each drug.** 52
- 3.3 **UV/Visible fluorescence emission spectrum of doxorubicin and ethidium bromide, using 488 nm excitation.** 53
- 3.4 **Fluorescence values of doxorubicin and ethidium bromide using 488 nm excitation wavelength and 470 nm and 480 nm emission wavelengths.** 54
- 3.5 **UV absorbance spectrum of DNA.** 55
- 3.6 **Overlaid spectral titrations of a series of molar DNA/drug ratios.** 57
- 3.7 **Spectroscopic analysis of (A) DNA/doxorubicin mixtures and (B) Scatchard plot.** 58
- 3.8 **Spectroscopic analysis of (A) DNA/mitoxantrone mixtures and (B) Scatchard plot.** 59
- 3.9 **Spectroscopic analysis of (A) DNA/ethidium bromide mixtures and (B) Scatchard plot.** 60

Characterisation of cell line models – MTT assay

- 3.10 **Calibration curve for MTT formazan in DMSO.** 66
- 3.11 **Standard curves for the MTT assay using MCF-7/S and MDA MB 231 cells.** 67
- 3.12 **Photomicrographs of MCF-7/S cells grown under normal growth conditions** 69
- 3.13 **Growth curves of MCF-7/S and MDA MB 231 cells analysed using the MTT assay.** 70

Cell viability studies

- 3.14 **Uptake of PI by non – viable MDA MB 231 cells analysed using FCM.** 75
- 3.15 **Uptake of FDA by viable MDA MB 231 cells analysed using FCM (FL1).** 76
- 3.16 **Analysis of calcein AM uptake FCM data from viable MCF-7/S and MCF-7/R cells.** 78

3.17	Uptake of calcein AM by viable and non – viable MCF-7/S cells and MCF-7/R cells analysed by FCM (FL1).	79
3.18	Analysis of calcein AM chamber slide LSC data from viable MCF-7/S cells.	80
3.19	Uptake of calcein AM by viable and non – viable MCF-7/S and MCF-7/R cells analysed by chamber slide preparations on the LSC.	81
3.20	LSC data dotplot and fluorescent images of MCF-7/S cells after incubation with calcein AM.	82
3.21	Cytocentrifuge preparation of 5×10^5 cell/ml of MCF-7/S cells.	84
3.22	Analysis of calcein AM cytocentrifuge LSC data from viable MCF-7/S cells.	85
3.23	Uptake of calcein AM by viable and non – viable MCF-7/S and MCF-7/R cells analysed by cytocentrifuge preparations on the LSC.	86
3.24	Uptake of sytox by non – viable MCF-7/S and MCF-7/R cells analysed by FCM (FL1).	87
3.25	The different contours encapsulating an event detected using LSC.	91
3.26	Laser scatter image and threshold contouring of a MCF-7/S cell as scanned by the LSC.	93
Anthracycline uptake and consequent viability of MCF-7/S and MCF-7/R cells		
3.27	Analysis of mitoxantrone uptake FCM data from viable MCF-7/S cells.	96
3.28	Uptake of mitoxantrone by viable MCF-7/S cells analysed by FCM.	97
3.29	Analysis of doxorubicin uptake FCM data from viable MCF-7/S and MCF-7/R cells.	99
3.30	Uptake of doxorubicin by viable and non – viable MCF-7/S cells and viable MCF-7/R cells, analysed by FCM (FL3).	100
3.31	Real colour images of a viable MCF-7/S cell after doxorubicin ($10 \mu\text{mol.L}^{-1}$) incubation.	101
3.32	Real colour images of a viable MCF-7/S cell after doxorubicin ($100 \mu\text{mol.L}^{-1}$) incubation.	102
3.33	Analysis of doxorubicin chamber slide LSC data from viable MCF-7/S cells.	105
3.34	Uptake of doxorubicin by viable and non-viable MCF-7/S and MCF-7/R cells analysed by chamber slide preparations on the LSC.	106
3.35	Analysis of doxorubicin cytocentrifuge LSC data from viable MCF-7/S cells.	107
3.36	Uptake of doxorubicin by viable and non - viable MCF-7/S and MCF/R cells analysed by cytocentrifuge preparations on the LSC.	108
3.37	Analysis of FCM data of doxorubicin uptake, sytox and annexin V binding of MCF-7/S cells.	111
3.38	Photomicrographs illustrating the growth of MCF-7/S and MCF-7/R at 144 hrs after doxorubicin incubation.	112
3.39	Uptake of doxorubicin measured by FCM over the time course 4-72 hours in MCF-7 cells.	113

3.40	Total cell number of MCF-7/S cells measured by trypan blue exclusion over the time course 4-72 hours.	114
3.41	Cell viability of MCF-7/S cells measured by trypan blue and sytox, over the time course 4-72 hours.	115
3.42	Percentage of MCF-7/S cells positive for annexin V binding, over the time course 4-72 hours.	116
3.43	Uptake of doxorubicin measured by FCM over the time course 96-144 hours, in MCF-7/S cells.	117
3.44	Total cell number of MCF-7/S cells measured by trypan blue exclusion over the time course 96-144 hours.	118
3.45	Cell viability of MCF-7/S cells measured by trypan blue and sytox, over the time course 96-144 hours.	119
3.46	Percentage of MCF-7/S cells positive for annexin V binding over the time course 96-144 hours.	120
3.47	Uptake of doxorubicin measured by FCM over the time course 4-72 hours, in MCF-7/R cells.	121
3.48	Total cell number of MCF-7/R cells measured by trypan blue exclusion over the time course 4-72 hours.	122
3.49	Cell viability of MCF-7/R cells measured by trypan blue and sytox, over the time course 4-72 hours.	123
3.50	Percentage of MCF-7/R cells positive for annexin V binding, over the time course 4-72 hours.	124
3.51	Uptake of doxorubicin measured by FCM, over the time course 96-144 in MCF-7/R cells.	125
3.52	Total cell number of MCF-7/R cells measured by trypan blue exclusion, over the time course 96-144 hours.	126
3.53	Cell viability of MCF-7/R cells measured by trypan blue and sytox, over the time course 96-144 hours.	127
3.54	Percentage of MCF-7/R cells positive for annexin V binding, over the time course 96-144 hours.	128
3.55	Percentage survival of MCF-7/S and MDA MB 231 cells after doxorubicin or mitoxantrone incubation.	129
Uptake of doxorubicin loaded microcapsules Cytocaps™ by MCF-7/S cells		
3.56	Analysis of Cytocaps™ uptake into MCF-7/S cells using FCM.	137
3.57	Uptake of Cytocaps™ measured by FCM over the time course 4-96 hours, in MCF-7/S cells.	138
3.58	Analysis of FCM data of sytox and annexin V measurement using MCF-7/S cells	139
3.59	Cell viability of MCF-7/S cells measured by trypan blue exclusion, over the time course 4-96 hours.	140
3.60	Cell viability of MCF-7/S cells measured by sytox uptake, over the time course 4-96 hours.	141
3.61	Annexin V binding of MCF-7/S cells over the time course 4-96 hours.	142
3.62	LSC dotplot of MCF-7/S cells after incubation with 0.5 μmol.L⁻¹ Cytocaps™.	145

3.63	False colour images of MCF-7/S cells incubated with CytocapsTM and analysis using LSC after 4 hours growth in culture.	146
3.64	False colour images of MCF-7/S cells incubated with CytocapsTM and analysis using LSC after 24 hours growth in culture.	147
3.65	False colour images of MCF-7/S cells incubated with CytocapsTM and analysis using LSC after 48 hours growth in culture.	148
3.66	False colour images of MCF-7/S cells incubated with CytocapsTM and analysis using LSC after 120 hours growth in culture.	149
Human breast carcinoma manipulation		
3.67	Mechanical disaggregation of T1, cytocentrifuge preparation stained with PAP, x40 magnification.	153
3.68	Mechanical disaggregation of T1, cytocentrifuge preparation stained with PAP, x100 magnification.	153
3.69	Mechanical disaggregation of T2, cytocentrifuge preparation stained with PAP, x40 magnification.	153
3.70	Mechanical disaggregation of T2, cytocentrifuge preparation stained with PAP, x100 magnification.	154
3.71	Mechanical disaggregation of T3, cytocentrifuge preparation stained with PAP, x40 magnification.	154
3.72	Enzymatic disaggregation of T3, cytocentrifuge preparation stained with PAP, x40 magnification.	154
3.73	Enzymatic disaggregation of T5, cytocentrifuge preparation stained with HE, x40 magnification.	155
3.74	Enzymatic disaggregation of T5, cytocentrifuge preparation stained with PAP, x40 magnification.	155
3.75	Mechanical disaggregation of T6, cytocentrifuge preparation stained with PAP, x40 magnification.	155
3.76	Mechanical disaggregation of T6, cytocentrifuge preparation stained with PAP, x100 magnification.	156
3.77	Enzymatic disaggregation of T7, cytocentrifuge preparation. stained with PAP, x40 magnification.	156
3.78	Enzymatic disaggregation of T7, cytocentrifuge preparation stained with HE, x40 magnification.	156
3.79	Total cell count per gram of tumour tissue disrupted from human breast tumours, comparing mechanical and enzymatic disaggregation.	157
3.80	Percentage of viable cells from tumour disaggregation using mechanical and enzymatic techniques.	158
3.81	Illustration of MCF-7/S cells incubated with doxorubicin and analysed using the LSC and 12 well PTFE coated slides.	163
3.82	Analysis of calcein AM PTFE slide data from human breast tumour FNA cells.	165

Human tumour proliferation

- 3.83 **FCM and LSC analysis of human nuclei labelled with PI and BrdUrd-FITC.** 175

Discussion

- 4.1 **Two cells contoured using (A) fluorescence computation and (B) light scatter.** 184
- 4.2 **A specific and non - specific assay for determining a resistant cell from a sensitive cell, using doxorubicin fluorescence** 190

List of tables

Introduction

- 1.1 Commonly used chemotherapy schedules for metastatic breast cancer (adapted from Smith, 1991). 5
- 1.2 Anthracyclines and associated compounds and their clinical use. 9

Materials and Methods

- 2.1 FCM settings for experiments within this study. 39

Results

Characteristics of drugs

- 3.1 Comparison of practical derivations of the extinction coefficients of doxorubicin, mitoxantrone and ethidium bromide and those used in literature. 50
- 3.2 Comparison of practical calculations of doxorubicin, mitoxantrone and ethidium bromide affinity constants and those used in literature. 61
- 3.3 Comparison of practical calculations of doxorubicin, mitoxantrone and ethidium bromide for the number of DNA phosphate groups bound per drug molecules for intercalative binding. 61

Characterisation of cell line models – MTT assay

- 3.4 Differences in various parameters of the MTT assay 72

Cell viability studies

- 3.5 Correlation results comparing the calcein AM values of mean fluorescence intensity measured using flow cytometry and peak maximum fluorescence measured using LSC with chamber slides. 84
- 3.6 Correlation results comparing the calcein AM values of mean fluorescence intensity measured using flow cytometry and integral fluorescence measured using LSC with chamber slides. 84

Anthracycline uptake and consequent viability of MCF-7/S and MCF-7/R cells

- 3.7 Correlation results comparing the doxorubicin values of mean fluorescence intensity measured using flow cytometry and red integral fluorescence measured using the LSC with chamber slides. 104
- 3.8 Correlation results comparing the doxorubicin values of mean fluorescence intensity measured using flow cytometry and red integral fluorescence measured using the LSC with cytocentrifuge preparations. 104

Human breast carcinoma manipulations

- 3.9 Total cell yield and viability of various human tumours using mechanical or enzymatic disruption techniques. 161
- 3.10 Total cell count and viability using trypan blue exclusion of FNAs taken from two human breast tumours. 163

3.11	Viability of human breast primary tumour cells disrupted using fine needle aspiration.	169
Human tumour proliferation		
3.12	Median values of each parameter assessed by LSC and FCM and paired t - test results comparing the two analysis techniques.	173
3.13	Rank correlation analysis of each measured parameter, comparing LSC and FCM.	174

INTRODUCTION

1. ***Introduction***

Aims

The general aims of the work described in this thesis are to develop a patient specific drug uptake assay using the fluorescence characteristics of common anthracycline cytotoxic drugs. To address these aims there are a number of subsidiary objectives:-

- To study drug/DNA binding by spectrofluorimetry
- To develop objective quantitative assays of cytotoxic drug uptake into human breast tumour cells *in vitro* :
 - (I) Using cell lines
 - (II) Using cells from human tumours
- To study drug uptake and cell viability by flow and laser scanning cytometry
- To investigate a proliferation marker which would enable doxorubicin treatment to be tailored for slow and rapid proliferating tumours
- To compare flow and laser scanning cytometry in multiparameter assays using an *in vivo* proliferation marker in human tumour samples
- To seek evidence for cell death mechanism after doxorubicin uptake using the apoptotic marker annexin V
- To provide scientific basis for extension of this project to *in vivo* studies

1.1 **Breast cancer**

Each year in Britain about 25 000 new cases are diagnosed and about 15 000 women die of breast cancer. It accounts for almost one in five of all cancer deaths among women. One in 12 Western women can expect to develop the disease in her lifetime, and one in 20 will die from breast cancer (Baum *et al.*, 1995). It is thus an important subject for therapeutic research.

1.1.1 **Normal breast tissue structure and growth**

The normal female breast ductal system is lined principally by epithelial cells, which are the origin of the majority of breast cancer. The metastases which often accompany primary breast cancer are facilitated by an extensive venous and lymph system within breast tissue. The cyclical levels of progesterone and oestrogen which influence breast tissue development and growth (Forsyth, 1991) maybe responsible for the irregular cellular growth (Walter, 1977). The reaction of breast epithelial cells to the stimulation of oestrogen can be judged by their oestrogen receptor (ER) status. The ER is a steroid - dependent DNA - binding protein, initially cloned from MCF-7 breast cancer cells (Sluyser, 1995). The functions of the ER include transcriptional activation and repression, nuclear localisation, DNA binding and hormone binding (Walker *et al.*, 1997). The ability of oestrogens to stimulate breast tumour growth is related to whether the tumour cells are ER positive or negative, ER positive cells are stimulated by oestrogens. The breast epithelium is a metabolically active tissue which is highly proliferative and sensitive to genetic, radiotherapeutic and chemotherapeutic damage.

Proliferating cells progress through a sequence of phases - the cell cycle. Normal and malignant cells traverse the cell cycle at various rates and the proliferating activity of a neoplastic mass may influence the treatment of a tumour.

Malignant breast tumour cells have lost the restriction of normal growth conditions and gained the ability to invade and colonize areas of the body normally reserved for other cells. For a breast tumour to survive and continue to grow the cells must stimulate angiogenesis and disrupt the normal proliferation cycle of cells to maintain 50% of stem cells.

1.2 **Types of breast cancer**

Breast cancer is a heterogenous disease both in terms of its cellular structure, and its response to treatment. There are two main types of breast lesions, ductal *in situ* carcinoma (DCIS) and invasive ductal carcinoma. DCIS is usually treated with surgery but patients do not receive chemotherapy (Graham *et al.*, 1991). The majority of invasive ductal carcinoma are of no special type (NST), other histological types include infiltrating lobular, colloid, tubular, cribriform, papillary, medullary, adenoid cystic, apocrine and argyrophilic, all of which are carcinomas (Sacks *et al.*, 1996). It is not uncommon for invasive disease to be accompanied by an *in situ* fraction. The description of a NST carcinoma is given as a grade I, II or III, calculated by the degree of glandular formation, nuclear pleomorphism and frequency of mitoses within the tumour. In general terms, grade III tumours are more aggressive and more likely to be treated using systemic chemotherapy.

1.3 **Therapeutic approaches to breast cancer**

The primary treatment for breast cancer is surgery to remove the entire tumour and its draining lymphatics and lymph nodes. This treatment cures many patients of the local disease, mortality is mainly due to metastatic tumours which have already formed at the time of diagnosis of the primary tumour (Sacks *et al.*, 1996). Other additional therapies which could be used in conjunction with surgery are radiotherapy, anti - oestrogen therapy and chemotherapy.

Radiotherapy is a directional treatment for locally advanced or metastatic disease, or to reduce the risk of recurrence in surgical fields, it is often used as an adjunct to surgery, dividing cells being sensitive to radiation damage.

Ovary ablation, by surgery or radiotherapy, can be performed to remove the proliferative stimulus of oestrogen when treating ER positive breast tumours (Baum, 1995). A second strategy is to block oestrogen and progesterone receptors, using an agent such as tamoxifen, which demonstrably improves disease free survival rates (Sacks *et al.*, 1996).

1.3.1 **Chemotherapy for breast cancer**

Chemotherapy for metastatic breast cancer was first described over 40 years ago (Schoenbach *et al.*, 1952) and systemic chemotherapy using intravenous cytotoxic drugs is now a major component of breast cancer treatment, although its use is very empirical.

Indications include grade III lesions, which tend to be aggressive tumours, the presence of axillary lymph node metastases, local or systemic recurrence, and patient age of less than 70 years. Efficacy of treatment is generally low; only 10 - 20% of patients receiving doxorubicin, an anthracycline cytotoxic drug, demonstrate complete remission from their tumour, and the median survival is generally less than 12 months (Young *et al.*, 1981). Part of the reason for these low response rates are that there are no clear indicators as to which agent or combination of agents should be prescribed to each patient. Knowledge of the properties of a tumour could give additional information indicating a more informed choice of drug regime and its administration strategy. The resistance status of the tumour and its proliferation rate are such key factors. Selective use of anthracyclines are important because there is substantial morbidity and significant mortality associated with their use. Chemotherapy can be used aggressively, to induce remission of a tumour, or as part of symptom palliation in those patients with terminal disease. Chemotherapy is associated with significant improvement in symptoms, mood and general sense of well-being (Coates *et al.*, 1987). To establish which patients will respond to chemotherapy would allow treatment targeting and prevent unnecessary treatment with inappropriate drugs.

In the 1970s combination therapy was pioneered, a drug schedule which incorporates anti - neoplastic agents with different modes of action. The dose and action of the three most common drug regimes used against breast cancer are illustrated in table 1.1. These drugs fall into the categories of; antimetabolites, alkylating agents or antibiotics. The mode of action of the antibiotics is complex, their pivotal action being the intercalation of DNA. The duration of these drugs within the body and concentration at which they interact with the cells are significant parameters within the study of the interaction of anti - neoplastic agents. The plasma concentrations of these drugs within patients is difficult to determine from the literature; plasma concentrations of doxorubicin have been found to be variable depending on drug schedule, the highest plasma concentration being reported to be $5 \mu\text{mol.L}^{-1}$ (Muller *et al.*, 1997).

Regime abbreviation	Drug	Class of drug	Dose range
CAF	Cyclophosphamide	Alkylation	600 - 750 mg/m ² i.v.
	Doxorubicin	Antibiotics	40 - 50 mg/m ² i.v.
	5 - Fluorouracil	Antimetabolite	600 mg/m ² i.v.
CMF	Cyclophosphamide	Alkylation	60 - 100 mg/m ² orally days 1 - 14
	Methotrexate	Antimetabolite	30 - 40 mg/m ² i. v. days 1 and 8
	5 - Fluorouracil	Antimetabolite	600 mg/m ² i.v.
MMM	Mitoxantrone	Antibiotic	7 - 8 mg/m ² i.v.
	Methotrexate	Antimetabolite	30 - 40 mg/m ² i.v.
	Mitomycin C	Antibiotic	7 - 8 mg/m ² i.v.

Table 1.1

Commonly used chemotherapy schedules for metastatic breast cancer (adapted from Smith and Powles, 1991)

CMF is the most commonly prescribed regime which demonstrates about 50% response rates, a response being a detrimental effect upon the tumour, which could range from a tumour remaining the same size to complete regression (Young *et al.*, 1981). Doxorubicin - containing regimes display the highest response rates (50 - 60%), but the cardio - toxicity of doxorubicin is high, and many patients are unable to withstand treatment. In some centres MMM is replacing the doxorubicin containing regimes, MMM has also shown 50% response rates (Powles *et al.*, 1991), but with less side effects than the doxorubicin containing regimes (Smith and Powles, 1991 and Greenall, 1996). The chemotherapy drugs used routinely against breast cancer and its metastasis cover various biochemical modes of action. Each class of drug elicits comparable response rates but their concurrent administration yields cumulative biological effect on the target tumour cells.

1.3.2 Mechanisms of action of chemotherapeutic drugs

Cytotoxic agents are categorised into five main groups. This classification is primarily biochemical and it has been mostly assumed that drugs of the same biochemical

nature have a similar mode of action. The classification of these drugs and their general mechanism is described briefly, some agents, including the anthracyclines (the focus of this study) have several mechanisms of action.

The anthracyclines probably form the most important group of antibiotics which have been used as treatment against neoplastic disease. They have many modes of action including DNA intercalation, inhibition of topoisomerase II, plasma membrane binding, free radical formation and alkylation.

Alkylation refers to the covalent attachment of alkyl groups to other molecules. Alkylation attacks a number of enzymes taking part in protein synthesis, and linking enzymes which are needed for the construction of new DNA strands. It prevents these enzymes from carrying out their biological role within the cell and so stops the formation of new DNA, which inhibits mitosis.

Antimetabolites mimic the structures of normal metabolic constituents, including folic acid, pyrimidines and purines. This leads to inhibition of specific enzymes preventing the synthesis of DNA or RNA in neoplastic cells. Methotrexate is an example of an antimetabolite which inhibits the action of dihydrofolate reductase, resulting in S phase inhibition which causes cell death.

Vinca alkaloids block microtubule formation and thereby disrupt mitotic spindle formation during mitosis, an example is taxol.

1.3.3 The anthracycline family

Doxorubicin (or adriamycin) is an anthracycline antibiotic isolated from a culture of *Streptomyces peucetius* var. *caesius*, or by chemical synthesis from daunorubicin (or daunomycin) (Carter *et al.*, 1975; Arcamore, 1978; Neidle, 1978 and Keizer *et al.*, 1990), its chemical structure is illustrated in figure 1.1. Doxorubicin is a widely used chemotherapy drug for many neoplastic diseases, namely breast cancer and haematological cancers (Young *et al.*, 1981 and Hortobagyi, 1997) and is the single most effective agent currently used for metastatic breast cancer (Greenall, 1996). The clinical use of doxorubicin and other members of the anthracycline family are illustrated in table 1.2, including an anthracycline derivative, the anthraquinone mitoxantrone, which has also been used successfully against breast cancer (Cornbleet *et al.*, 1984 and Stewart *et al.*, 1997).

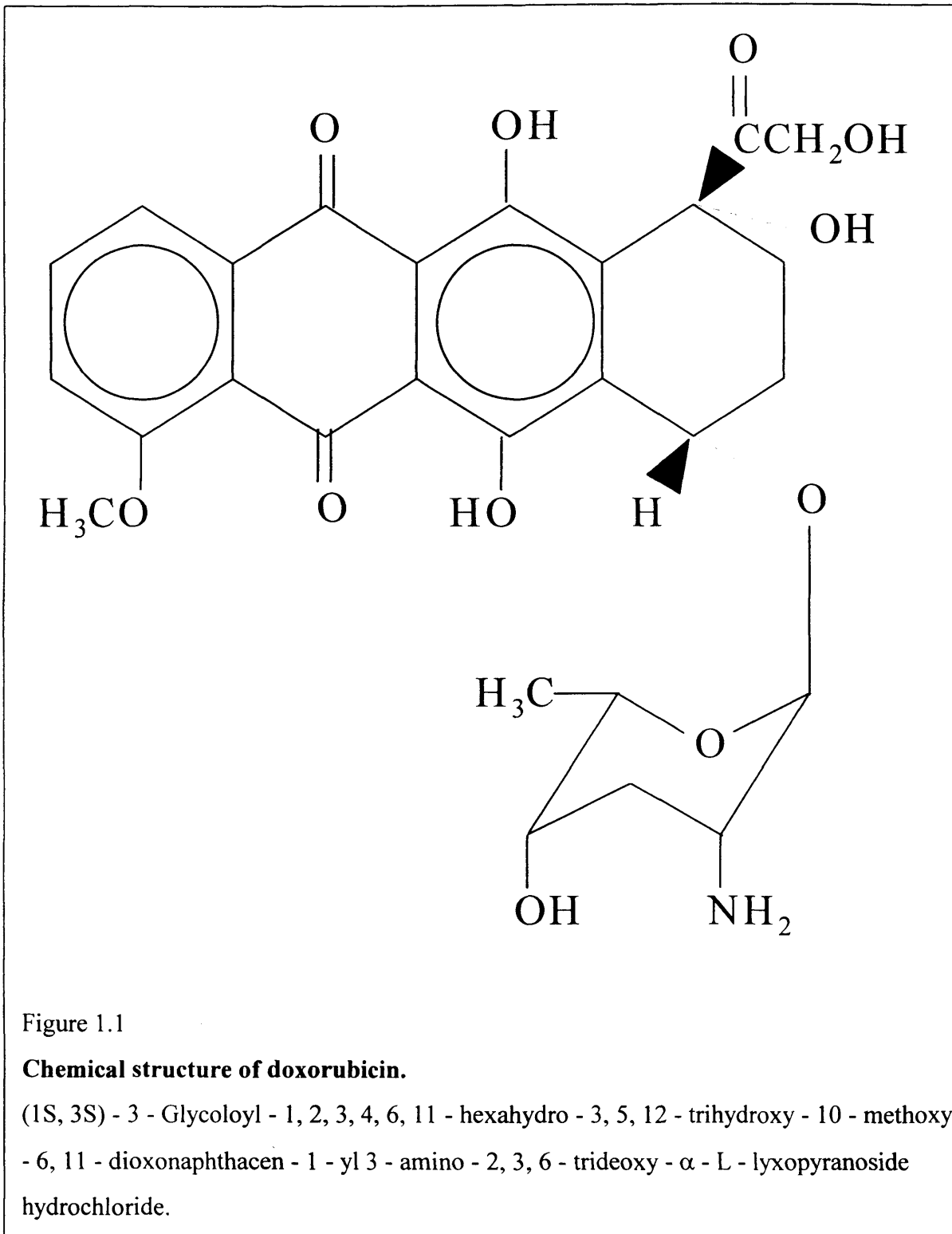


Figure 1.1

Chemical structure of doxorubicin.

(1S, 3S) - 3 - Glycoloyl - 1, 2, 3, 4, 6, 11 - hexahydro - 3, 5, 12 - trihydroxy - 10 - methoxy - 6, 11 - dioxonaphthacen - 1 - yl 3 - amino - 2, 3, 6 - trideoxy - α - L - lyxopyranoside hydrochloride.

Drug	Clinical Use
Daunorubicin	Leukaemias e.g. AML (a) (b)
Doxorubicin	Breast cancer (a) (d) Ovarian cancer (a) (b) Small cell lung cancer (a) (b) Hodgkin's and Non - Hodgkin's Lymphoma (a) (b)
Rubidazone (zorubicin)	Acute Leukaemia (b)
Carminomycin	Soft tissue sarcomas (b)
Pirarubicin	Breast cancer (a)
Idarubicin	Leukaemias (a) (c)
Epirubicin	Breast cancer (a) (d) Gastric cancer (a)
Aclacinomycin C	Acute Leukaemia (b)
AD 32	Acute Leukaemia (b)
Mitoxantrone (an aminoanthraquinone)	Breast Cancer (a) (d) (e)

(a) Hortobagyi, 1997; (b) Young *et al.*, 1981; (c) Tidefelt *et al.*, 1996; (d) Greenall, 1996 and (e) Cornbleet *et al.*, 1984.

Table 1.2

Anthracyclines and associated compounds and their clinical use.

1.3.3.2 Topoisomerase II inhibition

For efficient utilization of DNA during transcription, replication and chromosome segregation, mechanical and torsional stresses of the DNA superhelical structure need to be overcome (Alton, 1993). Topoisomerase II is a nuclear enzyme which breaks and rejoins phosphodiester bonds of DNA altering the degree of supercoiling of DNA. The topoisomerase II protein is predominantly active during S phase of the cell cycle (Deffie *et al.*, 1989) during DNA → RNA transcription and DNA replication. It creates double strand breaks in DNA, which are stabilized by doxorubicin which binds to the DNA - topoisomerase II composite creating a 'cleavable complex' (Tewey *et al.*, 1984; Fox and Smith, 1990 and Alton, 1993). The DNA strand breaks can be reversed by the removal of drug (Alton, 1993), but if the cell cycle progresses the cell will be irreparably damaged and

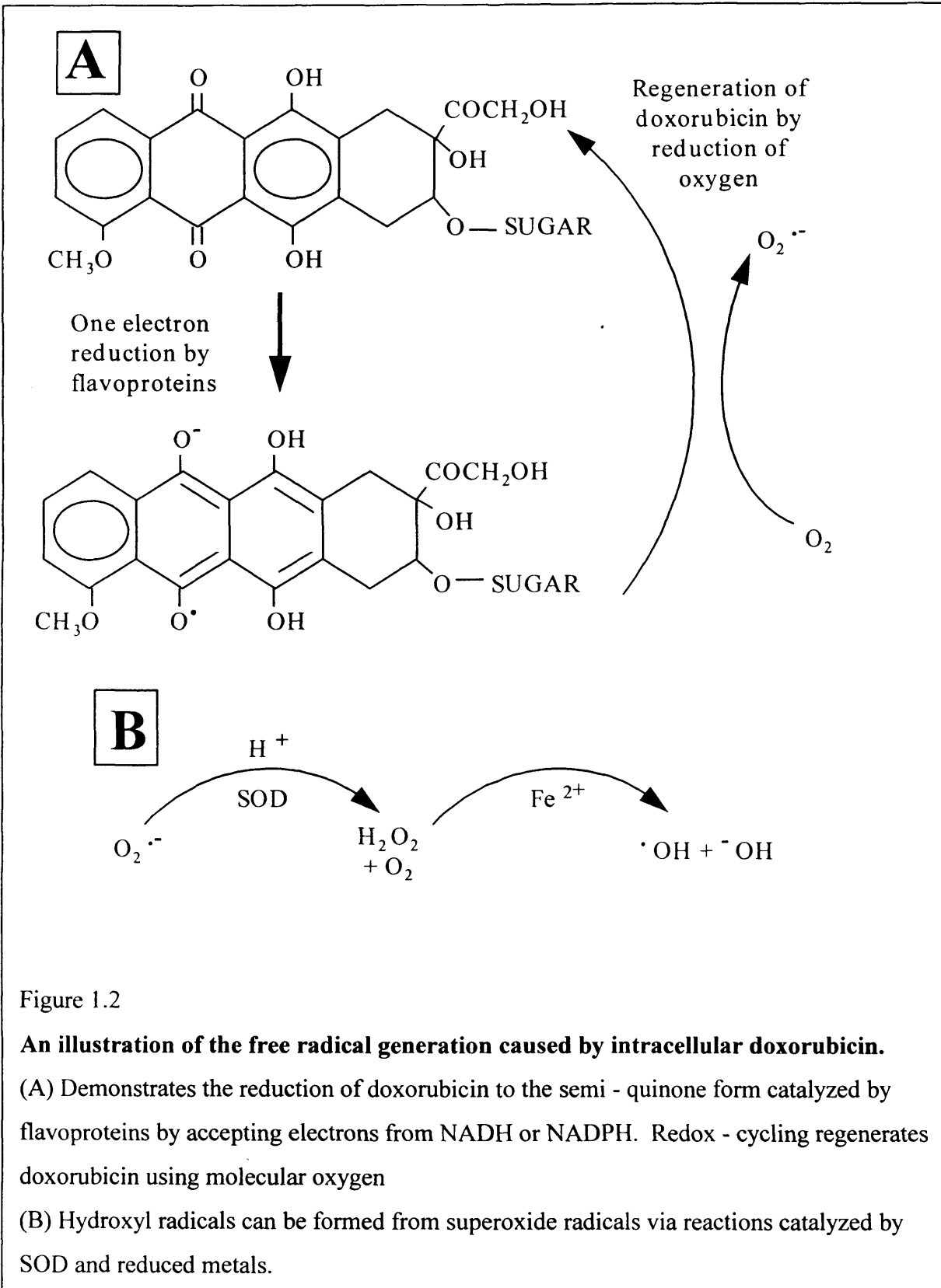
die. The DNA fragmentations caused by topoisomerase II stabilised strand breaks are not uniform using different anthracyclines (Capranico *et al.*, 1989). For example, idarubicin has been found to be more effective at inducing DNA fragmentation than doxorubicin (Capranico *et al.*, 1989 and Smith *et al.*, 1994). The quantity of DNA fragmentation caused by doxorubicin is not constant; DNA fragmentation decreased with increasing doxorubicin concentration (Smith *et al.*, 1994 ; Tewey *et al.*, 1984 and Pommier *et al.*, 1993). Increasing concentrations of doxorubicin are able to intercalate into the DNA and possibly inhibit the binding of topoisomerase II to DNA (Tewey *et al.*, 1984), therefore preventing DNA fragmentation by topoisomerase II.

1.3.3.3 Free radical formation and cell membrane interactions

The detection and action of free radicals generated by anthracyclines on, or within tumour cells, has been investigated by many groups (Doroshaw *et al.*, 1986; Sinha *et al.*, 1987; Bustamante *et al.*, 1990 and Ravid *et al.*, 1999). Doxorubicin, contains a quinone residue which can undergo a one - electron reduction to a semi - quinone by cellular flavoproteins e.g. microsomal cytochrome P450 reductase, NADH dehydrogenase and xanthine oxidase (Keizer *et al.*, 1990 and Ravid *et al.*, 1999). In the presence of oxygen this semi - quinone is oxidized back to its parent form to yield superoxide radicals shown in figure 1.2/A. Cellular superoxide dismutase (SOD) acts upon superoxide radicals to form hydrogen peroxide which can be converted to hydroxyl radicals in a reaction catalyzed by reduced metals, this is illustrated in figure 1.2/B. The hydroxyl radical is the most damaging species of the reactive oxygen species (ROS) (Keizer *et al.*, 1990 and Ravid *et al.*, 1999). Although these processes are widely accepted, their input towards the cytotoxicity of anthracyclines and the cellular locations of these events, is still debated. Hydrogen peroxide (Doroshaw, 1986 and Bustamante *et al.*, 1990) and hydroxyl radicals (Sinha *et al.*, 1987) have been shown to be generated by MCF-7/S cells incubated with doxorubicin concentrations of 0.4 - 2.5 $\mu\text{mol.L}^{-1}$ (Doroshaw, 1986) and 100 $\mu\text{mol.L}^{-1}$ (Sinha *et al.*, 1987). Suggesting these agents contribute to the toxicity of doxorubicin towards MCF-7/S cells. MCF-7/R cells have increased levels of mRNA for glutathione peroxidase compared with MCF-7/S cells (Sinha *et al.*, 1987 and Akman *et al.*, 1990) and do not generate detectable hydroxyl radicals in response to 100 $\mu\text{mol.L}^{-1}$ doxorubicin (Sinha *et al.*, 1987). The generation of this enzyme infers that it offers protection against doxorubicin cytotoxicity inhibiting the generation of ROS which are produced by MCF-

7/S cells which are sensitive to doxorubicin treatment. The use of agents which detoxified hydrogen peroxide and ROS abolished the cytotoxicity of doxorubicin $0.4 - 2.5 \mu\text{mol.L}^{-1}$ (Doroshaw, 1986). In addition, the hormonal form of vitamin D has been shown to increase the cytotoxicity of doxorubicin through the enhancement of the ROS mediated pathway (Ravid *et al.*, 1999). This evidence, strongly suggests that the ROS mediated pathways within MCF-7/S cells are critical to the cytotoxicity of doxorubicin. Many studies have centred around the action of radical scavengers and quenchers upon the cytotoxicity of these drugs (Sinha *et al.*, 1987 and Doroshaw *et al.*, 1986). Certainly the cytotoxicity of the anthracyclines can be reduced by removing the generated free radicals (Sinha *et al.*, 1987 and Doroshaw *et al.*, 1986).

Other non - DNA intercalation events may also lead to cytotoxic effects upon cells. Tritton and Yee (1982) have shown that doxorubicin does not need to enter the cells to cause these effects. Doxorubicin has a strong interaction with phospholipid membranes (Villalonga and Philips, 1978), via an electrostatic interaction between the ammonium group of doxorubicin and the phosphate group of the neutral phospholipids (Gaber *et al.*, 1998). Doxorubicin treatment of Sarcoma 180 cells has shown an increase in the fluidity of the plasma membrane (Siegfried *et al.*, 1983). Similar treatment of MCF-7/S cells, caused lipid peroxidation via a free radical mechanism (Bustamante *et al.*, 1990). It still remains to be finalised as to the relative importance of these non - DNA interacting mechanisms of anthracyclines, conflicting information seems to be generated dependent upon the cell type used. Keizer *et al.* (1990) has illustrated studies which appear to conclude that although free radical and cell membrane interactions may be important in the toxicity of the anthracyclines to normal cells such as cardiac tissue, they are not apparent in all cell lines which are sensitive to anthracycline treatment, therefore they are not universally important. Mitoxantrone and ametantrone (aminoanthraquinones) at $10^{-5} - 10^2 \mu\text{mol.L}^{-1}$ do not generate ROS when incubated with MCF-7/S cells although they are cytotoxic agents with many similar structural and mechanistic characteristics to the anthracyclines (Fisher and Patterson, 1992) Conversely it has been shown that N - tri fluoracetyl adriamycin - 14 - valerate (AD 32) is an active anthracycline with little or no ability to bind DNA (Tritton and Yee, 1982).



1.3.4 Resistance to anthracycline chemotherapy

Drug resistance is one reason, among many, why chemotherapy fails to cure cancer. Chemotherapy can only kill those tumour cells it can reach, anatomical sites such

as the meningeal space, peritoneal area and testes create sanctuary sites against nonspecific chemotherapy (Hedley *et al.*, 1993). Drug distribution is regulated by the vascular and lymphatic networks of the body and of the tumour itself, consequently a poorly vascularised tumour may be partially untouched by anti - neoplastic agents.

The failure of anthracycline chemotherapy is the result of complex mechanisms within each individual cell, and the heterogeneity of the cells within the tumour tissue. The heterogeneity of human tumours has many forms. The evidence for genetic heterogeneity has been offered by classical karyotypical analysis (Pandis *et al.*, 1995), more than one cell lineage has been demonstrated within a breast tumour mass (Teixeira *et al.*, 1995). The most relevant heterogeneity issue of this study is that of multiple drug resistant phenotypes. Drug resistant phenotypes maybe a result of genetic or epigenetic changes, or cell cycle variations (Heppner, 1984). For this study the detection of a drug - resistant cell population was through the reduction in anthracycline retention, regardless of the mechanisms for its appearance. A sub - population of tumour cells which are resistant to chemotherapy will increase the overall resistance of the tumour (Epstein, 1984). A patient - specific assay which could determine tumour resistance to anthracycline chemotherapy, could provide valuable drug targeting information.

MCF-7/S cells (human breast adenocarcinoma cell line) have been described in the literature with the assumption that they are oestrogen receptor positive (Brotherick *et al.*, 1995). Unfortunately not all MCF-7/S cells appear to express this receptor consistently, Palmari *et al.* (1997) found oestrogen receptor expression to increase as the culture of MCF-7/S cells grew, with distinct subpopulations noted. Response to anti - oestrogen therapy has also been inconsistent, MCF-7/S cells were used to induce breast tumours within nude mice (Kryprianou *et al.*, 1991) but only half of the induced tumours underwent regression with removal of oestrogens.

Biological drug resistance is multifactorial, it can be affected by the cell cycle phase and the proliferation status of the cell. For example, doxorubicin is most effective upon cells which are within S phase of the cell cycle, the determination of the proportion of tumour cells within the various stages of the cell cycle could provide more information for the choice of an appropriate drug regime. The biochemical mechanisms which contribute to the resistance of tumour cells to cytotoxic treatment include, detoxification mechanisms (e.g. SOD, catalase and glutathione - S - transferase), cellular drug transport systems (e.g. efflux and sub - cellular localisation), DNA replication mechanisms (e.g.

efficiency of topoisomerase II) and DNA repair mechanisms (enhancement) (Hedley, 1993).

The major biochemical resistance mechanism which influences anthracycline treatment is multidrug resistance (MDR), caused by the over expression of P - glycoprotein (P - gp) (Endicott and Ling, 1989) a 170 kD transmembrane protein. P - gp is a glycoprotein of the ABC (ATP - Binding Cassette) superfamily of active transporters (Krishan, 1997 and Higgins and Gottesman, 1992). It is an ATP dependent membrane pump, capable of efflux of cytotoxic agents, such as doxorubicin, (Beck, 1987) and their redistribution within the cell (Schuurhuis *et al.*, 1993) leading to drug resistance. The normal biological function remains unclear (Higgins and Gottesman, 1992), but it is highly expressed in normal tissues such as gut mucosa, endometrium (Hedley, 1993) and brain (Regev and Eytan, 1997). Tumours arising from these tissues will normally demonstrate resistance to chemotherapy agents sensitive to MDR (Goldstein *et al.*, 1992). Breast tissue does not constitutively express high levels of P - gp (Baldini, 1997), however many tumours acquire MDR resistance after exposure to chemotherapy agents such as doxorubicin. The ensuing resistance will cover numerous unrelated drugs (Flens *et al.*, 1994 and Krishan, 1997). Cells which present with the MDR phenotype have been shown to be resistant to doxorubicin and demonstrate a reduced cellular retention of the drug (Beck, 1987; Broxterman *et al.*, 1989; Drori *et al.*, 1995 and Hortobagyi, 1997).

Transport proteins such as P- gp and multidrug resistant associated protein (MRP) reduce the accumulation of cytotoxic agents within the cells but they also change the distribution of the drugs within the cells preventing their interaction with crucial intracellular targets, such as nuclear DNA. High levels of P - gp are found on cytoplasmic vesicles of MCF-7/R cells (doxorubicin resistant breast cancer cell line). Doxorubicin (and other anthracyclines) may be removed from these vesicles which ordinarily transfer the drug from the cytoplasm into the nucleus, as shown in MCF-7/S cells (doxorubicin sensitive breast cancer cell line) (Molinari *et al.*, 1994 and Arancia *et al.*, 1998). The mechanism of P - gp to allow the removal of a wide range of unrelated drugs may be as a flippase (Higgins and Gottesman, 1992). Drugs such as doxorubicin may enter the phospholipid membrane with its' hydrophobic planar chromophore, the hydrophilic amine group present in the daunosamine moiety interacting with the acidic headgroups of the phospholipids (Regev and Eytan, 1997). P - gp consists of two sets of six membrane

spanning segments (Higgins and Gottesman, 1992) which could transfer doxorubicin from one side of the plasma membrane to the other.

Other transport pumps which are associated with drug resistance include multidrug resistance associated protein (MRP) and lung resistance protein (LRP), both of which are involved with drug efflux (Krishan, 1997). These protein mechanisms are not of primary importance when investigating the resistance of breast tumour cells, but MRP may be present albeit in lower quantities than P - gp.

1.3.5 Clinical formulations and use of anthracyclines

Doxorubicin and most other anthracyclines are administered to patients via an intravenous line (Benjamin *et al.*, 1973) or by bolus injection (Ertman *et al.*, 1988). The optimum drug schedule of doxorubicin therapy has not yet been determined (Eksborg *et al.*, 1985). Intraperitoneal schedules have been used for ovarian cancer, and this type of administration has demonstrated higher plasma concentrations of doxorubicin than equivalent doses of i.v. therapy (Young *et al.*, 1981). Pirarubicin, idarubicin and mitoxantrone have been successfully formulated as effective oral preparations for breast cancer (Hortobagyi, 1997). An alternative to direct administration of anthracyclines into the systemic circulation of the body is encapsulating drugs which would allow the transport of the drug to various sites of the body before their release (Langer, 1998). The encapsulation of drugs such as doxorubicin can take various forms including pegylated liposomes (Muggia, 1997), lipid compositions (Lim *et al.*, 1997 and Cabanes *et al.*, 1998) and conjugation to transferrin (Kratz *et al.*, 1998a) or albumin (Kratz *et al.*, 1998b). The use of such types of drug delivery system will decrease side effects of anthracyclines and allow longer circulation of the drug (Muggia, 1997). Another approach to the use of liposomes was reported by Nam *et al.* (1998) where doxorubicin was encapsulated within a lipid based liposome which was coated with antibodies specific for B16BL6 and HRT - 18 tumour cell lines. Doxorubicin coupled to a proprietary albumin capsule (CytocapsTM Quadrant Healthcare UK Ltd) was investigated for this study.

1.3.5.1 Clinical limitations to anthracycline use

Doxorubicin has many adverse effects and a small therapeutic index (Cummings and Gardiner, 1997), its use is limited by its toxicity to normal host cells. The toxicity to the heart (Billingham, 1991) and bone marrow cause serious side effects, although others

include nausea and vomiting, stomatitis and oral ulceration, intestinal ulceration, mucosal shedding, diarrhoea, intestinal infections and notable alopecia. Patients receiving a total dose of $> 500 \text{ mg/m}^2$ doxorubicin have a mortality rate of 50% (Fenoglio, 1991). The toxicity of these drugs and the genuine mortality risk emphasises that a patient specific assay could determine their appropriate use. Tumours could be selected which would be most likely to respond at the cellular level to treatment and patients with high levels of cellular resistance would be detected and protected from futile therapeutic efforts.

1.4 **Research models for human primary breast tumours**

The intrinsic and acquired resistance of many tumour populations obliges us to determine those patients who will benefit from anthracycline therapy, from those patients who will not (Greenall, 1996 and Hortobagyi, 1997). Patients who have undergone inappropriate high dose chemotherapy may not survive the treatment, or be strong enough to cope with subsequent treatment with another class of drug.

One model system used to test drug action at the molecular level is the interaction of doxorubicin, mitoxantrone and ethidium bromide with 'free' mammalian DNA. This allows the determination of intracellular interactions of DNA and drug without the interference of other cellular processes (Zunino, 1972; Arcamore, 1978; Neidle, 1978 and Lown *et al.*, 1985).

Another model system utilises cell lines which are easily grown in culture to provide a constant supply of neoplastic cells. Examples of suitable cell lines include; MDA MB 231, MCF-7/S and MCF-7/R cells. MCF-7/S and MCF-7/R are a pair of cell lines, sensitive and resistant to doxorubicin therapy, respectively. These originate from human breast tumour metastases, cultivated and immortalised to produce 'continuous' cell lines. Cell lines offer a continuous supply of cells, but they have lost the structural organisation of the original tissue and the biochemical properties associated with it. Once extracted from a tumour, they dedifferentiate and the cell line created may have different characteristics to the original tumour cells. Despite this limitation cell lines are a useful model for establishing techniques to applied to freshly disaggregated cells from human tumours.

Another approach to the development of a patient specific drug uptake assay would be to use freshly disaggregated human breast tumour cells. However many difficulties are associated with such methods. The extraction of tumour cells from breast carcinomas is

difficult and unpredictable (Rong *et al.*, 1985 and Engelholm *et al.*, 1985). A wide range of viable tumour cells are yielded (Costa *et al.*, 1987 and Cerra *et al.*, 1990) which are often contaminated with other cells from the breast tissue, for example fibroblasts and blood. The disaggregation of tumour cells generates unpredictable yields of cells with varying viability however, the proliferation assay employed for this study used disrupted human tumour nuclei as an alternative use of human tumour cells. Nuclear extraction from tissue is much easier than disruption of viable intact cells and the proliferation assay provides crucial information about the proliferative state of cells within the tumour.

1.4.1 Drug sensitivity assays

The fluorescence of the anthracyclines can be used as a quantitative marker of uptake and retention of the drugs by individual cells, inferring their sensitivity or resistance to this therapy. The direct correlation of anthracycline fluorescence, with intracellular drug concentration is however hampered by the quenching of doxorubicin fluorescence when intercalated into DNA (Krishan and Ganapathi, 1980 and Durand and Olive, 1981). Intercalation into DNA creates an interaction between the doxorubicin molecule and DNA which prevents doxorubicin generating fluorescence, quenching of doxorubicin could be as great as 95% (Chaires *et al.*, 1982). Quenching would be greatest at low concentrations of doxorubicin, the doxorubicin available to the cell intercalates into the DNA, reducing the fluorescence observed. At higher drug concentrations doxorubicin is in excess, DNA intercalation sites are saturated, drug binds to the surface of DNA and is able to accumulate in the cytoplasm.

There are many parameters to be addressed within the design of a patient - specific drug sensitivity assay. Anthracycline drugs will pass through the plasma membrane of cells via passive diffusion (Eytan *et al.*, 1996) which means that they will pass into viable and non - viable cells. The detection and measurement of anthracycline retention only by viable cells is pertinent to this study. Thus the exclusion of non - viable cells from the analysis of anthracycline retention of a cell population is a requirement, the ability to obtain viable human tumour cells from primary breast tumours via fine needle aspiration or disaggregation is a major hurdle. Once a cell suspension has been obtained from a disaggregated breast tumour sample it will contain numerous cell types. Separation of the fluorescent anthracycline signals originating from tumour cells and contaminating cells is also required. Using cell lines, the viability and cell type are generally guaranteed but

human solid tumour suspensions may contain normal host epithelial cells, leukocytes and erythrocytes. Stripped human tumour nuclei can be used to demonstrate a technique to determine the proliferative rate and proportion of cells in the various stages of the cell cycle. The proliferation rate and where the cells are within the cell cycle is pertinent to the use of doxorubicin therapy. A slowly proliferating tumour may be most effectively targeted using a continuous course of treatment, whereas a rapidly proliferating tumour could be tackled using a rapid high regime.

1.4.1.1 Tumour cell growth assays

There are a variety of cell growth techniques that have been used to determine tumour cell sensitivity to drugs. These include colony formation assay (Salmon *et al.*, 1978), radiolabelled precursor inhibition assay (Bech - Hansen *et al.*, 1977) and subrenal capsule assay (Abrams *et al.*, 1986). The colony formation assay is based on the ability of cells to produce viable colonies in soft - agar plates after preincubation with a therapeutic agent. This technique is time consuming and labour intensive, and has a low plating efficiency 0.1 - 2.0% for ovarian carcinoma and 0.01 - 0.2% for myeloma cells (Salmon *et al.*, 1978). The length of time between the sampling of patient cells and the result is a crucial factor for the use of these procedures as a routine drug sensitivity assay. These assays may take 2 - 3 weeks, during which time chemotherapy would have already begun, therefore as a routine assay these techniques may be redundant.

Cell kinetic measurements incorporating radioactive or halogenated DNA precursors, for example, tritiated thymidine (^3H - TdR) or BrdUrd, allow the S - phase cells to be counted as they proceed through mitosis. The percentage of cells in each phase of the cell cycle can be determined using propidium iodide (PI), a dye which stoichiometrically binds DNA, and analysed by FCM (Rigg *et al.*, 1989 and Visscher *et al.*, 1990). Many other fluorescent dyes can also be used in a similar way (Traganos, 1990). This analysis offers a static view of the cells within a tumour, but it does not enable the determination of rates of cell cycle progression (Wilson, 1994). Another cell proliferation assay uses bromodeoxyuridine (BrdUrd), a halogenated pyrimidine which is incorporated into those cells in S - phase. BrdUrd can be administered *in vivo* to cancer patients prior to surgery, the proliferation of the tumour nuclei can thus be ascertained from BrdUrd and DNA content.

1.4.1.2 Fluorescence microscopy assays

Doxorubicin (and other anthracyclines) are naturally fluorescent, this property can be used to measure drug uptake into neoplastic cells.

The use of doxorubicin uptake has been harnessed as a drug sensitivity test, to determine the sensitivity of osteosarcoma cells to doxorubicin therapy (Baldini *et al.*, 1992 and Gebhardt *et al.*, 1994). Gebhardt *et al.* (1994) published their method model using P388/S and P388/R murine leukaemic cell lines, which were sensitive and resistant to doxorubicin treatment, respectively. Doxorubicin uptake was detected using fluorescence microscopy, fluorescence intensity was determined using photometers on a cell-by-cell basis. The cells were incubated for 30 min at 37°C with 1, 10 and 100 $\mu\text{g.ml}^{-1}$ doxorubicin. The 10 and 100 $\mu\text{g.ml}^{-1}$ concentrations were bright enough to be visible, but 1 $\mu\text{g.ml}^{-1}$ was not. The viability of these cells was determined using the green fluorescent viable cell dye fluorescein diacetate (FDA). The FDA and doxorubicin fluorescent signals were detected using detectors of different wavelengths. The quantity and location of fluorescence generated by doxorubicin is different in sensitive and resistant cells, doxorubicin can be detected within the nucleus of sensitive cells, with resistant cells showing only minimal fluorescence in the cytoplasm. This published work only described the assay using the murine leukaemic cell lines, although they had performed this assay on a number of clinical osteosarcoma patients and these samples demonstrated a variety of levels of cellular doxorubicin fluorescence. The labelling of viable cells with FDA and a cell-by-cell detection system enabled the analysis of viable cells only. Baldini *et al.* (1992) developed a very similar assay using human osteosarcoma primary cultures, they found all the clinical samples to be sensitive to doxorubicin treatment using nuclear fluorescence as a marker for sensitivity. Fluorescence microscopy enables individual cells to be analysed but this technique is slow and time consuming, and analyses only a small number of cells. Fluorescence microscopy can be used for quantitative analysis of small numbers of cells using image analysis software.

1.4.1.3 Confocal assays

Confocal microscopy has been extensively used to evaluate subcellular distributions of anthracyclines (Coley *et al.*, 1993; Bennis *et al.*, 1995 and Cooper *et al.*, 1996). Confocal microscopy has the ability to quantitatively analyse the fluorescence of individual planes of cells. These images can be reconstructed to create a very sharp 3D

image of the object. Confocal microscopy is a valuable tool for individual cell fluorescence quantification and visualisation, but quantification of large numbers of cells is slow. Unfortunately confocal microscopy was not easily accessible for this study but it would have been a useful parallel technique to flow and laser scanning cytometry, which could have created images definitively illustrating the sub - cellular localisation of doxorubicin and CytocapsTM over time.

1.4.1.4 Laser scanning microscopy assays

Laser scanning microscopy has been used in a similar way to confocal microscopy to determine subcellular drug retention and to examine differences between drug sensitive and resistant cells (Schuurhuis *et al.*, 1993; Lau *et al.*, 1994 and Arancia *et al.*, 1998). There is a distinct difference in the accumulation of doxorubicin between doxorubicin sensitive MCF-7/S and doxorubicin resistant MCF-7/R cells. Doxorubicin accumulates in the nucleus of MCF-7/S cells whereas MCF-7/R cells show lower levels of fluorescence mainly within the cytoplasm (Schuurhuis *et al.*, 1993 and Arancia *et al.*, 1998). Using very short incubations of doxorubicin with MCF-7/S cells, fluorescence was shown localised to cytoplasmic vesicles and the perinuclear area, as well as a faint signal from the nucleus, this 'punctate pattern' has been described by Keizer *et al.* (1989). The transport of doxorubicin to the nucleus via acidic vesicles may be important in the multidrug resistance phenomenon (Molinari *et al.*, 1994 and Arancia *et al.*, 1998). The distribution of P- gp within MCF-7/R cells has been demonstrated to be localised in the plasma membrane, perinuclear region and cytoplasmic vesicles including the golgi body (Coley *et al.*, 1993 and Arancia *et al.*, 1998). Schuurhuis *et al.* (1993) determined nuclear/cytoplasmic drug fluorescent ratios as an index for resistance using human breast cancer MCF-7/S and lung SW 1573 cell lines.

1.4.1.5 Flow cytometry assays

Flow cytometry (FCM) is a process in which measurements are made while cells or particles pass, in single file, through a focused laser beam in a fluid stream. Within a flow cell the cells or particles are measured for light scatter and fluorescent properties as they move through a focussed 488 nm argon laser beam. Once the sample has been measured the sample is lost into the waste collection tank. This presents with the disadvantage that the cells analysed by their light scatter and fluorescent properties can not be

morphologically visualised to confirm the flow cytometry results. The necessity of single cell analysis leads to the loss of structural integrity of the tissue and the relationship of the cell types within the tissue structure. Although FCM offers the ability to quantify cells quickly, accurately and precisely it can not elucidate information about the relationships of cells within a tissue, or show morphological characteristics.

The difference in fluorescence between anthracycline sensitive and resistant cells has been described (Krishan *et al.*, 1987; Durand and Olive, 1982; Frankfurt, 1987; Carpentier *et al.*, 1992 and Arancia *et al.*, 1998) and this difference can be detected and quantified using flow cytometry (FCM). Early use of FCM to determine doxorubicin intracellular fluorescence measured the decrease in PI fluorescence when doxorubicin was intercalated into double stranded DNA. The DNA sites occupied by doxorubicin were unavailable to PI, therefore the fluorescence measured was lower (Krishan and Ganapathi, 1979).

Many of the FCM studies using anthracycline uptake have been looking at the viability effects of cytotoxic drug incubations (Carpentier *et al.*, 1992, Fornari *et al.*, 1994 and Bennis *et al.*, 1997). These studies have generally used cell lines with a guaranteed high viability before cytotoxic treatment, the sensitivity of the cells to the drugs was then determined using colony formation assays (Ross *et al.*, 1989 and Carpentier *et al.*, 1992). The uptake of drug correlated with the clonogenicity of the cells inferring that those cells which were sensitive to the drug were unable to create colonies, unlike cells which did not retain drug which were able to produce colonies. FCM can measure viability using light scatter forward scatter (FSC) and side scatter (SSC) (Krishan, 1994), but it is insensitive and cells from tumours not only have different sizes because of viability but also morphology, and other cell types contaminate the sample.

The wide range of tumour cell sizes also inhibits the separation of normal host cells and tumour cells. Non - tumour cells can be physically separated from tumour cells, for example using density gradients (Resnicoff *et al.*, 1987; Kedar *et al.*, 1982 and Nygren *et al.*, 1994) or magnetic bead separation (Maas *et al.*, 1995). Alternatively cell types can be fluorescently labelled using appropriate antibodies. External markers, which enable the detection of un - permeabilised viable cells are appropriate for this study, the tumour cells can be labelled using epithelial cell markers (Davidson *et al.*, 1989 and Taylor - Papadimitriou *et al.*, 1989) or infiltrating lymphocytes could be labelled (Whiteside *et al.*, 1986). Neither system is flawless, an epithelial marker will label both tumour cells and

normal epithelial cells, but labelling of infiltrating leucocytes may not identify all non-tumour cells.

1.4.1.6 Other anthracycline assays

Other assay systems are available to determine the quantity of anthracycline retained within a population of tumour cells. These techniques include radiolabelling doxorubicin using ^{14}C , detected using liquid scintillation counting (Inaba *et al.*, 1979 and Schuurhuis *et al.*, 1993); spectrofluorimetry, extracting the drug from the cells then quantifying the drug using a fluorimeter (M^c Gown *et al.*, 1983 and Bennis *et al.*, 1997) and HPLC analysis after drug extraction from the cells (Herweijer *et al.*, 1989), this technique has also been used to determine the levels of doxorubicin and its metabolites in patient plasma (de Bruijn *et al.*, 1999). These techniques measure the doxorubicin retention of a population of cells rather than individual cell analysis which can be performed using FCM, LSC and confocal microscopy.

1.5 Laser scanning cytometry (LSC)

Laser scanning cytometry combines the benefits of light microscopy with flow cytometry. A prototype instrument was first described by Kamentsky and Kamentsky (1991). This was followed by a refined model, which came into commercial production in 1996, an advantage of the LSC, over conventional FCM and fluorescence microscopy, is its ability to view cells using light and fluorescence.

The LSC is a precise and accurate new technology which measures light and fluorescent parameters of cells held constrained on a microscope slide. Similar to FCM a standard 488 nm argon laser is used as the excitation energy source. The laser beam is directed to the microscope slide via a chain of mirrors through the optics of a Olympus BX50 fluorescent microscope, a schematic of the components of the LSC are shown in figure 1.3. The laser beam scans the microscope slide by precise step - wise movements of the computer controlled microscope stage, the diameter of the laser beam is dependent on the objective used, for example, a 20x objective creates a laser beam spot of 5 μm . The LSC makes measurements on each cell at 0.5 μm spatial intervals (Kamentsky *et al.*, 1997), therefore there is considerable multiple scanning over any given area of the slide creating a two-dimensional array of values, rather than the pulse spot analysis of flow

Introduction

cytometry (Reeve and Rew, 1997). Scattered laser light from each cell is collected by a solid state sensor located underneath the motorized stage (Clatch *et al.*, 1996). The fluorescence produced by fluorochromes within the analysed specimen are detected using photomultiplier tubes (PMT) which receive the signals via the microscope and chain of mirrors (Gorczyca *et al.*, 1998). Cell detection is performed using light scatter or fluorescence as the triggering signal, both parameters can be quantified independent of which is used as the event detection signal.

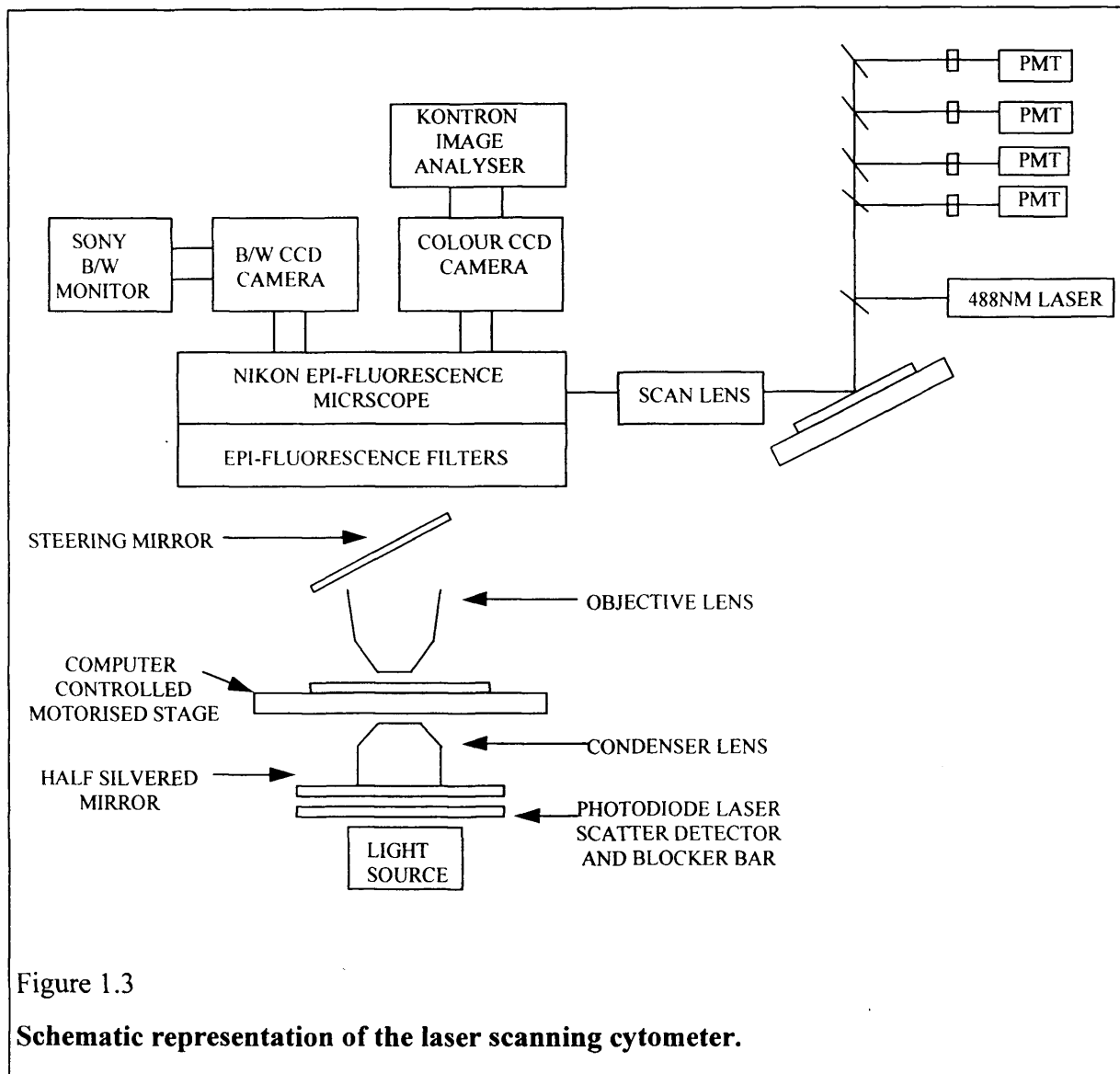


Figure 1.3

Schematic representation of the laser scanning cytometer.

The data generated by the LSC is comparable to that produced by FCM, but with many additional data sets. The fluorescence data calculated can be presented as either peak maximum fluorescence or integral fluorescence, peak maximum fluorescence for each cell is the highest fluorescent pixel reading within the data contour of the cell and

integral fluorescence is the sum of all the pixels in each cell. The benefits and appropriate use of either of these fluorescent values is dependent on the experiment, an example of the use of peak maximum and integral fluorescence is the analysis of DNA using a stoichiometric dye such as PI. PI fluorescence detected by the LSC, can be used to categorise cells of a population into the phases of the cell cycle. The red integral fluorescence of each cell infers DNA content, and peak maximum fluorescence the density of chromatin condensation (Luther and Kamentsky, 1996; Gorczyca *et al.*, 1996 and Kawasaki *et al.*, 1997), these parameters can be manipulated with 'nuclear area' to isolate nuclei within each cell cycle phase.

The LSC has been used for a variety of research applications but the majority of work has centred on DNA / cell cycle analysis (Gorczyca *et al.*, 1996; Kawasaki *et al.*, 1997; Luther and Kamentsky, 1996; Sasaki *et al.*, 1996; Clatch *et al.*, 1997; Gorczyca *et al.*, 1997; Kamada *et al.*, 1997 and Rew *et al.*, 1998). This work has established that the LSC can produce similar results to the flow cytometer (Bedner *et al.*, 1997; Kamentsky *et al.*, 1997; Musco *et al.*, 1998; Bedner *et al.*, 1998; Deptala *et al.*, 1998; Satoh *et al.*, 1999; Tomita *et al.*, 1999 and Bedner *et al.*, 1999). However, the LSC is more than an alternative to FCM, it offers the possibility of confirming many cellular parameters (e.g. cell type), by visualising the cells. Cells are retained on a microscope slide therefore they are not lost after fluorescence analysis. The X - Y co-ordinate of each cell is stored as an integral part of the data set, allowing the computer to position the stage accurately to visualise or re-scan any cell. A single cell or group of cells can be visualised using real-time CCD colour images or black and white images of the fluorescent signals. The ability to relocate can give confidence to the sensitivity of an assay, this is illustrated well by Woltmann *et al.* (1999). The analysis of induced sputum for eosinophils and bronchial epithelial cells is an assay developed as a potential marker for asthmatic airway inflammation (Woltmann *et al.*, 1999). The percentage of eosinophils within a induced sputum sample was from 0.1 to 22.6% (Woltmann *et al.*, 1999), sensitivity of 0.1% demonstrates that an assay can correctly label one cell in 1000 as positive, relocation confirmed these events are 'real' and not artefact.

Human breast tumours have been analysed by LSC using paraffin wax sections, the archival wax blocks were de - waxed then analysed for oestrogen receptor status, as a comparison to immunoperoxidase staining. The techniques compared well and the LSC

offered an automated analysis of slides, which would normally need to be counted manually using the immunohistochemical method (Gorczyca *et al.*, 1998).

1.6 **Viability determination**

Cells extracted from solid tumours are of variable viability and as anthracycline drugs are able to enter viable and non-viable cells, it is important to discriminate the viable cells from the non-viable cells and debris. There are many methods applicable to the use of microscopy and cytometry.

The determination of cellular viability can be assessed in several ways, and assays are generally categorised into two groups. The first group is based on the ability of unfixed viable cells to exclude dyes, positive staining with these dyes indicates a non-viable cell. The second group is based on a metabolic activity that only a viable cell can perform, producing or removing an agent from the cell that can be measured. Different viability assays measure different aspects of cell death and generate complementary information.

1.6.1 **The MTT assay**

The MTT cell viability assay was developed by Mosmann (1983) and determines the total viable cell population using the intracellular reduction of a soluble yellow tetrazolium dye, 3 - [4,5 - dimethyl (thiazol - 2 -yl) - 3, 5 - phenyl] tetrazolium bromide (MTT), to MTT formazan an insoluble purple product (Petty *et al.*, 1995). MTT is taken up into the cells and reduced by succinate dehydrogenase in the mitochondria (Denizot *et al.*, 1986) which is detected spectrophotometrically, cells which contain non-functioning mitochondria produce little colour and would be detected as non-viable.

The MTT assay is a means of determining the growth of cell lines, and of measuring the cytotoxicity of doxorubicin. The MTT is a classical cytotoxicity assay which has been used to determine the drug sensitivity of cells (Allen *et al.*, 1988), it is cheap, easy, and has been used by many groups studying various aspects of drug cytotoxicity (Fornari *et al.*, 1996).

1.6.2 **Trypan blue exclusion**

Trypan blue is a non - fluorescent, colloidal agent that is excluded from unfixed viable cells and detected using light microscopy and manual counting. Trypan blue

viability measurements correlate well with colony formation type assays, although rough handling of cells can lead to a falsely high percentage of non-viable cells (Tennant, 1964).

Individual cell analysis and the determination of cell type can not be performed using the MTT assay, a viability assay which was compatible laser cytometry was needed.

1.6.3 Propidium iodide (PI)

PI is a classic non-viable cell marker, two polar groups in the molecule prohibit its penetration into unfixed viable cells (Altman *et al.*, 1993 and Jones and Senft, 1985). PI intercalates with double stranded DNA (Dengler *et al.*, 1995) and the bright red fluorescent signal (617 nm emission) generated by PI is proportional to the DNA content of the cell. PI is widely used as a nuclear marker for LSC analysis (Kamentsky and Kamentsky, 1991; Gorczyca *et al.*, 1996 and Kawasaki *et al.*, 1997), and as a viability stain and for cell cycle analysis for FCM analysis (Krishan, 1975; Jones and Senft, 1985 and O'Brien and Bolton, 1995).

1.6.4 Fluorescein diacetate (FDA)

FDA is a commonly used viable cell marker (Jones and Senft, 1985), it is not fluorescent and enters all cells, within viable cells it is hydrolysed to produce fluorescein (Rotman and Papermaster, 1965) which emits a bright green fluorescence (515 nm emission).

1.6.5 Calcein acetoxymethyl ester (calcein AM).

Calcein AM is a non-fluorescent hydrophobic molecule which penetrates all cells. Non - specific cytoplasmic esterases within live cells cleave the ester bonds of the compound to produce calcein. Calcein demonstrates green fluorescence (530 nm emission), is hydrophobic and unable to efflux cells (De Clerck *et al.*, 1994; Homolya *et al.*, 1996 and Tiberghin & Loor, 1996). Calcein AM can be used as a viability marker (Wang *et al.*, 1993 and Papadopoulos *et al.*, 1994) or as a multidrug resistance marker (Hollo *et al.*, 1994 and Homolya *et al.*, 1993) because it is a substrate for P - gp.

1.6.6 Sytox

Sytox is a green fluorescent nucleic acid stain which labels non-viable cells, it is unable to penetrate the plasma membrane of viable cells (Haughland, 1996), its emission wavelength is 523 nm.

The fluorescent emission spectra of each of the described viability probes are suitable for the simultaneous detection with the red fluorescent doxorubicin, apart from PI. PI would have been a suitable viability probe for this study, unfortunately the emission wavelength of this dye is close to the emission peak of doxorubicin, and would be detected in the same fluorescent channel using laser cytometry.

The viability probes described here, are able to detect those cells which have died via necrosis, they are inconsistent with the detection of cells which die via 'programmed cell death' or apoptosis.

1.7 Apoptosis

Apoptosis is a process of 'programmed cell death' where a cell embarks upon a series of transitions leading to nuclear and cellular fragmentation (Poot *et al.*, 1997). During apoptosis the nuclear chromatin condenses, cell volume contracts, preserving the cell membrane integrity (Tounekti *et al.* and Ormerod *et al.*, 1993). The dying cell fragments into apoptotic bodies (Steller, 1993), which *in vivo* are rapidly phagocytosed (Ormerod *et al.*, 1993, Steller, 1995 and Tounekti *et al.*, 1995). Biochemically, the DNA fragments into large (50 - 300 kilobases) and subsequently small oligonucleosomal fragments (Steller, 1995 and Ormerod *et al.*, 1993). During the early stages of apoptosis the phosphatidylserine (PS) which resides in the inner leaflet of the plasma membrane of normal cells becomes exposed to the outer surface of the cell (Zhang *et al.*, 1997).

Cultured cells exposed to anti - cancer drug treatments have been shown to die via apoptosis (Hickman, 1992), but the mechanism is unknown (Huschtscha *et al.*, 1996). Apoptosis is also prevalent within tumours (Dive *et al.*, 1992). There are many genetic factors that influence the ability of a cell to proceed through apoptosis at any time, for example the overexpression of *bcl - 2* protects a cell against apoptosis (Kerr *et al.*, 1993), whereas products of *p53* tumour suppressor gene and *c - myc*, can lead to activation of apoptosis (White, 1993).

There are distinct features of apoptosis and necrosis that make them distinguishable from each other. Necrosis is characterised by cell swelling followed by rupture of the plasma membrane, the rupture leading to local inflammation (Ormerod *et al.*, 1993 and Dive *et al.*, 1992). Contrastingly an apoptotic cell shrinks, and does not cause an inflammation reaction.

An apoptotic cell has a short half life *in vivo* making its detection difficult, hampered by sample heterogeneity (Dive *et al.*, 1992). Microscopy offers an effective way to distinguish between necrotic and apoptotic cells, unfortunately this is not quantitative (Ormerod *et al.*, 1993).

Fragmented DNA sections are characteristic of apoptosis and can be detected using gel electrophoresis (Dive *et al.*, 1992 and Tounekti *et al.*, 1995). The cleaved ends of the DNA fragments can also be fluorescently labelled using TUNEL or ISEL techniques (Li and Darzynkiewicz, 1995 and Stokke *et al.*, 1998).

PS which becomes exposed to the outside of cells during apoptosis is a target for a specific label for apoptosis, the protein annexin V will bind to PS in a calcium dependent manner (Trotter *et al.*, 1997 and Martin *et al.*, 1997). The redistribution of PS to the external surface of cells is an early indicator of apoptosis, earlier than DNA associated changes and membrane leakage (Zhang *et al.*, 1997), which can be used with unpermeabilised cells. Annexin V can be labelled with FITC which enables detection and quantification using laser cytometry.

1.8 **Aim of the studies**

This study has set out to develop an assay which can be performed using human disrupted breast cancer cells to determine the anthracycline resistance status of the patient to enable an informed decision to be made about the subsequent therapy of the patient. Flow cytometry based work using anthracycline uptake has been carried out over the last two decades (Krishan and Ganapathi, 1979 and Krishan *et al.*, 1987 and Bennis *et al.*, 1997) but a patient assay has yet to be implemented. The LSC is the next generation of technology that combines fluorescent measurements of doxorubicin uptake and viability with visual characterisation. The aim of the present study was to compare FCM and LSC techniques for measuring anthracycline drug uptake, firstly using a tumour cell line model (MCF-7) and then using cells isolated from human tumours (breast carcinoma). As part of this, different anthracycline drugs were first characterised for their suitability for

cytometric detection, their cell/DNA binding characteristics were determined and the uptake of drug into sensitive and resistant cell lines were coupled with the effects of the drug on cell viability and growth. Comparisons to FCM were made of the use of the LSC for measuring cell proliferation in isolated tumour cell nuclei and in addition a novel delivery system (albumin capsule; CytocapsTM) was investigated. The cell proliferation investigation has contributed novel evaluation data that broadens the spectrum of techniques within the LSC repertoire, and offers further information leading to a more informed decision about the chemotherapy regime appropriate for each patient.

MATERIALS AND METHODS

2. ***Materials and methods***

2.1 **Selection and handling of cytotoxic drugs**

Doxorubicin was supplied in lyophilised form in vials containing 50 mg doxorubicin hydrochloride with lactose designed to be reconstituted for patient injection (Farmitalia Carlo Erba Ltd, Milan, Italy). Each vial was reconstituted under sterile conditions, with 25 ml distilled water to create a stock of 2 mg.ml^{-1} (3.45 mmol.L^{-1}). The stock of doxorubicin was stored in polypropylene screw top vials and frozen at $-20 \text{ }^{\circ}\text{C}$, an aliquot was thawed monthly and was kept refrigerated in the dark. All cytotoxic drugs were dispensed at low concentrations within a class II laminar flow hood using standard laboratory safety procedures. The majority of experiments using doxorubicin were carried out with doxorubicin solution reconstituted in distilled water, apart from the absorbance and fluorescence spectroscopy, which used doxorubicin prepared in Tris buffer (8 mmol.L^{-1} Tris in water; pH 7.4).

Mitoxantrone was provided in Tris buffer solution, by Prof. L. H. Patterson (De Montfort University), stored in a polypropylene tube, in the dark at $4 \text{ }^{\circ}\text{C}$.

Ethidium bromide (2, 7 - Diamino - ethyl - 9 - phenyl - phenanthridium bromide) (Sigma - Aldrich company Ltd, Poole, England) was reconstituted in Tris buffer solution and stored in a polypropylene tube, in the dark at $4 \text{ }^{\circ}\text{C}$.

2.1.1 **Study of the physical characteristics of fluorescent anthracycline compounds**

2.1.1.1 Absorbance measurements

Solutions of doxorubicin ($50 \text{ } \mu\text{mol.L}^{-1}$), mitoxantrone ($10 \text{ } \mu\text{mol.L}^{-1}$) and ethidium bromide ($40 \text{ } \mu\text{mol.L}^{-1}$) were transferred to quartz cuvettes for UV/Visible spectrophotometric analysis in a Perkin Elmer 552S spectrophotometer to determine the λ max. for each compound, all absorbance measurements were plotted using linear scales.

Titration of doxorubicin ($0 - 100 \text{ } \mu\text{mol.L}^{-1}$), mitoxantrone ($0 - 10 \text{ } \mu\text{mol.L}^{-1}$) and ethidium bromide ($0 - 100 \text{ } \mu\text{mol.L}^{-1}$) were analysed at the λ max. for each compound. Each solution was also analysed at 488 nm that is the wavelength of the argon laser used within flow and laser scanning cytometers. For each drug titration a straight line was plotted absorbance vs drug concentration $\mu\text{mol.L}^{-1}$, the graph was plotted using linear scales. The extinction coefficient for each compound was calculated using the equation for a straight line ($y = mx + c$), deriving the extinction coefficient from the gradient (m) of the line.

2.1.1.2 Fluorescence spectroscopy

Solutions of doxorubicin ($50 \mu\text{mol.L}^{-1}$) and ethidium bromide ($40 \mu\text{mol.L}^{-1}$) were placed in quartz cuvettes for fluorescence analysis using a Perkin Elmer 3000 fluorescence spectrometer. Each compound was excited at 488 nm, and the emission spectrum measured over the range of wavelengths 200 - 900 nm.

Titration of doxorubicin (0 - $10 \mu\text{mol.L}^{-1}$) and ethidium bromide (0 - $100 \mu\text{mol.L}^{-1}$) were measured at an excitation of 488 nm, the emission for each compound was read at the optimum wavelength, determined from the fluorescent spectra scans.

2.1.2 Study of the DNA binding characteristics of drugs

Glassware was silane coated using 2% v/v 3 - aminopropyltriethoxysilane (Sigma - Aldrich company Ltd, Poole, England) solution in standard grade acetone (Sigma - Aldrich company Ltd, Poole, England), each piece of glassware was filled with this solution for 5 - 10 secs. Then rinsed in acetone (2 - 5 secs. contact time) and distilled water (Milli Q) before being dried overnight.

Mammalian DNA (Sigma - Aldrich company Ltd, Poole, England) was reconstituted in Tris buffer, then incubated for 24 hours at room temperature, to allow the DNA to dissolve. The absorbance of DNA was measured at 260 nm and the concentration calculated using the extinction coefficient (6400).

2.1.2.1 Isosbestic point determination

The isosbestic point for each drug was determined by mixing DNA with doxorubicin, mitoxantrone or ethidium bromide in molar ratios of 0/25, 1/1, 2/1, 5/1, 10/1 and 15/1 (DNA : drug) and measuring the absorbance in a spectrophotometer over the visible region of the spectrum (320 - 700 nm). The absorbance scan for each solution was overlaid and the isosbestic point determined as the wavelength where the absorbance is equal regardless of DNA:drug ratio, all absorbance measurements were plotted on a linear scale.

2.1.2.2 Calculation of DNA binding coefficients of cytotoxic drugs (Scatchard plot analysis)

Solutions of DNA (2.3 mmol.L^{-1}) and doxorubicin, mitoxantrone and ethidium bromide (0.05 mmol.L^{-1}) were mixed in Tris buffer, using various ratios, and their

absorbance measured at 470, 480 or 660 nm, respectively, using a Unicam UV2 - 100 UV/Visible spectrometer. Using the absorbance measurements a Scatchard plot was produced to quantify the DNA binding of each drug. The Scatchard plot equation is :-
$$r/c = -Kr + Kn$$

Where r is the number of sites occupied by drug per DNA phosphate group; c is the concentration of drug; K is the affinity constant and n is the number of binding sites available for drug per DNA phosphate group. The affinity constant (K) and the number of available drug binding sites per DNA phosphate group (n) are determined by plotting r versus r/c, where K is the gradient of the line and n is the x intercept.

2.2 Cell studies

2.2.1 Culture of cell lines

The present study used human breast adenocarcinoma cell lines; MDA MB 231 obtained from Rachel Carter (Department of Surgery, University of Leicester) and MCF-7 cells from European Collection of Animal Cell Culture (ECACC), Porton Down, England. Alongside the parental MCF-7 cell line (MCF-7/S) a doxorubicin resistant subline (MCF-7/R) was maintained, obtained from Dr Tim Gant (Medical Research Council Toxicology unit, University of Leicester). The cells were routinely cultured in RPMI 1640 medium without phenol red, buffered with 0.04 mol.L⁻¹ HEPES and supplemented with 2 mmol.L⁻¹ L - glutamine (RPMI) containing 10% v/v fetal calf serum (FCS) (RPMI - FCS). Medium and supplements were obtained from Life Technologies Ltd (Paisley, Scotland) and FCS was from PAA Laboratories Ltd (Kingston-upon-Thames, England). Cells were grown at 37 °C in 5% CO₂ in air and 99% humidity (CO₂ incubator, Heraeus instruments, Brentwood, England) they were passaged twice weekly and used for experiments in log phase growth (75 - 80% confluence). Unless otherwise stated, all reagents were from Life Technologies Ltd (Paisley, Scotland).

2.2.1.1 Passaging cell lines

Confluent cells were passaged by treatment with trypsin/EDTA (0.1% trypsin/0.02% (w/v) EDTA). To passage, the growth medium was removed and the cells washed with minimal essential medium (MEM), an appropriate volume of trypsin/EDTA was added to each flask (4 ml to T₂₅ or 6 ml to T₈₀ flasks) and incubated for 10 min at 37 °C. The cells were transferred to a universal container, 7 ml RPMI - FCS was added to

neutralise the action of the trypsin/EDTA, centrifuged for 7 min at 454 g and resuspended in 1 ml RPMI - FCS then reseeded into RPMI - FCS at a dilution of 1:5. All cell line manipulations were carried out in class II laminar flow cabinets (Gelaire BSB 3). Media and trypsin/EDTA were warmed to 37 °C before use.

MCF-7/R cells were routinely maintained in medium containing 0.5 $\mu\text{mol.L}^{-1}$ doxorubicin, before each experiment MCF-7/R cells were grown in doxorubicin - free medium for four days.

2.2.1.2 Freezing, thawing and storage of cell lines

Cell stocks were maintained under liquid nitrogen at a concentration of 1 - 2 x 10⁶ cells.ml⁻¹ in medium containing 10% DMSO, 40% FCS and 50% RPMI. The cells were frozen slowly; 1 hour at 4 °C, followed by 1 hour at -20 °C, and then overnight at -80 °C, before transferring to liquid nitrogen. Each vial to be thawed was removed from liquid nitrogen and warmed to 37 °C in a water bath. The cell suspension was transferred to a universal of warm MEM, mixed and centrifuged at 454 g for 7 min then resuspended in 1 ml RPMI – FCS. T₂₅ flasks were seeded with cells and 8 ml RPMI - FCS. MCF-7/S and MDA MB 231 cells recovered well from freezing and confluence was achieved at around two days but MCF-7/R took at least 2 weeks to recover to their normal growth cycle and cells were not used for experiments until they were exhibiting a normal growth routine.

2.2.1.3 Trypan blue exclusion assay

A 10 μl aliquot of cells, was mixed in a small eppendorf tube with 10 μl trypan blue solution (0.2% trypan blue (PBS):0.9% saline in a 10:1 ratio) and counted in a dual chamber, improved Neubauer haemocytometer. The calculation used for the total number of cells is:-

Total cells per ml of cell suspension = cell count x 'dilution factor' x 10⁴.

Non-viable cells were identified by their incorporation of the blue dye.

2.2.1.4 Production of non-viable cells

Non-viable MDA MB 231, MCF-7/S and MCF-7/R cells were prepared by one of the following treatments: repeated freezing to -20 °C and thawing; refrigerating cells in PBS (8 g.L⁻¹ NaCl, 1.585 g.L⁻¹ K₂HPO₄.3H₂O and 0.34 g.L⁻¹ KH₂PO₄ dissolved in double distilled water, pH 7.4) for 4 - 5 weeks, or overnight incubation with hydrogen peroxide

(H₂O₂) at a concentration of 0.06% or 0.09% for MCF-7/S and MCF-7/R cells respectively, hydrogen peroxide incubations were carried out in serum free medium. A cell suspension was used as non - viable when viability was <20%, determined using trypan blue exclusion assay. For preliminary studies either of the first two techniques was used, but for the majority of studies non-viable cells were prepared using H₂O₂ treatment.

2.2.2 Cytotoxic free drug uptake studies

Suspensions of viable and non - viable MCF-7/S and MCF-7/R were incubated with a range of doxorubicin or mitoxantrone concentrations from 0.173 to 100 $\mu\text{mol.L}^{-1}$ in RPMI using a cell concentration of 5×10^6 cell/ml, for 1 hour at 37 °C. The cells were then centrifuged at 454g for 7 min and washed twice in PBS, the cells were either plated out for time course experiments or analysed using flow or laser scanning cytometry. For immediate analysis the cells were resuspended in 500 μl PBS and analysed within a period of 10 min to 4 hours after completion of the incubation, during which the cells were kept refrigerated at 4 °C. The cells destined for time course experiments were seeded into T₂₅ flasks (2.5×10^5 cells/ml) with 8 ml RPMI - FCS and incubated at 37 °C in 5% CO₂ in air, for 4, 24, 48, 72, 96, 120 or 144 hours. After incubation the cells were trypsinised and manually counted using the trypan blue exclusion assay and analysed for drug uptake, viability (sytox) and apoptosis status (annexin V) using laser cytometry. Analysis was performed after 10 min and by 4 hours of the completion of the assay, during which time the cells were refrigerated at 4 °C.

2.2.3 Cytotoxic Cytocaps™ uptake studies

Suspensions of MCF-7/S cells were incubated with a range of Cytocap™ (obtained as a gift from Quadrant Healthcare (UK) Ltd, Nottingham, England) concentrations 0.5 - 4 $\mu\text{mol.L}^{-1}$ using a cell concentration of 1×10^6 cell/ml in RPMI at 37 °C for 1 hour, which were mixed every 10 min. The Cytocap™ stock was a concentration of 100 mg.ml^{-1} human serum albumin (HSA) 0.68 mol.L^{-1} doxorubicin, which was kept until the best before date at 4 °C in the dark then disposed of as per the manufacturers instructions. After incubation 2×10^6 cells were seeded into each T₂₅ flask with 3 ml complete RPMI + FCS and grown in flasks for 4, 24, 48, 96, 120 and 144 hours, at 37 °C in 5% CO₂ in air. After incubation the cells were trypsinised and washed twice in PBS (7 min at 454g) then resuspended in 1 ml and analysed for viability (sytox), Cytocap™ uptake and apoptosis

status (annexin V). All quantitative analysis was carried out by flow cytometry and LSC was used to obtain images of the CytocapsTM within the cells. The LSC analysis was performed using chamber slides and light scatter detection. This work was carried out jointly with Ms Davinder Kaur, Department of Chemical Pathology, University of Leicester. Ms Kaur performed all flow cytometry using CytocapsTM.

2.2.4 The MTT assay

MTT (3 - [4, 5 - dimethylthiazol - 2 - yl] - 2, 5 - diphenyltetrazolium bromide) was obtained from Sigma - Aldrich company Ltd (Poole, England) and prepared weekly in Hank's balanced salt solution (Life Technologies Ltd, Paisley, Scotland) and stored at 4 °C. MTT solutions were used within a class II laminar flow cabinet and any spillages were neutralised using 2000 ppm chlorine solution (prepared weekly).

2.2.4.1 MTT formazan titration

Using a stock solution of MTT formazan (1 - [4, 5 - Dimethylthiazol - 2 - yl] - 3, 5 - diphenylformazan) (Sigma - Aldrich company Ltd, Poole, England) 1.19 mg.ml⁻¹ in DMSO, a range of concentrations were prepared from 60 to 240 µmol.L⁻¹. Aliquots (100 µl) of each dilution were placed in eight wells of a 96-well plate and the absorbance read at 540 nm on a microtitre plate reader (Titertek MCC).

2.2.4.2 Standard MTT assay

Using a 96 well plate 10 µl of MTT (5 mg.ml⁻¹ in Hanks salt solution) was added, then incubated at 37 °C with 5% CO₂ in air for 4 hours. After 4 hours the plate was centrifuged (Heraeus megafuge 1.0R, 417 g for 7 min) and the medium and MTT removed with care, using a pipette, to ensure that the MTT formazan crystals were not disturbed at the base of each well. DMSO (100 µl per well) was added to dissolve the MTT formazan crystals. The plates were agitated on a plate shaker (IKA/Schuttler MTS4) for 30 min to allow the formazan to dissolve, absorbance measurements were then made at 540 nm using a spectrophotometric plate reader (Titertek MCC).

2.2.5 Standard curves

MDA MB 231 and MCF-7/S cells were trypsinised, counted and prepared at a range of cell concentrations from 0.1 to 25 x 10⁴ cells/ml in RPMI - FCS. Aliquots (100

μl) of each cell suspension were pipetted in eight wells of a 96-well plate (Life Technologies Ltd, Paisley, Scotland), leaving one row of wells containing medium only as a blank. If the sample numbers allowed the outside wells of the 96 well plate were left empty or filled with medium only as these wells were prone to greater evaporation than the wells from the main body of the plate. The MTT assay was then carried out, as described previously.

2.2.5.1 Growth curves of MCF-7/S and MDA MB 231 cell lines

MDA MB 231 and MCF-7/S cells were trypsinised, counted and prepared at cell concentrations of 0.1 to 2.5×10^4 cells/ml in RPMI - FCS, aliquots ($100 \mu\text{l}$) of each cell solution were pipetted into eight wells of 96-well plates and were incubated at 37°C , 5% CO_2 in air, for 4, 24, 72 or 172 hours. Each morning $50 \mu\text{l}$ medium were removed and replaced with $50 \mu\text{l}$ fresh medium to feed the cells, at the end of each incubation time the plates were analysed using the MTT assay as described previously.

2.2.5.2 Cytotoxic studies using MCF-7/S and MDA MB 231 cells

MDA MB 231 and MCF-7/S cells were trypsinised, counted and prepared at 2.5×10^5 cells. ml^{-1} in RPMI - FCS medium, aliquots ($100\mu\text{l}$) of each cell line were pipetted into wells of 96 well plates. The plate was incubated for 24 hours at 37°C after which, $50 \mu\text{l}$ medium was removed and replaced with $50 \mu\text{l}$ of medium containing doxorubicin or mitoxantrone at a range of concentrations $0.1 - 5 \mu\text{mol.L}^{-1}$. The plates were incubated for a further 24 hours, centrifuged for 7 min at 417 g (Heraeus), resuspended in $100 \mu\text{l}$ of fresh RPMI - FCS medium, then analysed using the MTT assay.

2.3 Cytometric studies

2.3.1 Viability markers

2.3.1.1 Propidium iodide (PI)

PI (Sigma - Aldrich company Ltd, Poole, England) was dissolved in distilled water under sterile conditions to create a stock of 1 mg.ml^{-1} which was stored in 1 ml aliquots at -20°C . One vial of stock was routinely kept refrigerated at 4°C in the dark and replaced monthly.

Aliquots ($500 \mu\text{l}$) of MDA MB 231 (2.5×10^5 cell. ml^{-1} in PBS) were incubated for 10 min at room temperature with a range of PI concentrations ($0.25 - 500 \mu\text{g.ml}^{-1}$). After

incubation the cells were centrifuged for 7 min at 454 g and resuspended in 1 ml PBS. Analysis was carried out on the flow cytometer between 10 min and 4 hours of the completion of the assay, during this time the cells were refrigerated at 4 °C.

2.3.1.2 Fluorescein diacetate (FDA)

Fluorescein diacetate (FDA obtained from Sigma - Aldrich company Ltd, Poole, England) was dissolved at 10 mg.ml⁻¹ in acetone and stored at -20 °C. A working stock of 0.1 mg.ml⁻¹ in PBS was freshly prepared for each experiment.

MDA MB 231 cells (2.5 x 10⁵ cells.ml⁻¹ in PBS) were incubated in 500 µl for 10 min at room temperature with FDA at concentrations ranging between 0.78 - 12.5 ng.ml⁻¹, centrifuged for 7 min at 454 g and resuspended in 1 ml PBS. Analysis was carried out on the flow cytometer between 10 min and 4 hours of the completion of the assay, during this time the cells were refrigerated at 4 °C.

2.3.1.2 Preliminary calcein AM experiments

MCF-7/S (viable and non - viable) and MCF-7/R (viable and non - viable) cells were titrated using a range of calcein AM (Molecular Probes, Oregon, USA) concentrations from 0.05 to 1.05 µmol.L⁻¹. Calcein AM was stored at -20 °C at 1 mmol.L⁻¹ concentration, and a fresh working stock of 10 µmol.L⁻¹ in PBS was prepared for each experiment. Aliquots of 100 µl cells (5 x 10⁶ cells.ml⁻¹) were incubated with calcein AM in PBS for 10 min at 37 °C washed twice in PBS, then resuspended in 500 µl PBS. The cells were analysed using flow cytometry or LSC, cells were refrigerated for between 10 min and 4 hours before analysis.

2.3.1.4 Standard calcein AM assay

Calcein AM (1 mmol.L⁻¹) was diluted 1 : 4000 in PBS, for use in the assay at 1.05 µmol.L⁻¹. Aliquots (100 µl) of cells (5 x 10⁶ cell.ml⁻¹) were incubated with calcein AM for 10 min at 37 °C, washed twice (7 min, 454 g), then resuspended in 500 µl of PBS. The cells were measured in the flow cytometer or LSC between 10 min and 4 hours of the completion of the assay, during which time the cells were kept refrigerated at 4 °C.

2.3.1.5 Preliminary sytox experiments

Sytox (Molecular Probes, Oregon, USA) was dissolved at 5 mmol.L⁻¹ in anhydrous DMSO and kept at -20 °C. Aliquots (100 µl) of non - viable MCF-7/S and MCF-7/R cells (5 x 10⁶ cells.ml⁻¹), were incubated with a range of sytox concentrations from 0.0625 to 1.25 nmol.L⁻¹ in PBS for 15 min at 37 °C washed twice (7 min, 454 g) and resuspended in 500 µl PBS. Once the assay was complete the cells were analysed using flow cytometry between 10 min and 4 hours of preparation, during which time the cells were kept refrigerated at 4 °C.

2.3.1.6 Standard sytox assay

Sytox was stored at -20°C at 5 mmol.L⁻¹ a working stock of 5 nmol.L⁻¹ was freshly prepared each day. An aliquot of 100 µl of cells (5 x 10⁶ cells.ml⁻¹) were incubated for 15 min at 37 °C with 0.6 nmol.L⁻¹ sytox in PBS, washed twice, centrifuged at 454 g for 7 min, then resuspended in 500 µl PBS. The cells were kept refrigerated until FCM or LSC analysis between 10 min and 4 hours of the completion of the assay.

2.3.2 Measurement of apoptosis

2.3.2.1 Annexin V - FITC binding

Detection of apoptosis using the annexin V - FITC binding kit from Boehringer Ingelheim Bioproducts Partnership, Heidelberg, Germany was used as described by the manufacturer, with the exception of the volume of annexin V - FITC reagent which was optimised after preliminary experiments from 5 µl to 1 µl. The cells were washed in PBS, before being resuspended in annexin V binding buffer (1:4 in distilled water (Milli Q)) at 5 x 10⁵ cells/ml. Aliquots of cells (195 µl) were incubated for 10 min at room temperature with 1 µl annexin V - FITC reagent then analysed by flow cytometry between 10 min and 4 hours of the completion of the assay, during which time the samples were refrigerated at 4 °C.

2.3.3 Flow cytometry - FACScan

2.3.3.1 Instrumentation and settings

Flow cytometry analysis was performed on a Becton - Dickinson FACScan (Becton - Dickinson, Oxford, UK). This instrument uses a fixed excitation wavelength of

Materials and Methods

an argon laser at 488 nm, which is air cooled. The alignment and precision of the light scatter and fluorescence were checked weekly using CaliBRITE beads (Becton - Dickinson, Oxford, UK). The FACScan is equipped with two light scatter detectors - forward (FSC) and side scatter (SSC) which enable a measure of particle size and granularity, respectively, and has the capacity to measure three fluorescent signals simultaneously. The three fluorescent detectors broadly measure green (FL1) (bandpass filter 480 +/- 10 nm), orange (FL2) (bandpass filter 530 +/- 30 nm) and red (FL3) (bandpass 580 +/- 30 nm) fluorescence. The individual photomultiplier voltages for each detector are user defined, which are illustrated in table 2.1. Generally 10 000 events were collected as a dotplot using 'FSC vs SSC'. The cell lines used were usually fairly uniform in size and granularity enabling a region to be drawn which includes the majority of single cells excluding cell debris and obvious cell clumps. This procedure was performed for all FCM data analysis, using only single cells for fluorescence analysis. All FCM analysis was performed using a FCS threshold value of 72 and setting of E -01 and a SSC setting of 352, apart from DNA analysis which used a SSC setting of 400.

Experiment	FL1	FL3
PI	/	385
FDA	385	/
Sytox	380	/
Calcein AM	258	/
Doxorubicin	/	507
Annexin V	380	/
Mitoxantrone	/	507
Cytocaps™	/	380
DNA analysis	400	410

Table 2.1

FCM settings for experiments within this study.

2.3.3.2 Analysis of data

Control cells which were not incubated with a fluorescent probe or drug were used to set the negative peak or threshold values for positive fluorescence. A marker was set

for each experiment to include up to 5% of the negative population, most data was presented as mean fluorescence and/or percentage of cells positive.

2.3.3.3 DNA analysis of human dissociated nuclei

Samples were analysed by laboratory staff on a FACScan (Beckon Dickinson, Oxford, England) equipped with the doublet discrimination module at the Gray Laboratory Cancer Research Trust, Mount Vernon Hospital, Northwood, Middlesex, England, this work was undertaken as a collaboration with Dr George D. Wilson. Up to 10 000 events were collected for each sample with PI being collected into FL3 (>650 nm) and FITC into FL1 (515-545 nm), data was analysed using LYSYS II software.

2.3.4 Laser scanning cytometry (LSC)

The LSC (Compucyte, Mass., USA) uses an air cooled excitation 488 nm argon laser similar to the flow cytometer. Unlike the flow cytometer there was only one light scatter detector but contains three fluorescence photomultiplier tubes (PMT), channel 1 - 530 +/- 15 nm (green); channel 2 - 570 - 630 nm (red/orange) and channel 3 - >650 nm (far red).

Cells analysed using LSC are detected using either light scatter or fluorescence, which ever was appropriate for the individual experiment. The data produced by the LSC has similarities and differences to flow cytometry, the data collected for this study included red and green integral fluorescence, red and green peak fluorescence and laser scatter area. The LSC calculates fluorescence in two ways, integral fluorescence is the summation of all the fluorescent pixels within the data contour and peak maximum fluorescence is the maximum pixel reading from within the data contour.

The data collected for all experiments, except the tumour nuclei work, was not gated, the fluorescence data was produced from all the events detected. The analysis of the data was performed using histograms similar to those produced by flow cytometry, a region was set to include up to 5% of the negative population and data was presented as either mean fluorescence and/or percentage of cells positive.

2.3.4.1 Sample preparation and positioning using the LSC

The LSC analyses cellular (particle, nuclei etc.) samples that are held statically in a microscope slide format. The machine can analyse cells prepared in various ways, for

example, cytocentrifuged preparations of cells, cells grown on slides or cells pipetted into chamber slides, depending on the detection method required and the experimental design.

Once the sample was prepared the slide was fixed on the motorised stage, the exact positioning of the slide was crucial as it allowed relocation, repeated scans and additional staining to be carried out.

2.3.4.2 Cytocentrifuge preparations - cell lines

In preliminary experiments MCF-7/S cells were prepared at 0.5 , 1 and 5×10^6 cells/ml and aliquots of $65 \mu\text{l}$ of each cell suspension were placed in a Shandon Cytospin II (Life Sciences International (UK) Ltd, Basingstoke, England) with the addition of $10 \mu\text{l}$ FCS. The cytocentrifuge was run at 1000 rpm for 5 min , then the cytocentrifuge preparations were allowed to air dry then mounted with 25% glycerol in PBS with a glass coverslip. Having established the optimal cell concentration, cell suspensions of 5×10^5 cells/ml were used in all subsequent experiments.

2.3.4.3 Cytocentrifuge preparations - human tumour nuclei

Each dissociated nuclei sample (in PBS) were cytocentrifuged using $65 \mu\text{l}$ aliquots with $10 \mu\text{l}$ FCS, spun at 1000 rpm for 5 min using a Shandon Cytospin II. The density of the nuclei varied between samples, therefore after the initial cytocentrifuge preparation serial dilutions with PBS (e.g. $1:100$ or $1:1000$) or concentrations were made appropriately, to create a cytocentrifuge preparation which gave an even spread of isolated nuclei.

2.3.4.4 Chamber slides for analysis on the LSC

Chamber slides were constructed from normal glass microscope slides. The two long sides of the slides were lined using a thin strip of multilayered adhesive tape, the two strips were joined at one end with a short piece of tape. A cover slip was positioned carefully on the tape and pressure applied to the edges to seal the coverslip in place as shown in figure 2.1. Samples were prepared in the same manner as for FCM analysis, and an aliquot of approximately $20 \mu\text{l}$ of the cell suspension ($1 \times 10^6 \text{ cells.ml}^{-1}$) was pipetted into the chamber. The slide was sealed with nail varnish to prevent from drying out and the cells were allowed to settle on the slide before LSC analysis. All analysis was

completed within 30 min of slide preparation, during this time the cells remained rounded, enabling light scatter to be used as the detection method.

Cells incubated with doxorubicin or calcein AM were examined using the LSC with both cytocentrifuge preparations and chamber slides. Cytocentrifuge preparations used a fluorescent detection signal, doxorubicin treated cells were detected using a red signal with a contouring threshold of 500 pixels and the red PMT set at 58 mV. Calcein AM treated cells were detected using a green signal with a contouring threshold of 400 pixels and the green PMT set at 40 mV. Cells in chamber slides were detected using light scatter with contouring thresholds of 100 or 200 (doxorubicin and calcein AM, respectively) and the fluorescence detected in the red or green channels with PMTs set at 58 (doxorubicin) or 14 (calcein AM), the offset remained constant at 1900 for all LSC slide analysis.

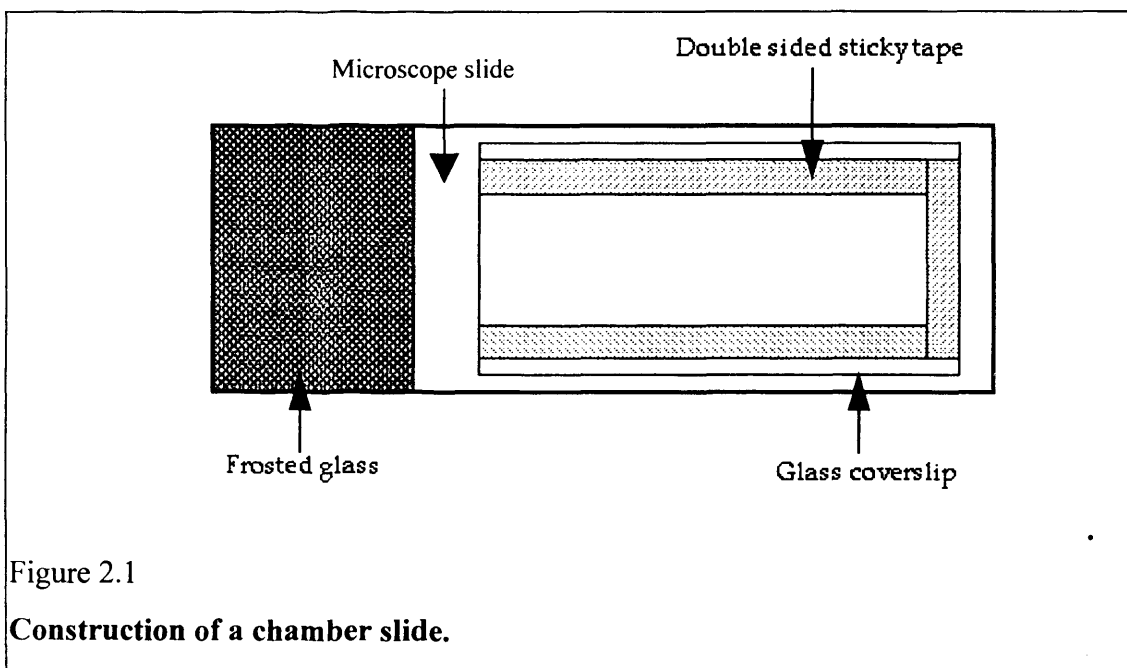


Figure 2.1

Construction of a chamber slide.

2.3.4.5 Relocation and image capturing using the LSC

The fluorescence and light scatter data for each cell detected using the LSC has been saved with the X - Y co - ordinate of the event. To individually analyse a cell or group of cells, they are isolated by creating a region incorporating them e.g. on a dotplot. The LSC can be asked to relocate to these events, but the slide must be positioned exactly as it was when the original data was collected. The re-analysis of the slide can be performed using fluorescence or light scatter detection, each cell which is re-scanned

produces an individual data set and a black and white image of fluorescence or light scatter. A true colour image could also be produced using light microscopy and the colour (CCD) camera. Relocation and image scanning can be performed on a individual cell basis or in 'galleries' of cells, the smallest containing 16 cells. False colour images were produced using sequential black and white scans of red and green fluorescence and light scatter, these images were overlaid and manipulated in Paint Shop Pro 5.0 (JASC).

2.3.5 Cytometric measurement of DNA content in cells

The data from FCM and LSC was analysed similarly. Doublet discrimination was used on the FCM data to generate a 'FL3 Area vs Width' dotplot, a region was created which excluded debris and aggregates from further analysis. On the LSC, a dotplot of 'Red Integral vs Area' were used similarly, using the data from the 'nuclei' region of the dotplots (FCM and LSC), a dotplot of 'FL3 Area vs FL1 Height' (FCM) or 'Red Integral vs Green Integral' (LSC) was generated. A region was then set around the BrdUrd labelled cells for FCM and LSC analysed nuclei.

Analysis was performed on single parameter DNA histograms generated from the total nuclei population and from the BrdUrd labelled population. Specific regions were marked to calculate the various parameters. M1 and M2 were used to calculate the DNA index, M2 and M3 were set around the G1 and G2 populations from which the mean fluorescence values were noted for relative movement and calculation of T_s and M4 delineated the aneuploid population. M1 and M2 were set around the divided G1 cells (to correct the labelling index) and the S and G2 population for relative movement analysis was contained within M3, M4 defined the aneuploid population. The labelling index (LI), duration of S phase (T_s) and potential doubling time (T_{pot}) were calculated as previously described (Wilson, 1991 and Begg *et al.*, 1985). In aneuploid tumours, this analysis was restricted to the population with abnormal DNA.

2.3.6 Manipulations of fresh primary human breast tumours

DMEM (Dulbecco's Modified Eagle Medium) without phenol red or L- glutamine was obtained from Life Technologies Ltd, Paisley, Scotland. Penicillin/Streptomycin solution (1×10^5 units.ml⁻¹) was obtained from Life Technologies Ltd, Paisley, Scotland. Collagenase type I, hyaluronidase, DNase type I and xylene were obtained from Sigma - Aldrich company Ltd, Poole, England. Harris' Haemotoxylin, OG6 (Orange G), Eosin,

DPX mountant and EA50 (eosin - azure) and were obtained from CellPath, Hemel Hempstead, England. DMEM medium was buffered with 0.04 mol.L^{-1} HEPES and supplemented with 2 mmol.L^{-1} L - glutamine and $1 \times 10^5 \text{ IU.L}^{-1}$ penicillin/streptomycin solution and 10% FCS.

2.3.6.1 Disaggregation of tumour

Fresh human breast tissue was routinely received by the histopathology laboratory and processed by a histopathologist. The tumour was located macroscopically, part of the tumour was used for routine diagnostic purposes and the remaining tissue was made available for research. All manipulations were carried out in a class II laminar flow cabinet and disaggregation processes followed all COSHH and biological hazard procedures.

2.3.6.2 Mechanical disaggregation

Tumour tissue was transferred to a class II laminar flow cabinet in cold MEM and processed within an hour of receipt, during this time the tumour was kept at $4 \text{ }^{\circ}\text{C}$. The tumour was bathed in cold MEM in a 3.5 cm diameter sterile petri dish (Life technologies Ltd, Paisley, Scotland) and trimmed of any obvious fat. If the tumour tissue was large enough ($0.25 \text{ cm} \times 0.5 \text{ cm} \times 0.5 \text{ cm}$) it was divided into two halves, one for mechanical disaggregation and one for enzymatic disaggregation and each section of tumour tissue weighed and recorded. If the material was too small for division the sample was randomised to mechanical or enzymatic digestion. Mechanical disaggregation was performed using scapel blades and skin graft blades, thin strips of tissue were cut and then pressure applied to the sections using the edge of the scapel blade in a scraping motion. Once the bathing MEM medium became cloudy with cells, it was transferred to a sterile universal using a Pasteur pipette then replaced with fresh MEM. This process was continued until the tissue was soft and non - cellular and no further cells were released. The resultant cellular MEM solution was sieved through a $100 \text{ }\mu\text{m}$ nylon cell strainer (Fisher Scientific, Loughborough, England) washed in PBS and centrifuged in sterile universals at 454 g for 7 min at room temperature.

2.3.6.3 Enzymatic disaggregation

Tissue for enzymatic disaggregation was bathed in cold MEM and cut into small pieces (1 - 3 mm³) using skin graft blades and scapel blades. After the tissue had been sectioned it was incubated in DMEM, 0.1% collagenase type I, 0.01% hyaluronidase and 0.002% DNase type I (Rong *et al.*, 1985) using 5 ml for every gram of wet tumour. Samples were agitated for 3.5 hours at 37 °C then sieved through a 100 µm cell strainer, washed in PBS and centrifuged at 454 g, for 7 min at room temperature.

2.3.6.4 Viability of disrupted tumour suspensions

Cell viability for each procedure was determined using trypan blue exclusion, PI and FDA. Tumour cells were incubated with 50 µg.ml⁻¹ PI or 12.5 ng/ml⁻¹ at a concentration of 2.5 x 10⁵ cells/ml in PBS for 10 min at room temperature, centrifuged for 7 min at 454 g and resuspended in PBS, analysis was carried out using flow cytometry between 10 min and 4 hours of the completion of the assay.

2.3.6.5 Histological staining of disrupted tumour cells

Concurrently with viability analysis two cytocentrifuge preparations of mechanical and enzymatic disaggregated cells were produced. The slides were air dried before being stained histologically, one with Papanicolaou cytological stain and the second with Haemotoxylin and eosin.

2.3.6.6 Papanicolaou staining procedure

Slides were incubated for 5 min in Harris' Haemotoxylin, rinsed for 2 min in tap water, incubated in IMS (Sigma - Aldrich company Ltd, Poole, England) for 1 min, followed by 2 min in OG6. They were rinsed again for 2 min in IMS, then incubated in EA50 for 3 min, then repeat rinses in IMS for 2 min and 4 min. Finally the slides were incubated in xylene for 10 min before mounting with DPX.

2.3.6.7 Haemotoxylin and eosin staining procedure.

Slides were incubated in Haemotoxylin for 2 min, rinsed for a few seconds in tap water, counterstained in eosin for 5 min, and rinsed in tap water for a few seconds. The slides were then taken from water through increasing concentrations of ethanol, incubating

for 5 min in 70%, 90% then 100% ethanol. The slides were then incubated in xylene for 10 min before mounting in DPX. All staining procedures were performed in a fumehood.

2.3.7 Fine needle aspirate (FNA) samples

Preliminary experiments were carried out to determine the best conditions for examining cell suspensions using the LSC, viable MCF-7/S cells at concentrations from 0.1 to 100×10^4 cells/ml were used on three types of slide. The cells (5×10^6 cells.ml⁻¹) were incubated with doxorubicin at 100 $\mu\text{mol.L}^{-1}$, 1 mmol.L^{-1} or untreated (control) for one hour in RPMI, washed in PBS (454 g, 7 min) and adjusted to concentrations ranging from 0.1 - 100×10^4 cells/ml.

The three slide systems were:- 12 well PTFE coated multispot slide (Henley, Essex), 8 well Permanox plastic chamber slide (Life Technologies Ltd, Paisley, Scotland) and 16 well glass chamber slide (Life Technologies Ltd, Paisley, Scotland). The volumes of cell suspensions used for each well or chamber were 50 μl for the PTFE coated slide, 200 μl for the 8 well slide and 100 μl for the 16 well slide. The cell suspensions were loaded onto the slides and incubated at 37 °C for 30 min in a wet chamber constructed of a perspex box lined with saturated blotting paper, then washed in PBS. The PTFE coated slide was then mounted with a coverslip (22 x 64 mm) in 25% glycerol in PBS. The 8 and 16 well chamber slides had their medium decanted before the chambers were removed using the key supplied by the manufacturer, then the rubber gaskets which attached the chambers to the slides were removed using a scapel blade and then washed in PBS and mounted with 25% glycerol in PBS. The cellular spread and fluorescence was observed using light and fluorescence microscopy.

2.3.7.1 Processing of FNAs

Tumour material was received from the Department of Histopathology, and transferred to a class II laminar flow cabinet in cold MEM. Tumour sections were selected from the edge of the tumour which was likely to be cellular, rather than the centre of the tumour which could have been necrotic and stromal. The tumour was kept moist with PBS containing 1% FCS, then cells aspirated with a 19 gauge needle using a 20 ml syringe. After several passes the residual tumour was washed with PBS containing 1% FCS, and this solution transferred to a universal together with the aspirated tumour cells,

centrifuged (454 g, 5 min) and resuspended in 1 ml PBS containing 1% FCS and counted using trypan blue exclusion then adjusted to 5×10^6 cells/ml.

After counting the cells they were used for doxorubicin incubation (1 hour at 1, 100 and 1000 $\mu\text{mol.L}^{-1}$ doxorubicin concentrations) and calcein AM incubation. After incubation with doxorubicin and calcein AM the cells were centrifuged (454 g, 7 min) and resuspended in PBS at 1×10^6 cells/ml, aliquots (50 μl) of cells were pipetted onto each well of a PTFE coated slide, then allowed to settle for 30 min in a wet chamber at 37 °C. The excess media was removed and washed in PBS containing 1% FCS, the slides were mounted immediately in 25% glycerol in PBS then analysed using light scatter contouring using the LSC.

2.3.8 Studies of BrdUrd uptake into nuclei of primary human tumours

Patients with invasive ductal breast carcinoma and gastric adenocarcinomas were labelled with 250 mg 5' - bromo - 2' - deoxyuridine (Sigma - Aldrich company Ltd., Poole, England) (BrdUrd) *in vivo* by intravenous injection between 3 and 15 hours prior to surgery (Rew *et al.*, 1992). The specimens consisted of 19 breast carcinomas and 12 gastric adenocarcinomas. Tumours were selected from an archive on the basis of their DNA and BrdUrd profiles from samples preserved for up to seven years in 70% ethanol at - 20°C, during which period the samples physically had shown no significant deterioration. All nuclei preparation was carried out by laboratory staff at the Gray Laboratory Cancer Research Trust, Mount Vernon Hospital, Northwood, Middlesex, England, as part of a collaboration with Dr George D. Wilson.

2.3.8.1 Sample preparation and staining

Specimens were processed and analysed as previously described (Rew *et al.*, 1992). Briefly, fragments of solid tumour were dissociated into a nuclei suspension using 0.4 mg.ml^{-1} pepsin (Sigma - Aldrich company Ltd., Poole, England) in 0.1 mol.L^{-1} HCl for 45 to 60 min at 37°C. The resultant suspension was filtered through 35 μm nylon mesh and denatured with 2 mol.L^{-1} HCl for 15 min at room temperature. After washing twice in PBS, the nuclei were incubated with a 1:20 dilution of a mouse anti-BrdUrd monoclonal antibody (Dako Ltd, High Wycombe, England) in 200 μl of PBS containing 0.5% Tween-20 (Sigma - Aldrich company Ltd., Poole, England) and 0.5% normal goat serum (Sigma - Aldrich company Ltd., Poole, England). After 1 hour, the nuclei were washed and

resuspended in a 1:20 dilution of a goat anti-mouse IgG FITC conjugate (Sigma - Aldrich company Ltd., Poole, England) in 200 μ l of PBS containing 0.5% Tween-20 and 0.5% normal goat serum. After 30 min the nuclei were washed and resuspended in 1 ml of PBS containing 10 μ g.ml⁻¹ PI. Each sample was analysed using FCM and LSC, LSC analysis was performed the next day after over - night refrigeration at 4 °C. The nuclei were prepared as cytocentrifuge preparations and the bright red nuclear fluorescence of PI was used as the triggering signal for contouring, up to 5000 events were collected using WinCyte software.

2.3.9 Statistical analysis

Various statistical analysis was employed for this study. The Scatchard plot ($r/c = -K_r + K_n$) was used to determine the affinity of doxorubicin, mitoxantrone and ethidium bromide had for DNA in solution. Pearson r and Spearman's rank order correlation have been used to determine the similarity between two sets of data. These tests have been used to compare the results of analysis by different methods. In both cases the null hypothesis = 0, that is, that there is no correlation between the two sets of data. A correlation calculation of 1 would indicate a perfect positive correlation between the two sets of data. A two tailed Student t test was employed to determine whether there was a statistical difference between the two sets of breast tumour disaggregation data and various parameters of the proliferation assay of tumour nuclei analysed by FCM and LSC. The tumour nuclei proliferation assay also employed coefficient of variation analysis of areas of the cell cycle.

RESULTS

CHARACTERISTICS OF DRUGS

3.1 **Characteristics of drugs**

The fluorescence characteristics of doxorubicin, mitoxantrone and classical intercalator ethidium bromide have been investigated using spectrophotometry, fluorimetry and DNA binding studies.

3.1.1 **Physical characteristics of drugs**

3.1.1.1 Absorbance

Spectroscopic analysis was carried out on doxorubicin, mitoxantrone and ethidium bromide to assess their compatibility for use with flow and laser cytometers, their absorbance spectra are illustrated in figures 3.1. The absorbance maximum (λ) in the visible region of the spectra was 472, 660 and 480 nm, for doxorubicin, mitoxantrone and ethidium bromide, respectively. Each compound had a large absorbance peak in the UV region of the spectrum, but only the absorbance peaks of the visible region are of interest. Doxorubicin and ethidium bromide have λ max. values close to 488 nm which is the wavelength of the argon laser light source available in standard flow and laser scanning cytometers, making them suitable fluorescent agents for use with these cytometry detection systems, mitoxantrone was less suitable with a higher λ max. of 660 nm.

3.1.1.2 Spectrophotometric titrations

The dose dependent relationship between the absorbance and concentration of doxorubicin (10 - 100 $\mu\text{mol.L}^{-1}$), mitoxantrone (1 - 10 $\mu\text{mol.L}^{-1}$) and ethidium bromide (10 - 100 $\mu\text{mol.L}^{-1}$), are shown in figure 3.2. The absorbance readings for each drug were measured at the λ max. for each compound and at 488 nm. The absorbance values for doxorubicin and ethidium bromide were comparable measured at their λ max. and 488 nm, but the absorbance yield of mitoxantrone was lower at 488 nm than 660 nm (λ max.).

3.1.1.3 Extinction coefficient derivation

The linear relationship between drug concentration and absorbance value as illustrated in figure 3.2 for doxorubicin, mitoxantrone and ethidium bromide can be used to calculate extinction coefficients for each compound. Using the equation for a straight line ($y = mx + c$), m , the gradient, was used to determine the extinction coefficient. The calculated extinction coefficients and those found in literature are shown in table 3.1.

Drug	Extinction coefficient (graphically calculated)			Extinction coefficient (literature)		
	value (mol.cm ⁻¹)	λ	solvent	value (mol.cm ⁻¹)	λ	solvent
Doxorubicin	9800	470	Tris HCl	13600 (a)	478	methanol + HCl (a)
				13050 (b)	477	methanol (b)
Mitoxantrone	23500	660	Tris HCl			
Ethidium bromide	5000	480	Tris HCl			

(a) Rizzo *et al.*, 1988 and (b) Vigevani and Williamson, 1980

Table 3.1.

Comparison of practical derivations of the extinction coefficients of doxorubicin, mitoxantrone and ethidium bromide and those used in literature.

3.1.1.4 Fluorescence

The fluorescent emission peaks of doxorubicin and ethidium bromide are 559 and 601 nm, respectively, as shown in figure 3.3. The second peak at 488 nm is the excitation light being detected within the emission spectra. The emission peaks of doxorubicin and ethidium bromide are compatible for FCM and LSC as these wavelengths are within the band of wavelengths detected by their PMTs. Mitoxantrone was not included in this analysis as the fluorimeter was unable to detect the wavelength of fluorescence which mitoxantrone would produce (>660 nm).

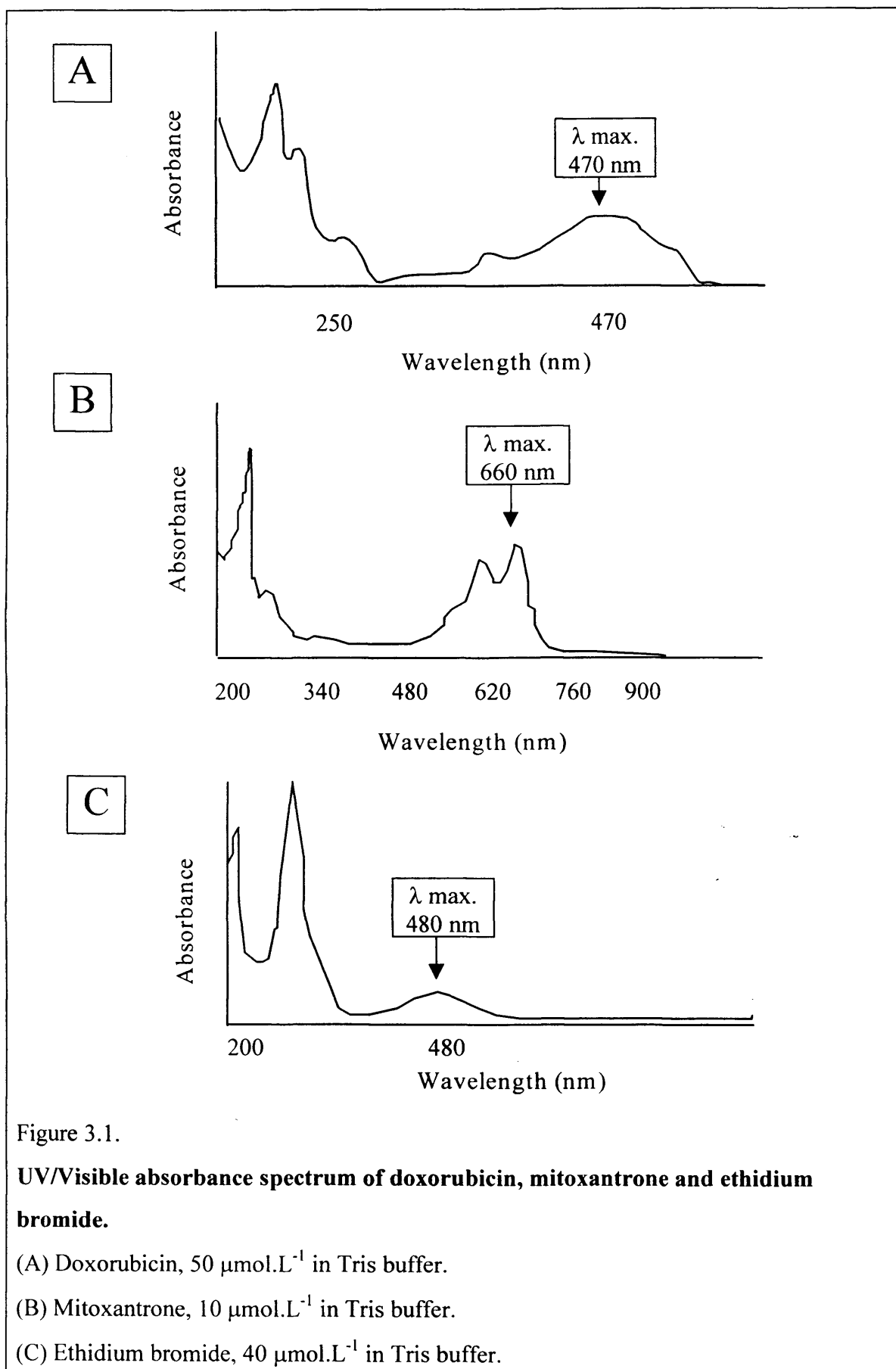


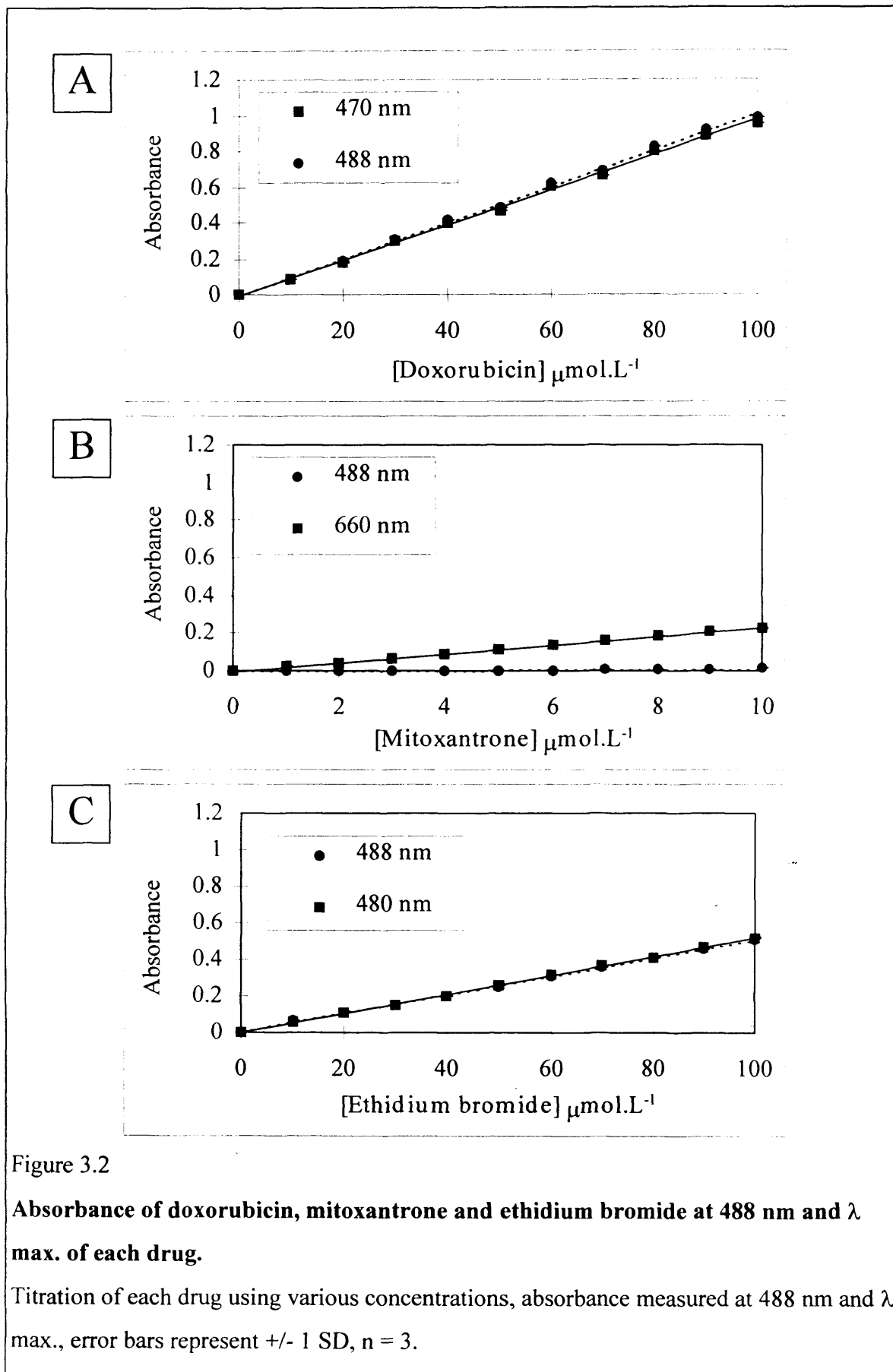
Figure 3.1.

UV/Visible absorbance spectrum of doxorubicin, mitoxantrone and ethidium bromide.

(A) Doxorubicin, 50 $\mu\text{mol.L}^{-1}$ in Tris buffer.

(B) Mitoxantrone, 10 $\mu\text{mol.L}^{-1}$ in Tris buffer.

(C) Ethidium bromide, 40 $\mu\text{mol.L}^{-1}$ in Tris buffer.



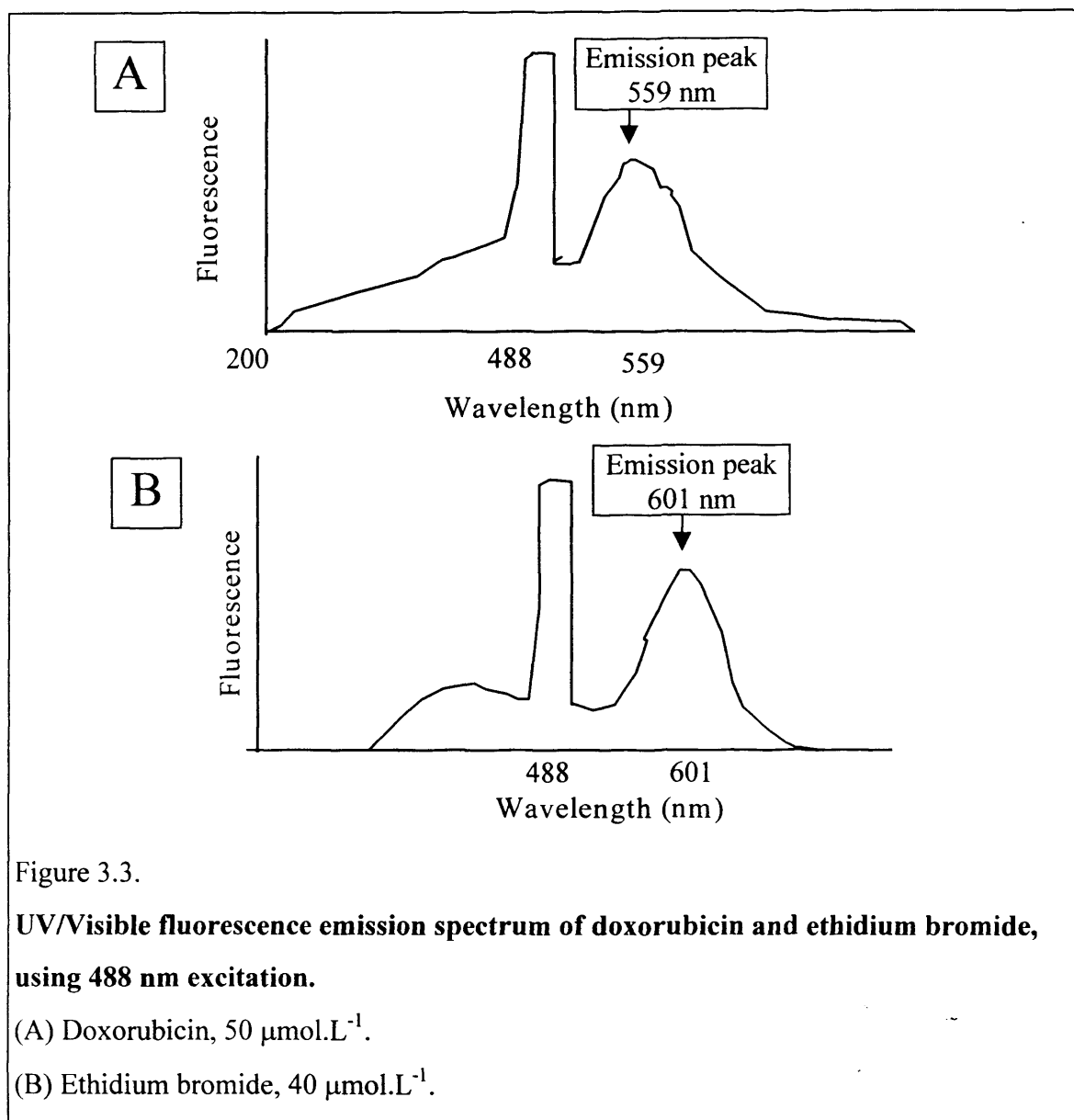


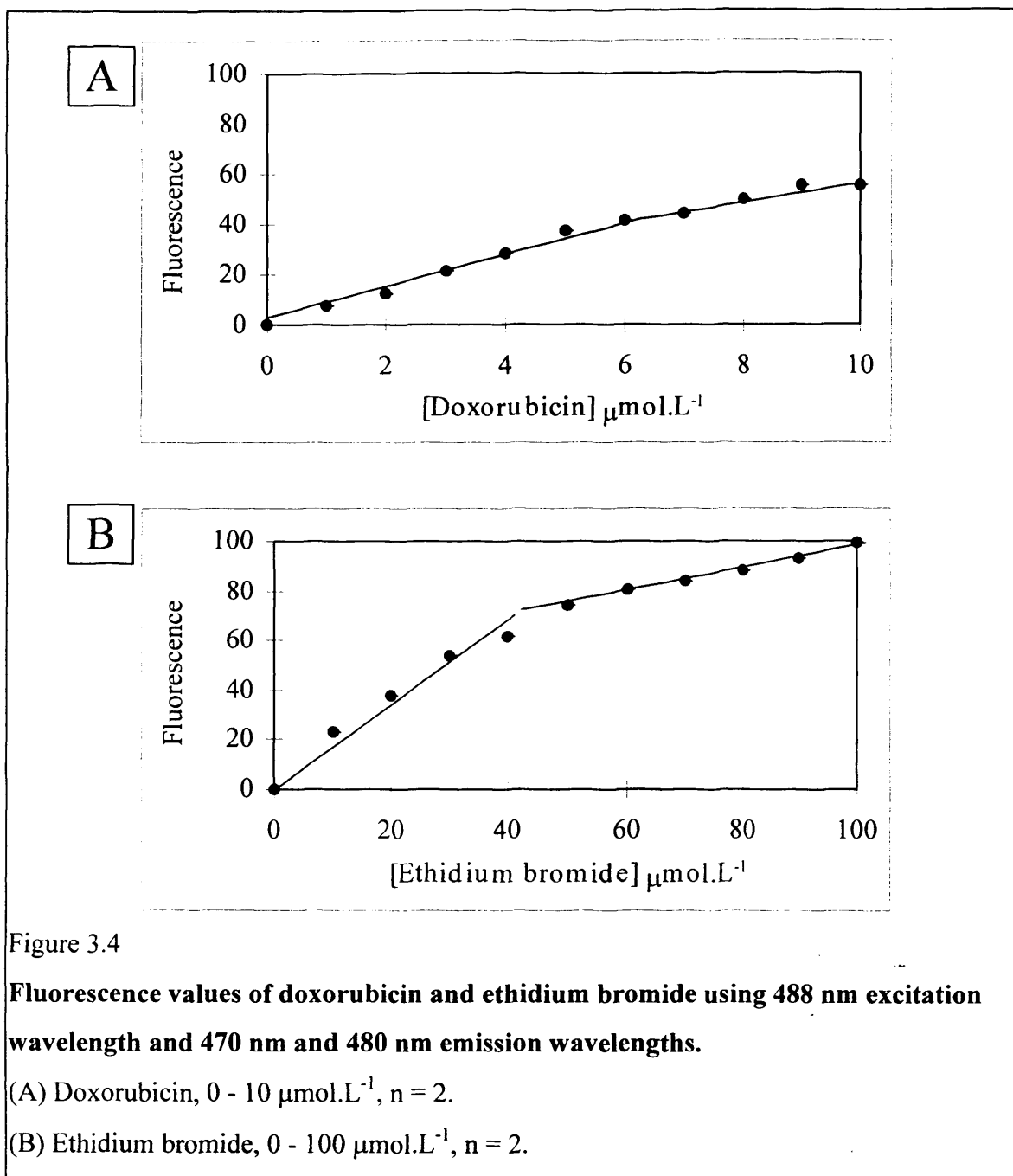
Figure 3.3.

UV/Visible fluorescence emission spectrum of doxorubicin and ethidium bromide, using 488 nm excitation.

(A) Doxorubicin, 50 $\mu\text{mol.L}^{-1}$.

(B) Ethidium bromide, 40 $\mu\text{mol.L}^{-1}$.

Fluorescent titrations of doxorubicin (1 - 10 $\mu\text{mol.L}^{-1}$) and ethidium bromide (10 - 100 $\mu\text{mol.L}^{-1}$) were carried out using an excitation of 488 nm and emission wavelengths of 560 and 601 nm, respectively, these data are shown in figure 3.4. A dose dependent relationship was seen between concentration and fluorescence at lower concentrations, but at higher concentrations quenching occurs, a plateau was reached at > 6 $\mu\text{mol.L}^{-1}$ doxorubicin and > 50 $\mu\text{mol.L}^{-1}$ ethidium bromide.



3.1.2 DNA binding characteristics of drugs

The λ max. of 260 nm for DNA solution, as shown in figure 3.5, is at a lower wavelength than the absorbance peaks of doxorubicin, mitoxantrone and ethidium bromide which have absorbances >400 nm. The absorbance values detected using the DNA/drug solution were as a result of the influence of the drugs not the DNA.

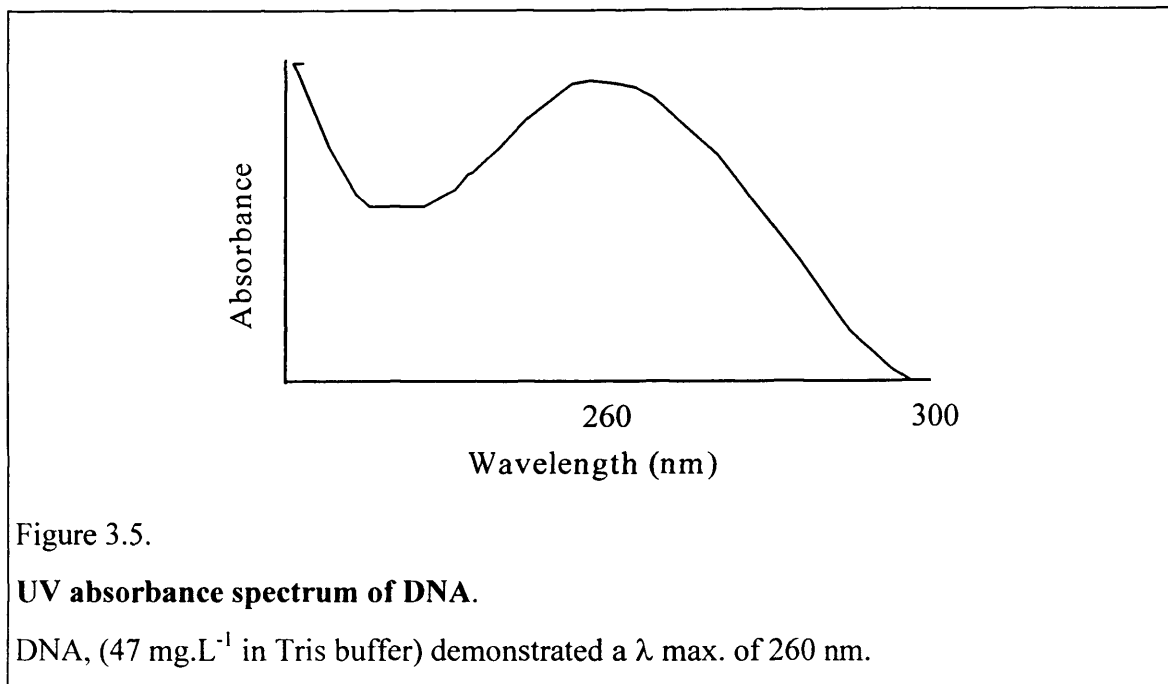


Figure 3.5.

UV absorbance spectrum of DNA.

DNA, (47 mg.L^{-1} in Tris buffer) demonstrated a $\lambda \text{ max.}$ of 260 nm.

3.1.2.1 Isosbestic point determination

The isosbestic points for doxorubicin, ethidium bromide and mitoxantrone are 570, 515 and 700 nm, respectively, as shown in figure 3.6. The isosbestic point is a wavelength where the absorbance of bound and unbound drug (to DNA) in solution are equal, regardless of DNA/drug ratio. The chance of there being a third form of drug, in solution, which has the same absorbance was infinitely small, therefore the detection of an isosbestic point indicates that there are only two forms of drug present in solution. The isosbestic point for doxorubicin and ethidium bromide are clear and definite, for mitoxantrone this point was not so precise.

3.1.2.2 Spectral titration

The affinity of doxorubicin, mitoxantrone and ethidium bromide for DNA was calculated from the spectral titrations and Scatchard plots shown in figures 3.7, 3.8 and 3.9, for doxorubicin, mitoxantrone and ethidium bromide, respectively.

Equation (1) is the Scatchard plot equation.

$$r/c = -Kr + Kn \quad (1)$$

Where r is the number of sites occupied by drug per DNA phosphate group; c is the concentration of drug; n is the number of binding sites for the drug per DNA phosphate group and K is the affinity constant. A plot of ' r/c vs r ' gives a line of slope $-K$ and intercept Kn on the x axis. The Scatchard plot for doxorubicin, mitoxantrone and ethidium bromide was divided into two parts as each plot was curved, allowing affinity constants to be determined for intercalation and surface binding, the $-K$ slope and Kn intercept were determined for intercalation and surface binding.

The high and low affinity binding constants from intercalative and surface binding of doxorubicin, mitoxantrone and ethidium bromide to DNA were calculated from the Scatchard plots shown in figures 3.7, 3.8 and 3.9, respectively. Each Scatchard plot was divided into vertical and horizontal sections, the vertical portion of the plot was used to determine the high affinity intercalation and the horizontal portion was used to determine the low affinity surface binding. The calculated affinity binding constants are shown in table 3.2, compared with values found in literature. From the Scatchard plots the number of drug molecules per DNA phosphate groups were also calculated and the results from this study and those from literature are shown in figure 3.3.

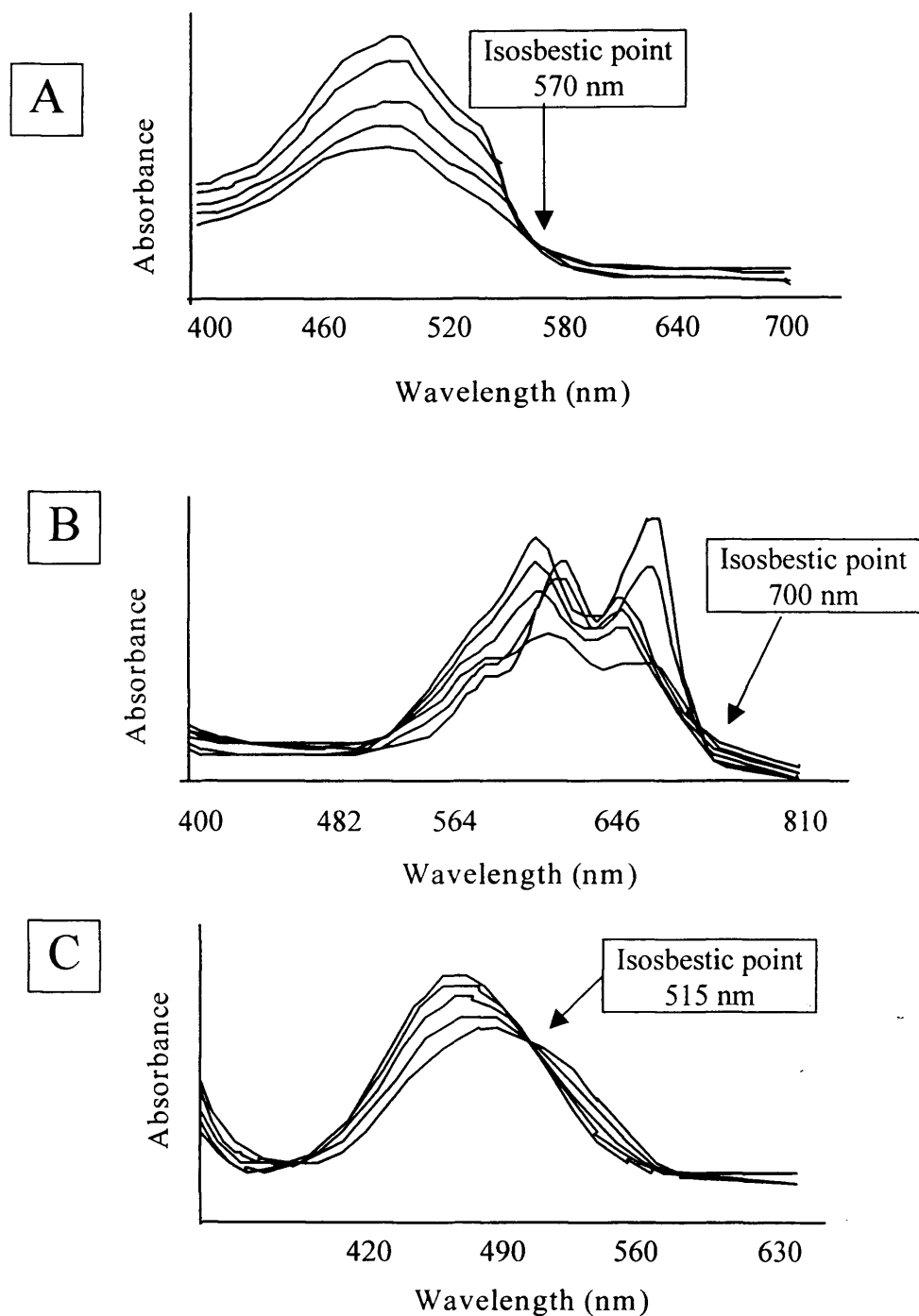


Figure 3.6

Overlaid spectral titrations of a series of molar DNA/drug ratios.

(A) Doxorubicin, (B) mitoxantrone and (C) ethidium bromide, using DNA/drug ratios of 0/25, 1/1, 2/1, 5/1, 10/1 and 15/1.

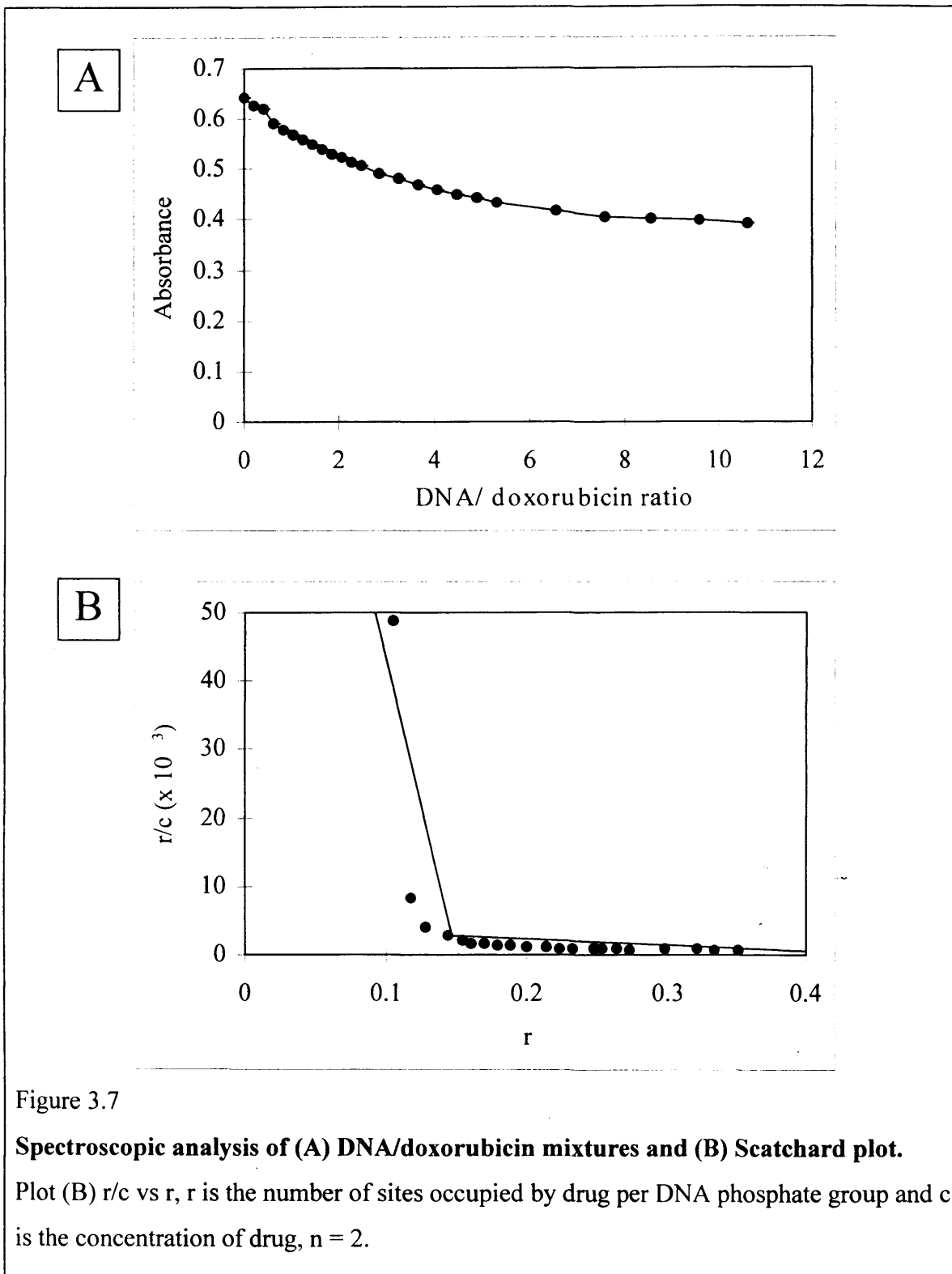


Figure 3.7

Spectroscopic analysis of (A) DNA/doxorubicin mixtures and (B) Scatchard plot.

Plot (B) r/c vs r , r is the number of sites occupied by drug per DNA phosphate group and c is the concentration of drug, $n = 2$.

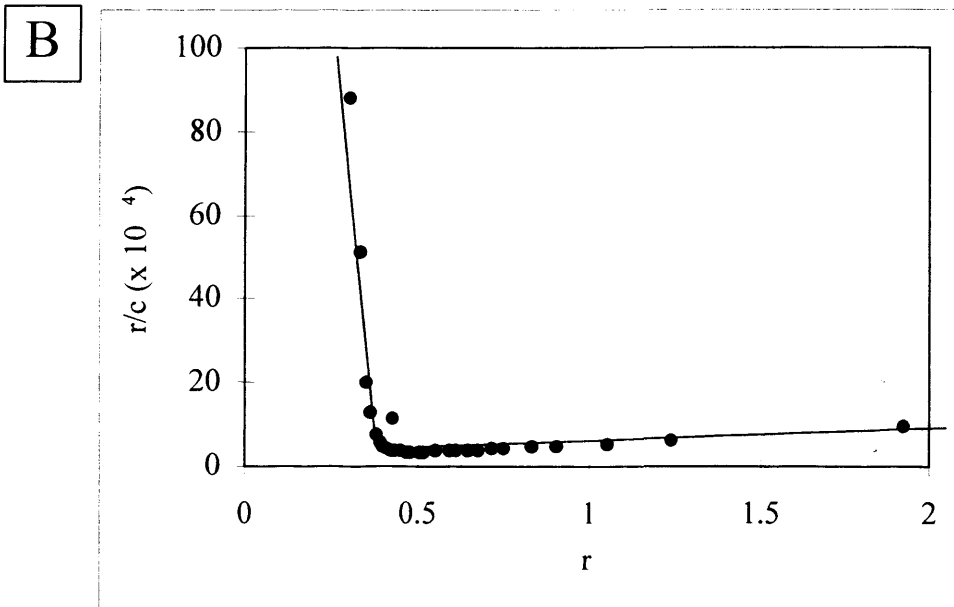
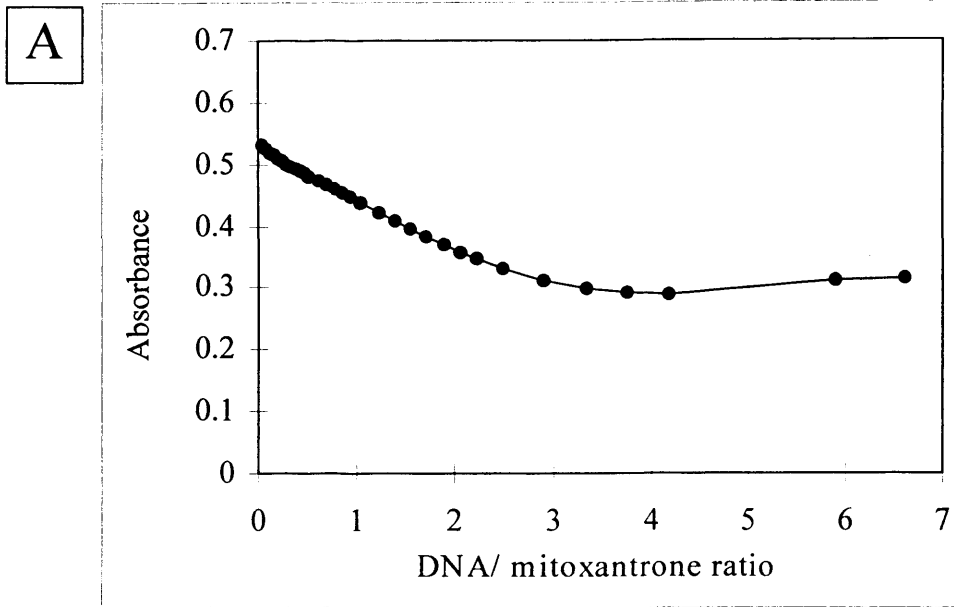
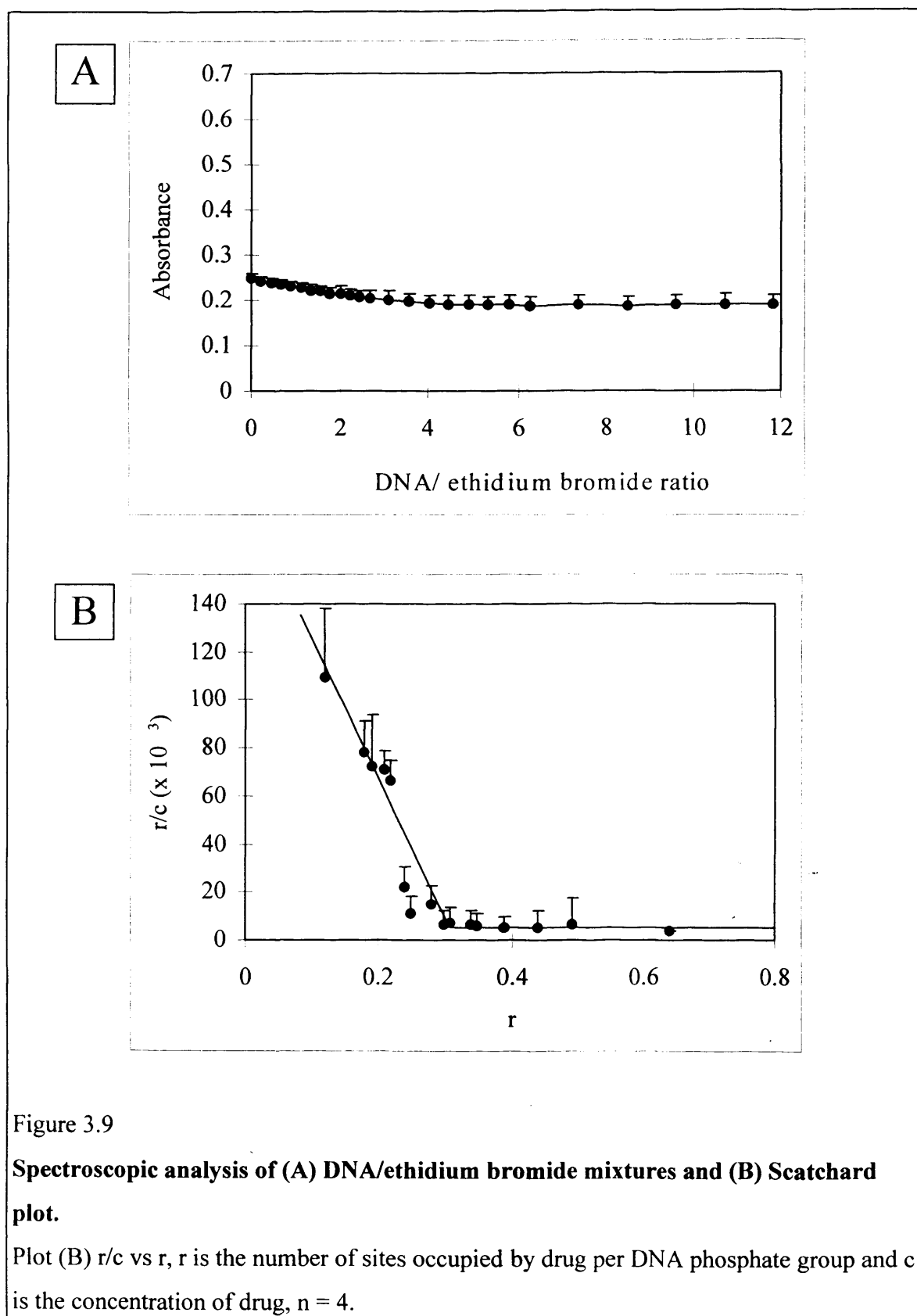


Figure 3.8

Spectroscopic analysis of (A) DNA/mitoxantrone mixtures and (B) Scatchard plot.

Plot (B) r/c vs r , r is the number of sites occupied by drug per DNA phosphate group and c is the concentration of drug, $n = 2$.



Compound	Affinity constant (intercalation) (mol.L ⁻¹) Graphically	Affinity constant (surface binding) (mol.L ⁻¹) Graphically	Affinity constant (intercalation) (mol.L ⁻¹) Literature Source
Doxorubicin	0.13×10^3	0.92×10^3	4.42×10^6 (a); 6.5×10^6 (b); 2.8×10^6 (e); 3.0×10^6 (f).
Mitoxantrone	0.45×10^4	/	1.8×10^6 (c); 2.6×10^8 (d); 1.78×10^5 (g).
Ethidium bromide	0.29×10^3	1.21×10^3	0.26×10^6 (c); 6×10^5 (g).

(a) Gandecha, 1985, PhD thesis; (b) Capranico, 1989; (c) Kapuscinski *et al.*, 1981; (d) Hartley *et al.*, 1988; (e) Zunino *et al.*, 1972; (f) Neidle, 1978 and (g) Lown *et al.*, 1985.

Table 3.2.

Comparison of practical calculations of doxorubicin, mitoxantrone and ethidium bromide affinity constants and those used in literature.

Compound	DNA phosphate groups per 1 intercalating drug molecule (graphically determined)	DNA phosphate groups per 1 intercalating drug molecule (literature)
Doxorubicin	8	5 (a); 5.3 (b); 3.6 (c);
Mitoxantrone	2.2	/
Ethidium bromide	3.5	/

(a) Zunino *et al.*, 1972; (b) Neidle, 1978; (c) Cummings *et al.*, 1991.

Table 3.3

Comparison of practical calculations of doxorubicin, mitoxantrone and ethidium bromide for the number of DNA phosphate groups bound per drug molecules for intercalative binding.

3.1.3 Discussion

The natural fluorescence and DNA binding characteristics of the chemotherapy agents doxorubicin and mitoxantrone were compared to that of the classical intercalator, ethidium bromide. Doxorubicin fluorescence in solution was shown to be linear to a concentration of $6 \mu\text{mol.L}^{-1}$. The deviation from Beer - Lambert law is probably due to the dimerization of doxorubicin, this phenomenon was also detected using daunorubicin at a concentration $> 2 \text{ mmol.L}^{-1}$, as previously described (Arcamore, 1978). The wavelengths of absorbance and fluorescence were measured and found to compare with those reported in the literature (Vigevani and Williams, 1980 and Smyth *et al.*, 1986), doxorubicin was shown to be compatible with FCM and LSC analysis as its absorbance was close to 488nm; the excitation wavelengths of the lasers in both machines. The excitation wavelength of mitoxantrone at 660 nm is not compatible with a high yield fluorescence using FCM or LSC, although cellular mitoxantrone content has been quantified using confocal microscopy (Fox and Smith, 1995), and could be detected by FCM as shown previously (Smith *et al.*, 1992) and within this study.

In a cell suspension doxorubicin binds to DNA (Carter, 1975) and other cellular structures, including the plasma membrane (Siegfried *et al.*, 1983 and Gaber *et al.*, 1998). Doxorubicin fluorescence will be detectable from all sites of the cell, although intercalation of DNA causes considerable fluorescent quenching (Zunino *et al.*, 1972 and Krishan and Ganapathi, 1979) which is a consideration with the use of doxorubicin fluorescent for a quantitative assay.

The isosbestic points shown in figure 3.6 identify the binding of drugs to DNA in solution, and the use of the Scatchard plot quantifies this binding. Ionic strength of the solutions used for isosbestic point determination and Scatchard plot analysis may influence the results. The isosbestic point determination of mitoxantrone is sensitive to ionic strength < 0.1 and high drug concentrations, use of solutions with alternative ionic strengths can lead to the isosbestic point being lost (Lown *et al.*, 1985).

The DNA binding studies used for this investigation were to re - iterate the intercalation model of anthracyclines (Zunino *et al.*, 1972; Arcamore, 1978 and Quigley *et al.*, 1980) and aminoanthraquinones (e.g. mitoxantrone) (Lown *et al.*, 1985 and Durr, 1988). The isosbestic point determination and affinity binding constants calculated from Scatchard plots, utilised the change in visible absorbance of the drugs as they bound to DNA.

The Scatchard plot (Scatchard, 1949) is the most common method used for the presentation of ligand binding data (Bordbar *et al.*, 1996). Two general classes of plot are usually encountered, linear and non - linear. Linear Scatchard plots result from a single class of binding site (Dombi, 1984) and non - linear plots are produced when two or more non - equivalent binding sites exist (Dombi, 1984 and Bordbar *et al.*, 1996). The analysis of non - linear Scatchard plots precisely can be prone to misinterpretation (Crabbe, 1990). The Scatchard plots obtained in this study were analysed assuming there were two modes of binding between drug and DNA, similar to those described by Chaires *et al.* (1982) investigating the binding of daunomycin to DNA, and by Zunino (1971) measuring the elution of drug from DNA - cellulose columns.

The binding affinities determined in this study were lower than those from other studies (Kapusinski *et al.*, 1981; Lown *et al.*, 1985 and Hartley *et al.*, 1988). The discrepancy of these results were consistent for all three drugs tested, experimental differences could have created the low results possibly as a result of the DNA not being sonicated (Neidle, 1978) and by the use of drug/DNA solutions of inappropriate ionic strength (Chaires *et al.*, 1982 and Lown *et al.*, 1985).

A variety of methods to determine drug intercalation can be employed which either measure changes in the properties of the drug or DNA (Neidle, 1978). Other changes such as, the reduction of fluorescence as the drug chromophore binds to DNA, and circular dichroism studies, which highlight the changes in the CD spectrum of the drug through DNA interaction (Rizzo *et al.*, 1988) can be used to characterise the binding of drug. Properties that can be used to measure changes in DNA include utilising DNA's well documented hydrodynamic properties. The intrinsic viscosity of DNA increases when the drug binds to DNA (Zunino *et al.*, 1972); buoyant density and sedimentation coefficient are both decreased (Arcamore, 1978), and the thermal denaturation of DNA helix to coil increases (Chaires *et al.*, 1982).

Throughout this study doxorubicin concentrations were used over a range of 1 - 100 $\mu\text{mol.L}^{-1}$, often using concentrations $> 6 \mu\text{mol.L}^{-1}$, comparable to other studies (Krishan *et al.*, 1979 and Muller *et al.*, 1997). These higher drug concentrations are not pharmacologically relevant. The highest recorded plasma concentration from a chemotherapy patient receiving doxorubicin therapy is 5 $\mu\text{mol.L}^{-1}$ (Muller *et al.*, 1997). For this study it would have been informative to titrate doxorubicin to a lower concentration range e.g. 0.1 - 1 $\mu\text{mol.L}^{-1}$ to establish the lower level of sensitivity of

Results

cytometric doxorubicin detection. The use of the higher doxorubicin concentrations for monitoring uptake into tumour cells is justified for this study, to assess individual patients resistance to anthracycline therapy, doxorubicin needs to be easily detectable. The high concentrations of doxorubicin are more easily detected using their fluorescence than the lower, more clinically relevant concentrations.

**CHARACTERISATION
OF CELL LINE
MODELS-
MTT ASSAY**

3.2 **Characterisation of cell line models - MTT assay**

The growth characteristics of the human breast carcinoma cell lines, MCF - 7/S and MDA MB 231 cells were performed using the MTT assay. Once characterised the MCF - 7/S cells were used to develop the doxorubicin uptake assay.

3.2.1 **MTT formazan calibration**

The directly proportional linear relationship between MTT formazan and absorbance over a concentration range of 1 - 0.24 $\mu\text{mol.L}^{-1}$ is shown in figure 3.10. All absorbance values are plotted as linear values.

3.2.2 **Standard curves for the MTT assay**

The standard curves for the MTT assay using MCF-7/S and MDA MB 231 cells from 0.1 - 25 x 10⁴ cell/ml are shown in figure 3.11. The assay was linear using the absorbance values 0.1 - 3.0 using the MDA MB 231 cells and between 0.1 - 0.65 absorbance units for MCF-7/S cells.

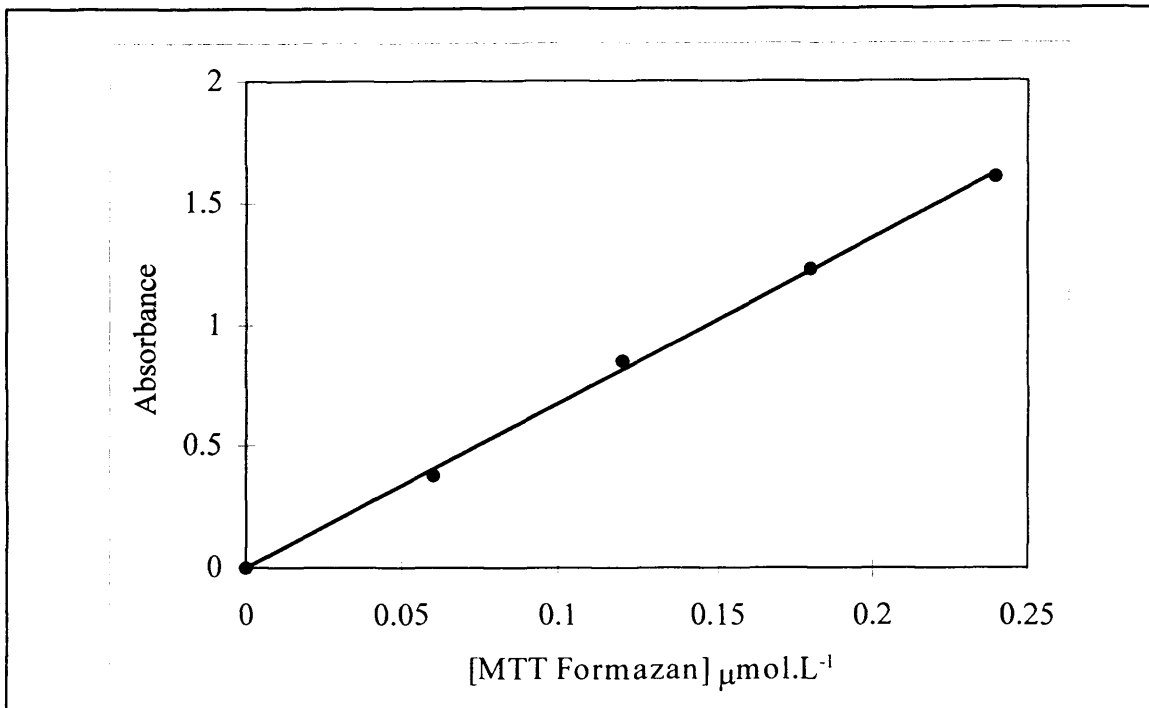
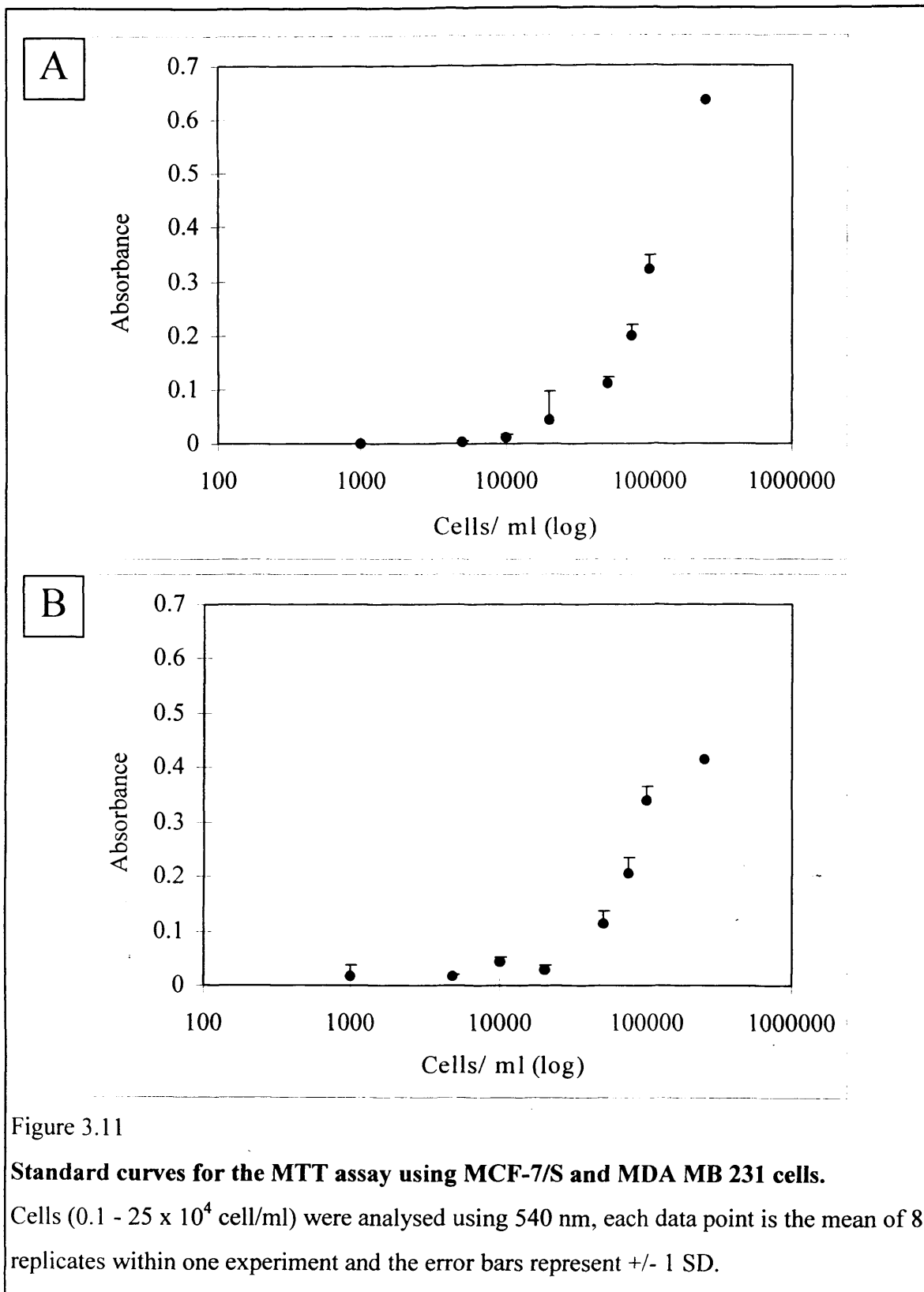


Figure 3.10

Calibration curve for MTT formazan in DMSO.

The absorbance of the MTT formazan (0 - 240 μmol.L⁻¹) was measured at 540 nm (n = 1).



3.2.3 Growth curves

Experiments were performed using the MTT assay with MDA MB 231 and MCF-7/S cells to determine the optimal seeding concentration which produced a steep growth curve and exponential growth over a defined length of time. These cell seeding concentrations would then be used for future experiments.

The growth of MCF-7/S cells are illustrated in figure 3.12, demonstrating the cells at 4 hours beginning to adhere to the surface of the flask, they are still rounded and appear to have a bright outline. With increasing time the cells became more densely populated as seen in figure 3.12/B - D, by 144 hrs the cells have reached confluence and have started to grow on top of one another. Growth curves using MCF-7/S and MDA MB 231 cells, using a range of seeding concentrations from 0.01 to 2.5×10^5 cells/ml were grown for 4 - 172 hours, then assayed using MTT, as shown in figure 3.13. These data show that the cells are still in exponential growth at 172 hours, although the 144 hour photo (2.5×10^5 cells/ml seeding concentration) shown in figure 3.12/D suggests that the cells are confluent. The lowest cell concentrations 0.01 to 0.2×10^5 cells/ml, for both cell lines, remained in lag phase until at least 72 hours, when their growth was very slow. The higher cell concentrations from 0.5 to 2.5×10^5 reached exponential growth by 24 hours and continued to multiply up until 172 hours. A seeding concentration of 2.5×10^5 cells/ml was chosen as the one to be used in subsequent experiments.

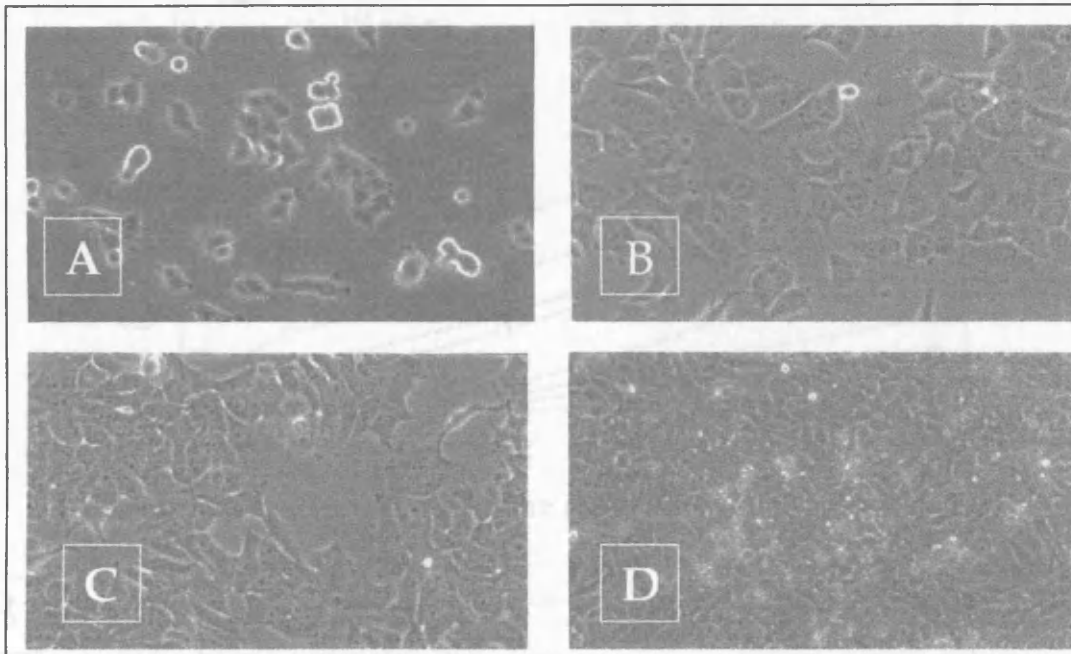


Figure 3.12

Photomicrographs of MCF-7/S cells grown under normal growth conditions.

MCF-7/S cells grown in T₂₅ tissue culture flasks with RPMI - FCS medium.

Photographs (x 40 objective) demonstrating what these cells look like under normal growth conditions at (A) 4 hours, (B) 24 hours, (C) 72 hours and (D) 144 hours.

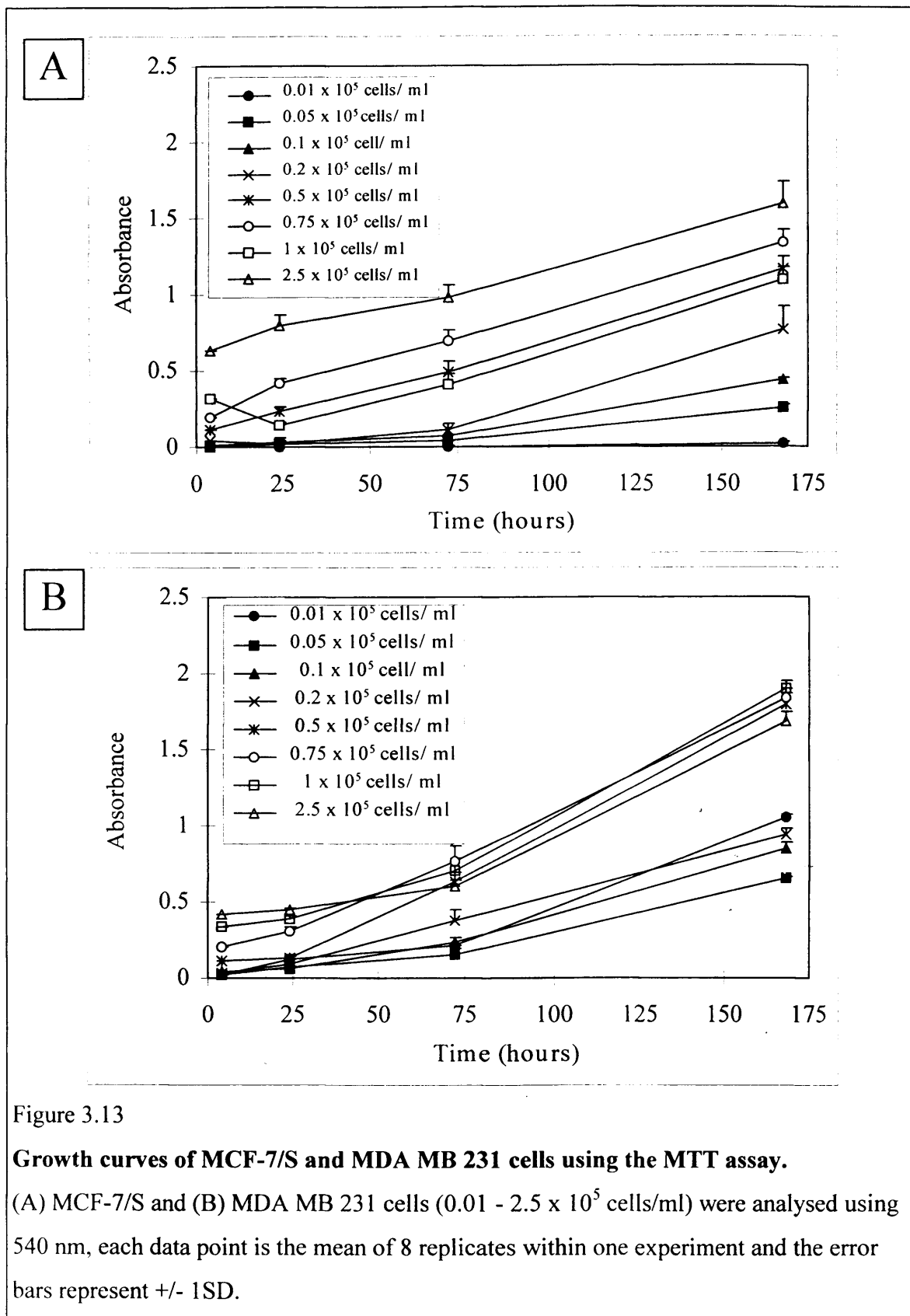


Figure 3.13

Growth curves of MCF-7/S and MDA MB 231 cells using the MTT assay.

(A) MCF-7/S and (B) MDA MB 231 cells ($0.01 - 2.5 \times 10^5$ cells/ml) were analysed using 540 nm, each data point is the mean of 8 replicates within one experiment and the error bars represent +/- 1SD.

3.2.4 Discussion

Since their establishment MCF-7/S cells have been utilised extensively in breast cancer research (Bustamante *et al.*, 1990, Davies *et al.*, 1996 and Bargou *et al.*, 1997). Before using them for drug uptake studies their growth characteristics were established using the MTT assay.

This model was sufficient to determine the best cell concentration for the subsequent cytotoxicity assay (section 3.3) which was also performed using 96 well plates. Growth curves were not translated into cell numbers, hence the standard curve could not be extended beyond an absorbance reading of 0.65 because linearity could not be assumed.

Since the introduction of the MTT assay, it has been compared to various other viability assays (Petty *et al.*, 1995). There have also been modifications made to the original procedure (Denizot *et al.*, 1986) and various limitations acknowledged (Siewerts *et al.*, 1995). The MTT procedure has been performed in the literature, using a variety of MTT concentrations, MTT formazan solubilising solutions and detection wavelengths, table 3.4 highlights the variety of procedures used.

The procedure for the MTT assay used for this study was the same as described by Petty *et al.* (1995). The solubilising solution used to dissolve the MTT formazan crystals is the main source of variety between the procedures adopted by different laboratories, the pH of this solution influences the absorbance of MTT formazan (Siewerts *et al.*, 1995 and Denizot and Lang, 1986). Mosmann (1983) acidified the solubilising solution (isopropanol) to change the pH indicator (phenol red) of the growth medium to yellow, as yellow does not produce an interfering absorbance signal, unlike red, unfortunately acidifying the medium changes the absorbance spectrum of the MTT formazan. The procedure used in this study removed as much medium as possible to avoid a change in pH and phenol red free medium was used. The DMSO used as a solubilising agent does not cause protein precipitation, which was another technical limitation of the use of an organic solvent such as isopropanol (Denizot and Lang, 1986).

Literature source	MTT concentration (mg.ml ⁻¹)	Solubilising solution	Wavelength (nm)
Mosmann, 1983	5	Acid - isopropanol	570
Denizot and Lang, 1986	5	Propanol	560
Alley <i>et al.</i> , 1988	5	DMSO	540
Klumper <i>et al.</i> , 1995	5	Acid - isopropanol	565
Petty <i>et al.</i> , 1995	5	DMSO	540
Sieuwerts <i>et al.</i> , 1995	6.5	DMSO	540
Yamaue <i>et al.</i> , 1996		DMSO	570
Liu <i>et al.</i> , 1997	2.5	50% N,N' - dimethylformamide and 20% sodium dodecyl sulphate in PBS	570

Table 3.4
Differences in various parameters of the MTT assay.

Most laboratories used two wavelengths, the first around 570 nm to detect the absorbance of MTT formazan and the second over 600 nm, to eliminate artefacts such as scratches on the wells. For this study a second wavelength was not used, only cell blanks measured at 570 nm, which were subtracted from the test wells.

Liu *et al.* (1997) has shown that it may not be only the mitochondria which reduce MTT, they have shown MTT formazan crystals in endosomes and liposomes. It was concluded that MTT formazan accumulates in the endosomal/lysosomal compartment and is then transported to the cell surface through exocytosis.

Other assays which could have been used to determine viability and cell number, include the ATP assay, which detects ATP using the firefly luciferase - luciferin system producing luminescence. ATP degrades quickly after death therefore its detection indicates the viability of a cell, the assay has better reproducibility and sensitivity than the MTT assay (Petty *et al.*, 1995). Manual cell counting using trypan blue exclusion could also have been used.

It has been established using the MTT assay that MCF-7/S and MDA MB 231 cells grow exponentially between 24 - 172 hours and using a seeding concentration of 2.5×10^5 cells/ml demonstrates a steep growth curve which was considered to be a suitable cell

concentration for the investigation of the cytotoxicity of doxorubicin and mitoxantrone using the MTT assay.

MCF-7/S cells were used throughout the study. The MTT assay was useful to study growth curves of the cell lines, but it was not considered suitable for simultaneous detection of doxorubicin. Trypan blue exclusion could have been used instead of the MTT assay to determine cell number and viability. The investigation of alternative viability probes, are described in the next chapter.

CELL VIABILITY STUDIES

3.3 **Cell viability studies**

The MCF-7/S and MCF-7/R cell lines were used to determine a suitable cytometric viability probe which could be used for FCM and LSC analysis. The most suitable presentation of samples to the LSC, for this study, was also investigated.

3.3.1 **Propidium iodide (PI)**

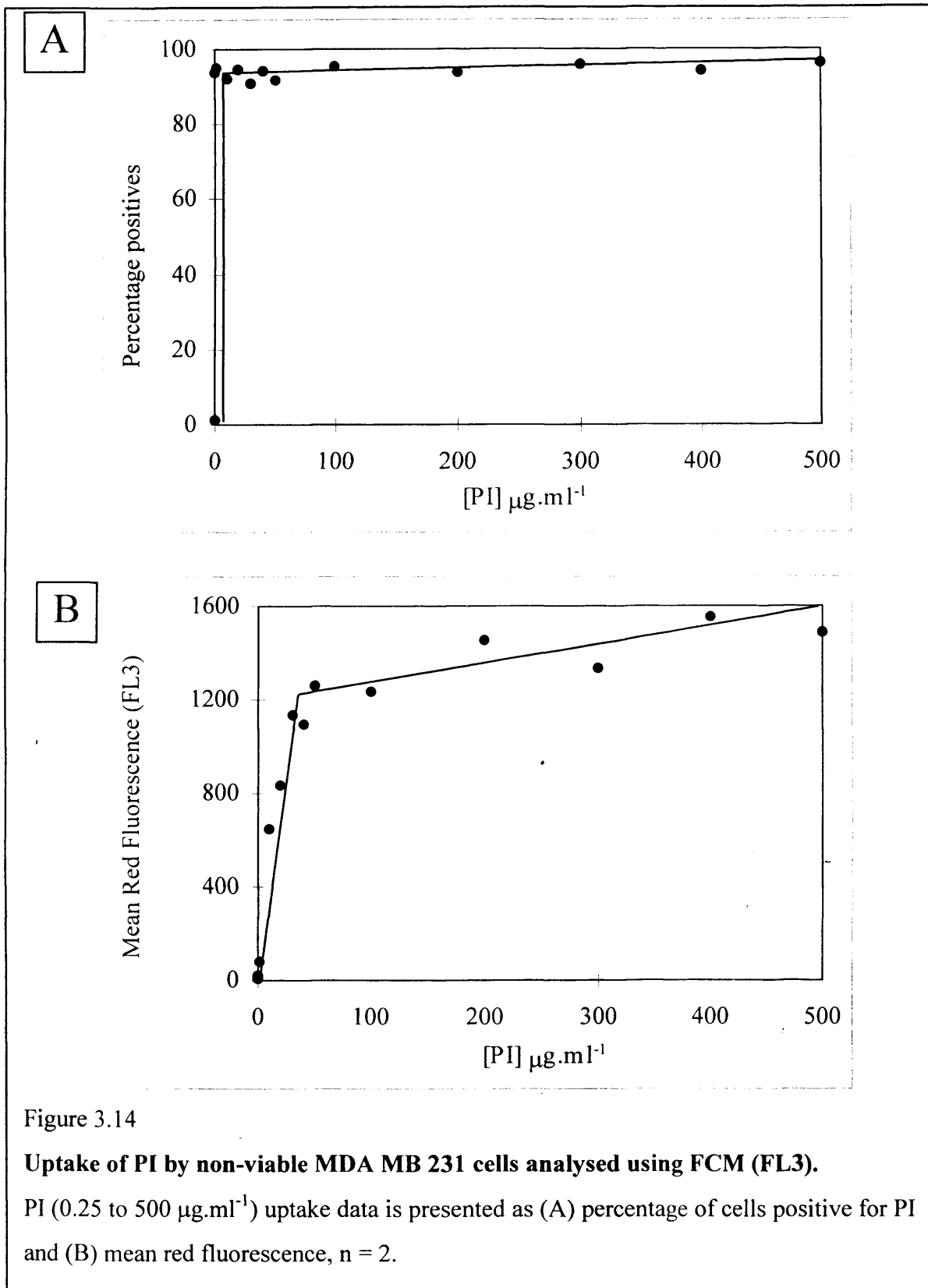
PI labels non - viable cells with a bright red/orange nuclear stain. The titration of PI ($0.25 - 500 \mu\text{g.ml}^{-1}$) using non - viable MDA MB 231 cells analysed by FCM is shown in figure 3.14, the cells became saturated $> 50 \mu\text{g.ml}^{-1}$ PI when the maximum fluorescence and percentage of positive cells was reached. A concentration of $50 \mu\text{g.ml}^{-1}$ and above would be suitable for a non-viable cell assay.

3.3.2 **Fluorescein diacetate (FDA)**

FDA labels viable unfixed cells with green fluorescence. Viable MDA MB 231 cells were titrated with $0.78 - 12.5 \text{ ng.ml}^{-1}$ FDA then analysed by FCM, the data is shown in figure 3.15. FDA $> 6.25 \text{ ng.ml}^{-1}$ demonstrated the maximum percentage of cells positive for fluorescence, although over the range of concentrations used the mean fluorescence has not reached maximum.

3.3.3 **Calcein AM**

Calcein AM labels viable unfixed cells with bright green fluorescence. The analysis of FCM data of calcein AM uptake ($0.05 - 1.05 \mu\text{mol.L}^{-1}$) using viable MCF-7/S and MCF-7/R cells are shown in figure 3.16. Single cells were isolated from cell debris using the light scatter parameters side scatter (SSC) and forward scatter (FSC) (SSC vs FSC). The fluorescence data produced was generated from the gated region (figure 3.16) which was used to generate the mean fluorescence data. Figure 3.16 illustrates two discrete populations of MCF-7/S calcein AM labelled cells.



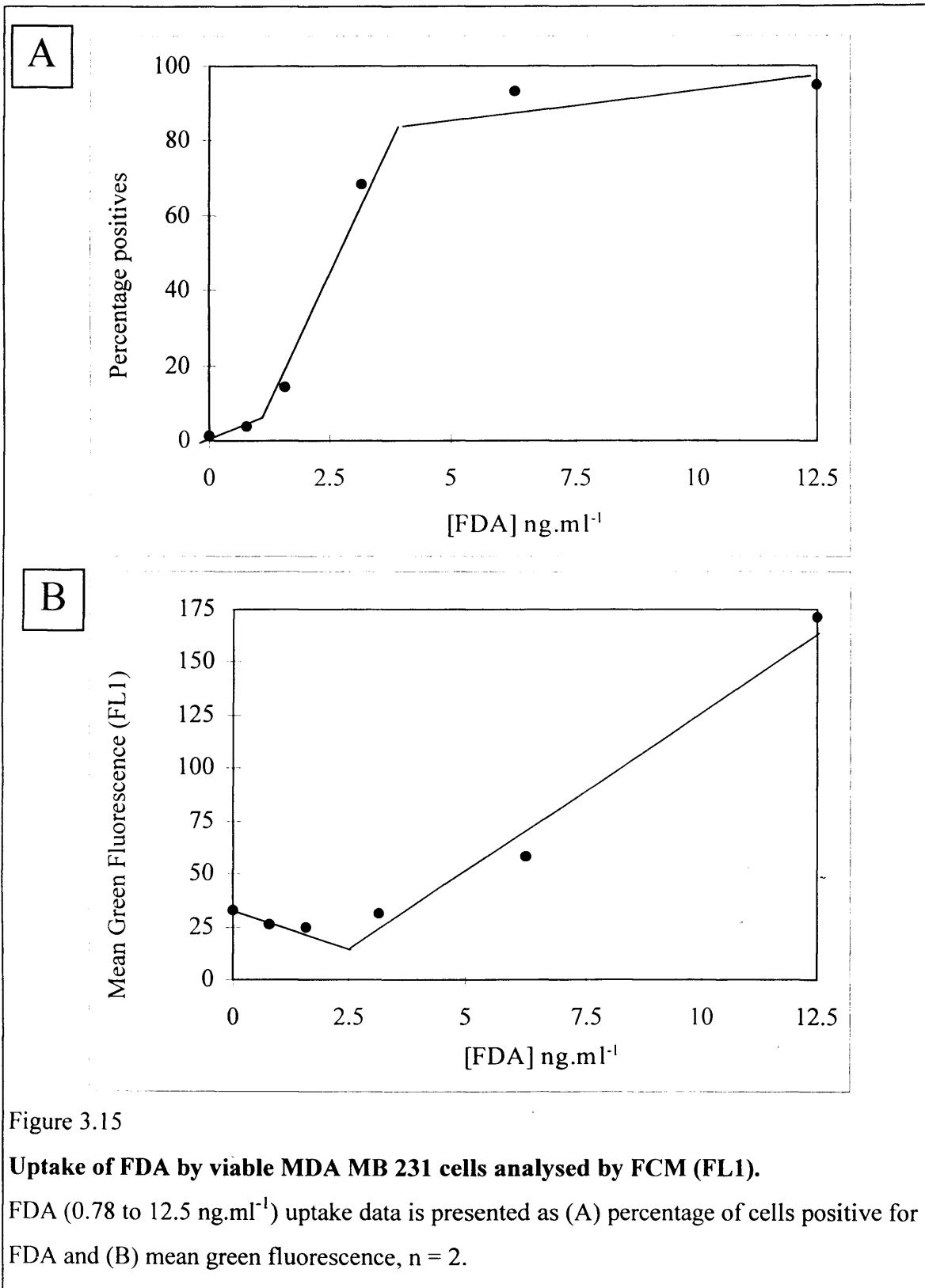


Figure 3.15

Uptake of FDA by viable MDA MB 231 cells analysed by FCM (FL1).

FDA (0.78 to 12.5 ng.ml⁻¹) uptake data is presented as (A) percentage of cells positive for FDA and (B) mean green fluorescence, n = 2.

The uptake of calcein AM (0.05 to 1.05 $\mu\text{mol.L}^{-1}$) using viable and non - viable MCF-7/S and MCF-7/R cells are shown in figure 3.17. A directly proportional linear

relationship between calcein AM concentration and fluorescence was demonstrated using viable MCF-7/S cells but only low levels of fluorescence were detected using other cells.

The calcein AM titration of viable and non-viable MCF-7/S and MCF-7/R cells were also analysed by LSC with chamber slide (light scatter computation) (figure 3.19) and cytocentrifuge preparation (green fluorescence computation) (figure 3.23). The LSC analysis of data collected using light scatter as the triggering signal was demonstrated in figure 3.18. LSC data was not regioned into 'single' cells like FCM, but histograms were created similarly, containing a positive region that would generate the mean integral and peak green fluorescence. Integral and peak fluorescence are illustrated for positive and negatively incubated viable MCF-7/S, which were overlaid to demonstrate the increases in fluorescence of the calcein AM incubated cells.

The titration of viable and non - viable MCF-7/S and MCF-7/R cells using chamber slides on the LSC, shown in figure 3.19, gave a very similar pattern of results to FCM, shown in figure 3.17. The mean integral and peak fluorescence measured from the chamber slides gave a similar pattern, although the levels of integral fluorescence were much higher.

Viable MCF-7/S cells incubated with $1.05 \mu\text{mol.L}^{-1}$ generate a bright green fluorescence, as detected by LSC and FCM. Figure 3.20 demonstrates a LSC dotplot from which, cells positive for calcein AM staining were visualised and images captured via a fluorescent microscope and the Kontron 100 image analysis system. The green fluorescent cells were relocated from the red region highlighted in the dotplot, demonstrating that this area contains single cells. The green calcein AM fluorescence images are true colour.

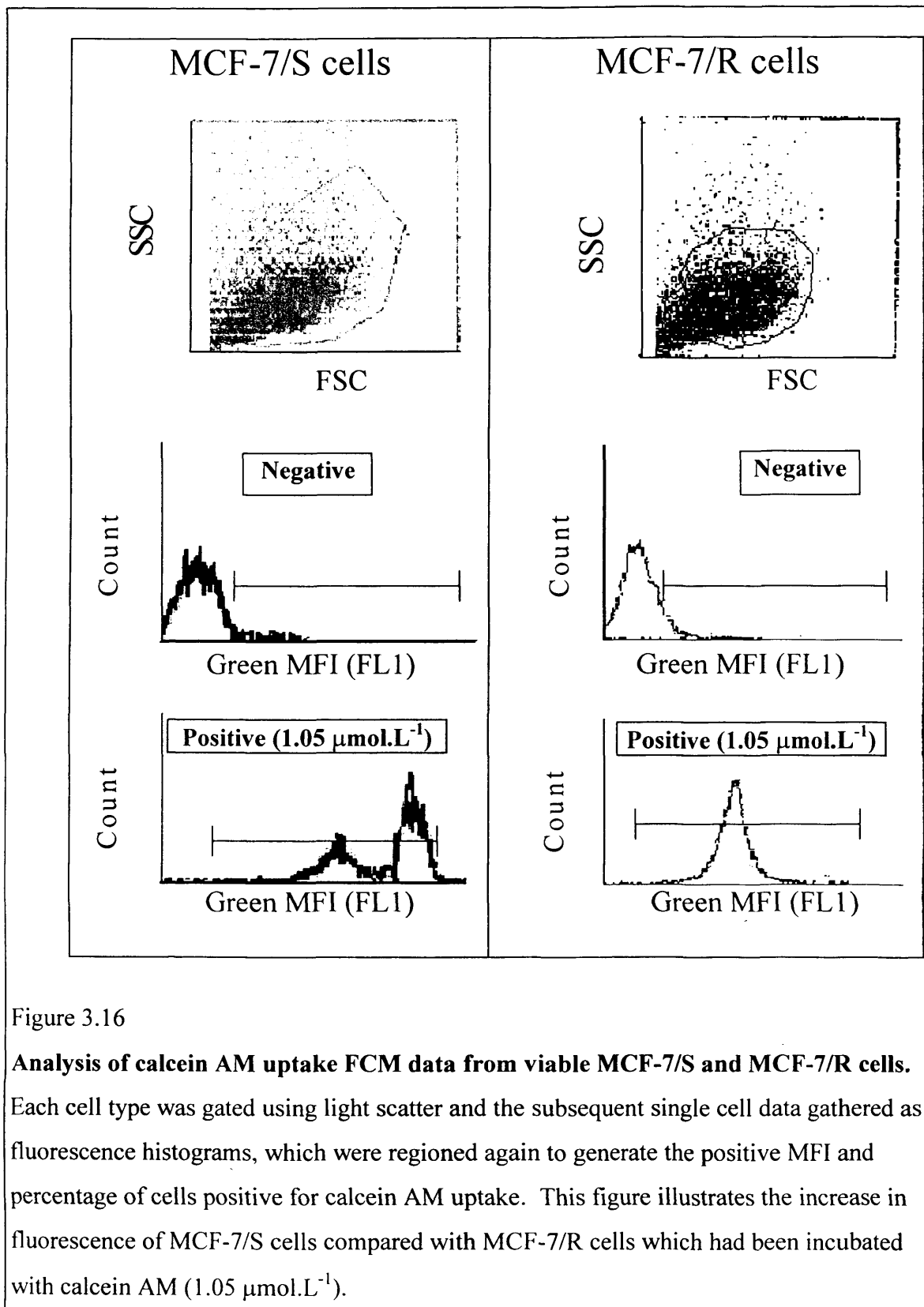


Figure 3.16

Analysis of calcein AM uptake FCM data from viable MCF-7/S and MCF-7/R cells.

Each cell type was gated using light scatter and the subsequent single cell data gathered as fluorescence histograms, which were regioned again to generate the positive MFI and percentage of cells positive for calcein AM uptake. This figure illustrates the increase in fluorescence of MCF-7/S cells compared with MCF-7/R cells which had been incubated with calcein AM (1.05 μmol.L⁻¹).

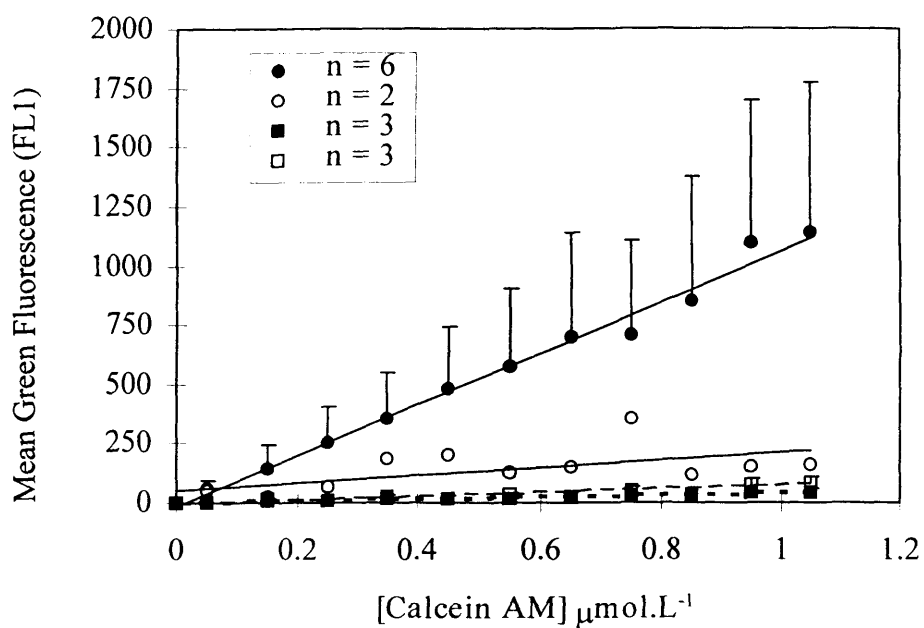


Figure 3.17

Uptake of calcein AM by viable and non - viable MCF-7/S and MCF-7/R cells analysed by FCM (FL1).

Calcein AM ($0 - 1.05 \mu\text{mol.L}^{-1}$) uptake data was presented as mean green fluorescence using MCF-7/S (●, ○) and MCF-7/R (■, □), viable (closed symbols) and non -viable (open symbols) cells. Error bars represent +/- 1SD.

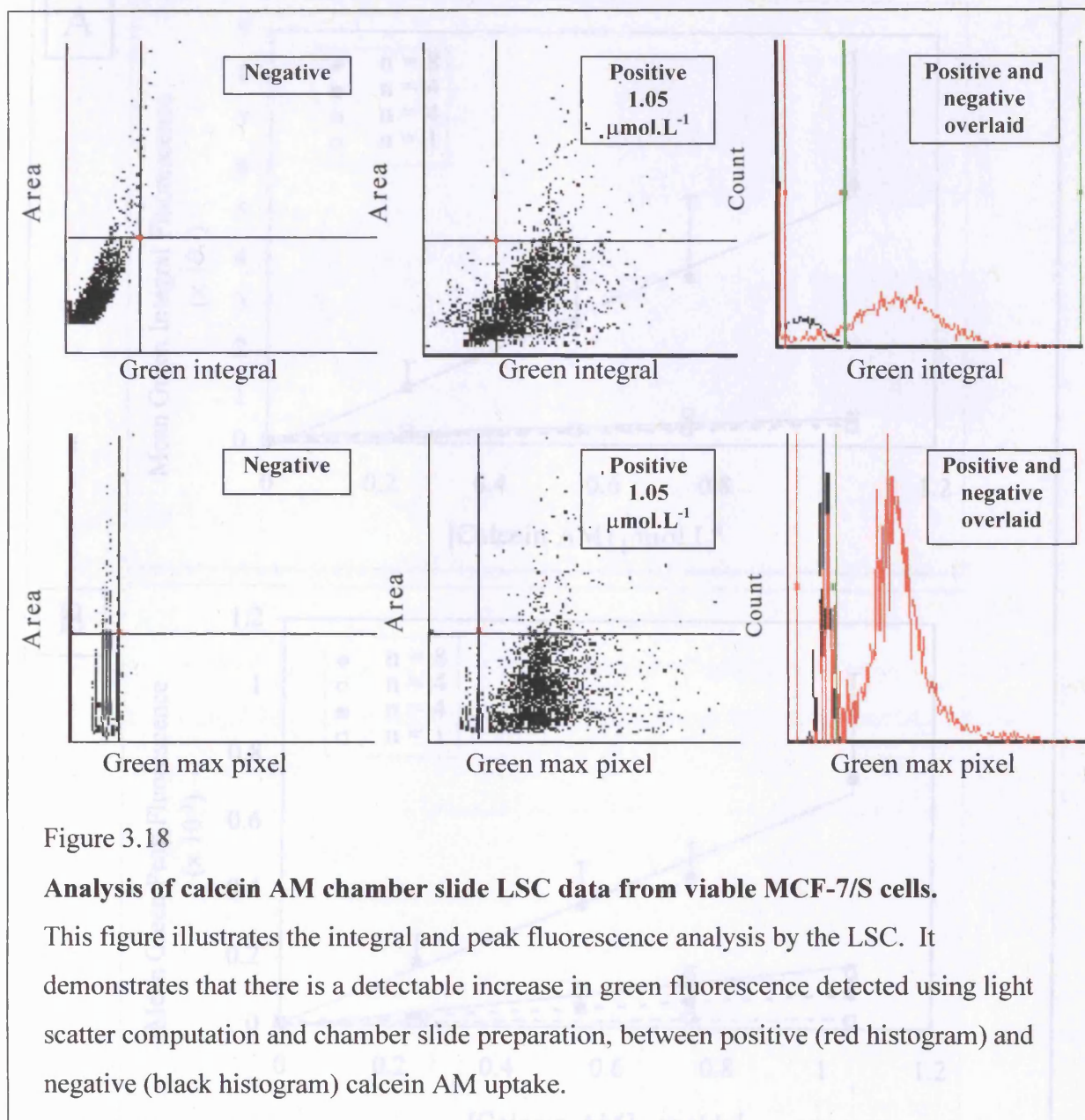
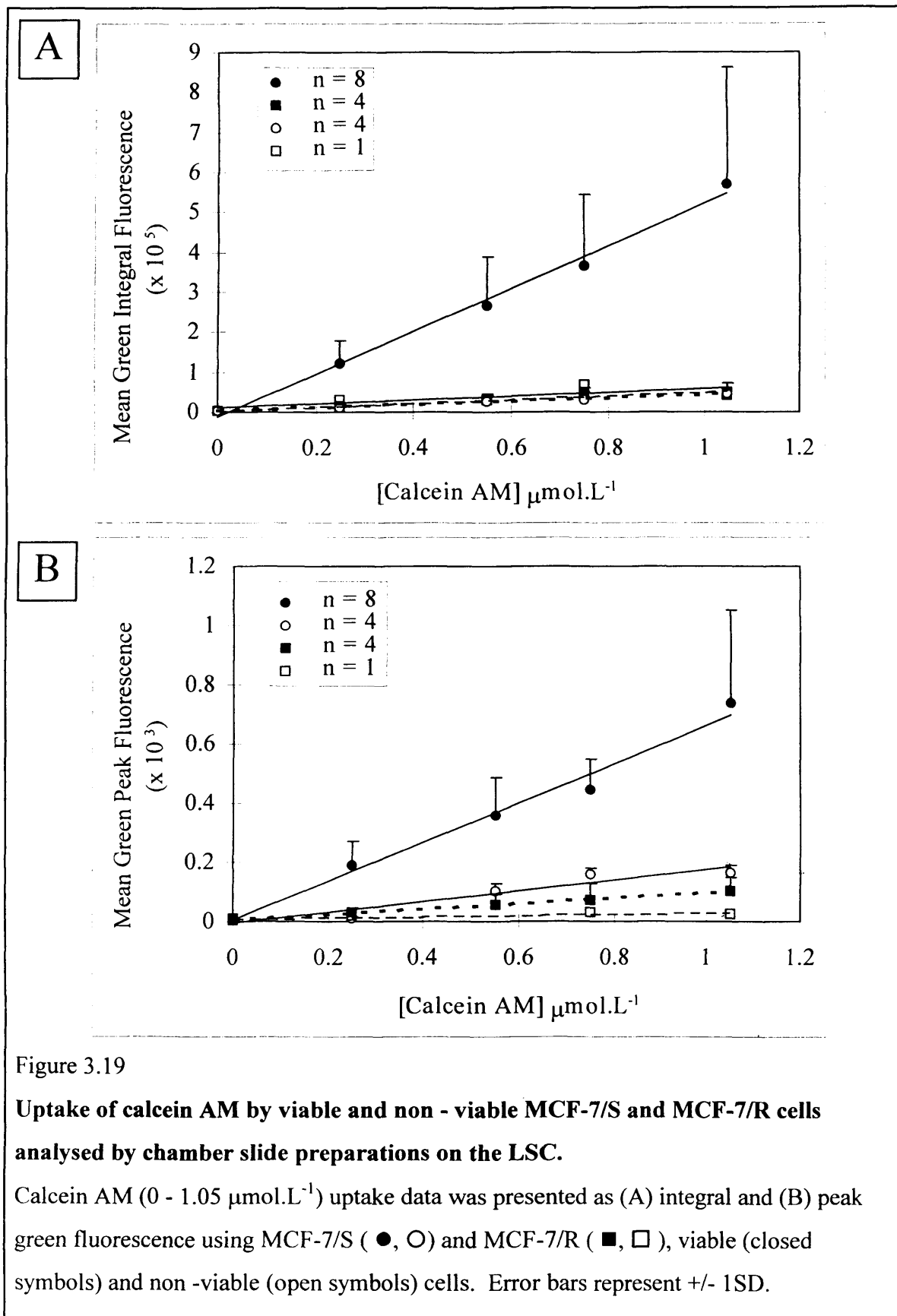


Figure 3.18

Analysis of calcein AM chamber slide LSC data from viable MCF-7/S cells.

This figure illustrates the integral and peak fluorescence analysis by the LSC. It demonstrates that there is a detectable increase in green fluorescence detected using light scatter computation and chamber slide preparation, between positive (red histogram) and negative (black histogram) calcein AM uptake.



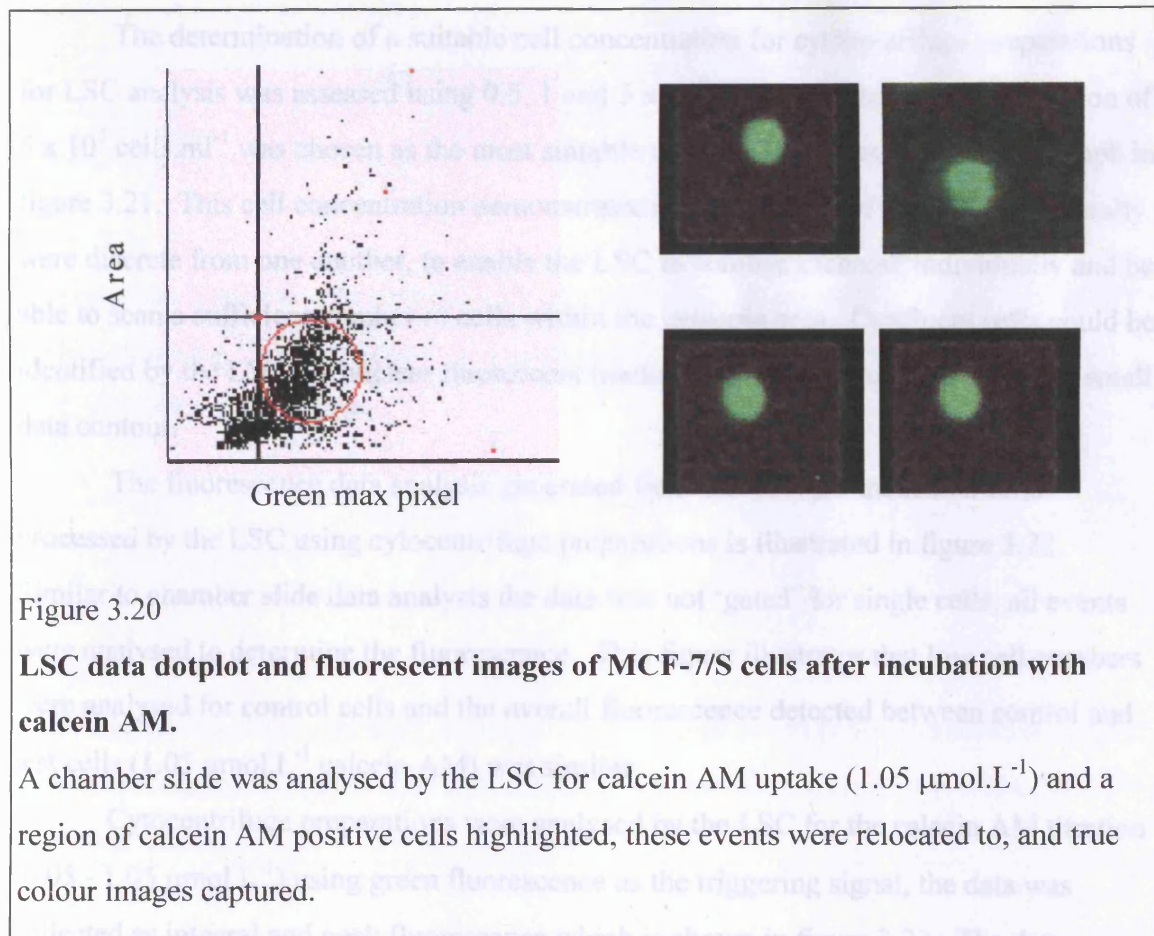


Figure 3.20

LSC data dotplot and fluorescent images of MCF-7/S cells after incubation with calcein AM.

A chamber slide was analysed by the LSC for calcein AM uptake ($1.05 \mu\text{mol.L}^{-1}$) and a region of calcein AM positive cells highlighted, these events were relocated to, and true colour images captured.

The determination of a suitable cell concentration for cytocentrifuge preparations for LSC analysis was assessed using 0.5, 1 and 5×10^5 cells/ml. The cell concentration of 5×10^5 cells.ml⁻¹ was chosen as the most suitable which is shown as a photomicrograph in figure 3.21. This cell concentration demonstrated an even spread of cells which generally were discrete from one another, to enable the LSC to contour each cell individually and be able to scan a sufficient number of cells within the cytospin area. Confluent cells could be identified by the LSC if a nuclear fluorescent marker was used in conjunction with a small data contour.

The fluorescence data analysis generated from calcein AM incubated cells processed by the LSC using cytocentrifuge preparations is illustrated in figure 3.22. Similar to chamber slide data analysis the data was not 'gated' for single cells, all events were analysed to determine the fluorescence. This figure illustrates that low cell numbers were analysed for control cells and the overall fluorescence detected between control and test cells ($1.05 \mu\text{mol.L}^{-1}$ calcein AM) was similar.

Cytocentrifuge preparations were analysed by the LSC for the calcein AM titration ($0.05 - 1.05 \mu\text{mol.L}^{-1}$) using green fluorescence as the triggering signal, the data was collected as integral and peak fluorescence which is shown in figure 3.23. The data produced from the cytocentrifuge preparations do not reveal a dose effect and exhibit very high standard deviation between results, the data, in general, was higher than the chamber slide equivalent.

Calcein AM uptake and its detection using flow cytometry or the LSC with chamber slides, could be used to distinguish between viable and non - viable MCF-7/S cells. Viable and non - viable MCF-7/R cells have a low calcein AM uptake therefore this vital dye could not distinguish between them.

There was a strong correlation between the fluorescence measured by FCM and LSC chamber slide, for integral and peak values, as described in tables 3.5 and 3.6. Using the Pearson r correlation, a perfect correlation between two sets of results would yield a result of 1 and two sets of results which demonstrate no correlation yield a correlation value of 0. The best correlation of results was for the analysis of viable MCF-7/S cells using integral and peak fluorescence.

	MCF-7/S viable	MCF-7/S non - viable	MCF-7/R viable
Pearson r	0.99	0.93	0.98

Table 3.5

Correlation results comparing the calcein AM values of mean fluorescence intensity measured using flow cytometry and peak maximum fluorescence measured using LSC with chamber slides.

	MCF-7/S viable	MCF-7/S non - viable	MCF-7/R viable
Pearson r	0.99	0.92	0.99

Table 3.6

Correlation results comparing the calcein AM values of mean fluorescence intensity measured using flow cytometry and integral fluorescence measured using LSC with chamber slides.

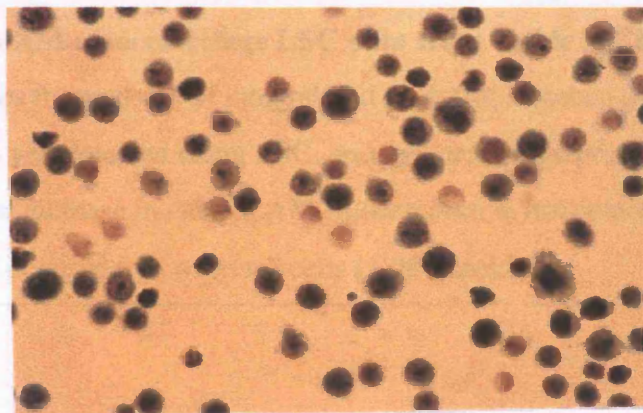


Figure 3.21

Cytocentrifuge preparation of 5×10^5 cells/ml MCF-7/S cells.

The cells were stained with Papanicolaou and the photomicrograph was taken using a light microscope using x 40 objective.

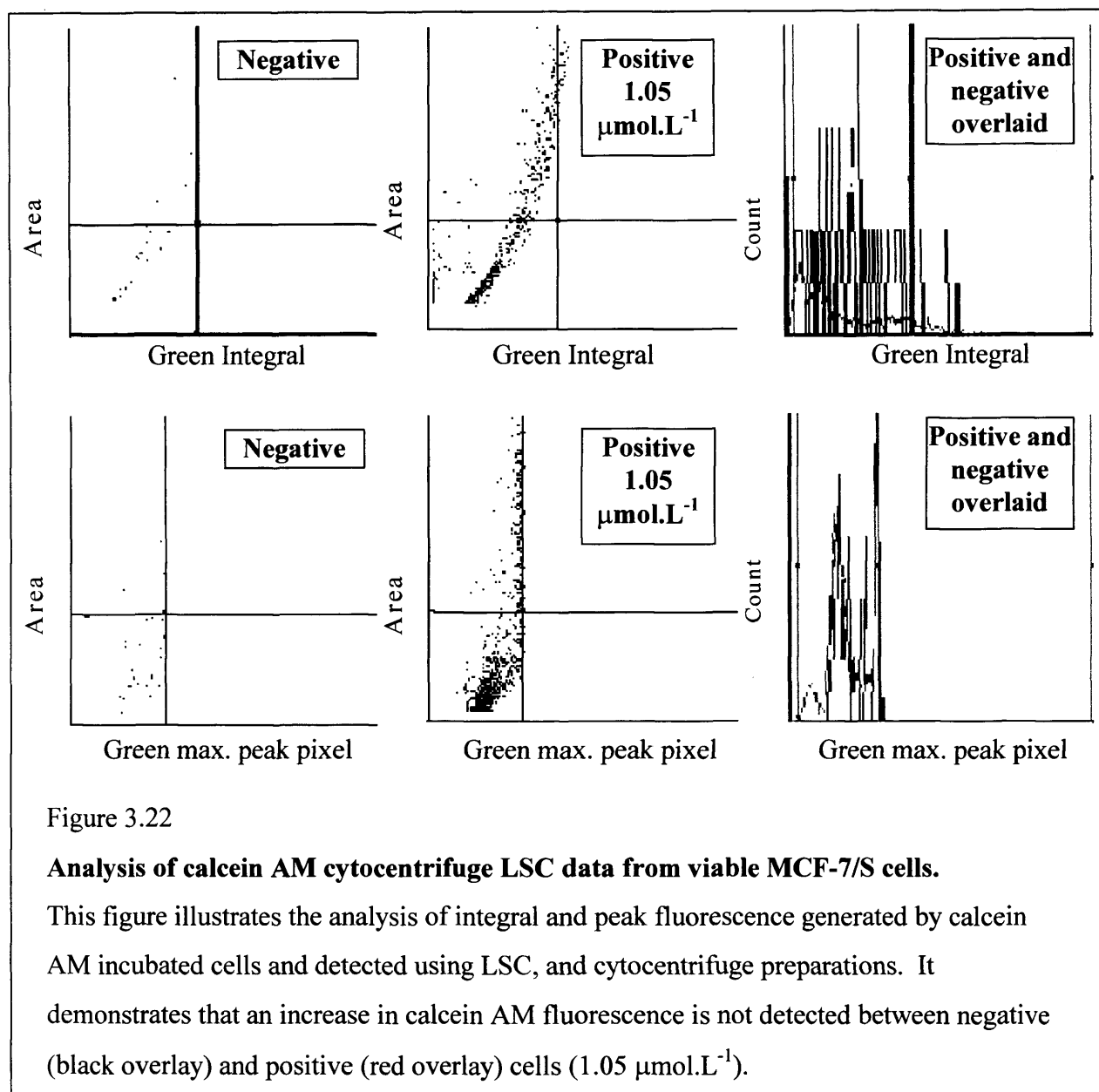


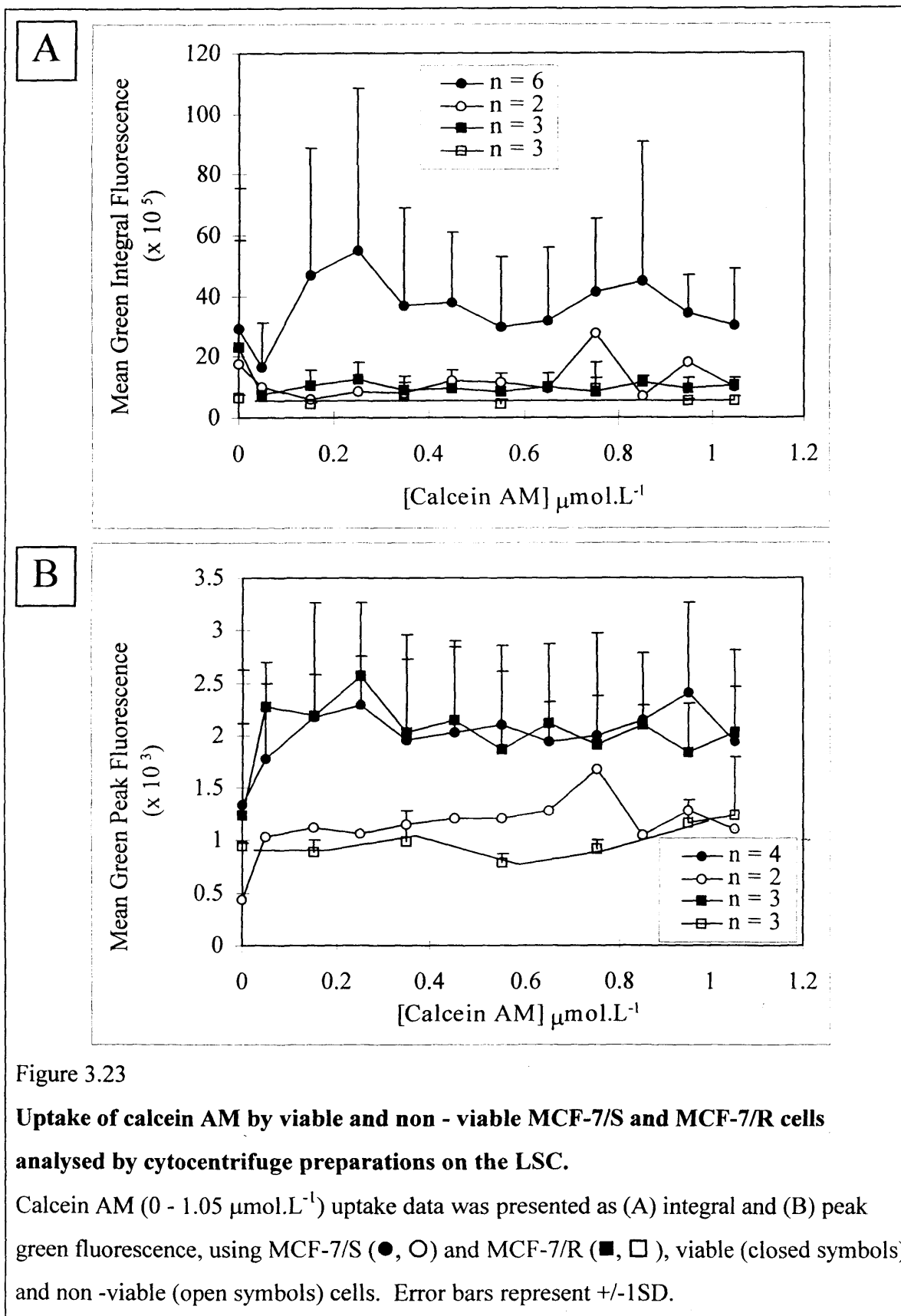
Figure 3.22

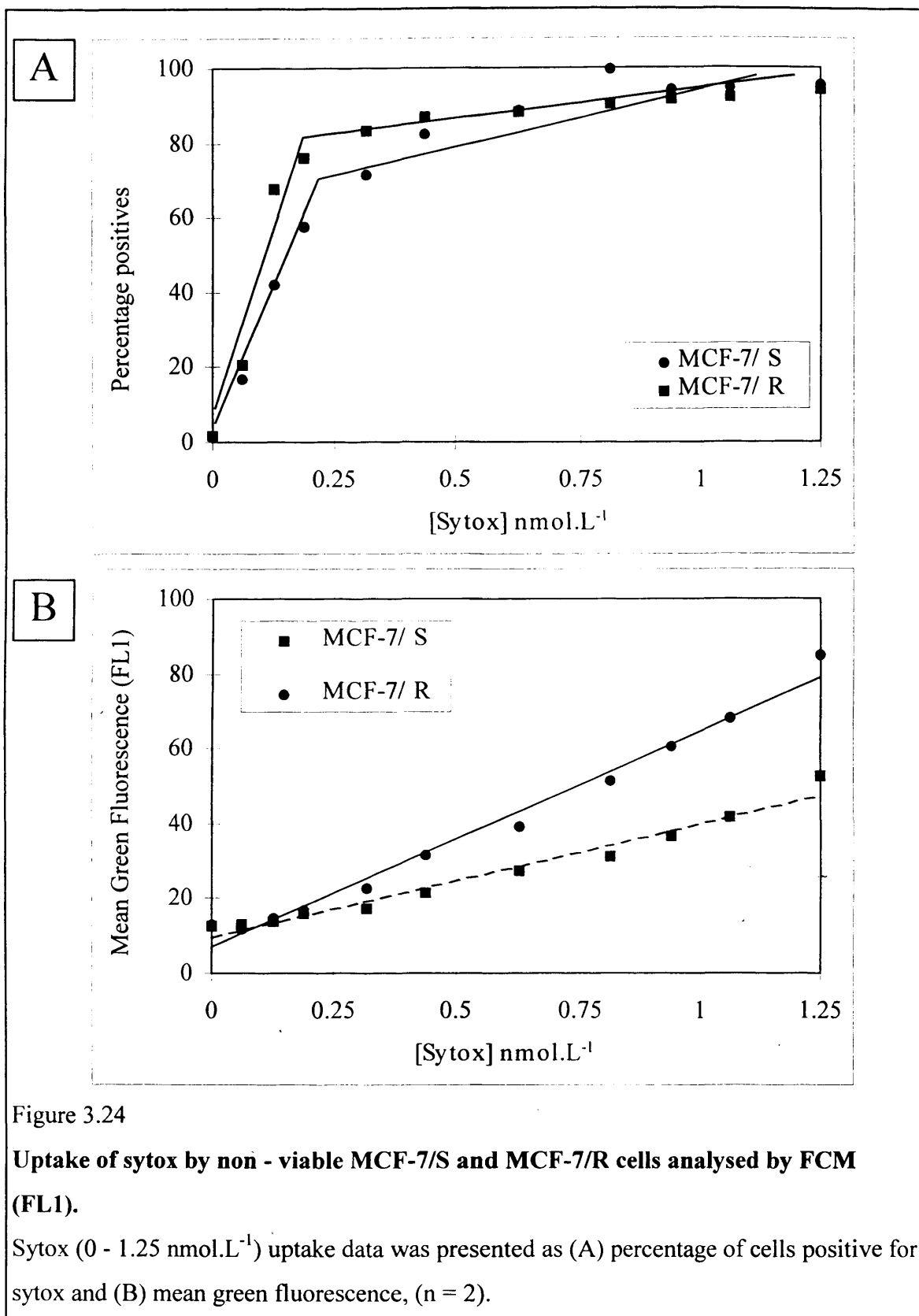
Analysis of calcein AM cytocentrifuge LSC data from viable MCF-7/S cells.

This figure illustrates the analysis of integral and peak fluorescence generated by calcein AM incubated cells and detected using LSC, and cytocentrifuge preparations. It demonstrates that an increase in calcein AM fluorescence is not detected between negative (black overlay) and positive (red overlay) cells ($1.05 \mu\text{mol.L}^{-1}$).

3.3.4 Sytox

Sytox labels non-viable cells with a green nuclear fluorescence. The sytox titration ($0.0625 - 1.25 \text{ nmol.L}^{-1}$) using non-viable MCF-7/S and MCF-7/R cells was analysed using FCM data shown in figure 3.24. The maximum percentage of positive cells was at $>0.6 \text{ nmol.L}^{-1}$ sytox. The relationship between sytox concentration and detected fluorescence was directly proportionally linear.





3.3.5 Discussion

The objective of these experiments was to assess the best fluorescent reagent for determining the viability of cells using LSC and FCM, allowing simultaneous doxorubicin detection. PI (Krishan, 1975 and Dengler *et al.*, 1995) is often used for distinguishing between viable and non-viable as it demonstrates a bright nuclear signal, but its red/orange fluorescence is a similar wavelength to doxorubicin and therefore is detected using the same PMT of FCM and LSC, differentiating between these signals would be difficult.

FDA (Rotman and Papermaster, 1965) produces a bright green fluorescence from viable unfixed cells, which can be detected simultaneously with doxorubicin. However, FDA has inherent problems as a viability probe, once it has been cleaved to produce fluorescein it can leak out of cells. Other agents which have been used as viability probes include calcein AM, BCECF - AM, acridine orange and carboxyFDA, of which calcein was found to be the least pH sensitive (Haughland, 1996 and Moore *et al.*, 1990). The loading of calcein AM and BCECF AM creates brightly fluorescent viable cells with a low extracellular background, but FDA and carboxyFDA exhibited dimly green fluorescent cells and gave a high extracellular background (Moore *et al.*, 1990). The use of calcein AM staining as a viability probe has been shown to demonstrate agreement with trypan blue exclusion cell counts (Moore *et al.*, 1990). Calcein fluorescence can decrease over time, after 4 hours its fluorescence had decreased by 12% (Wang *et al.*, 1993), therefore the measurement of calcein fluorescence for this study, was measured within 4 hours of the assay being completed. The decline in calcein fluorescence was less than other agents including carboxyFDA (Wang *et al.*, 1993).

Calcein AM could have been a good option for this study. The non-fluorescent calcein AM is cleaved by esterases only within viable cells to yield the fluorescent calcein agent which is retained in the cell. Thus it labels viable cells creating an inclusion criteria for cells, which could subsequently also be analysed for doxorubicin uptake. However calcein AM could not distinguish between viable and non-viable resistant MCF-7/R cells, as the viable MCF-7/R cells only demonstrate a weak calcein fluorescence. This is because calcein AM is also a multidrug resistant analyte (Liminga *et al.*, 1996 and Homolya *et al.*, 1993) which has been utilised as a functional test for the presence of the MDR ATPase pump, P-glycoprotein (P-gp), (Liminga *et al.*, 1996). P-gp is commonly found in large quantities within the plasma membranes of certain tumour cell

types (Goldstein *et al.*, 1992), including the MCF-7/R cells (Davies *et al.*, 1996) as well as constitutively in some normal tissues (Tiberghien and Loor, 1996). Therefore high expression of the pump prevents the accumulation of calcein AM within the cell, thus decreasing the conversion of calcein AM to calcein. As the retention difference of calcein is so pronounced between sensitive and resistant cells this fluorescent probe was considered not to be ideal for this study.

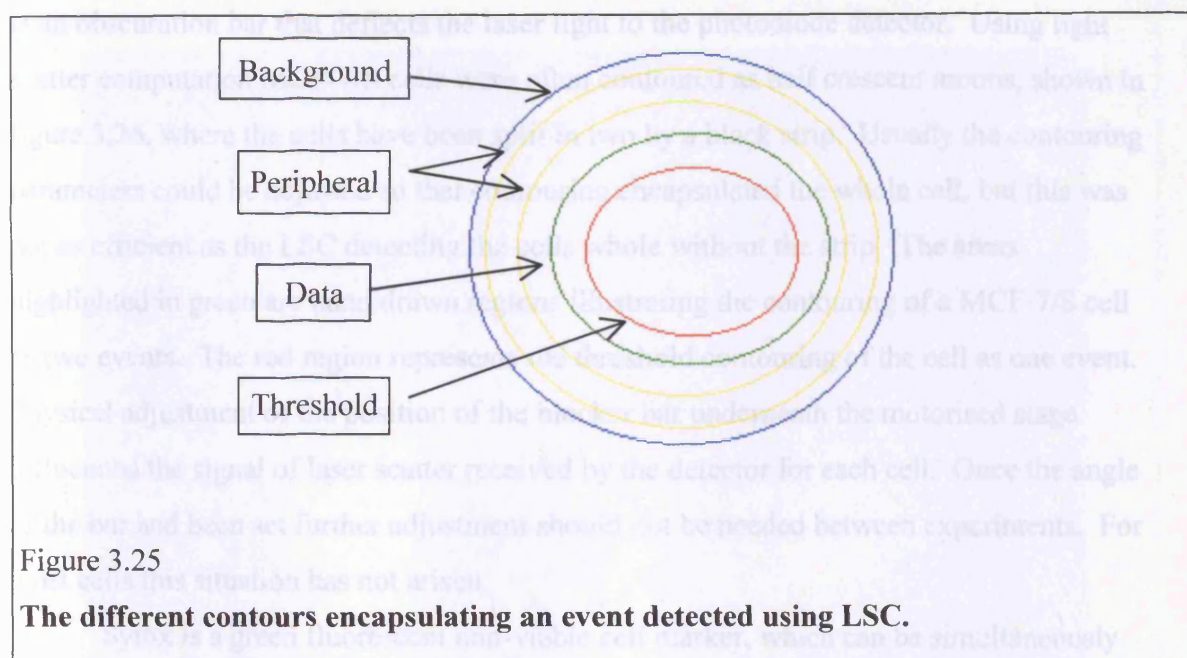
The incubation of viable MCF-7/S cells with calcein AM demonstrated two fluorescent populations (figure 3.16). As the cells used for these experiments were all >85% viable, the low green fluorescent population of about 50% of the cells could not represent the non-viable cells. The reasons for the heterogeneity in the MCF-7/S cell population have not been investigated in this study. It could be caused by different levels of esterase activity within the cell population. Alternatively, it could be possible that there was a subset of doxorubicin resistant cells within the MCF-7/S cells, but this would have been seen when the cells were incubated with doxorubicin (section 3.4.2), where only a single cell population was seen. Subsequent studies by Davinder Kaur in which MCF-7/S cells were cultured in the presence of doxorubicin showed this line to be 100% drug sensitive. The presence of P - gp on cells could have been measured with an antibody that blocks P - gp activity, which could have been used to block leakage of calcein AM from the cells. Anti - P - gp antibodies have been produced including MRK16, UIC2, JSB - 1 and C219 (Shi *et al.*, 1995 and Lehne *et al.*, 1995). MRK16 and UIC2 are directed against surface epitopes of P - gp and therefore can be used to label viable cells. JSB - 1 and C219 are directed against intracellular epitopes and are thus intracellular markers of P - gp. Using sensitive and resistant human hepatoma (HB8065) and leukaemic (KG1a) cell lines the surface antibodies MRK16 and UIC2 were reported to show better discrimination between resistant (P - gp positive), and sensitive (P - gp negative) cells than the internal epitopes antibodies (Lehne *et al.*, 1995). P - gp can also be blocked easily using a variety of calcium channel blockers, such as verapamil and vincristine (Krishan, 1994). Using different combinations of modulators and inhibitors, transport protein - specific assays can be created. Feller *et al.* (1995) demonstrated that the use of daunorubicin and the inhibitor genistein could be used in combination as a multidrug resistance - associated protein (MRP) specific assay, whereas calcein AM and vincristine demonstrated the effects of MRP and MDR (P- gp). The mitochondrial polarisation dye Rh123 has also been

demonstrated to show a decrease in accumulation within cells which have MRP but are MDR negative (Twentyman *et al.*, 1994).

The LSC data for calcein AM titration was considerably different between the chamber slide and cyto centrifuge preparations, figure 3.19 and 3.23, respectively. The titration of calcein AM using light scatter detection (chamber slides) on the LSC gave a good correlation between both green integral, and maximum peak pixel fluorescent values and the MFI detected using FCM. These results highlight that the data produced by the LSC using chamber slides for single colour analysis of calcein AM is very similar and comparable to flow cytometry data. The integral and maximum peak pixel results using cyto centrifuge preparations whilst giving comparable data to each other, did not display an increase in fluorescence as the calcein AM concentration increased.

The triggering signal for cell detection using calcein AM cyto centrifuge preparations on the LSC was green fluorescence. After a fluorescence signal has been accepted as an event the outline of this signal was surrounded by a threshold contour, shown in figure 3.25. The threshold contour will encapsulate the green fluorescent signal, it is dependent on user-defined variables including cell size and fluorescent signal triggering level. The data contour is a function of the threshold contour, it contains the area within the threshold contour with the addition of a user - defined number of pixels. The pixels detected within the data contour create the data set of fluorescence measurements for each cell. The contour arrangement using laser scatter as the triggering parameter is the same as described above.

Using light scatter as the triggering signal for the threshold contour should, on the other hand, encapsulate the majority of the cell, not just the area which contains fluorescent signal. The data contour therefore would create a small extension of the threshold contour, surrounding the cell without a large area of slide. For this study using light scatter gave a better representation of the cell fluorescence, enabling all the fluorescence to be measured within the cell.



Nuclear staining and fluorescent triggering (Kamentsky and Kamentsky, 1991; Rew *et al.*, 1998 and Woltmann *et al.*, 1999) is more commonly used for LSC analysis than laser scatter contouring (Musco *et al.*, 1998 and Clatch *et al.*, 1996). PI is often used as a nuclear marker (Luther and Kamentsky, 1996; Gorczyca *et al.*, 1996 and Deptala *et al.*, 1998) as it is bright and consistently localised within the nucleus. Broad cytoplasmic stains may not be suitable triggering signals if they create patches of fluorescence that could lead to single cells being contoured as many small events. Nuclear fluorescent staining is sufficient as the triggering event for single colour quantification if the signal is bright and staining consistent. PI or other DNA stains, could be used as cell markers for threshold contouring and other probes used to simultaneously label other cellular constituents of quantitative interest. Woltmann *et al.* (1999) developed quantitative analysis of eosinophils and bronchial epithelial cells from induced sputum. A cytocentrifuge preparation system was used staining all cells with PI, the red fluorescence was used as the contouring trigger, with eosinophils and epithelial cells detected with Oregon Green labelled specific antibodies. Although this threshold trigger is nuclear in location, the data contour was extended several pixels from the threshold contour to ensure all cytoplasmic staining was detected. The setting of the data contour is not ideal, for all the cells to be included within a contour inevitably area of the slide will be included, unless the cell is the same shape as the nucleus.

Underneath the motorised stage and above the laser scatter detector assembly there is an obscuration bar that deflects the laser light to the photodiode detector. Using light scatter computation MCF-7/S cells were often contoured as half crescent moons, shown in figure 3.26, where the cells have been split in two by a black strip. Usually the contouring parameters could be adjusted so that contouring encapsulated the whole cell, but this was not as efficient as the LSC detecting the cells whole without the strip. The areas highlighted in green are hand drawn regions illustrating the contouring of a MCF-7/S cell as two events. The red region represents the threshold contouring of the cell as one event. Physical adjustment of the position of the blocker bar underneath the motorised stage influenced the signal of laser scatter received by the detector for each cell. Once the angle of the bar had been set further adjustment should not be needed between experiments. For most cells this situation has not arisen.

Sytox is a green fluorescent non-viable cell marker, which can be simultaneously detected with doxorubicin. This viability probe was measured in this study exclusively using FCM. Sytox is a relatively new fluorescent agent which is marketed by Molecular Probes, it has been described as producing DNA histograms equivalent to the quality of those produced by PI (Haughland, 1996). Sytox strongly and specifically stains nuclear DNA and it suitable for use as a nuclear marker for laser confocal microscopy (Matsuzaki *et al.*, 1997). Sytox gave a different level of fluorescence with non-viable MCF-7/S and MCF-7/R in the FCM. This difference was not so pronounced as that described for calcein AM (figure 3.17), therefore sytox was a more suitable choice of viability probe for this study. The titration of sytox was not performed on viable MCF-7/S and MCF-7/R cells, which would have been a good comparison to ensure that sytox uptake of non-viable cells was significantly higher than using viable cells. Comparison of FCM and LSC sytox uptake results should also have been carried out.

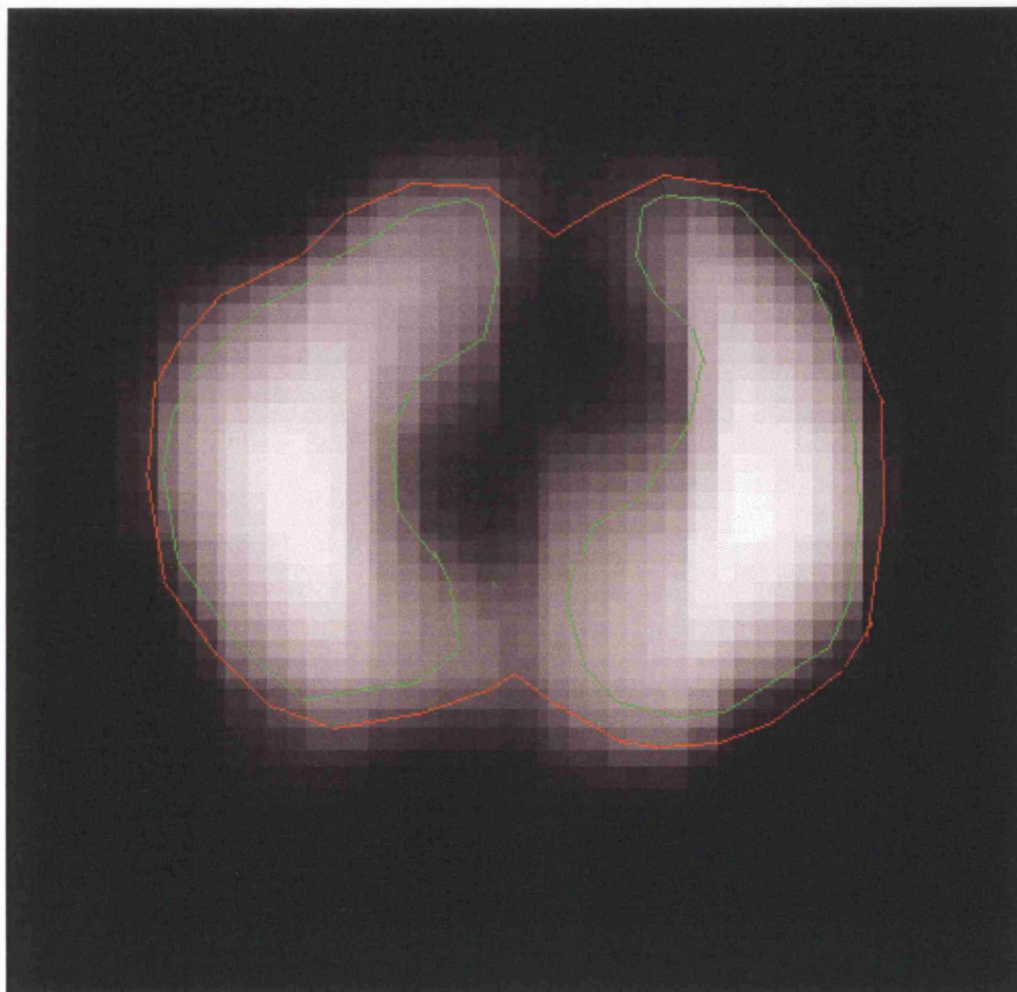


Figure 3.26

Laser scatter image and threshold contouring of a MCF-7/S cell scanned by the LSC.

The green regions are illustrating how the LSC can contour one cell as two, and the red region shows the LSC contouring the cells as a whole, compensating for the black strip.

There are other fluorescent agents available commercially which are claimed to be capable of determining cell viability using flow cytometry and other fluorescent detection systems. The majority of these agents are available from Molecular Probes, Inc. (Eugene, Oregon, USA). Calcein AM is advertised by Molecular Probes as both a constituent of a viability kit (Live/Dead viability/cytotoxicity kit) but also for multidrug resistance assays (Vybrant multidrug resistance assay kit). Another possible agent is DiOC₁₈ which is included in a kit for measuring cell - mediated cytotoxicity. Dioctadecyloxycarbocyanine

(DiO) is a derivative of cyanine dyes, the octadecyl (C_{18}) side chain of this probe attaches to the lipid bilayer of the cell, whilst the chromophore remains on the cell surface (Shapiro, 1995). DiOC₁₈ is a green stain which labels live cells, within the kit it is coupled with PI, which stains non - viable cells red/orange. Another family of dyes available from Molecular Probes, are the syto dyes. Syto 16 has been used by Luther and Kamensky (1996) to detect live COS-7 cells. Rhodamine 123 (Rh123) is a cationic dye which accumulates in the mitochondria of live cells, and emits a green fluorescence. The green viability dyes such as syto 16 and Rh123 could be other agents that are suitable for use in this study.

**ANTHRACYCLINE
UPTAKE AND
CONSEQUENT
VIABILITY OF
MCF-7/S AND
MCF-7/R CELLS**

3.4 Anthracycline uptake and consequent viability of MCF-7/S and MCF-7/R cells

3.4.1 Mitoxantrone uptake of MCF-7/S cells

The FCM analysis of a mitoxantrone titration is illustrated in figure 3.27. All events were regioned using 'SSC vs FCS' dotplot determining single cells using size parameters. From the positive region histograms were produced to generate the MFI and percentage positive data for each sample. This figure illustrates the difference in fluorescence between a positive and negative sample.

MCF-7/S cells were incubated in 1 – 100 $\mu\text{mol.L}^{-1}$ mitoxantrone and analysed using FCM to measure fluorescence, these data are shown in figure 3.28. The maximum number of cells retained mitoxantrone at $>15 \mu\text{mol.L}^{-1}$, and fluorescence was directly proportional to fluorescence up until $\geq 25 \mu\text{mol.L}^{-1}$, after which concentration the fluorescence began to plateau.

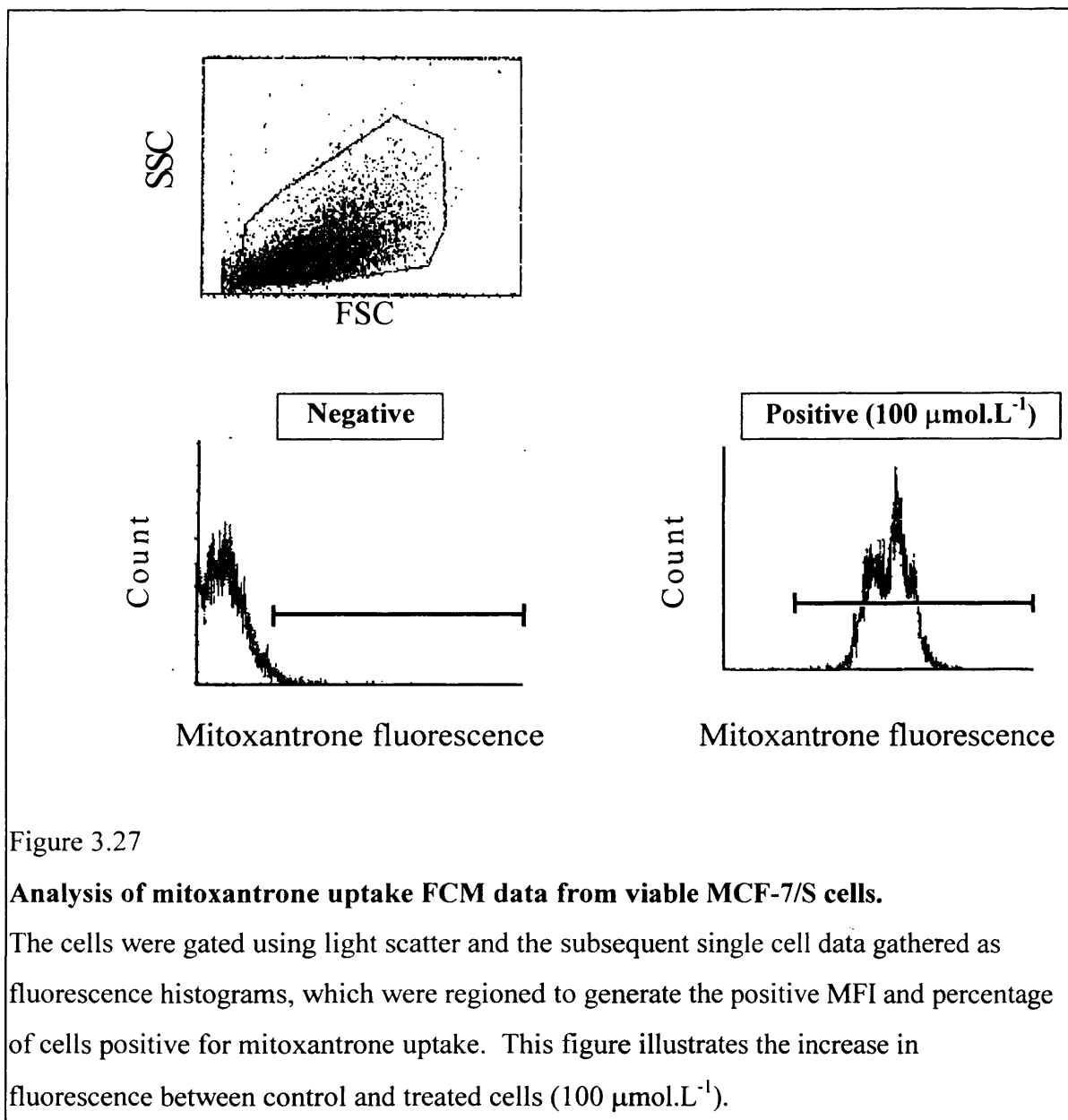
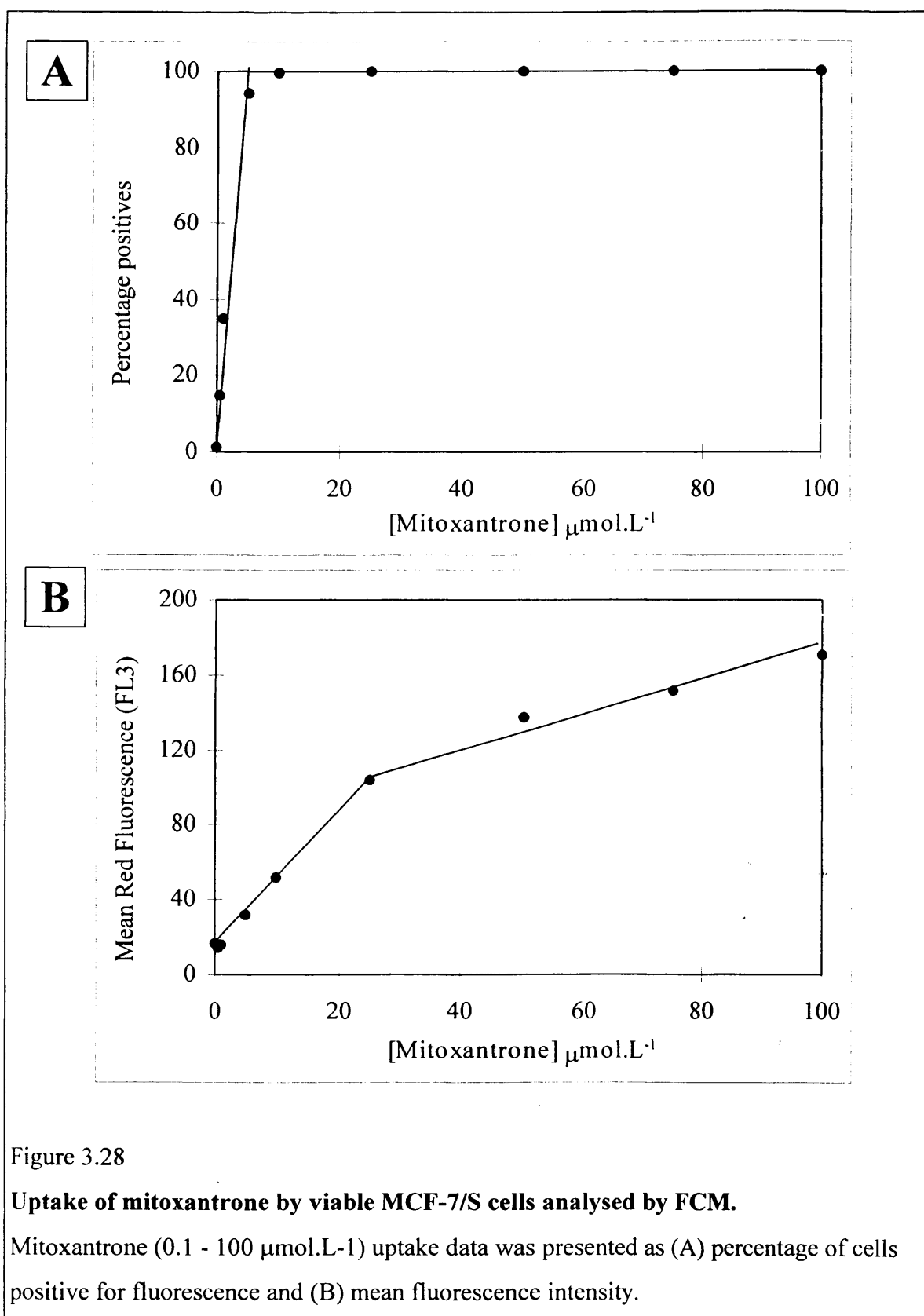


Figure 3.27

Analysis of mitoxantrone uptake FCM data from viable MCF-7/S cells.

The cells were gated using light scatter and the subsequent single cell data gathered as fluorescence histograms, which were regioned to generate the positive MFI and percentage of cells positive for mitoxantrone uptake. This figure illustrates the increase in fluorescence between control and treated cells (100 μmol.L⁻¹).



3.4.2 Doxorubicin uptake and consequent viability.

MCF-7/S and MCF-7/R cells were incubated with doxorubicin and analysed on FCM and LSC, using cytocentrifuge and chamber slide preparations. After the time course of 4 – 144 hours, uptake of doxorubicin, viability and apoptotic status of the cells were measured by FCM.

3.4.2.1 Flow cytometry

The FCM analysis of the doxorubicin titration using MCF-7/S and MCF-7/R cells is illustrated in figure 3.29. Single cells were gated using ‘SSC vs FCS’ dotplot, producing histograms for the MFI and percentage positive data. This figure illustrates the characteristically higher doxorubicin fluorescence of the MCF-7/S cells compared with the MCF-7/R cells.

The results from the titration of viable and non - viable MCF-7/S cells and viable MCF-7/R cells using a one hour incubation with 0 - 86.25 $\mu\text{mol.L}^{-1}$ doxorubicin, are shown in figure 3.30. The fluorescence detected for each cell line was directly proportional to the lower doxorubicin concentrations, but at the high concentrations the fluorescence began to plateau as it became quenched. Viable MCF-7/S cells demonstrated a greater retention of doxorubicin than viable MCF-7/R cells, but the highest fluorescence was measured from the non-viable MCF-7/S cells.

The doxorubicin retention of viable MCF-7/S cells after incubation with 10 and 100 $\mu\text{mol.L}^{-1}$ of drugs is illustrated in figures 3.31 and 3.32. At these high doxorubicin concentrations fluorescence is noted in the whole cell, not just isolated to the nucleus. These light and fluorescent microscopy images were captured using an image analysis system (Kontron 100).

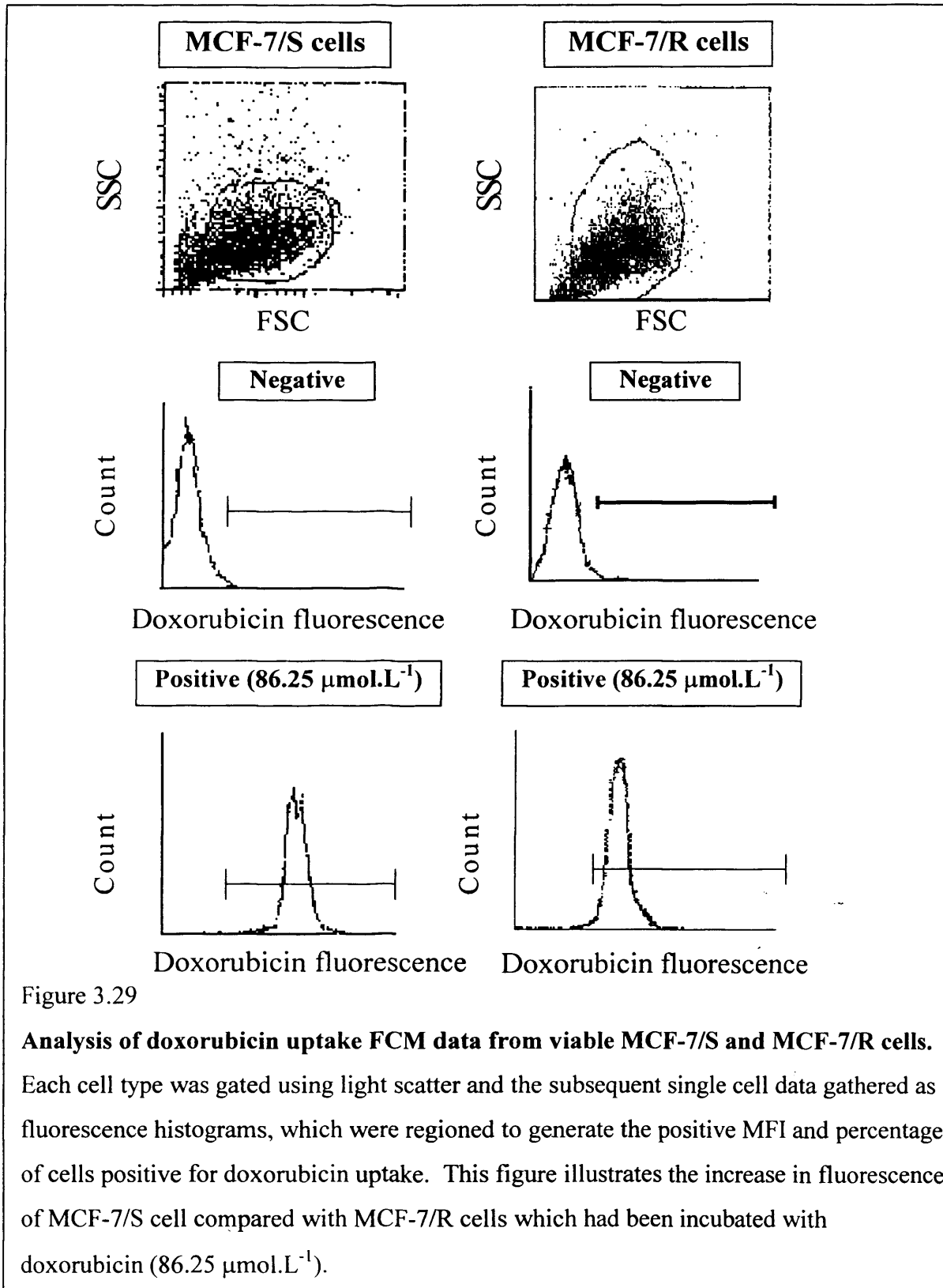


Figure 3.29

Analysis of doxorubicin uptake FCM data from viable MCF-7/S and MCF-7/R cells. Each cell type was gated using light scatter and the subsequent single cell data gathered as fluorescence histograms, which were regioned to generate the positive MFI and percentage of cells positive for doxorubicin uptake. This figure illustrates the increase in fluorescence of MCF-7/S cell compared with MCF-7/R cells which had been incubated with doxorubicin (86.25 μmol.L⁻¹).

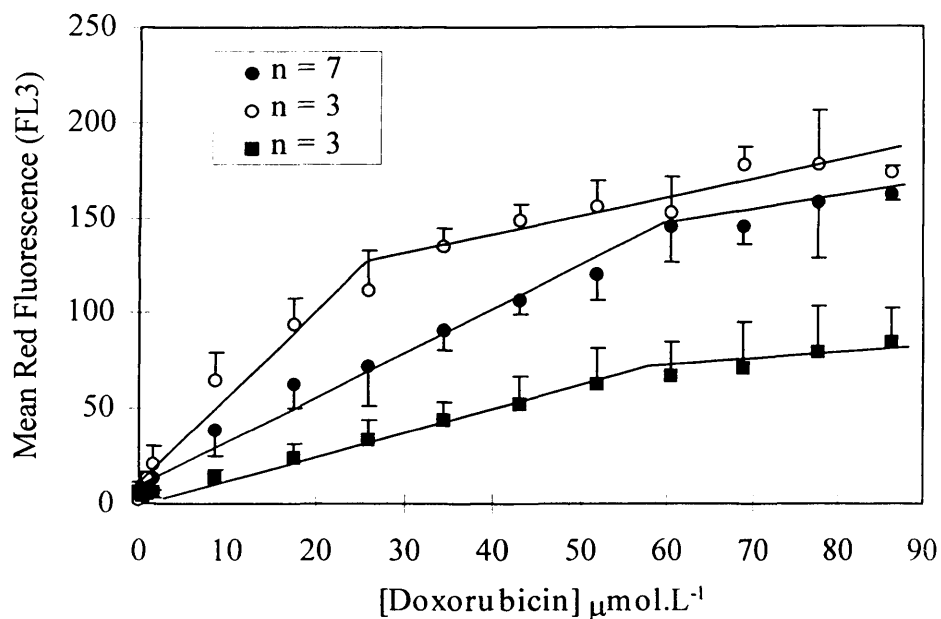


Figure 3.30

Uptake of doxorubicin by viable and non - viable MCF-7/S cells and viable MCF-7/R cells, analysed by FCM (FL3).

Doxorubicin (0 - 86.25 $\mu\text{mol.L}^{-1}$) uptake data was presented as mean red fluorescence using MCF-7/S (●, ○) and MCF-7/R (■) viable (closed symbols) and non - viable (open symbols) cells. Error bars represent +/- 1SD.

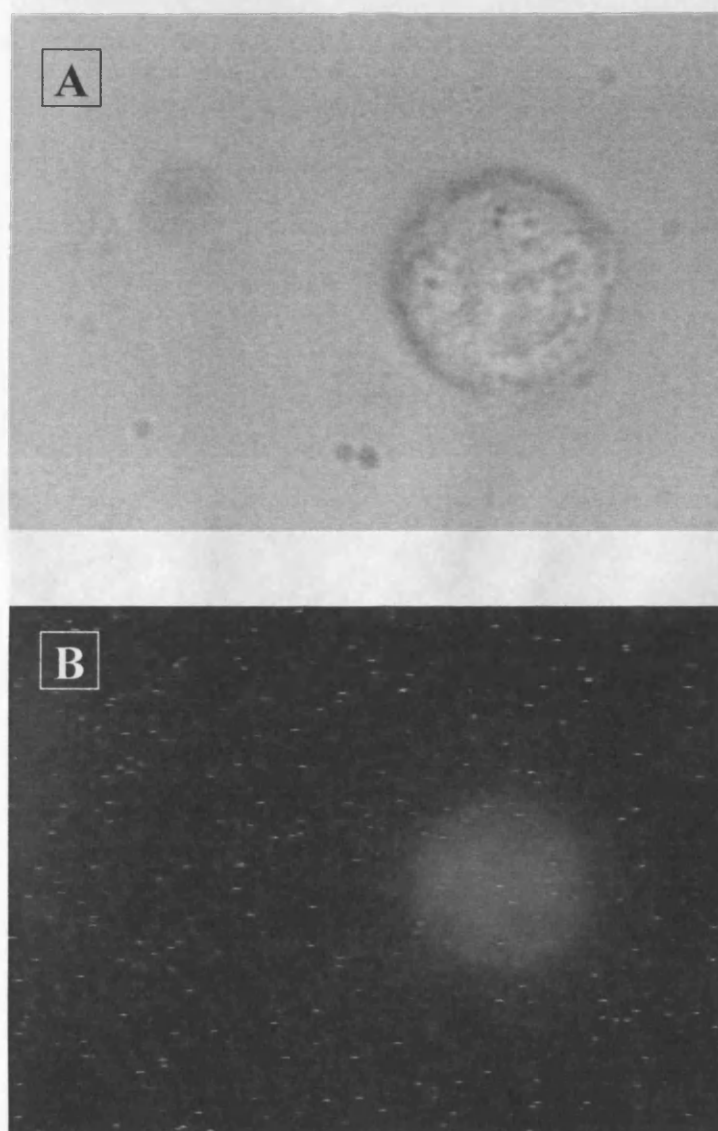


Figure 3.31

Real colour images of a viable MCF-7/S cell after doxorubicin ($10 \mu\text{mol.L}^{-1}$) incubation.

Image (A) represents a light microscopy image (x 100) and image (B) represents the red fluorescence of the cell. The fluorescence was excited using blue light cube filter. The images were captured using the Kontron 100 image analysis system.

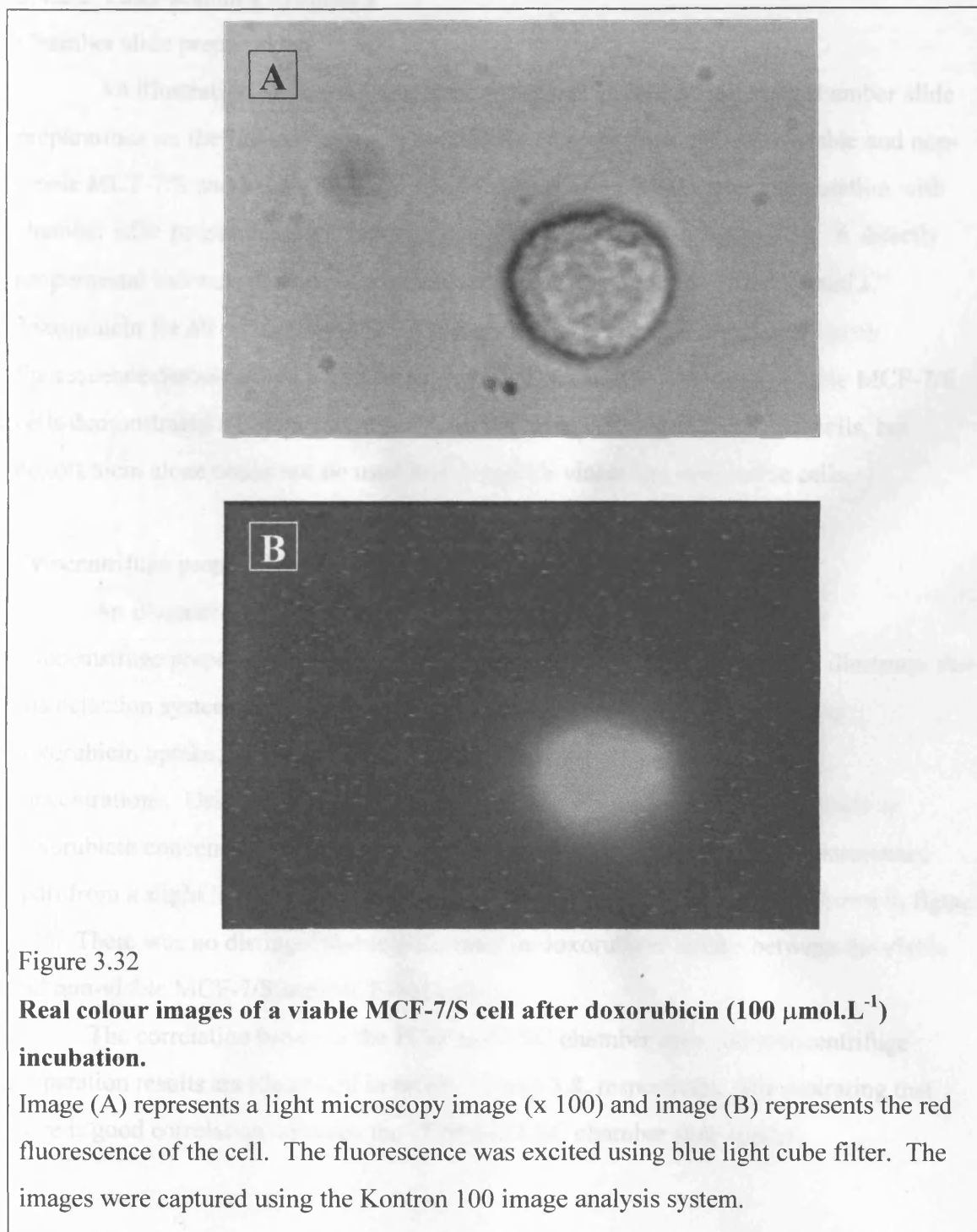


Figure 3.32

Real colour images of a viable MCF-7/S cell after doxorubicin ($100 \mu\text{mol.L}^{-1}$) incubation.

Image (A) represents a light microscopy image (x 100) and image (B) represents the red fluorescence of the cell. The fluorescence was excited using blue light cube filter. The images were captured using the Kontron 100 image analysis system.

3.4.2.2 Laser scanning cytometry

Chamber slide preparations

An illustration of doxorubicin uptake analysis of data collected by chamber slide preparations on the LSC is shown in figure 3.33. Doxorubicin uptake of viable and non-viable MCF-7/S and MCF-7/R cells were analysed using light scatter computation with chamber slide preparations on the LSC, these data are shown in figure 3.34. A directly proportional increase in fluorescence was seen at concentrations $\leq 42.13 \text{ mmol.L}^{-1}$ doxorubicin for all cells, after which fluorescence plateau. Red integral and peak fluorescence demonstrated a similar pattern to each other and to FCM. Viable MCF-7/S cells demonstrated a higher retention of doxorubicin than viable MCF-7/R cells, but doxorubicin alone could not be used to distinguish viable and non-viable cells.

Cytocentrifuge preparations

An illustration of doxorubicin uptake analysis of data collected using cytocentrifuge preparations on the LSC is shown in figure 3.35. This figure illustrates that this detection system using single colour computation and quantification using doxorubicin uptake, can not easily distinguish between varying doxorubicin concentrations. Using cytocentrifuge preparations a dose response to an increase in doxorubicin concentration was not measured using integral or mean peak fluorescence apart from a slight increase in fluorescence using viable MCF-7/S cells, as shown in figure 3.36. There was no distinguishable difference in doxorubicin uptake between the viable and non-viable MCF-7/S and MCF-7/R cells.

The correlation between the FCM and LSC chamber slide and cytocentrifuge preparation results are illustrated in tables 3.7 and 3.8, respectively, demonstrating that there is good correlation between the FCM and LSC chamber slide results.

	MCF-7/S viable	MCF-7/S non - viable	MCF-7/R viable
Pearson r	0.98	0.54	0.94

Table 3.7

Correlation results comparing the doxorubicin values of mean fluorescence intensity measured using flow cytometry and red integral fluorescence measured using LSC with chamber slides.

	MCF-7/S viable	MCF-7/S non - viable	MCF-7/R viable
Pearson r	0.78	-0.24	-0.61

Table 3.8

Correlation results comparing the doxorubicin values of mean fluorescence intensity measured using flow cytometry and red integral fluorescence measured using LSC with cytocentrifuge preparations.

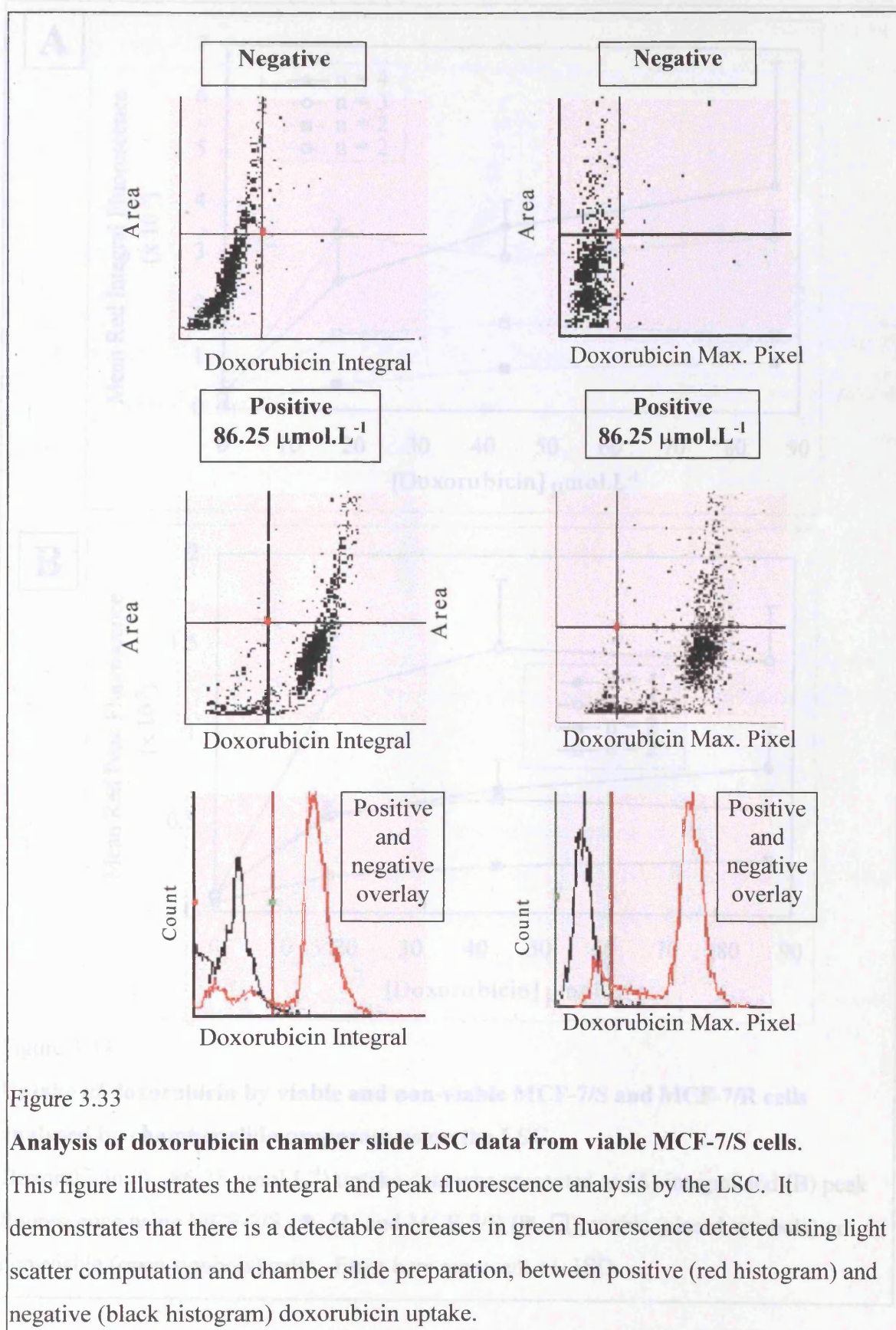
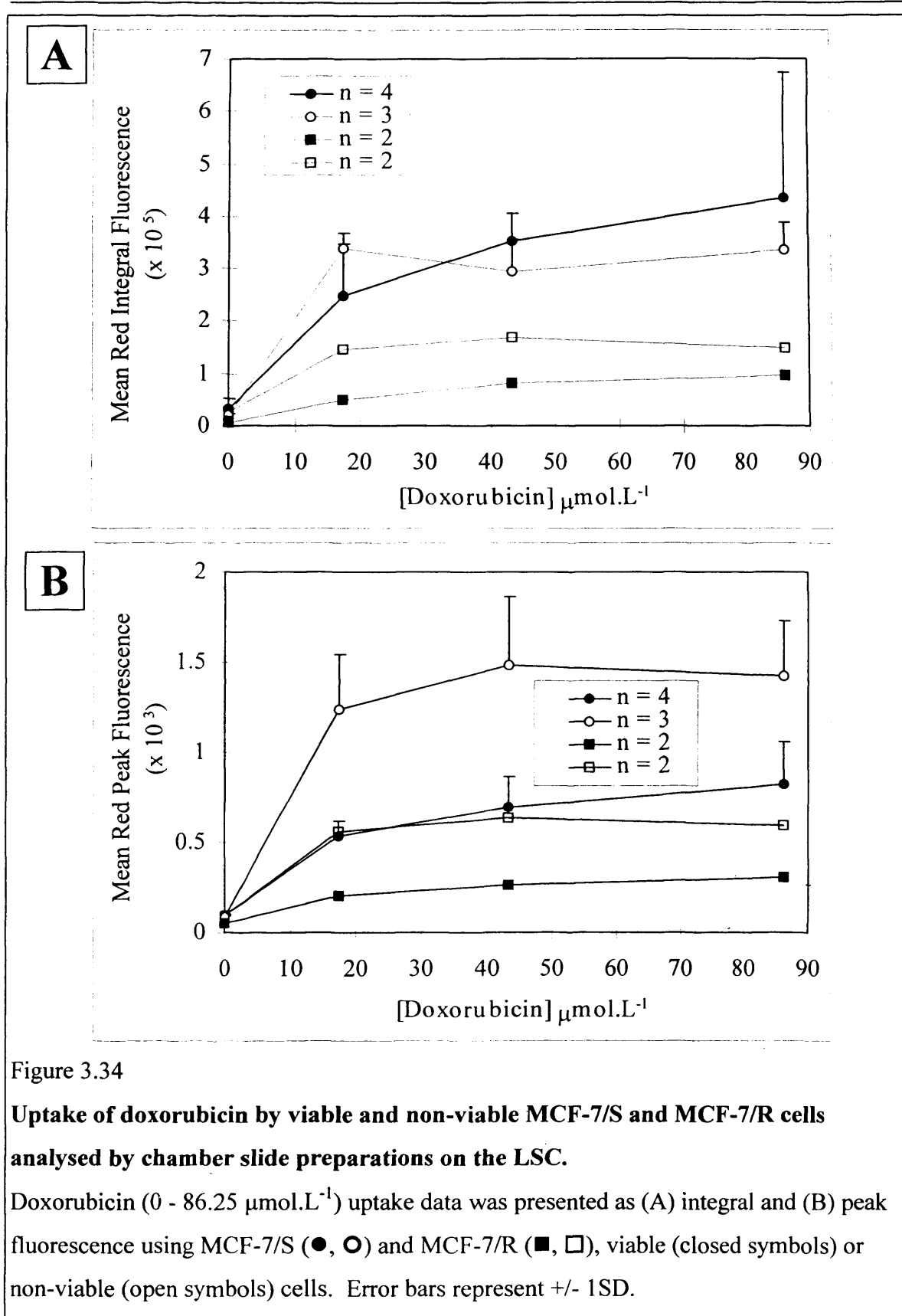


Figure 3.33

Analysis of doxorubicin chamber slide LSC data from viable MCF-7/S cells.

This figure illustrates the integral and peak fluorescence analysis by the LSC. It demonstrates that there is a detectable increase in green fluorescence detected using light scatter computation and chamber slide preparation, between positive (red histogram) and negative (black histogram) doxorubicin uptake.



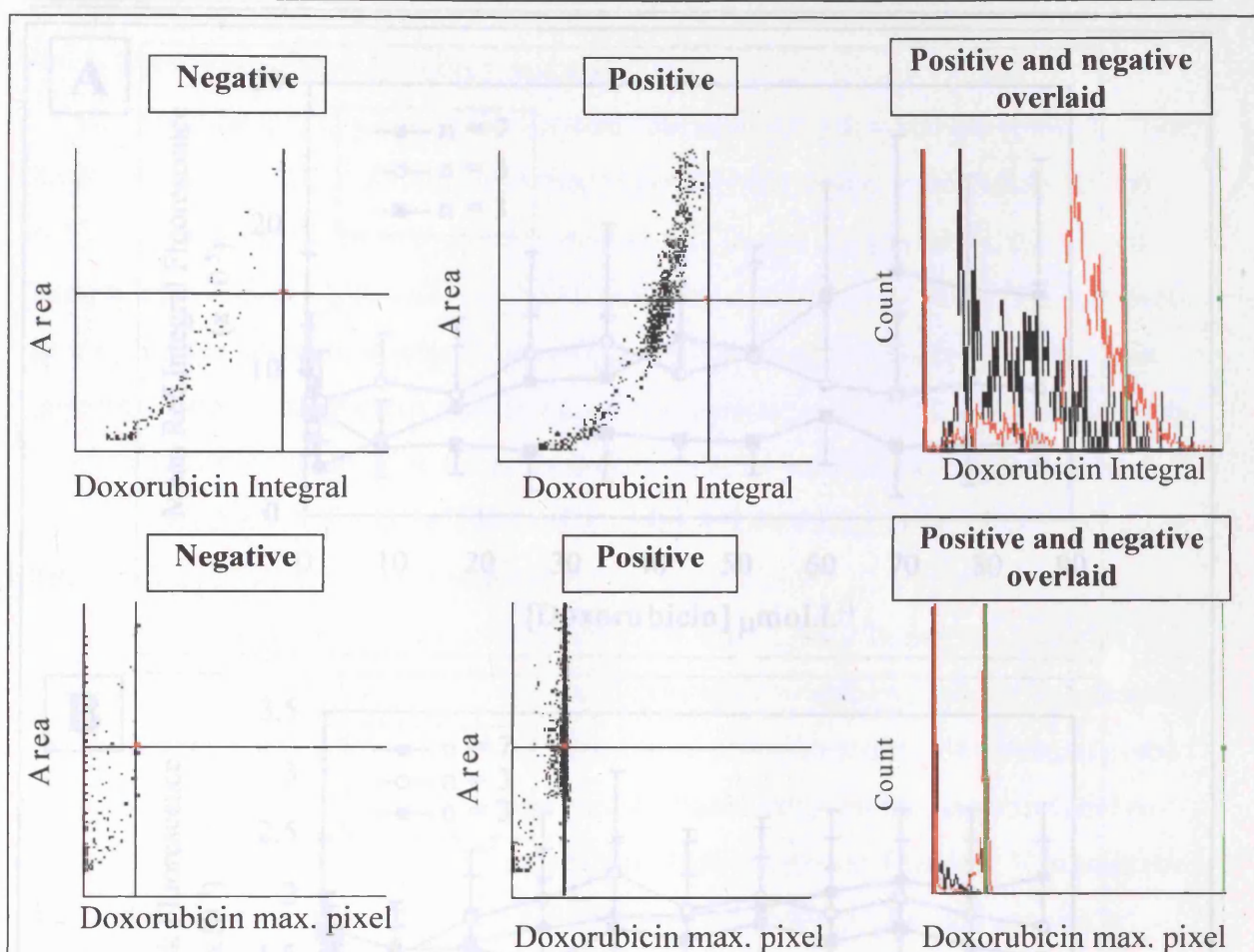


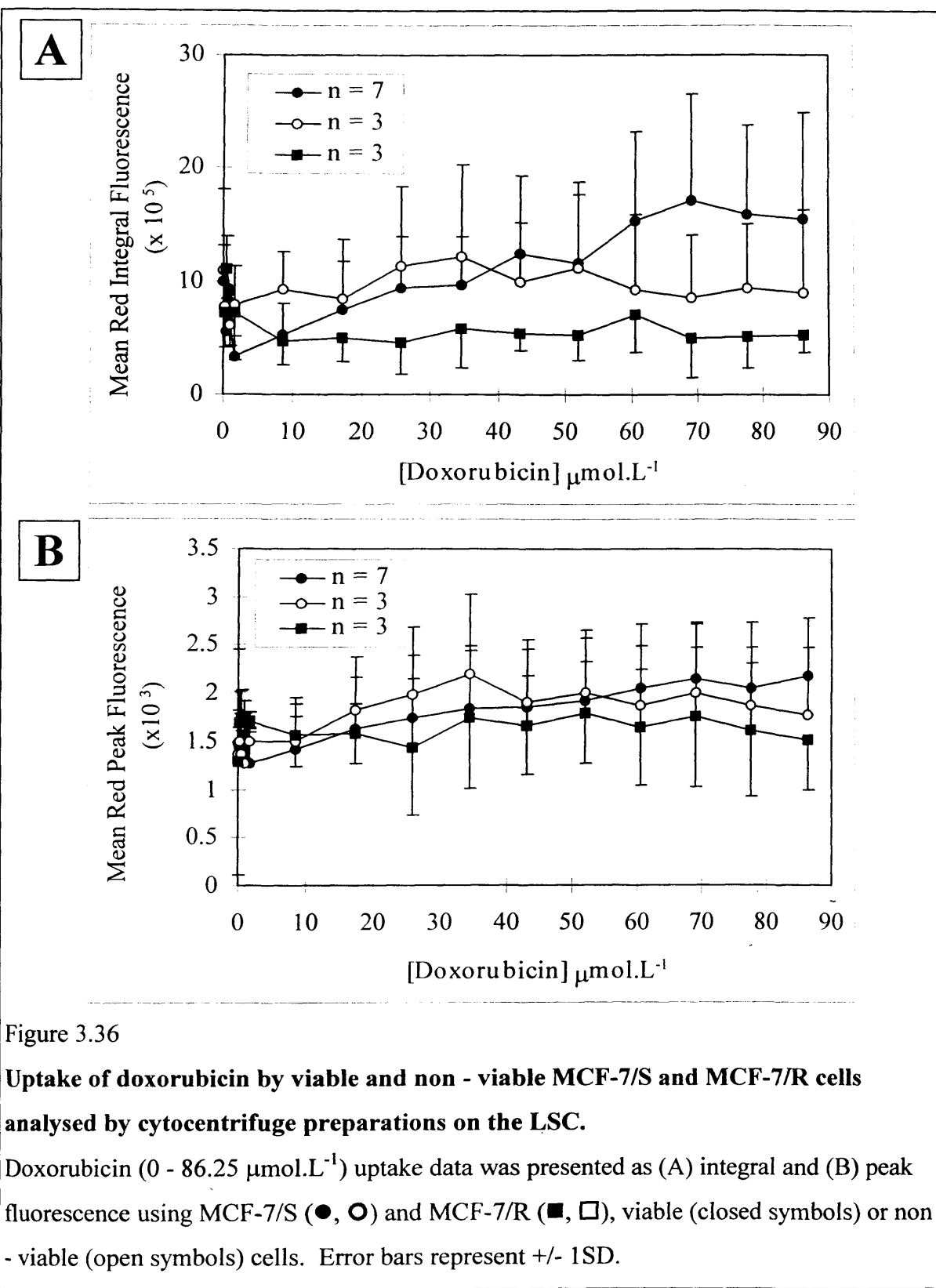
Figure 3.35

Analysis of doxorubicin cytocentrifuge LSC data from viable MCF-7/S cells.

This figure illustrates the integral and peak fluorescence analysis by the LSC. It demonstrates that there is not a great detectable increase in red fluorescence detected using red fluorescence computation and cytocentrifuge preparation, between positive (red histogram) and negative (black histogram) doxorubicin uptake.

Uptake of doxorubicin by viable and non-viable MCF-7/S and MCF-7/R cells analysed by cytocentrifuge preparations on the LSC.

Doxorubicin (10^{-20} $\mu\text{mol/L}$) uptake data was presented as (A) integral and (B) peak fluorescence using MCF-7/S (\blacklozenge , \circ) and MCF-7/R (\blacktriangle , \square), viable (closed symbols) or non-viable (open symbols) cells. Error bars represent $\pm 1\text{SD}$.



3.4.3 Time course of doxorubicin uptake

After the initial doxorubicin titrations, the analysis of doxorubicin uptake had been established. A time course study was then undertaken incubating viable MCF-7/S and MCF-7/R cells for one hour with doxorubicin (0, 1, 10 and 100 $\mu\text{mol.L}^{-1}$), then grown in culture for 4, 24, 48, 72, 96, 120 and 144 hours, then analysed using FCM. The two main goals of these experiments were to determine whether a doxorubicin concentration that gave an effective inhibition of growth also gave a detectable level of fluorescence, and the second point was to determine the optimal time point for incubation of the cells with doxorubicin. MCF-7/S and MCF-7/R cells were incubated with doxorubicin to compare and establish the differences in responses.

At the completion of the incubations 4, 24, 48, 72, 96, 120 and 144 hours the MCF-7/S and MCF-7/R cells were assayed for doxorubicin uptake, viability and apoptosis status. Viability was determined using trypan blue exclusion and the fluorescence probe sytox, measured using FCM. Apoptosis was measured using the fluorescently labelled probe - annexin V. The analysis of doxorubicin uptake, sytox and annexin V fluorescence is illustrated in 3.37, which demonstrates the small increases in sytox and annexin V fluorescence, caused by doxorubicin incubation.

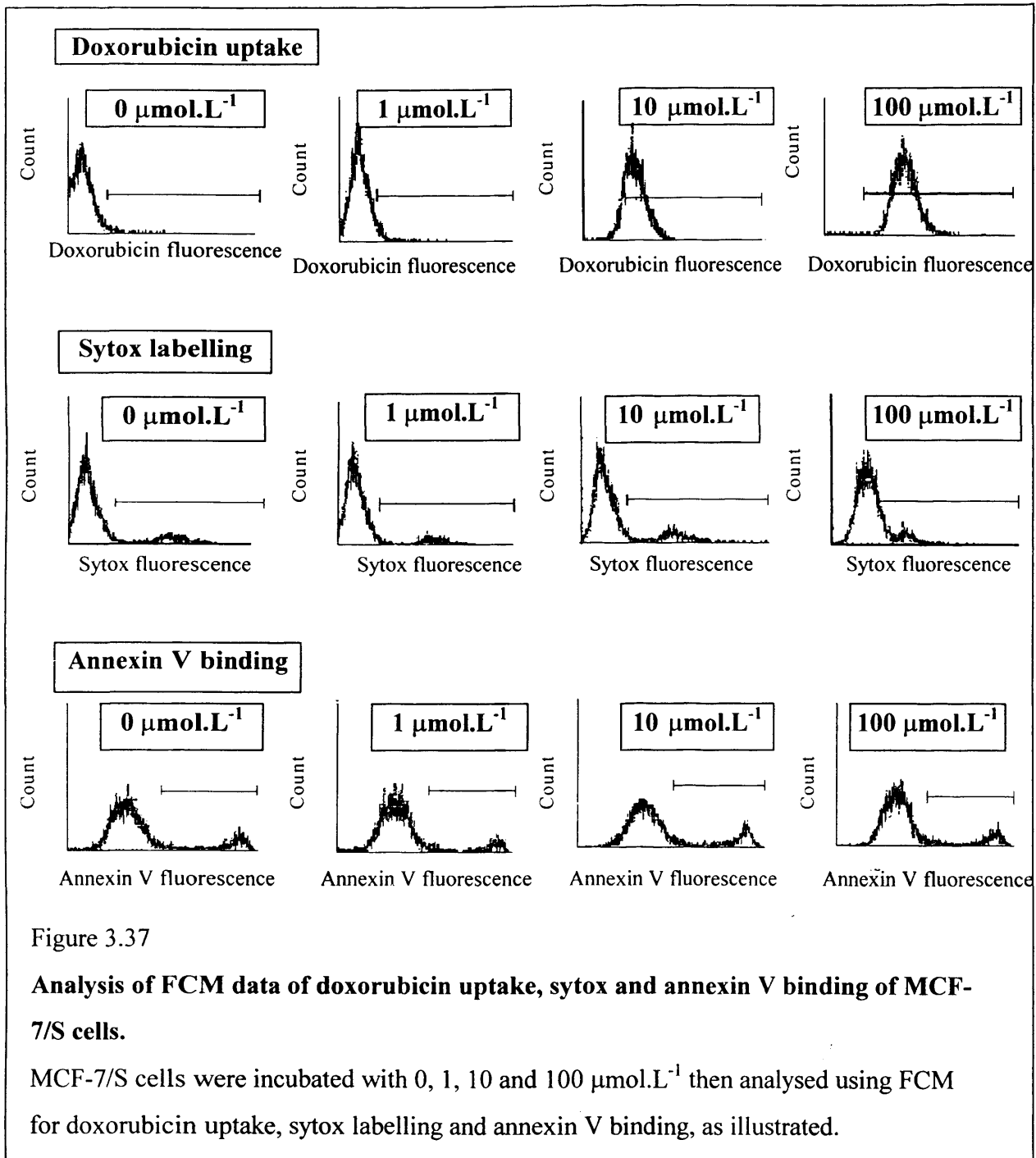
MCF-7/S and MCF-7/R cells which were incubated with 10 and 100 $\mu\text{mol.L}^{-1}$ doxorubicin then grown in culture for 144 hours are compared in figure 3.38. At 144 hours the MCF-7/S control cells were confluent, but the cells which had been incubated with 10 $\mu\text{mol.L}^{-1}$ and 100 $\mu\text{mol.L}^{-1}$ were elongated, stressed and no longer uniform in size or shape. In contrast the MCF-7/R cells were all confluent, demonstrating that the doxorubicin treatment had not affected the growth of the cells.

The set of data describing MCF-7/S cells incubated with doxorubicin and grown in culture for 4, 24, 48 and 72 hours are shown in figures 3.39 - 3.42. Percentage of cells positive for doxorubicin uptake and the mean fluorescence intensity generated are shown in figure 3.39. The percentage of cells positive for doxorubicin is dependent upon the concentration, 100 $\mu\text{mol.L}^{-1}$ demonstrating a maximum percentage uptake, and the lower concentrations showing a reduced percentage uptake. In this study 100 $\mu\text{mol.L}^{-1}$ doxorubicin concentration was the only one which demonstrated a considerably higher fluorescence intensity than control cells. The cell count for each time point illustrated in figure 3.40 shows that all cells were growing until 72 hours, after which only control cells had an increase in cell number, all other samples incubated with doxorubicin demonstrated

a decrease in cell number proportional to doxorubicin concentration. Viability data measured by trypan blue exclusion and sytox staining analysed by FCM are shown in figure 3.41, which remained constantly high over the time course. Apoptosis status was low as measured using annexin V labelling and remained constant over the time course but unfortunately annexin V was not assayed at 72 hours, as shown in figure 3.42.

The data shown in figure 3.43 - 3.47 describes similar data to the previous set of figures, using longer time courses - 96, 120 and 144 hours of growth. The mean red fluorescence of the MCF-7/S cells remained at similar levels to cells assayed at 48 and 72 hours as shown in figure 3.43/B, but the percentage of cells positive for doxorubicin uptake had dropped for 10 and 100 $\mu\text{mol.L}^{-1}$ doxorubicin concentrations. The total cell count demonstrated in figure 3.44 shows that cell number for all doxorubicin concentrations remained at a constant level which they had reached by 72 hours as shown in figure 3.40. Viability remained constant over 96 - 144 hours, as shown in figure 3.45, although in general the viability was slightly lower than the shorter incubation times described in figure 3.41. Apoptosis over 96 - 144 hrs was rising slightly for all samples especially cells incubated with 100 $\mu\text{mol.L}^{-1}$ doxorubicin, this is shown in figure 3.46.

The data from the doxorubicin incubations of MCF-7/R over 4 - 144 hours are shown in figure 3.47 - 3.54. Mean doxorubicin fluorescence and the corresponding percentage of positive cells are shown in figure 3.47, describing very low fluorescence and control levels of positive cells, for all samples. Total cell numbers increase exponentially over the time course, as described in figure 3.48. Viability demonstrated in figure 3.49 remained constantly high over the time course and apoptosis was detected at control cell levels, as shown in figure 3.50. The doxorubicin uptake, viability and apoptotic status for 96 - 144 hrs time course using MCF-7/R cells generated similar data to the 4 - 72 hrs time course. The data from 96 - 144 hours are shown in 3.51 - 3.54. The MCF-7/R cells do not demonstrate significant levels of red fluorescence after doxorubicin incubation and the drug appears not to induce cell death (figure 3.53) or apoptosis (figure 3.54), as determined using trypan blue exclusion assay, sytox uptake and annexin V binding, respectively. The total cell number described in figure 3.52 shows that the cells were no longer in exponential growth after 72 hours but had become quiescent.



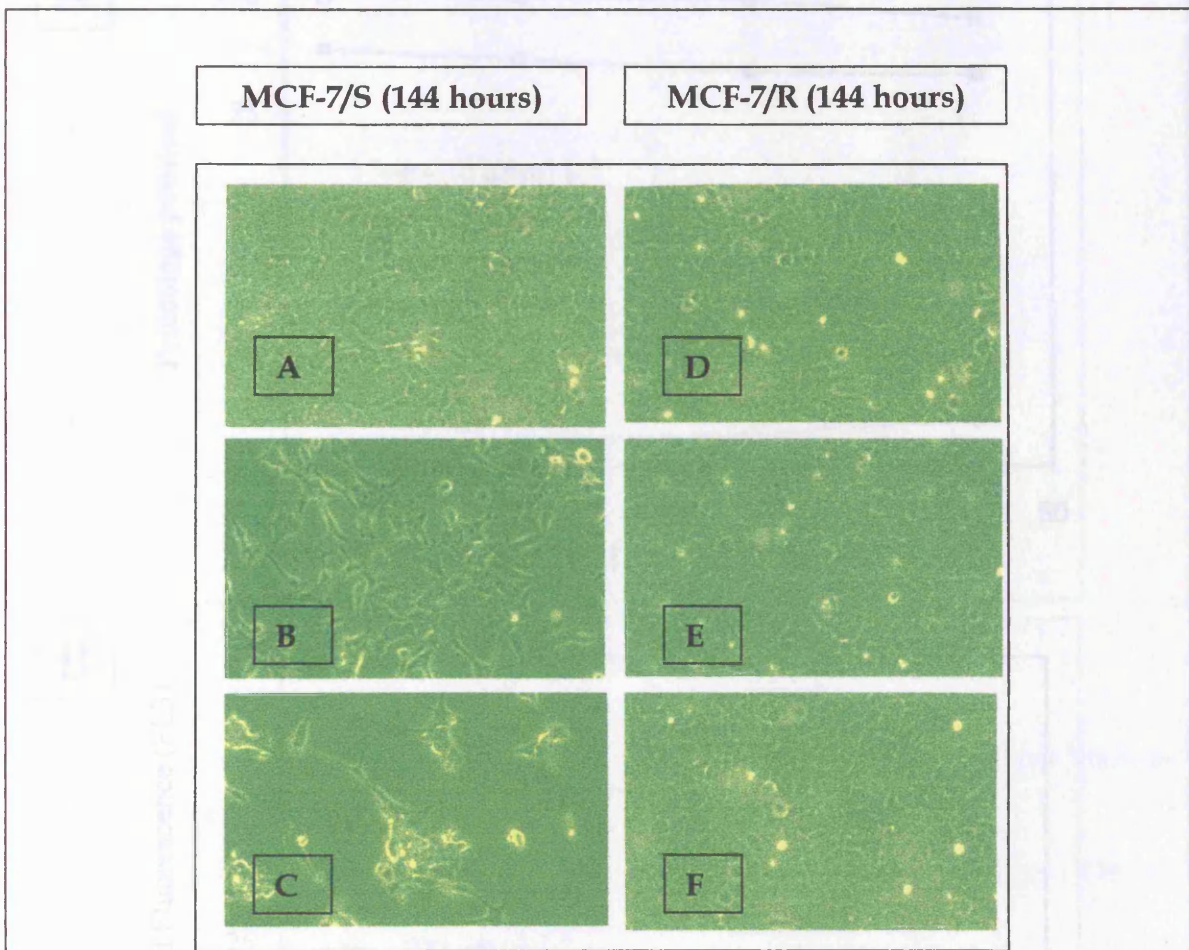


Figure 3.38

Photomicrographs illustrating the growth of MCF-7/S and MCF-7/R cells at 144 hours after doxorubicin incubation.

Images (A) and (D) are the control cells, (B) and (E) cells incubated with $10 \mu\text{mol.L}^{-1}$ doxorubicin and (C) and (F) cells which have been incubated with $100 \mu\text{mol.L}^{-1}$ doxorubicin.

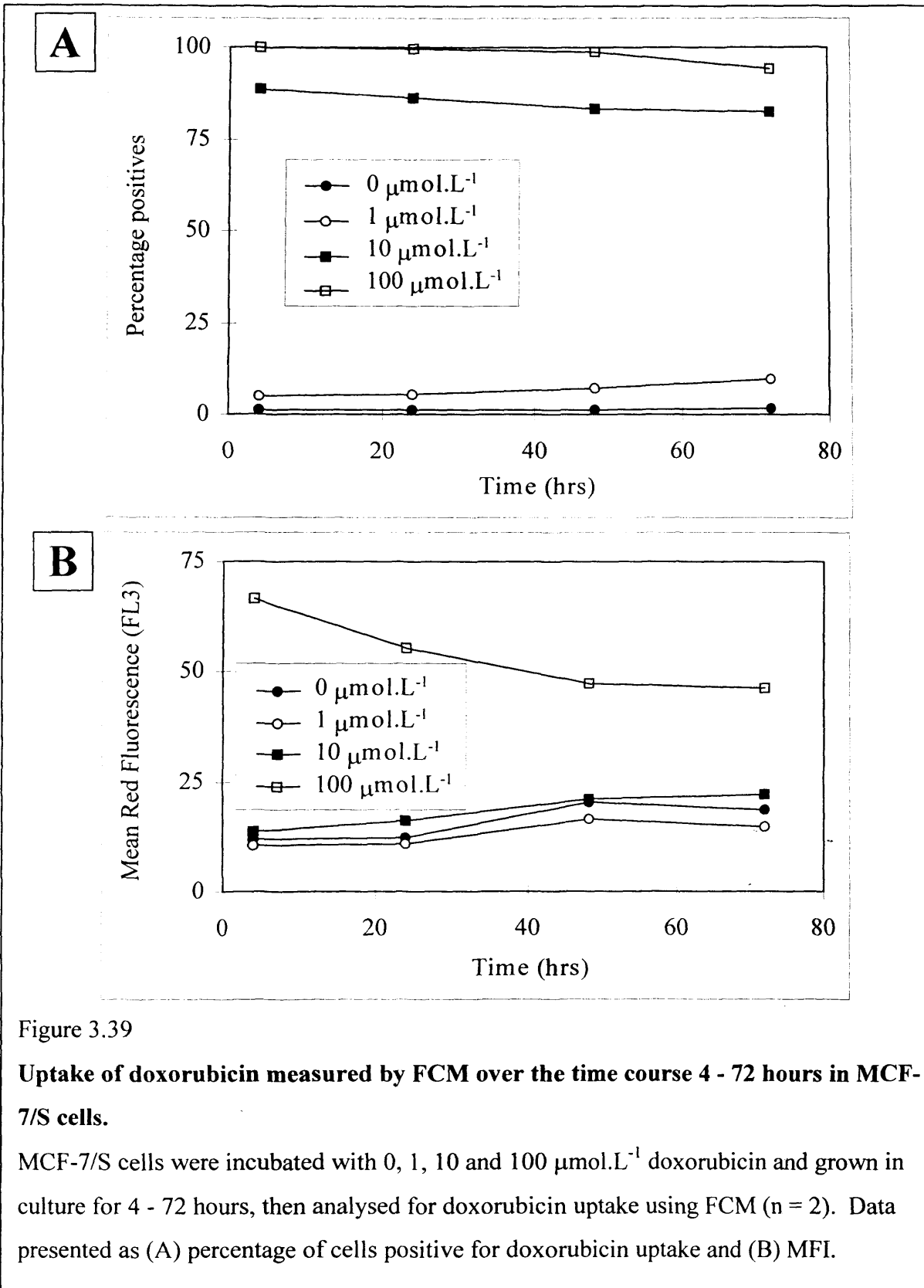


Figure 3.39

Uptake of doxorubicin measured by FCM over the time course 4 - 72 hours in MCF-7/S cells.

MCF-7/S cells were incubated with 0, 1, 10 and 100 $\mu\text{mol.L}^{-1}$ doxorubicin and grown in culture for 4 - 72 hours, then analysed for doxorubicin uptake using FCM (n = 2). Data presented as (A) percentage of cells positive for doxorubicin uptake and (B) MFI.

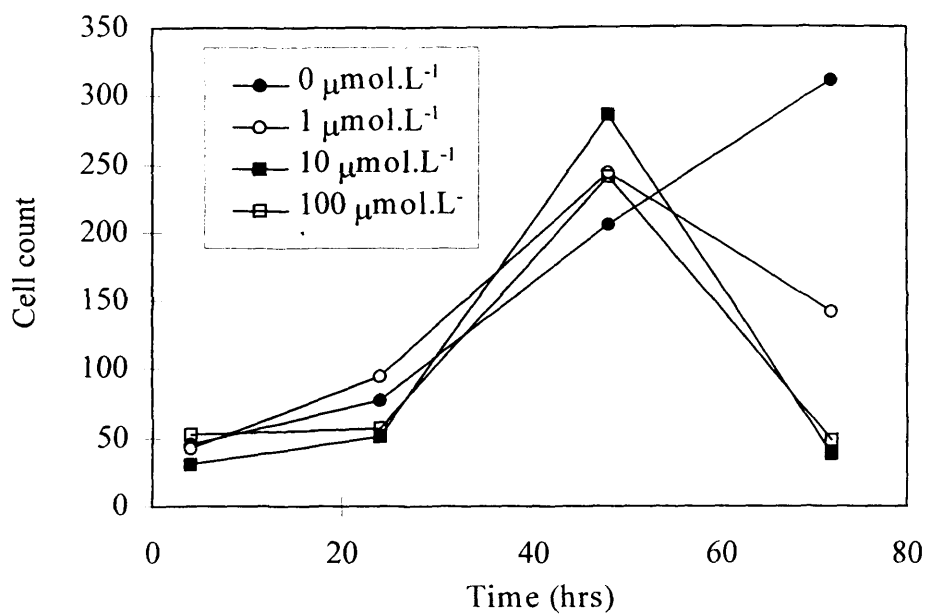
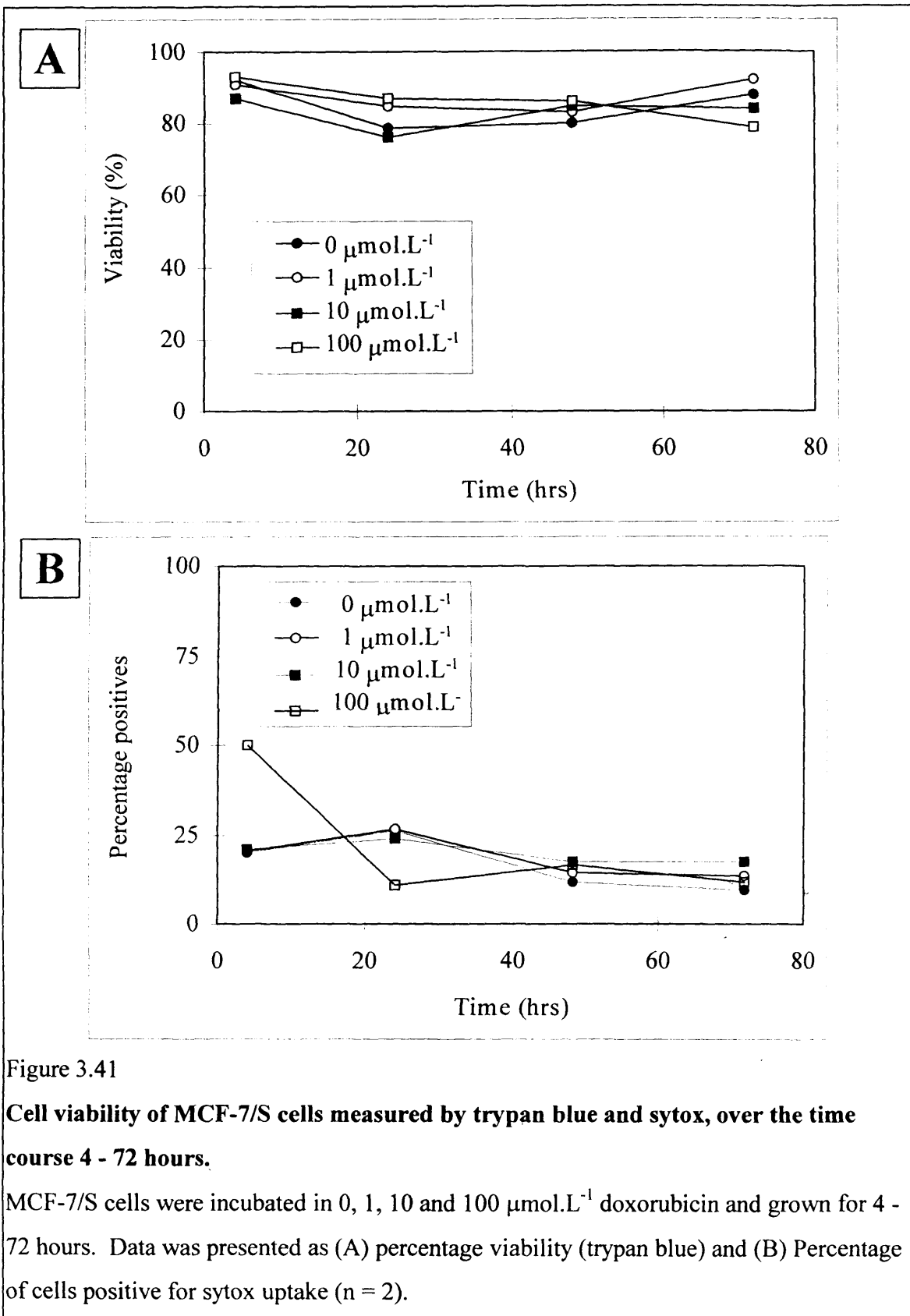


Figure 3.40

Total cell number of MCF-7/S cells measured by trypan blue exclusion over the time course 4 - 72 hours.

MCF-7/S cells were incubated in 0, 1, 10 and 100 μmol.L⁻¹ doxorubicin and grown for 4 - 72 hours, then analysed for cell number using trypan blue exclusion.



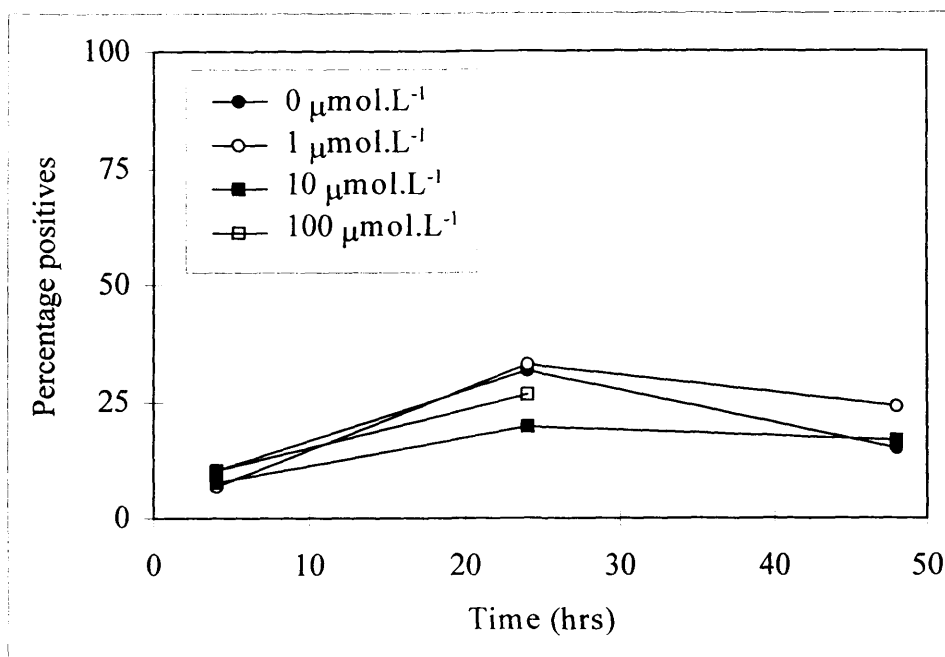


Figure 3.42

Percentage of MCF-7/S cells positive for annexin V binding over the time course 4 - 72 hours.

MCF-7/S cells were incubated with 0, 1, 10 and 100 $\mu\text{mol.L}^{-1}$ doxorubicin and grown for 4 - 72 hours, then analysed for annexin V binding using FCM (n = 2).

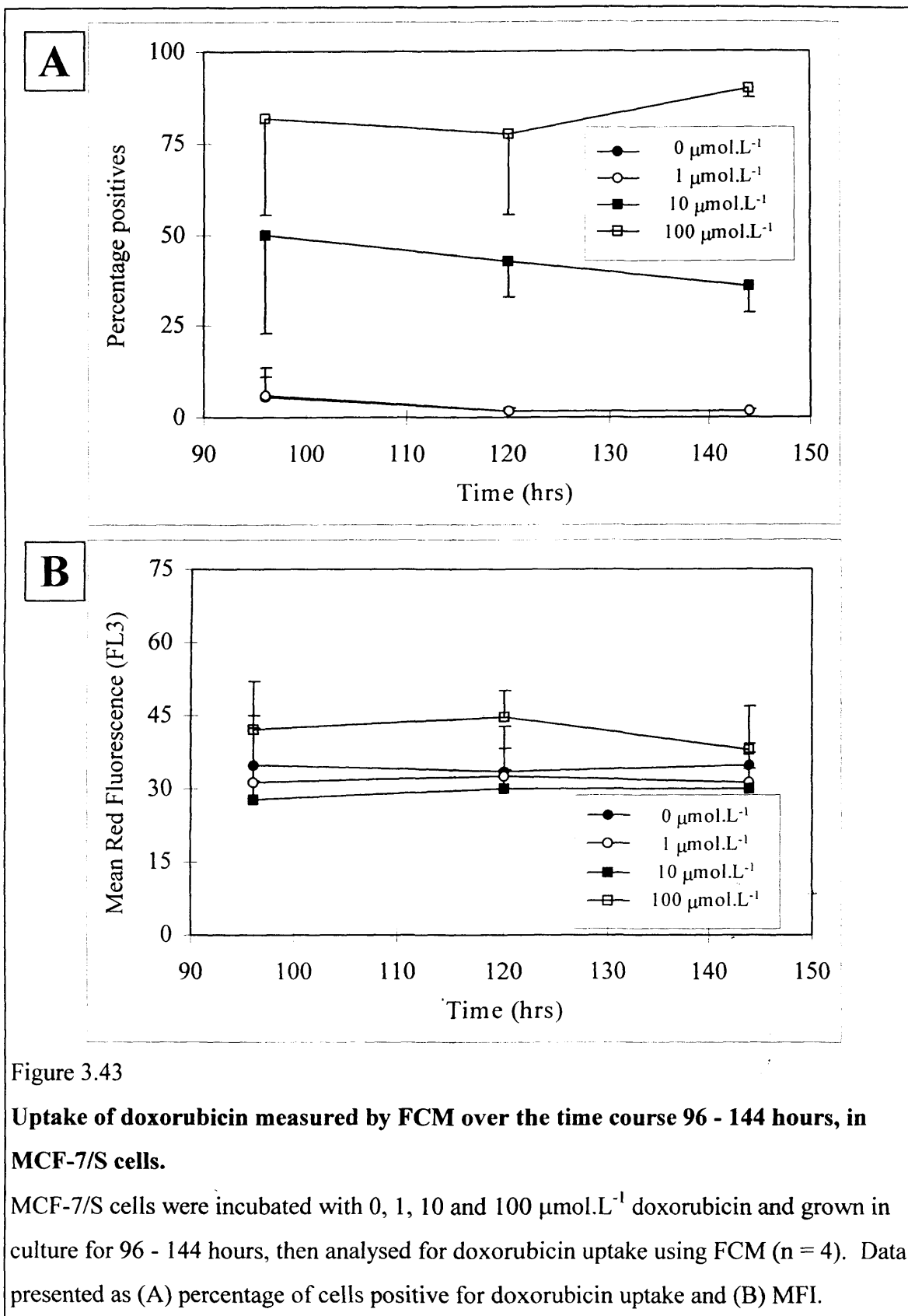


Figure 3.43

Uptake of doxorubicin measured by FCM over the time course 96 - 144 hours, in MCF-7/S cells.

MCF-7/S cells were incubated with 0, 1, 10 and 100 $\mu\text{mol.L}^{-1}$ doxorubicin and grown in culture for 96 - 144 hours, then analysed for doxorubicin uptake using FCM (n = 4). Data presented as (A) percentage of cells positive for doxorubicin uptake and (B) MFI.

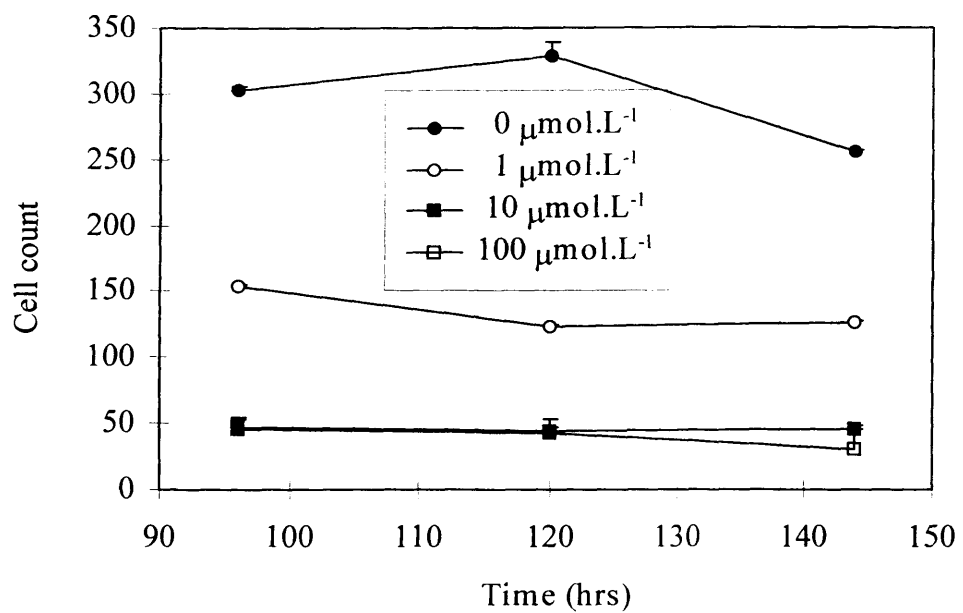


Figure 3.44

Total cell number of MCF-7/S cells measured by trypan blue exclusion over the time course 96 - 144 hours.

MCF-7/S cells were incubated in 0, 1, 10 and 100 µmol.L⁻¹ doxorubicin and grown for 96 - 144 hours, then analysed for cell number using trypan blue exclusion.

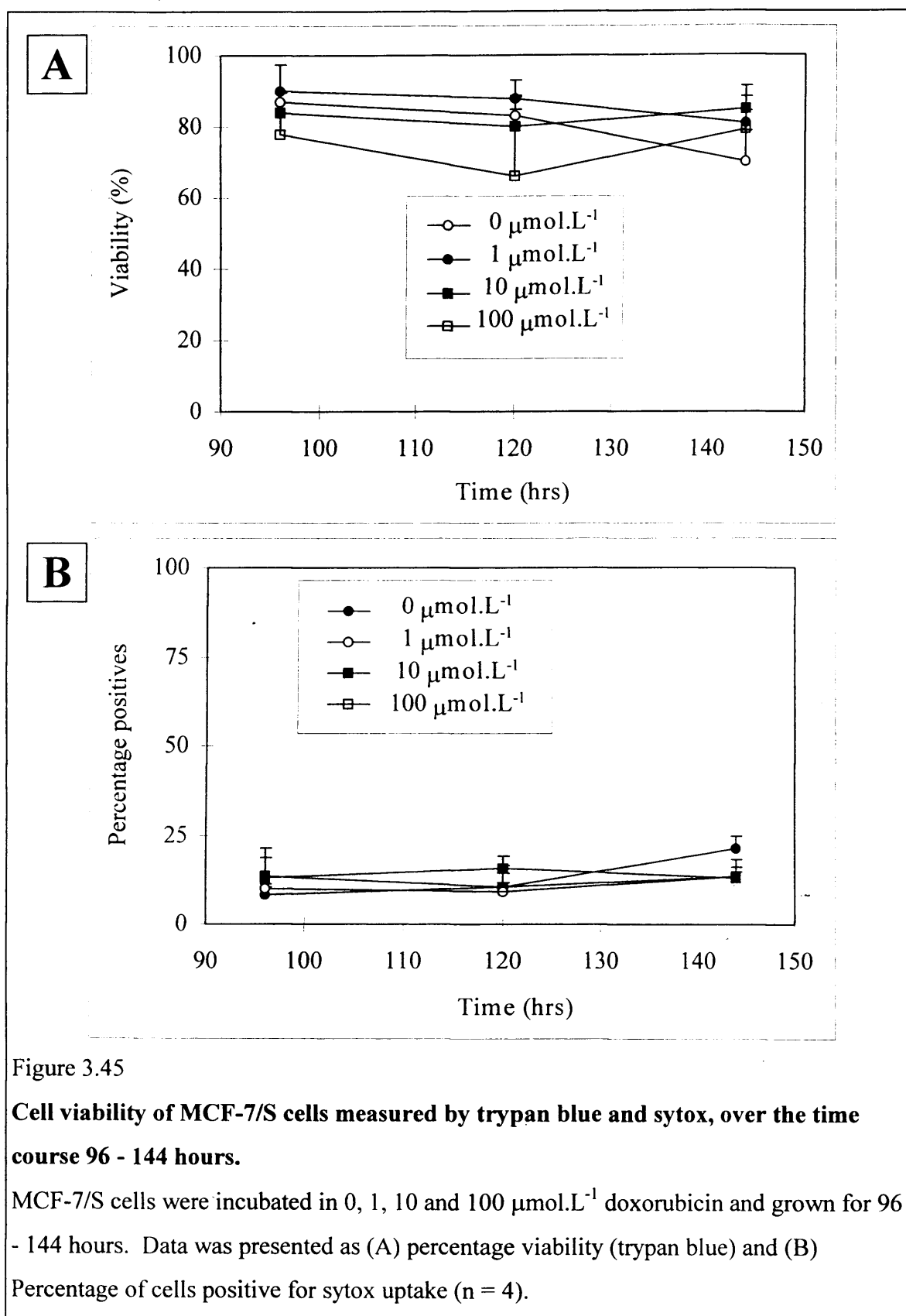


Figure 3.45

Cell viability of MCF-7/S cells measured by trypan blue and sytox, over the time course 96 - 144 hours.

MCF-7/S cells were incubated in 0, 1, 10 and 100 $\mu\text{mol.L}^{-1}$ doxorubicin and grown for 96 - 144 hours. Data was presented as (A) percentage viability (trypan blue) and (B) Percentage of cells positive for sytox uptake (n = 4).

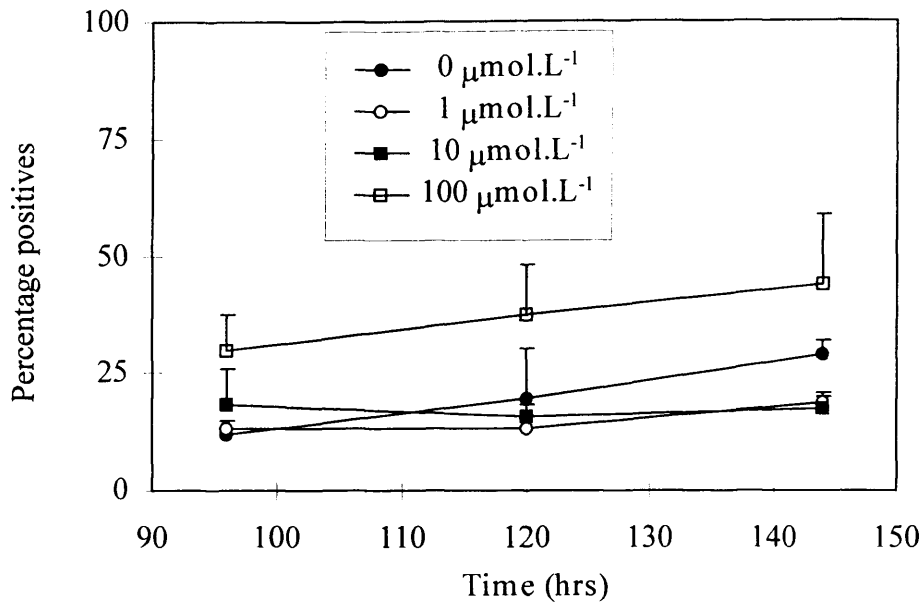


Figure 3.46

Percentage of MCF-7/S cells positive for annexin V binding over the time course 96 - 144 hours.

MCF-7/S cells were incubated with 0, 1, 10 and 100 µmol.L⁻¹ doxorubicin and grown for 96 - 144 hours, then analysed for annexin V binding using FCM (n = 4).

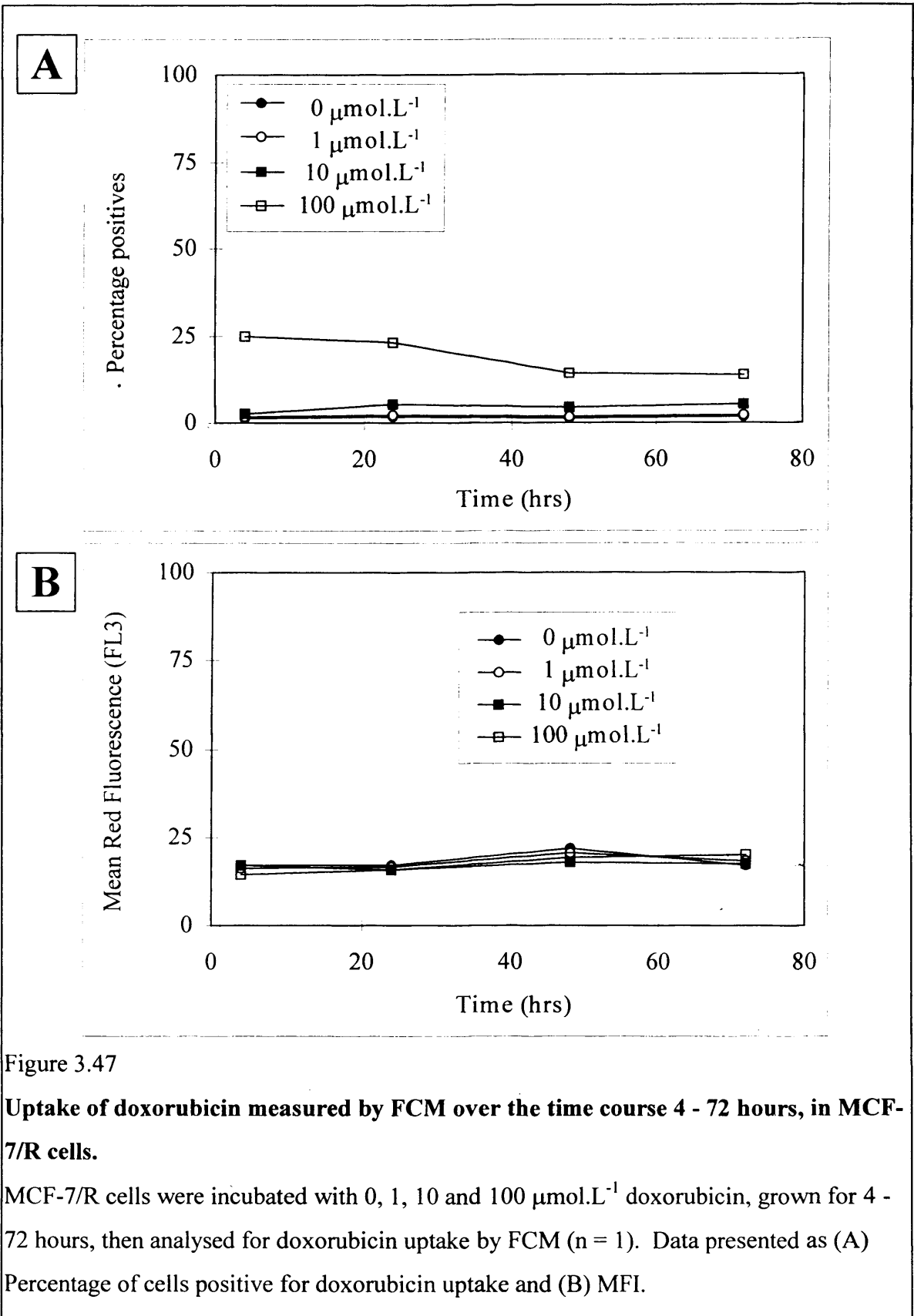


Figure 3.47

Uptake of doxorubicin measured by FCM over the time course 4 - 72 hours, in MCF-7/R cells.

MCF-7/R cells were incubated with 0, 1, 10 and 100 $\mu\text{mol.L}^{-1}$ doxorubicin, grown for 4 - 72 hours, then analysed for doxorubicin uptake by FCM (n = 1). Data presented as (A) Percentage of cells positive for doxorubicin uptake and (B) MFI.

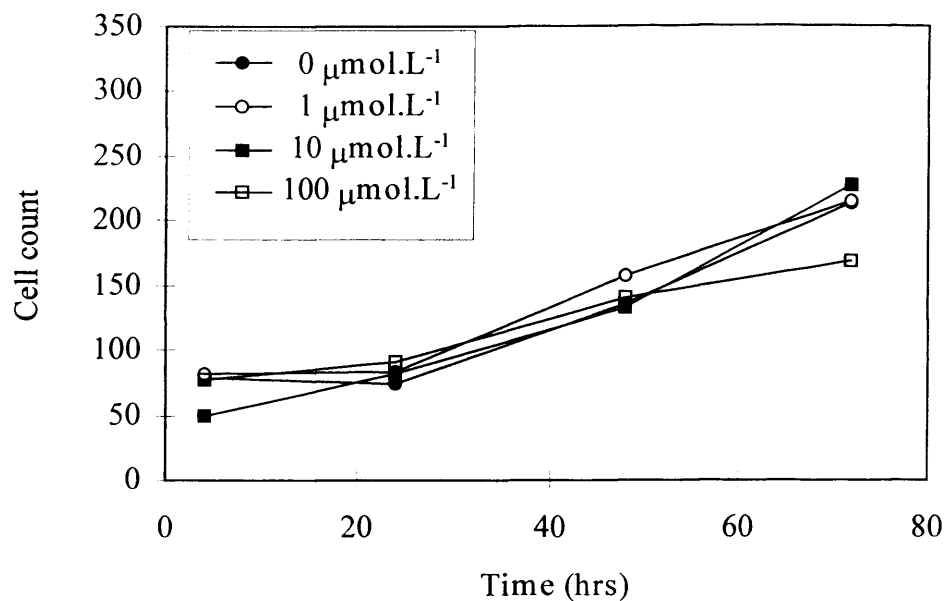


Figure 3.48

Total cell number of MCF-7/R cells measured by trypan blue exclusion over the time course 4 - 72 hours.

MCF-7/R cells were incubated with 0, 1, 10 and 100 μmol.L⁻¹ doxorubicin and then grown for 4 - 72 hours, then analysed for cell number using trypan blue exclusion.

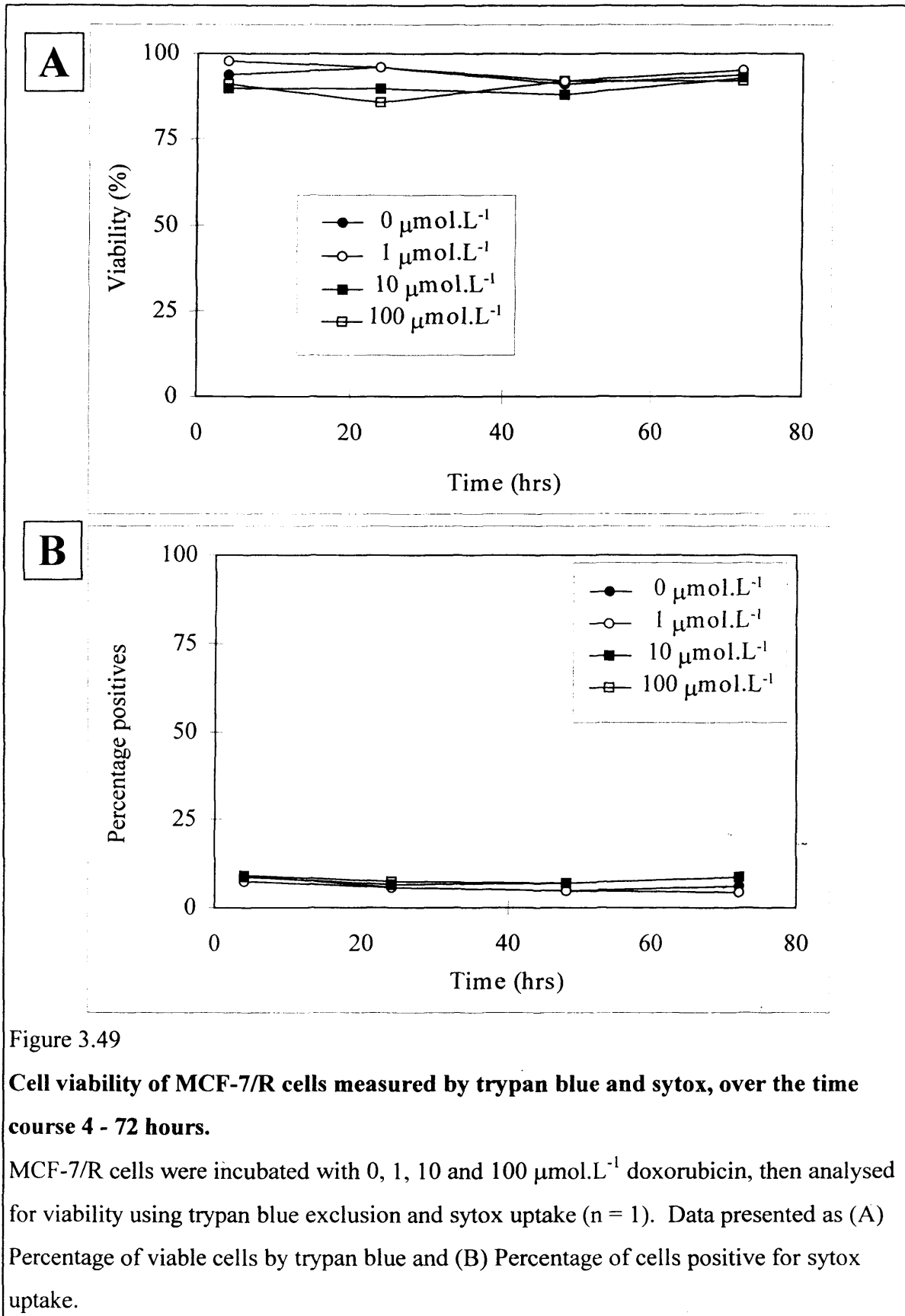


Figure 3.49

Cell viability of MCF-7/R cells measured by trypan blue and sytox, over the time course 4 - 72 hours.

MCF-7/R cells were incubated with 0, 1, 10 and 100 $\mu\text{mol.L}^{-1}$ doxorubicin, then analysed for viability using trypan blue exclusion and sytox uptake ($n = 1$). Data presented as (A) Percentage of viable cells by trypan blue and (B) Percentage of cells positive for sytox uptake.

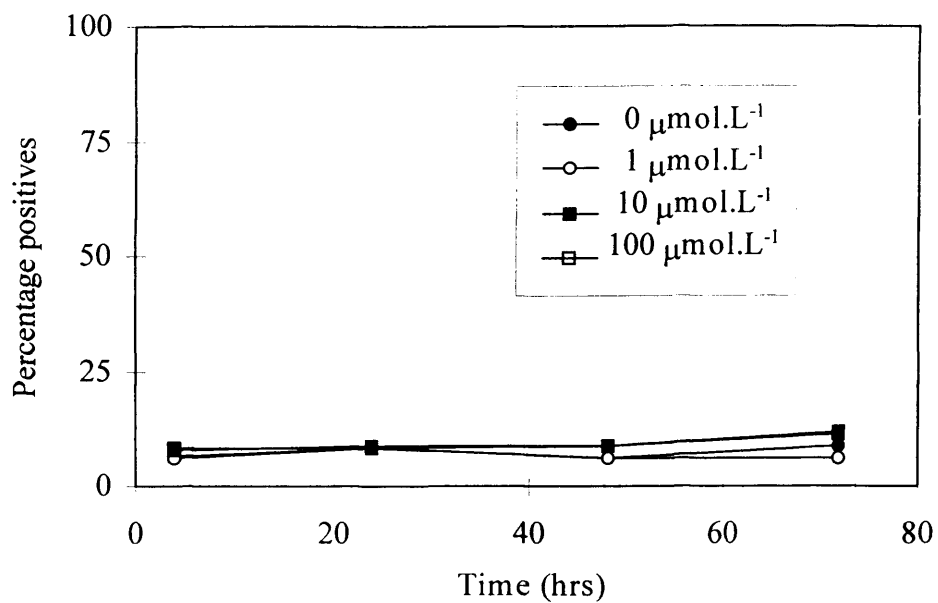


Figure 3.50

Percentage of MCF-7/R cells positive for annexin V binding , over the time course 4 - 72 hours.

MCF-7/R cells were incubated with 0, 1, 10 and 100 µmol.L⁻¹ doxorubicin grown for 4 - 72 hours then analysed for annexin V binding by FCM (n = 1).

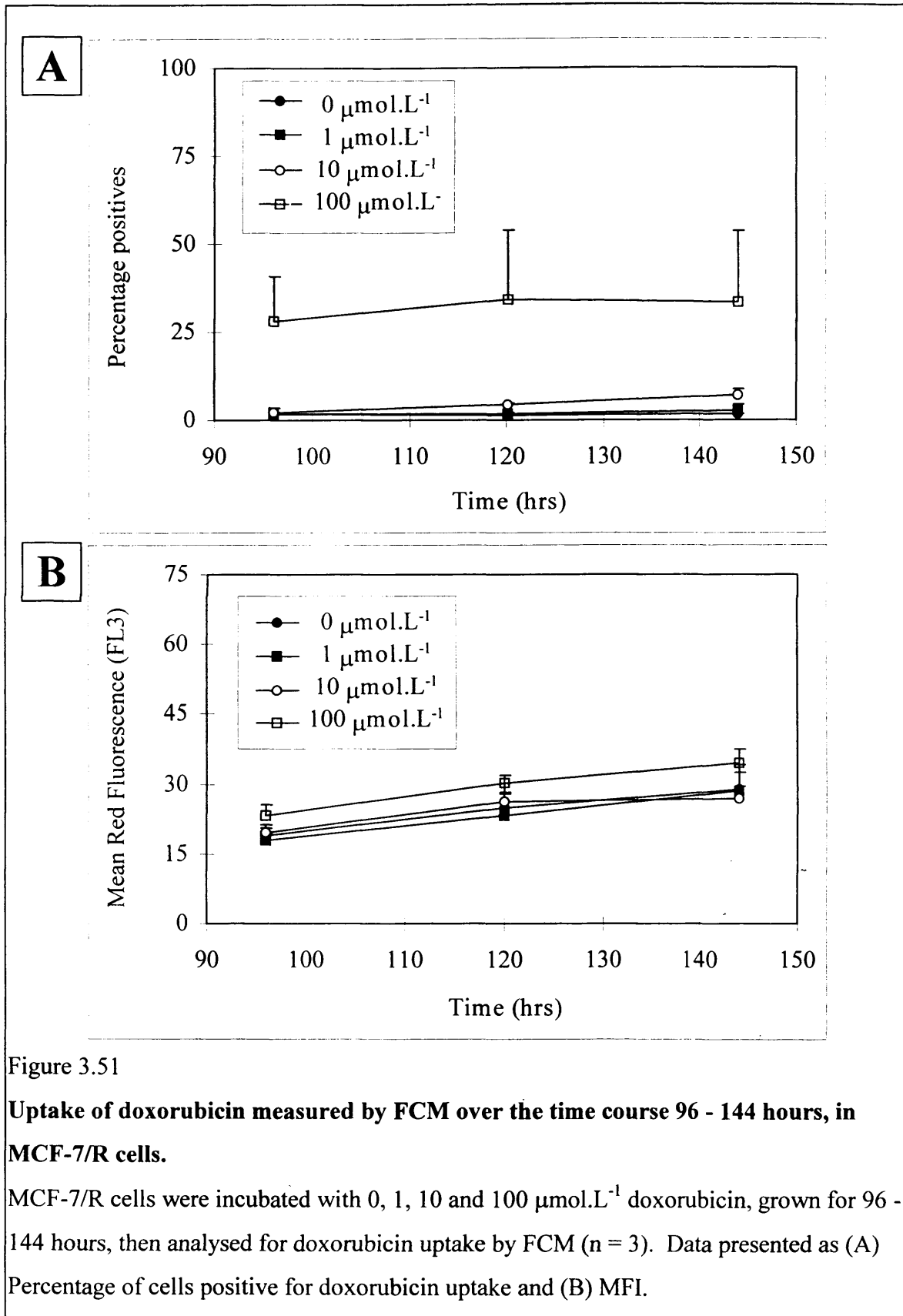
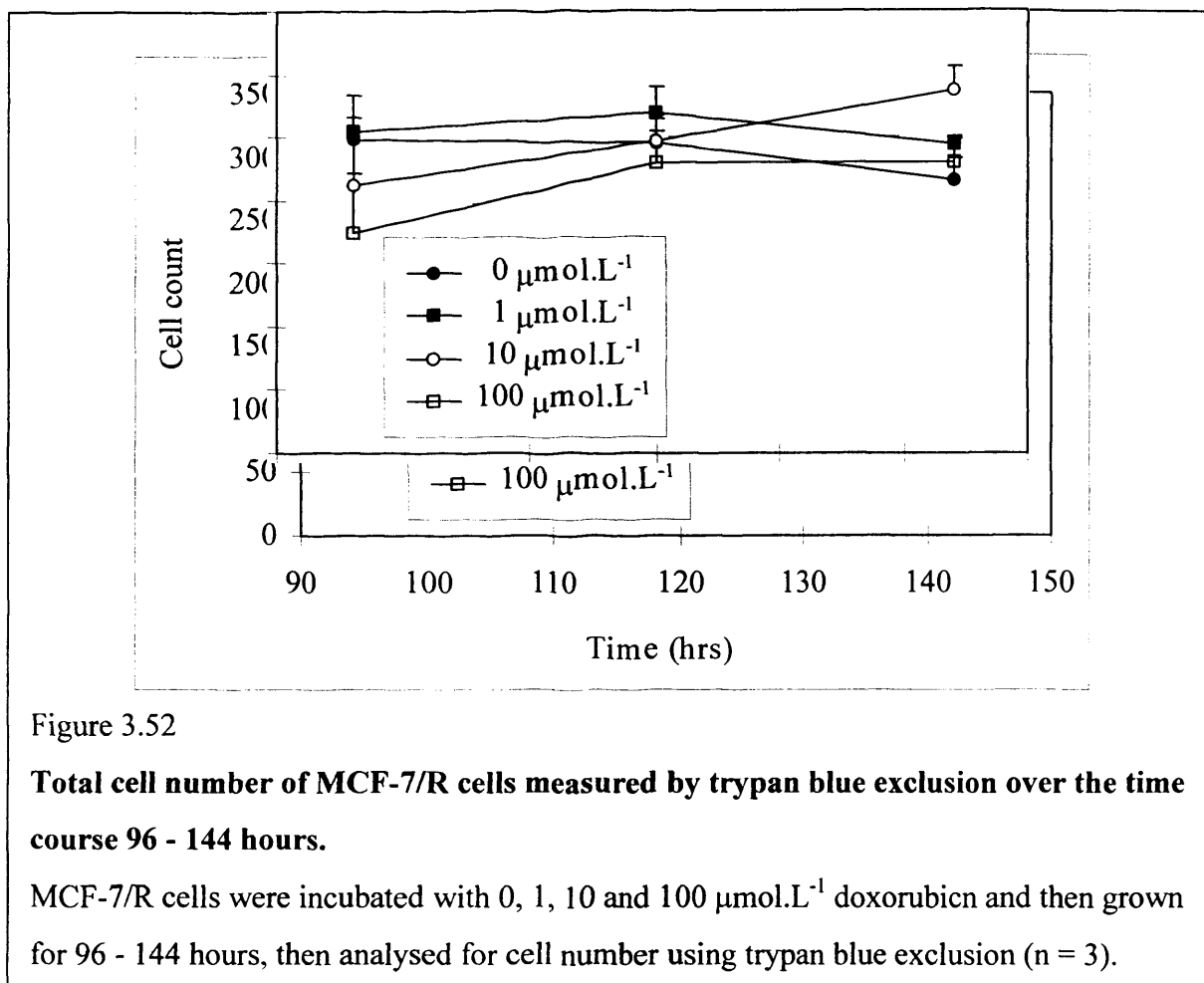


Figure 3.51

Uptake of doxorubicin measured by FCM over the time course 96 - 144 hours, in MCF-7/R cells.

MCF-7/R cells were incubated with 0, 1, 10 and 100 $\mu\text{mol.L}^{-1}$ doxorubicin, grown for 96 - 144 hours, then analysed for doxorubicin uptake by FCM ($n = 3$). Data presented as (A) Percentage of cells positive for doxorubicin uptake and (B) MFI.



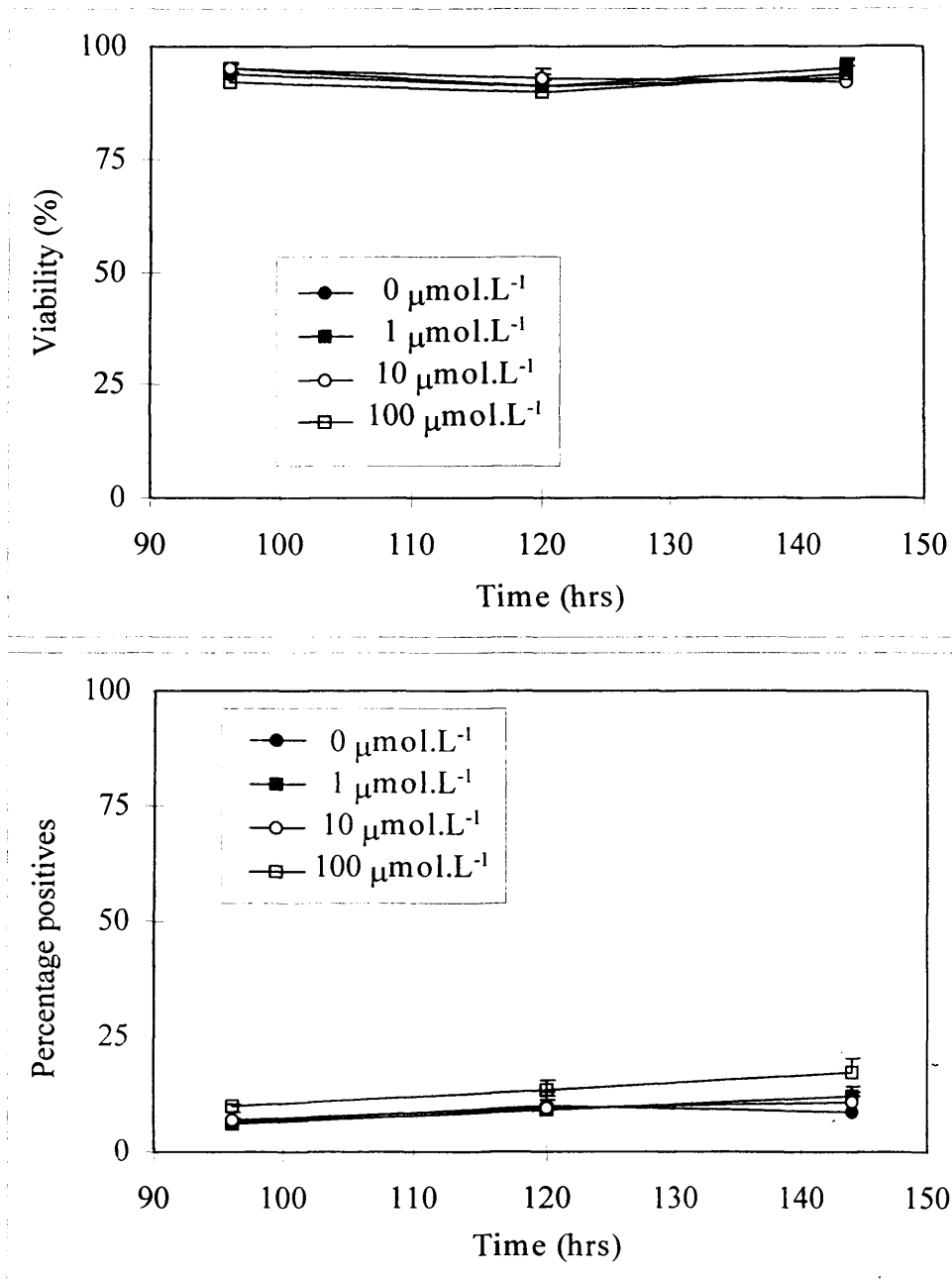


Figure 3.53

Cell viability of MCF-7/R cells measured by trypan blue and sytox, over the time course 96 - 144 hours.

MCF-7/R cells were incubated with 0, 1, 10 and 100 $\mu\text{mol.L}^{-1}$ doxorubicin, then analysed for viability using trypan blue exclusion and sytox uptake (n = 3). Data presented as (A) Percentage of viable cells by trypan blue and (B) Percentage of cells positive for sytox uptake.

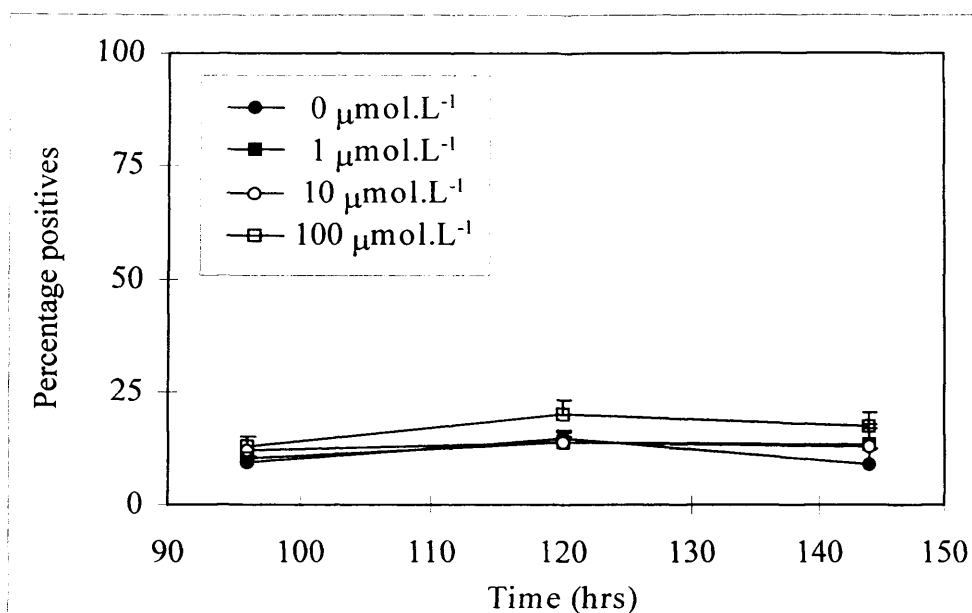


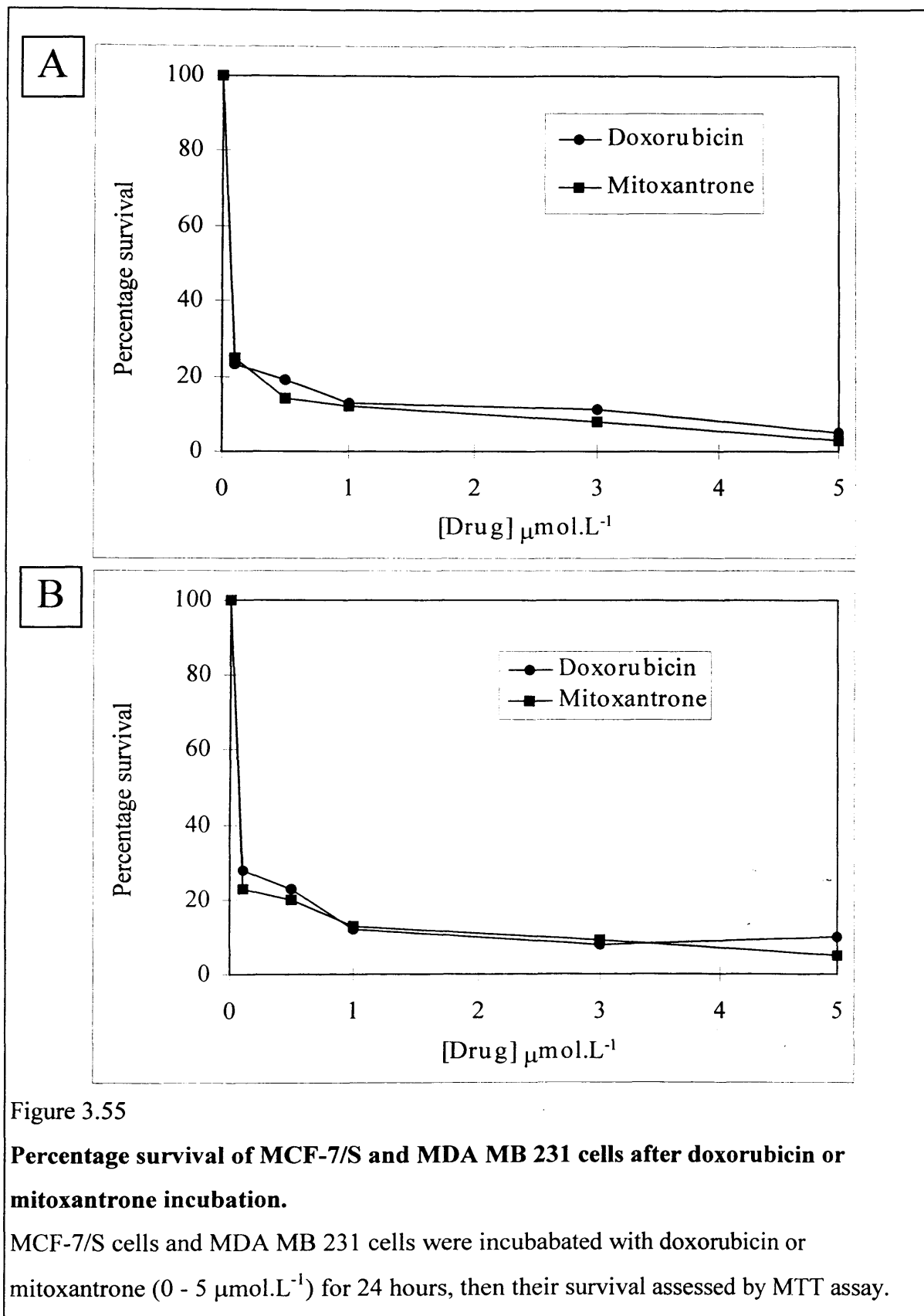
Figure 3.54

Percentage of MCF-7/R cells positive for annexin V binding, over the time course 96 - 144 hours.

MCF-7/R cells were incubated with 0, 1, 10 and 100 $\mu\text{mol.L}^{-1}$ doxorubicin grown for 96 - 144 hours then analysed for annexin V binding by FCM (n = 3).

3.4.4 Cytotoxicity of doxorubicin and mitoxantrone

Viable MCF-7/S and MDA MB 231 cells were incubated with 0 - 5 $\mu\text{mol.L}^{-1}$ concentrations of doxorubicin or mitoxantrone for 24 hours before viability analysis using the MTT assay. The percentage survival of MCF-7/S and MDA MB 231 cells after 24 hour drug incubation are shown in figures 3.55. Both cell lines reacted in a similar way, all drug concentrations used caused a drop in viability to <30%. Doxorubicin and mitoxantrone caused very similar patterns of death using both MDA MB 231 and MCF-7/S cells, both drugs were effective at causing the majority of cells to die at all drug concentrations. IC_{50} calculations were not performed on these data because of a lack of data points at drug concentrations lower than 1 $\mu\text{mol.L}^{-1}$.



3.4.5 Discussion

The concentration and length of time doxorubicin and its metabolites circulate the blood stream of chemotherapy patients is dependent on the drug schedule used although its optimisation is still unclear. A doxorubicin infusion should be high enough to reach saturation initially, but to remain in the blood stream at the highest tolerated concentration, for as long as possible. Doxorubicin levels in peripheral blood decrease rapidly a few minutes after infusion, the half life of doxorubicin and its metabolites being about 27 hours (Benjamin *et al.*, 1972 and Erttmann *et al.*, 1988). The concentration of doxorubicin present in peripheral blood depends on the concentration of the bolus and the frequency of injections (Erttmann *et al.* 1988). The initial i.v. infusion of doxorubicin is usually 1 mg.ml⁻¹, (Erttmann *et al.*, 1988) the minimum effective dose being 30 mg/m² body surface, creating a plasma concentration of 51 ng.ml⁻¹ (0.09 µmol.L⁻¹) at 30 min postinjection, and a dose of 60 mg/m² body surface gave a serum concentration of 120 ng.ml⁻¹ (0.21 µmol.L⁻¹). Similar concentrations of doxorubicin and its metabolites have been reported in other studies (Fornari *et al.*, 1996 and de Bruijn *et al.*, 1999). These plasma concentrations are lower than the concentrations of doxorubicin used for the present study which was in the range of 0.173 to 100 µmol.L⁻¹. The primary reason for studying these high concentrations of drug was for the purpose of visualisation. The study of the action of the high concentrations of drug upon tumour tissue/models and normal tissue may, however be important and useful to determine the mechanisms and consequences of its action. The cells of the peripheral blood stream, the heart and the linings of the blood vessels could encounter doxorubicin in high concentrations, immediately after administration. A solid breast tumour has to undergo extensive angiogenesis to grow more than a few millimeters in diameter, this vascularisation is inefficient compared to normal tissue, and the vessels are characteristically leaky. These capillaries could create areas of the tumour where drugs can accumulate to a higher level than those found in the plasma.

A variety of conditions alter the levels of anthracycline fluorescence measured by FCM including incubation time and concentration of drug. For this study one hour was generally used as the incubation time for doxorubicin, which from previous studies was generally determined to give maximum uptake e.g. Durand and Olive, 1981. The incubation of doxorubicin was carried out using a cell suspension of 5 x 10⁶ cell/ml which may have reduced the doxorubicin uptake compared to other studies which used ≤ 5 x 10⁵

cell/ml (M^c Gown *et al.*, 1983; Luk and Tannock, 1989 and Carpentier *et al.*, 1992). It has also been demonstrated that monolayers of cells retained a higher drug fluorescence than cells in suspension (Durand and Olive, 1981). The cell density and incubation time used for 'free' doxorubicin and CytocapsTM time course studies were consistent, within these studies and demonstrated measurable fluorescence. The pH of the growth medium was not checked during this study, and as phenol red indicator was not included in the medium, there was no visual pH but fresh medium was used for all drug incubations.

The time course of doxorubicin uptake shows that MCF-7/R cells do not retain large amounts of doxorubicin compared with MCF-7/S cells. Over the 4- 144 hour time course the MCF-7/S cells incubated with doxorubicin showed no decrease in viability or increase in apoptosis. However, all doxorubicin concentrations used (1, 10 and 100 $\mu\text{mol.L}^{-1}$) exerted a cytostatic effect upon the cells. They continued to increase in number up until 48 hours but by 72 hours the cell number dropped, although viability remained stable and high.

The definitive action of cell death via doxorubicin has not been categorically confirmed. Various processes have been outlined including free radical damage (Sinha *et al.*, 1987), topoisomerase II inhibition (Alton *et al.*, 1993), DNA intercalation (Waring, 1970) and various effects on cell membranes (Tritton and Yee, 1982). It appears that doxorubicin acts via multiple mechanisms. It is not yet clear whether each one may be needed in a synergistic manner to cause cell death or if any one mechanism alone maybe sufficient. The nature of the effect of the drug may vary with concentration. The molecular mechanism of the events after the penetration of doxorubicin within the cell, or as a consequence of membrane interaction are incompletely defined. Doxorubicin has been demonstrated to cause apoptosis in tumour cell lines (Ling *et al.*, 1993 and Muller *et al.*, 1997) at the concentrations which have been used in the present study but this has not been confirmed by this work. An individual cell's transcriptional status should be considered as well as doxorubicin concentration when determining whether it will die or not. The apoptotic schedule is a complex cascade of signals and protein generation. MCF-7/S cells used for this study have been documented to have oestrogen stimulated growth activity which would complicate the issue further, all cells were cultured without phenol red pH indicator (Hickman, 1992) or any other known oestrogenic substances. It has been speculated that there are different clones of MCF-7/S cells (Kyprianou *et al.*, 1991), some which undergo apoptosis and others which do not. The *c-myc* oncogene has

been isolated and been discovered to hold a critical role in growth regulation of MCF-7/S cells (Fornari *et al.*, 1996), the protein which it codes for is thought to represent a component in the apoptotic pathway (Fornari *et al.*, 1996). The tumour suppressor gene *p53* also has a pivotal role inducing apoptosis, therefore possible specific mutations of this gene could prevent apoptosis within a human tumour population (Aas *et al.*, 1996). The lack of apoptosis shown by the MCF-7/S cells of this study may have been because they were part of a clone that were not destined to die through apoptosis. Over the 144 hours viability remained high for all cells. As the doxorubicin had exhibited cytostatic action over the cells, it would seem that there was only a matter of time before all the cells would die, what mechanism would this be from? how long would they remain in this quiescent state?

The MCF-7/R cells did not respond to the doxorubicin treatment. They demonstrated a reduced red fluorescence, but the cell growth was not affected until 96 hours, when all the cells appeared quiescent, including the control. This was probably because the cells were confluent and had become starved of nutrients. The MCF-7/R cells were not affected by the doxorubicin treatment as they are able to pump the drug out of the cell and away from the sites within the cell which causes the cytostatic/cytotoxic effect of the drug, namely the nucleus. Davies *et al.* (1996) studied the MCF-7/R cells used for this work. The designation which was given to these cells was HP - gp. These cells have MDR1 mRNA levels of $6.65 \pm 2.29 \text{ amol.ng}^{-1}$, the level of detected P - gp by MRK16 was correlated with Rh123 accumulation. The high levels of P - gp enable the unusual compartmentation of anthracyclines as well as the removal of the drug from the cell. This transport protein can be found within the membranes of cytoplasmic organelles and on the nuclear envelope (Arancia *et al.*, 1998). Many studies have confirmed that there is reduced anthracycline accumulation in resistant cells compared with their sensitive counterparts (Inaba *et al.*, 1979; Frankfurt, 1987; McGown *et al.*, 1983; Konen *et al.*, 1989; Fox and Smith, 1995 and Arancia *et al.*, 1998).

The use of flow cytometry to determine a population of drug resistant cells using an anthracycline (usually doxorubicin or daunorubicin) as a transport protein (P - gp) modulator is well documented (Inaba *et al.*, 1979; Herweijer *et al.*, 1989; Mc Gown *et al.*, 1983; Frankfurt, 1987 and Krishan, 1994). The fluorescence detection of drugs within cells has also been coupled with many other measurements including cell growth inhibition, DNA damage and P-gp cellular localization. Resistance to anthracycline

therapy has been detected using other detection methods specific to P-gp, as an alternative to the carcinogenic anthracyclines. Other fluorescent agents have also been utilised in a similar manner to the anthracyclines to determine the resistance of a cell population via the reduction of an agent within the cell (Neyfakh, 1988; Feller *et al.*, 1995 and Kessel *et al.*, 1991).

Using the MTT assay it was found that incubation with doxorubicin or mitoxantrone at 0.1 - 5 $\mu\text{mol.L}^{-1}$ for 24 hours caused MCF-7/S and MDA MB 231 cells to become >70% non - viable. This was not seen after a one hour incubation with 1 - 100 $\mu\text{mol.L}^{-1}$ doxorubicin, using trypan blue exclusion, sytox or annexin V binding, even when cells were incubated for a further 4 - 144 hours. The discrepancy between the two sets of results could be the result of the differences in incubation times. The drug may require longer than one hour to interact with the cells, or more damage can be caused the longer the drug is in contact with the cells. A short incubation time of one or two hours has been used for similar investigations (Feller *et al.*, 1995; Fisher and Patterson, 1992 and Schuurhuis *et al.*, 1993). The MTT assay fundamentally measures different cellular functionality than sytox and trypan blue exclusion, it determines the ability of the mitochondria of the cell to hydrolyse MTT to MTT formazan. This assay is a measure of an energy dependent cellular process. Sytox and trypan blue are a measure of the ability of a cell to retain an effective plasma membrane, a cell with a compromised plasma membrane will allow entry into the cell of both trypan blue and sytox. There maybe discrepancy in the timing of the end of mitochondrial activity and the permeability of the plasma membrane as two of the events leading up to the demise of a cell, which may also be dependent of the mechanism of death.

Although the IC_{50} could not be accurately determined for in this study, it was less than 1 $\mu\text{mol.L}^{-1}$ for both doxorubicin and mitoxantrone using both MCF-7/S and MDA MB 231 cell lines. Many definitions of IC_{50} can be found in the literature for these drugs, using numerous cell lines, using various viability or cell proliferation assays, with varying time incubations of drug and the incubation time after the drug incubation and before the assay. The differences between the assays makes direct comparisons difficult.

Schuurhuis *et al.* (1993) investigated the relationship between doxorubicin resistance of MCF-7/S cells and the accumulation and distribution of the drug within the cells, the IC_{50} of MCF-7/S cells was 0.19 $\mu\text{mol.L}^{-1}$. This figure was determined after using a two hour incubation with doxorubicin, the cells were then allowed to complete at

least three doubling times before being counted (Schuurhuis *et al.*, 1987). A parallel experiment was also carried out using MCF-7/R cells which exhibited a IC_{50} of 290 $\mu\text{mol.L}^{-1}$. The IC_{50} of mitoxantrone and doxorubicin were calculated in parallel, using a one hour drug incubation time, followed by 6 days of drug free growth before being counted (Fisher and Patterson, 1992). Mitoxantrone was found to be more toxic to the MCF-7/S cells than doxorubicin. Mitoxantrone IC_{50} was 5.2 nmol.L^{-1} and doxorubicin IC_{50} was 3 $\mu\text{mol.L}^{-1}$. Mitoxantrone has been found to be significantly more toxic towards human cells than other antineoplastic drugs such as doxorubicin (Epstein and Smith, 1988).

For this study the apoptotic status of MCF-7/S and MCF-7/R cells were determined using an annexin V binding kit (Boehringer Ingelheim Bioproducts Partnership, Heidelberg, Germany). The main biochemical methods of detection of apoptosis are - (a) detection of DNA breaks, caused by endonucleases, (b) detection of DNA fragments using gel electrophoresis and (c) detection of specific apoptotic related proteins, receptors or ligands from Western blots and (d) detection of the translocation of phosphatidylserine (PS). The DNA fragments can be labelled *in situ* by using terminal deoxynucleotidyl transferase (TdT) (TUNEL) or using a DNA polymerase (ISEL), on fixed cells. Apoptosis detection on individual unfixed cells can be performed using the detection of the translocation of phosphatidylserine (PS) from the inner face of the plasma membrane to the cell surface (Martin *et al.*, 1996) by the binding of annexin V. PS is an external signal of apoptosis and is detectable without fixation or DNA extraction. The annexin V binding assay can be easily performed concurrently with the detection of doxorubicin uptake. The annexin V protein is FITC labelled for detection, the green fluorescence can then be simultaneously measured with the red fluorescence of doxorubicin using FCM and LSC. Normally annexin V binding is used alongside PI staining. The double labelling enables the PI to exclude all those cells which are necrotic. PI was not used for this study as its red fluorescence would overlap with that of doxorubicin.

**UPTAKE OF
DOXORUBICIN
LOADED
MICROCAPSULES
CYTOCAPSTM BY
MCF-7/S CELLS**

3.5 Uptake of doxorubicin loaded microcapsules Cytocaps™ by MCF-7/S cells

For this study a new drug delivery system produced by Quadrant Ltd (Nottingham, England) has been investigated for its binding and cytostatic capabilities against the human breast carcinoma MCF-7/S cell line. The product Cytocaps™ are 3 µm microcapsules of HSA covalently coated with doxorubicin, 0.68 mol.L⁻¹ doxorubicin per mole HSA.

3.5.1 Cytocaps™ time course

Viable MCF-7/S cells were incubated for one hour with a range of Cytocaps™ concentrations of 0.5 to 2 µmol.L⁻¹, grown in culture for 4, 24, 48, 72 and 96 hours, and then analysed using FCM. The FCM analysis of Cytocap™ uptake is described in figure 3.56 and the uptake data is shown in figure 3.57. There was a proportional response between Cytocaps™ uptake and concentration, the highest percentage uptake was 75% at 24 hours, for 2 µmol.L⁻¹. All Cytocap™ concentrations generated levels of fluorescence that were higher than in the control cells. After Cytocap™ incubation viability was determined by trypan blue exclusion and sytox uptake (FCM), apoptosis was also measured using annexin V binding (FCM), the FCM analysis of these analytes was illustrated in figure 3.58. This figure shows MCF-7/S cells incubated with 0.5 µmol.L⁻¹ Cytocaps™ and incubated with sytox or annexin V.

The trypan blue counts and percentage viability of the cell suspensions after being grown in culture for 4 - 96 hours are shown in figure 3.59. The control cell culture increased in cell number until 48 hours after which it reached a plateau, at 72 hours the cell numbers started to decrease, presumably as the cells had become overgrown and lacked essential nutrients. All concentrations of Cytocaps™ prevented cell growth and caused a fall in cell count after 72 hours. Cell viability only dropped at 96 hours, this was greater in the cultures including Cytocaps™ than in the control.

The results generated by sytox staining to determine viability using FCM are shown in figure 3.60. The red fluorescence of the Cytocaps™ is very bright and a small amount of this fluorescence leaks into the FL1 PMT which is used to analyse sytox levels. Cells incubated with each concentration of Cytocaps™ alone, were analysed and the leakage into FL1 was calculated and subtracted from the overall percentage positive cells when analysing the sytox signal in dual labelled samples. The general trend of sytox uptake was similar for all Cytocap™ concentrations, the peak sytox signal is at 24 hours,

indicating the highest percentage of non - viable cells. This is the same time point that demonstrated the highest percentage CytocapsTM uptake and fluorescence. There appears to be no difference in the percentage of non - viable cells between the CytocapTM concentrations.

The percentage of cells positive for annexin V - FITC binding and the corresponding mean green fluorescence are shown in figure 3.61. The level of apoptosis is constant and low for all samples until 72 hours when there was an increase in the percentage of annexin V positive cells, in both the control and CytocapTM treated samples at 96 hours. There was an apparent dose effect on apoptosis with the control cells showing the least and cells treated with 1 and 2 $\mu\text{mol.L}^{-1}$ CytocapsTM showing the most apoptosis. The green fluorescence of annexin V was very bright and therefore was not affected by leakage of red fluorescence from the CytocapsTM.

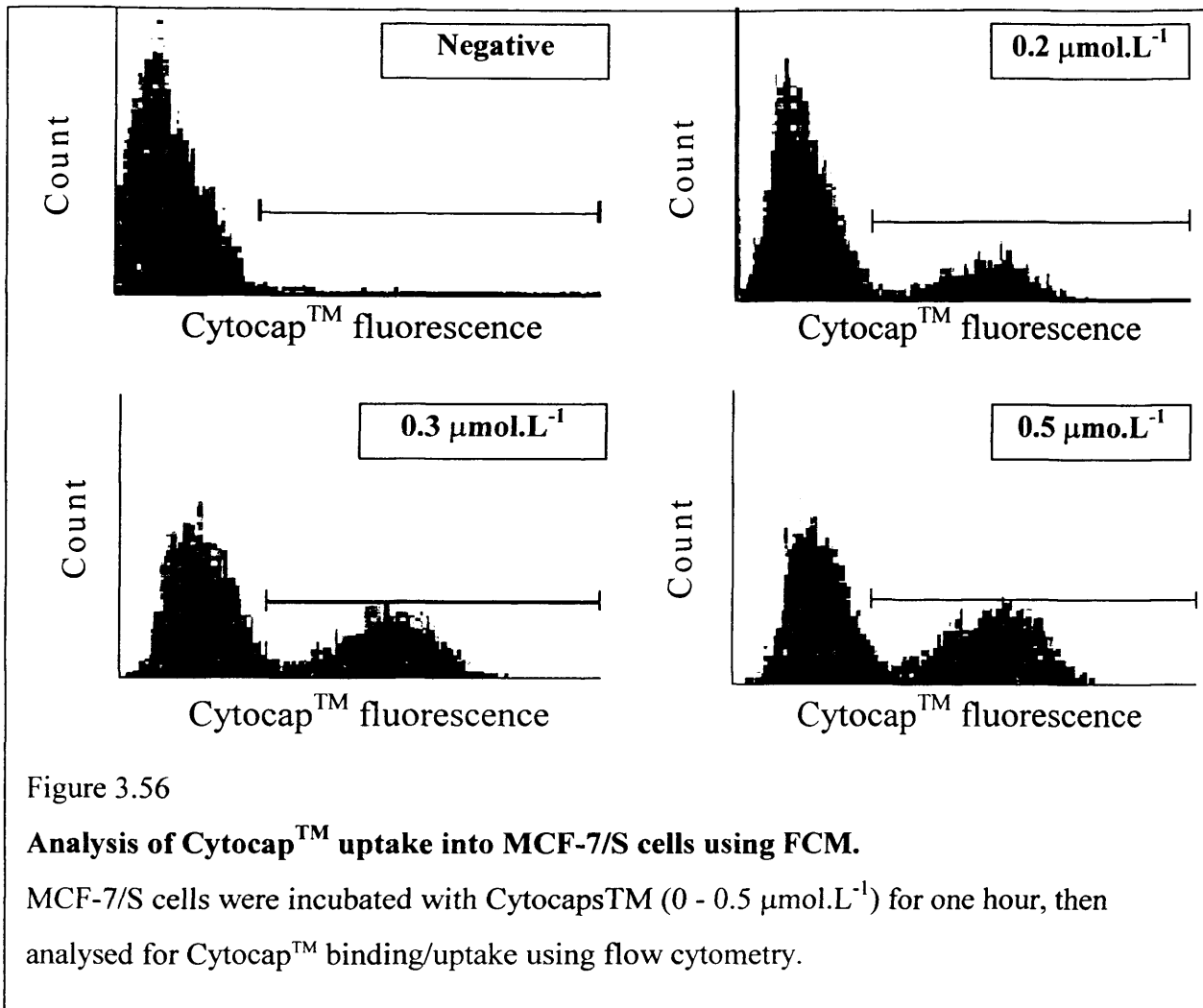


Figure 3.56

Analysis of Cytocap™ uptake into MCF-7/S cells using FCM.

MCF-7/S cells were incubated with Cytocaps™ (0 - 0.5 μmol.L⁻¹) for one hour, then analysed for Cytocap™ binding/uptake using flow cytometry.

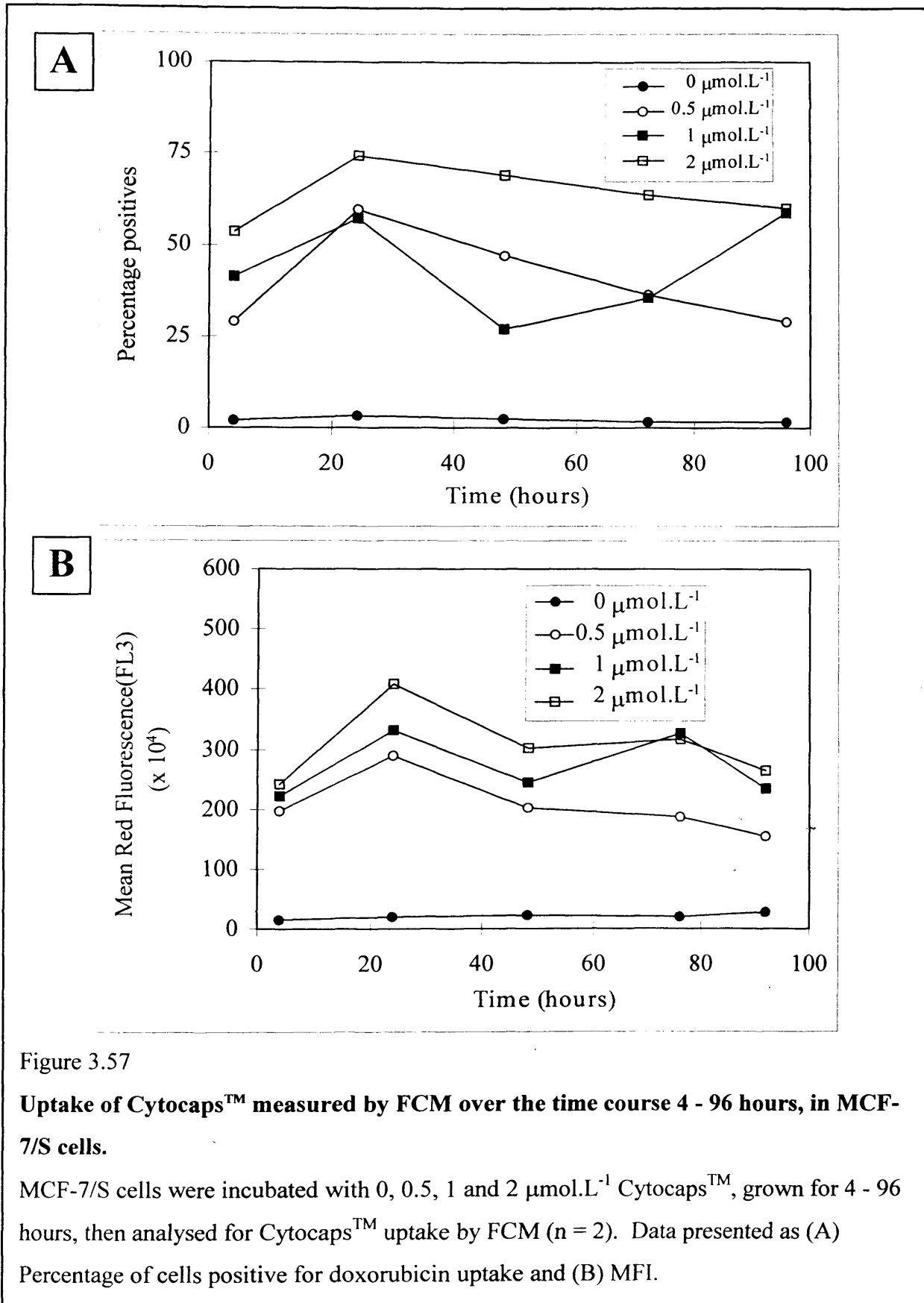


Figure 3.57

Uptake of Cytocaps™ measured by FCM over the time course 4 - 96 hours, in MCF-7/S cells.

MCF-7/S cells were incubated with 0, 0.5, 1 and 2 $\mu\text{mol.L}^{-1}$ Cytocaps™, grown for 4 - 96 hours, then analysed for Cytocaps™ uptake by FCM (n = 2). Data presented as (A) Percentage of cells positive for doxorubicin uptake and (B) MFI.

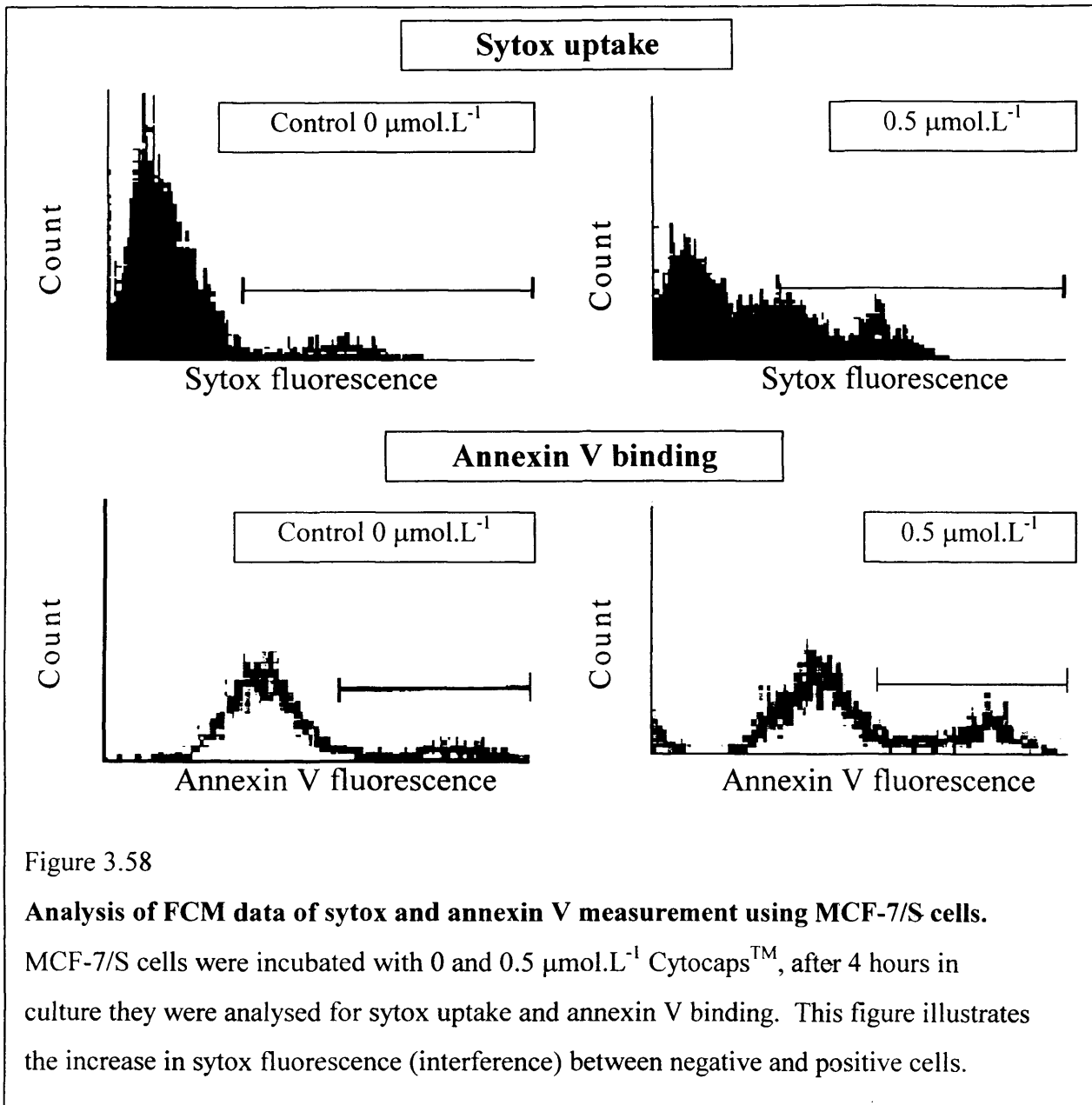


Figure 3.58

Analysis of FCM data of sytox and annexin V measurement using MCF-7/S cells.

MCF-7/S cells were incubated with 0 and 0.5 $\mu\text{mol.L}^{-1}$ CytocapsTM, after 4 hours in culture they were analysed for sytox uptake and annexin V binding. This figure illustrates the increase in sytox fluorescence (interference) between negative and positive cells.

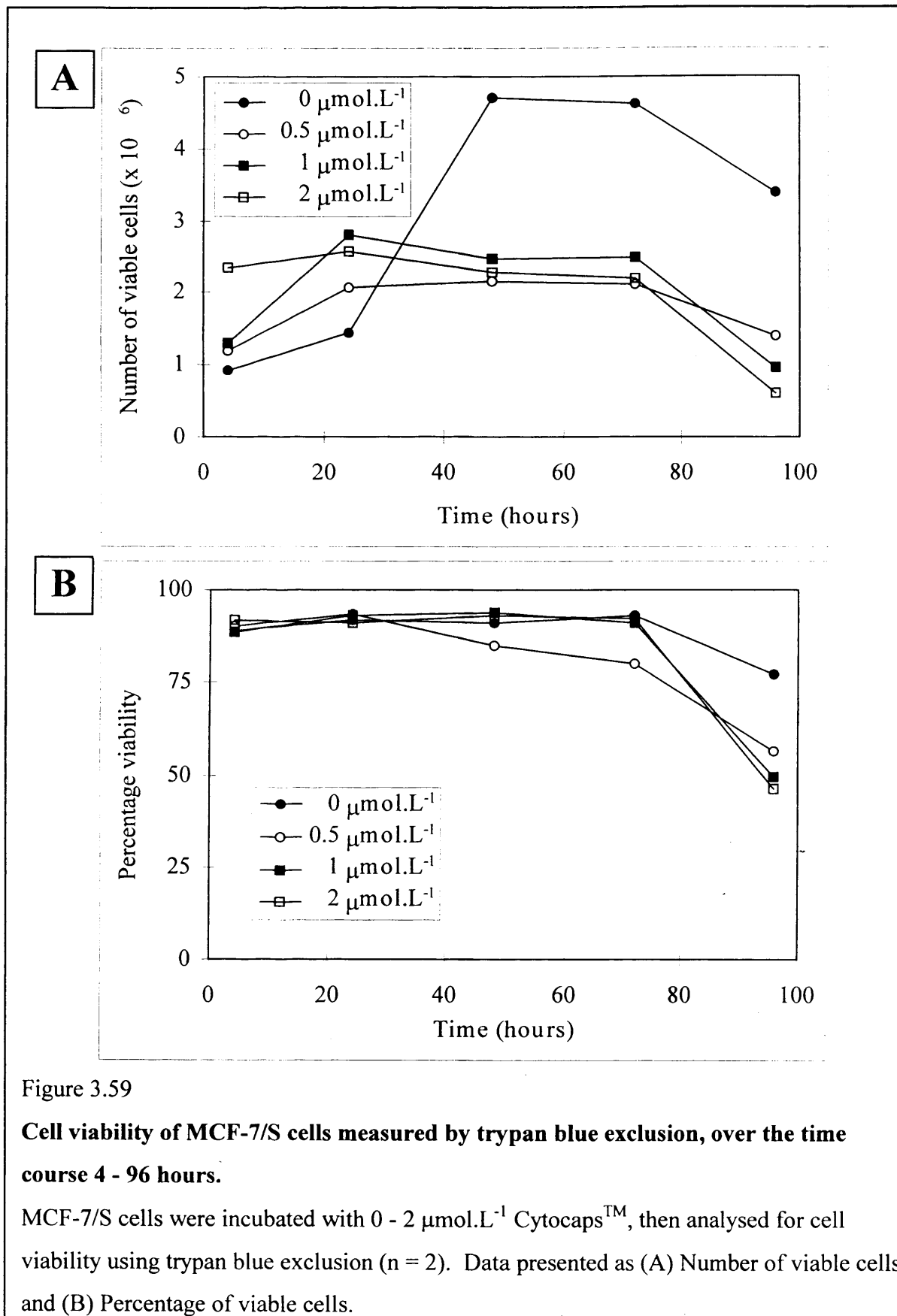


Figure 3.59

Cell viability of MCF-7/S cells measured by trypan blue exclusion, over the time course 4 - 96 hours.

MCF-7/S cells were incubated with 0 - 2 $\mu\text{mol.L}^{-1}$ CytocapsTM, then analysed for cell viability using trypan blue exclusion (n = 2). Data presented as (A) Number of viable cells and (B) Percentage of viable cells.

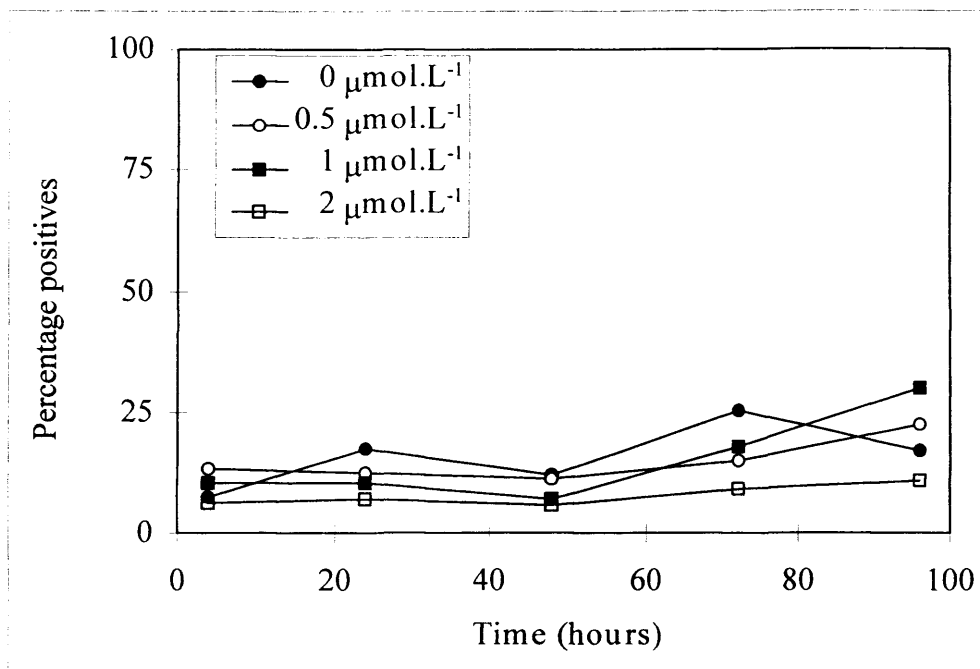
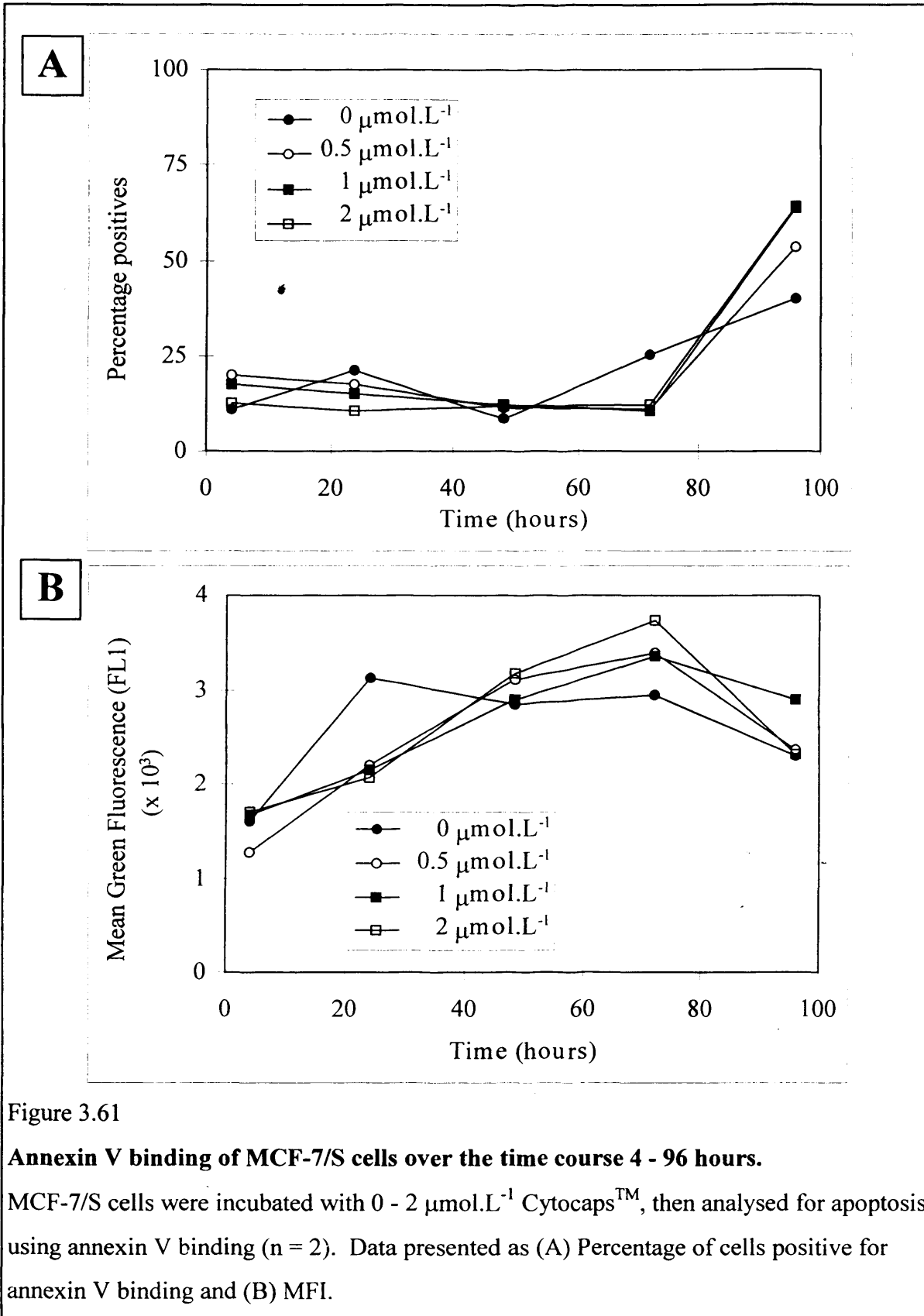


Figure 3.60

Cell viability of MCF-7/S cells measured by sytox uptake, over the time course 4 - 96 hours.

MCF-7/S cells were incubated with 0 - 2 μmol.L⁻¹ CytocapsTM, then analysed for viability using sytox uptake (n = 2).



3.5.2 LSC analysis

Aliquots of MCF-7/S cells incubated with $0.5 \mu\text{mol.L}^{-1}$ CytocapsTM were analysed using the LSC and chamber slides. Although this analysis was standardised between the samples it was not used quantitatively. A dot plot such as described in figure 3.62 was produced for each time point, the figure demonstrates the 'Area vs Red Max. Pixel' data for the 24 hour time point, which was indicated from figure 3.57 to represent the time point with the maximum binding of CytocapsTM to cells. The LSC detected the MCF-7/S cells using light scatter and measured the red fluorescence of the CytocapsTM detected simultaneously. The 'Area' of the cells is determined from the light scatter signal, the number of pixels within the threshold contour of each cell, and 'Red Max. Pixel' is the highest red pixel signal within the data contour of each cell. This dot plot separates MCF-7/S cells, from unbound CytocapsTM, the regions 1 - 3 highlighted in the dotplot represent the following (1) MCF-7/S cells attached to CytocapsTM, (2) CytocapsTM alone and (3) MCF-7/S cells alone. The images produced in figures 3.63 - 3.66 are produced from galleries of the first 16 cells recorded from the highlighted region (1), for each of the time points.

The images in figures 3.63 - 3.66 are created from black and white laser images, the LSC relocates to the highlighted region (1) of the 'Area vs Red Max. Pixel' dotplot and rescans the first 16 cells. The laser images of these cells can be obtained for light scatter, red and green fluorescence, to create the false colour images in figures 3.63 - 3.66 a laser scan of each parameter was obtained sequentially. Each black and white image was transferred to Paintshop Pro 5 where they were split into the three primary colours red, green and blue, each image was allocated one of the three colours and then recombined to produce the false colour images.

The 16 images in figure 3.63 represent the first 16 cells which have been incubated with $0.5 \mu\text{mol.L}^{-1}$ CytocapsTM and have been grown for 4 hours in culture. The cells (blue) appear small and only slightly larger than the CytocapsTM (red), these cells have received two incubations of trypsinization within 6 hours, when they were plated out to grow in culture they were given insufficient time to recover from their original trypsinization and CytocapsTM incubation. The cells therefore appear small because they are round and have only adhered sufficiently to remain at a constant position, they have not begun to spread out, as they are normally seen in culture. Each of the cells, in the centre of each individual image, have at least one CytocapTM attached, the position of each

Cytocap™ is on the outside of the MCF-7/S cell. The images taken from the same region of the 'Area vs Red Max. Pixel' dotplot at 24 hours are shown in figure 3.64. The cells (blue) at 24 hours visually look larger than the cells at 4 hours. Each cell has one or more Cytocap™ (red) attached which appear to be on the outside of the cells. The images in figure 3.65 were created at 48 hours, the Cytocaps™ have penetrated into the cells. By 120 hours incubation (FCM data not shown) a number of the Cytocaps™ appear to have released their doxorubicin within the cells to create a diffuse red fluorescence, as shown in figure 3.66, rather than the bright discreet Cytocaps™ at the earlier time points. Not all the Cytocaps™ at 120 hours were at the same stage of break down as some still appeared as discreet bright red fluorescent images.

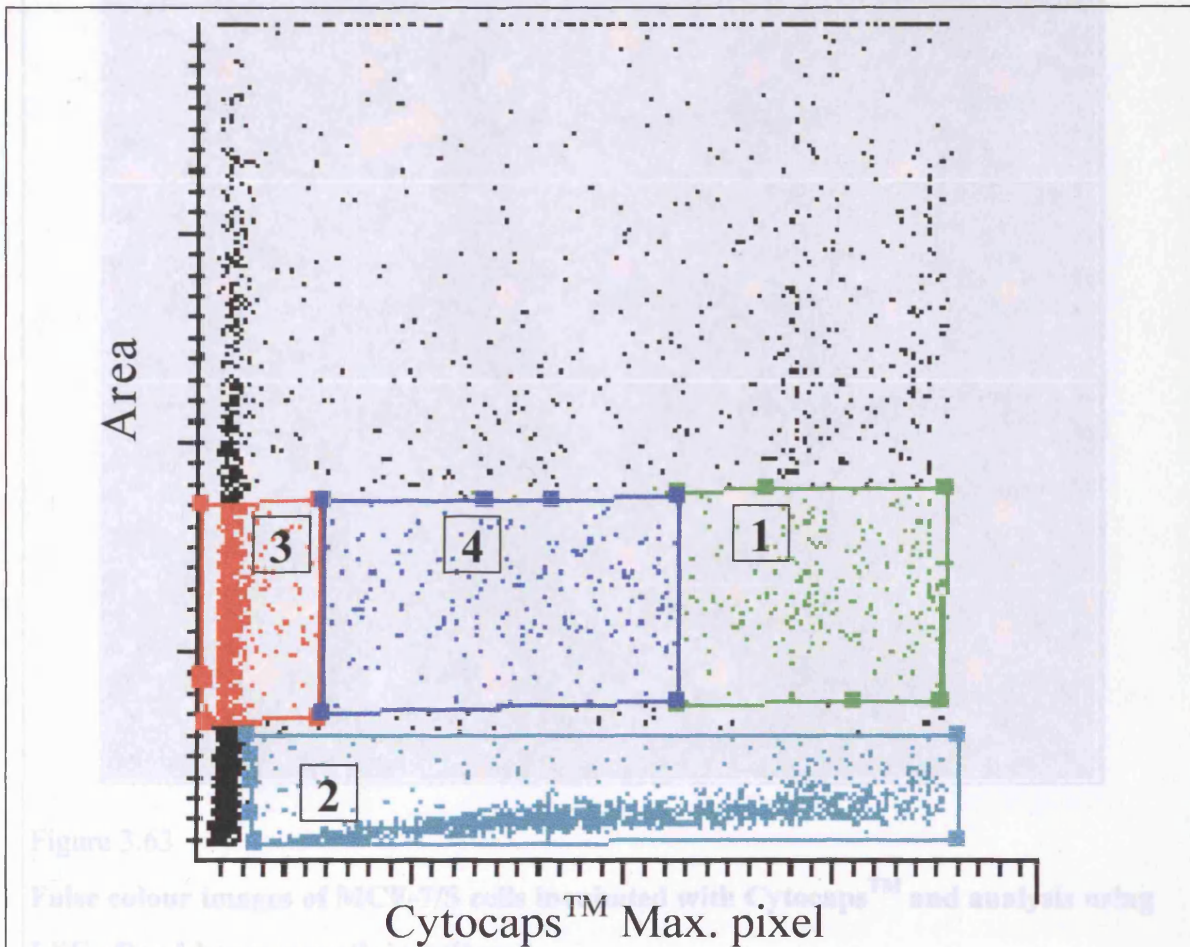


Figure 3.62

MCF-7/S cells were incubated with $0.5 \mu\text{mol.L}^{-1}$ Cytocaps™, then grown for 4 hours in culture, then analysed using the LSC for Cytocaps™ uptake.

Figure 3.62 shows the LSC dot plot of MCF-7/S cells after incubation with $0.5 \mu\text{mol.L}^{-1}$ Cytocaps™, then grown for 4 hours in culture, then analysed using the LSC for Cytocaps™ uptake.

LSC dot plot of MCF-7/S cells after incubation with $0.5 \mu\text{mol.L}^{-1}$ Cytocaps™.

MCF-7/S cells were incubated with $0.5 \mu\text{mol.L}^{-1}$ Cytocaps™ for one hour and then grown in culture for 24 hours, then analysed using the LSC for Cytocaps™ uptake.

Region 1 represents MCF-7/S single cells attached to a Cytocaps™ of the brightest fluorescence, region 2 represents Cytocaps™, region 3 represents MCF-7/S cells alone and region 4 represents MCF-7/S cells attached to various size or fluorescent Cytocaps™.

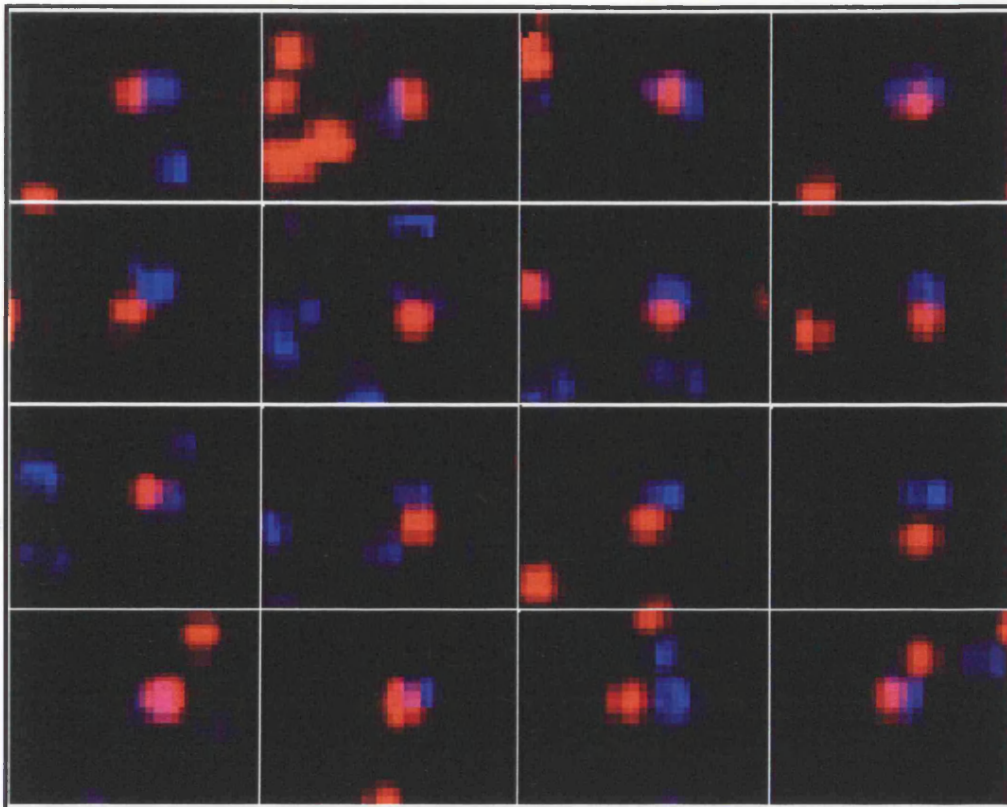


Figure 3.63

False colour images of MCF-7/S cells incubated with Cytocaps™ and analysis using LSC after 4 hours growth in culture.

MCF-7/S cells were incubated with $0.5 \mu\text{mol.L}^{-1}$ Cytocaps™, then grown for 4 hours.

The cells were analysed using light scatter on the LSC. False colour gallery images of the cells were produced, 'red' represents the Cytocaps™ and 'blue' the light scatter images of the cell.

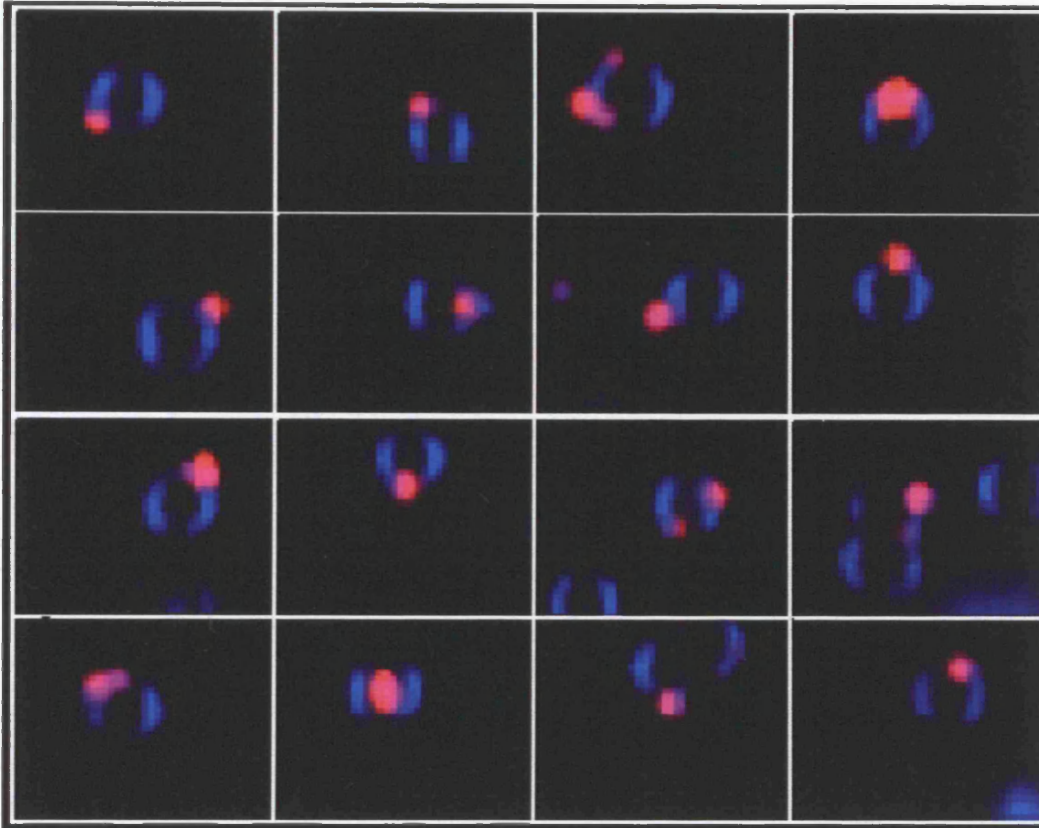


Figure 3.64

False colour images of MCF-7/S cells incubated with Cytocaps™ and analysis using LSC after 24 hours growth in culture.

MCF-7/S cells were incubated with $0.5 \mu\text{mol.L}^{-1}$ Cytocaps™, then grown for 24 hours. The cells were analysed using light scatter on the LSC. False colour gallery images of the cells were produced, 'red' represents the Cytocaps™ and 'blue' the light scatter images of the cell.

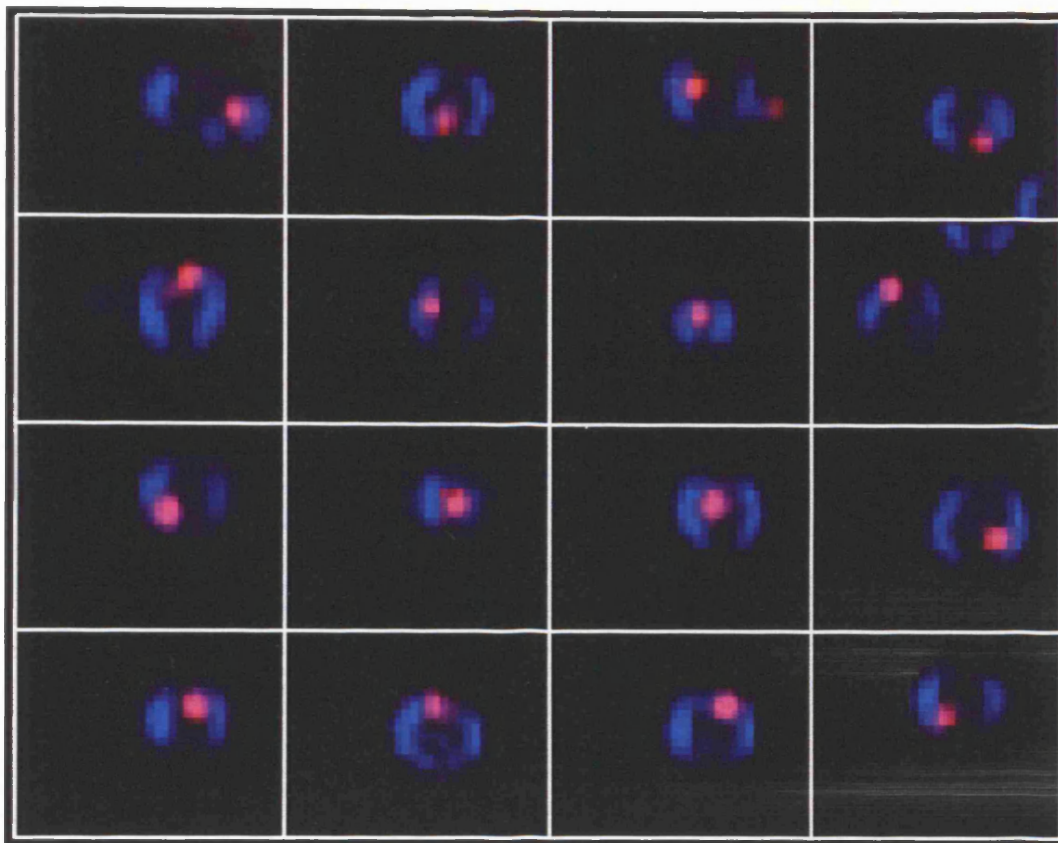


Figure 3.65

False colour images of MCF-7/S cells incubated with Cytocaps™ and analysis using LSC after 48 hours growth in culture.

MCF-7/S cells were incubated with $0.5 \mu\text{mol.L}^{-1}$ Cytocaps™, then grown for 48 hours.

The cells were analysed using light scatter on the LSC. False colour gallery images of the cells were produced, 'red' represents the Cytocaps™ and 'blue' the light scatter images of the cell.

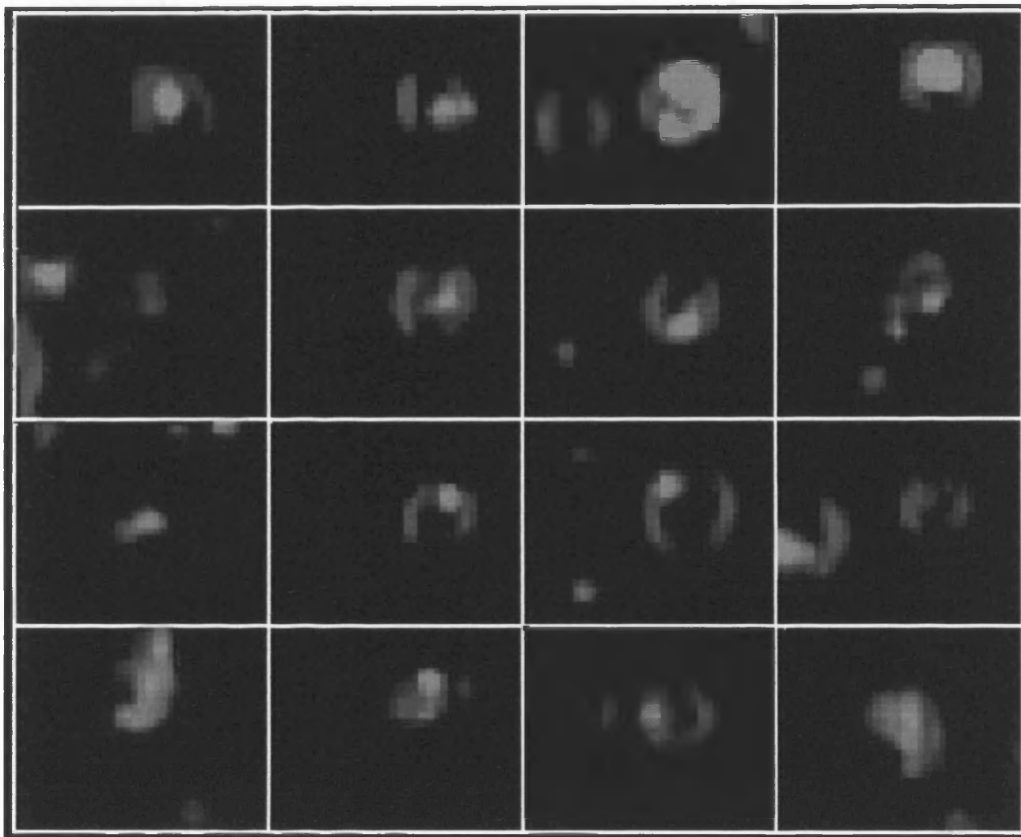


Figure 3.66

False colour images of MCF-7/S cells incubated with Cytocaps™ and analysis using LSC after 120 hours growth in culture.

MCF-7/S cells were incubated with $0.5 \mu\text{mol.L}^{-1}$ Cytocaps™, then grown for 120 hours. The cells were analysed using light scatter on the LSC. False colour gallery images of the cells were produced, 'red' represents the Cytocaps™ and 'blue' the light scatter images of the cell.

3.5.3 Discussion

Cytocaps™ and other drug delivery systems offer an opportunity to increase response to chemotherapeutic agents such as doxorubicin and reduce the harmful side effects. Drug delivery systems such as Cytocaps™ may enable drug to be delivered to tumour sites in a concentrated form which may be more effective than the systemic diffuse treatment which is offered, i.e. i.v. doxorubicin.

From this investigation Cytocaps™ were detectable using LSC and FCM at the concentrations 0.5 - 2 $\mu\text{mol.L}^{-1}$ used. The uptake of Cytocaps™ appeared to reach a peak at 24 hours (figure 3.57) and to enter the cell at 48 hours (figure 3.64). A cytostatic effect of Cytocaps™ was seen at all concentrations used. Very similar results were obtained with both methods for measuring cell viability (trypan blue and sytox). Annexin V - FITC binding generally remained at a similar level to that of the control cells, reinforcing the trypan blue counts, that growth was arrested but the cells were not dying, until 96 hours when an increase in apoptosis was detected.

The use of sytox simultaneously with Cytocaps™ in the future would need further experimental adjustment. The Cytocaps™ are very bright compared with sytox and the FL1 PMT on the FCM was set at a fairly sensitive setting to detect sytox, but consequently it was also detecting leakage of red fluorescence from the Cytocaps™. To use these agents simultaneously the sytox signal could be increased (use a higher concentration) and/or the sensitivity of the FL1 PMT could be decreased. The leakage was largely masked by the brighter fluorescence of the annexin V - FITC, compared to sytox staining. This problem was compounded by the lack of colour compensation between FL1 and FL3 on the particular FCM used.

As shown in figure 3.62 a large number of Cytocaps™ that did not attach to the cells over the incubation times used for this study. It has been suggested from the results in figure 3.57 that Cytocaps™ which are going to become attached to the MCF-7/S cells they will have done so by 24 hours. It would be interesting to remove the unattached Cytocaps™ at different stages of the time course and compare these to uptake results with a constant pool of unattached Cytocaps™. Because in this study the cells were incubated with the Cytocaps™ in suspension it was not possible to remove the unattached Cytocaps™ from the cell suspensions using simple centrifugation, as they sedimented at similar g force.

The use of the LSC for this part of the study has demonstrated its unique ability to offer morphological data as to the location and kinetics of these CytocapsTM over time. With further work the measurement of CytocapsTM into MCF-7/S cells can be quantified and the movement of the CytocapsTM more accurately assessed. The LSC could determine the levels of fluorescence within the nucleus and cytoplasm separately and a ratio generated as performed by Schuurhuis *et al.* (1993). The relationship between the subcellular localisation of the CytocapsTM and the subsequent events and timing before cell death could be investigated. The investigation of the CytocapsTM and their interaction with human tumour cells can offer a wealth of research possibilities, including investigations into the mechanisms which lead to the internalisation of the capsule and the sites on the cell surface which the CytocapsTM are able to bind to and why.

**HUMAN BREAST
CARCINOMA
MANIPULATIONS**

3.6 Human breast carcinoma manipulations

The technique to disaggregate human breast tumour cells from a solid tumour was investigated to produce a tumour cell suspension with a high viability and yield. The techniques used for this study were mechanical, enzymatic disruption and fine needle aspirates (FNA). All the tumours used for mechanical and enzymatic disaggregation were infiltrating ductal carcinomas, tumour 1 and 5 were undefined infiltrating ductal carcinomas, tumour 2 was a grade I, tumours 4 and 7 were grade II and tumours 3 and 6 were grade III.

3.6.1 Cytocentrifuge preparations of human disrupted tumour cells

Illustrations of the breast tumour cell suspensions are shown in figures 3.67 - 3.78. These are photographs of cytocentrifuge preparations that were stained with H & E or PAP. These photos illustrate the variety of the appearance of tumour cells, and the other cell types found within tumour cell disruptions.

Figures 3.67, 3.71 and 3.75 highlight major points about mechanical disaggregation, they demonstrate a large number of tumour cells, many of which are still in clumps. Large quantities of cellular debris and extracellular matrix material is particularly noticeable in figure 3.69. Many of the tumour cells appear to have lost the majority of their cytoplasm and are no longer round in appearance, figure 3.68 illustrates at x 100 magnification the larger nuclei of the tumour cells, which have retained a minimal cytoplasm. In contrast with the numerous tumour cells of figures 3.67, 3.71 and 3.75, figure 3.70 illustrates a low number of tumour cells, compared to a large quantity of lymphoid and stromal cells. A higher magnification of tumour and lymphocytes is illustrated in figure 3.70, many of these cells have retained more cytoplasm than those shown in figure 3.69.

Results

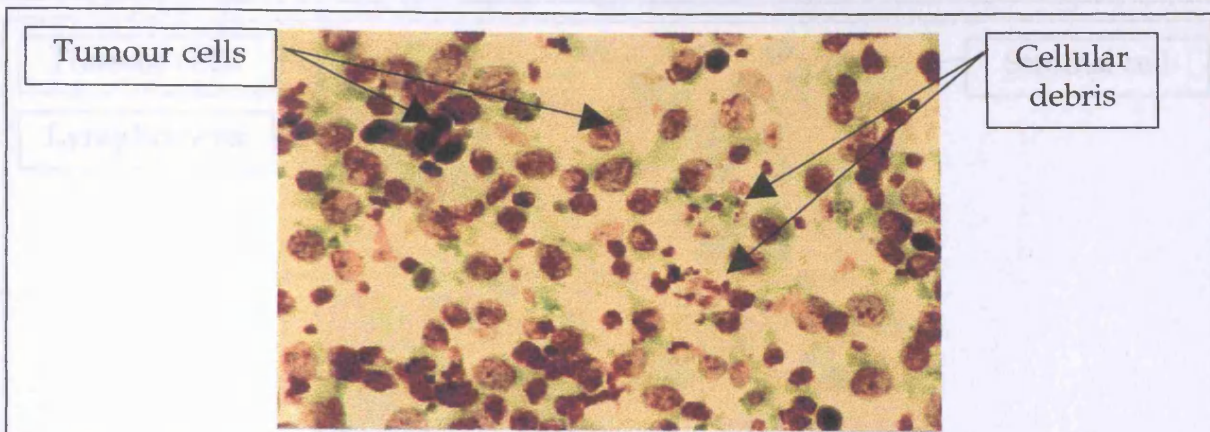


Figure 3.67

Mechanical disaggregation of T1, cytocentrifuge preparation stained with PAP, x40 magnification.

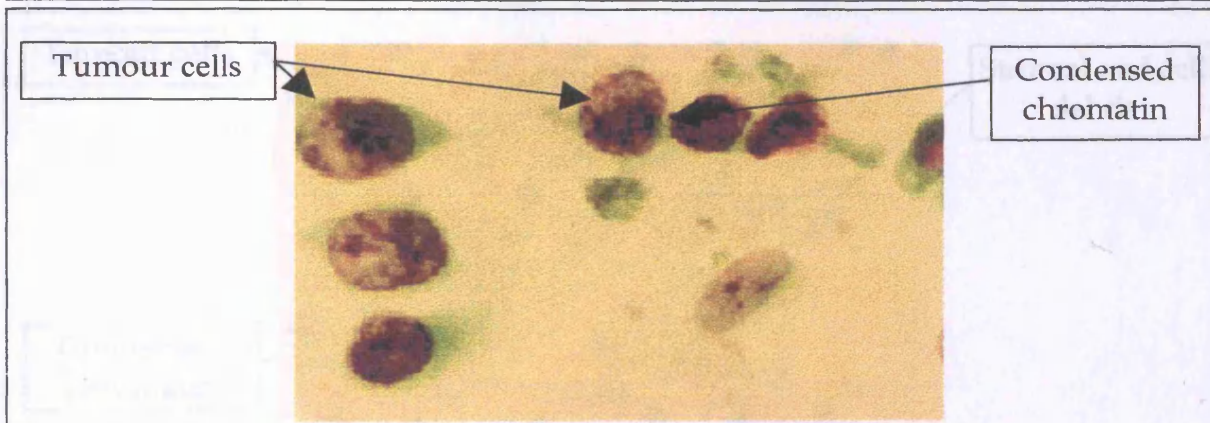


Figure 3.68

Mechanical disaggregation of T1, cytocentrifuge preparation stained with PAP, x100 magnification.

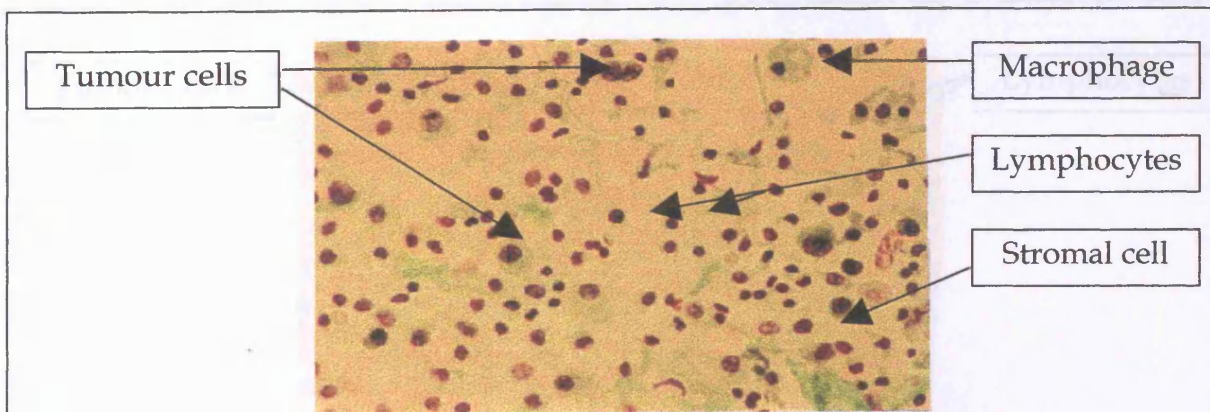


Figure 3.69

Mechanical disaggregation of T2, cytocentrifuge preparation stained with PAP, x40 magnification.

Results

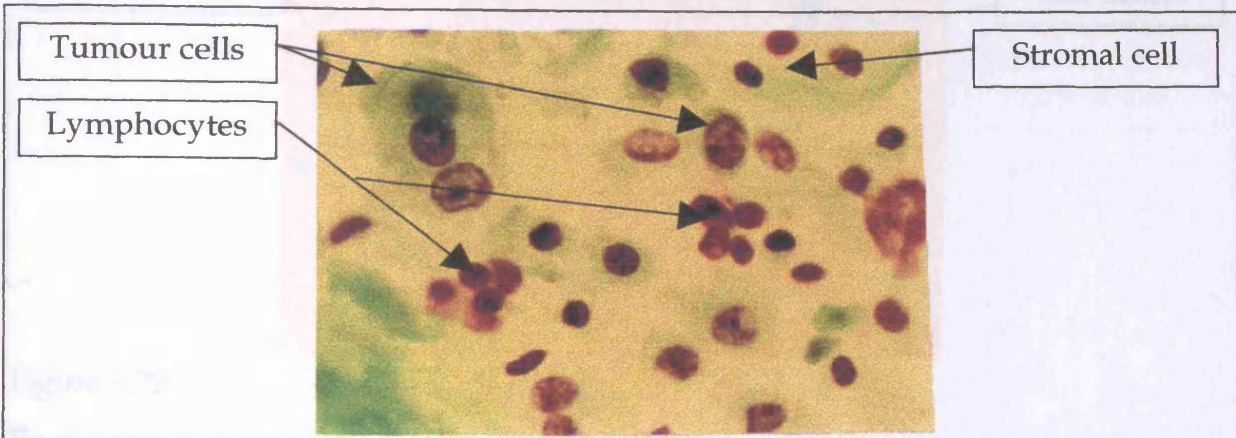


Figure 3.70
Mechanical disaggregation of T2, cytocentrifuge preparation stained with PAP, x100 magnification.

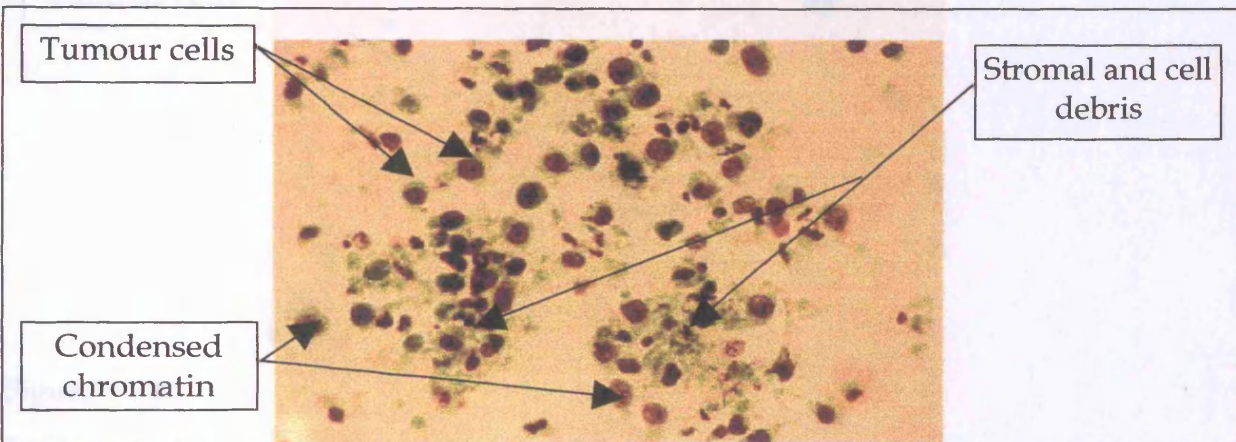


Figure 3.71
Mechanical disaggregation of T3, cytocentrifuge preparation stained with PAP, x40 magnification.

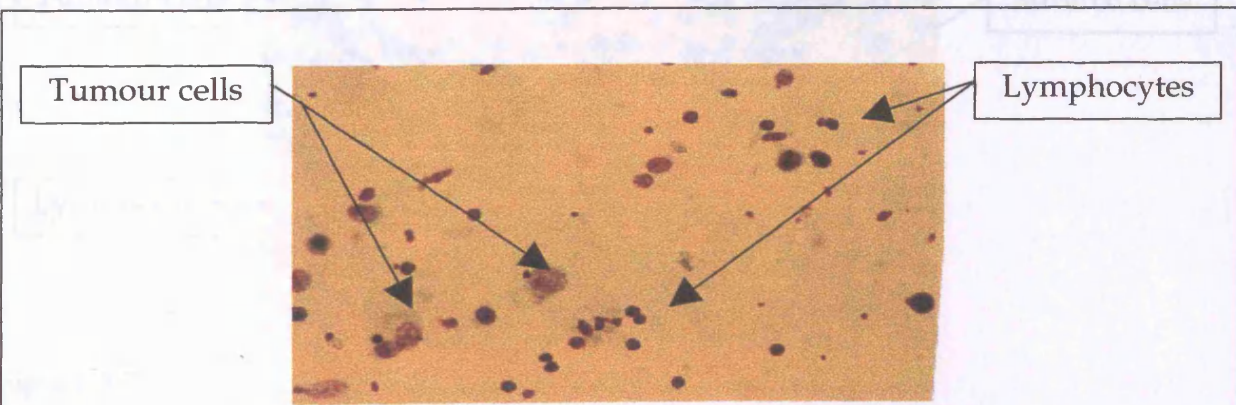


Figure 3.72
Enzymatic disaggregation of T3, cytocentrifuge preparation stained with PAP, x40 magnification.

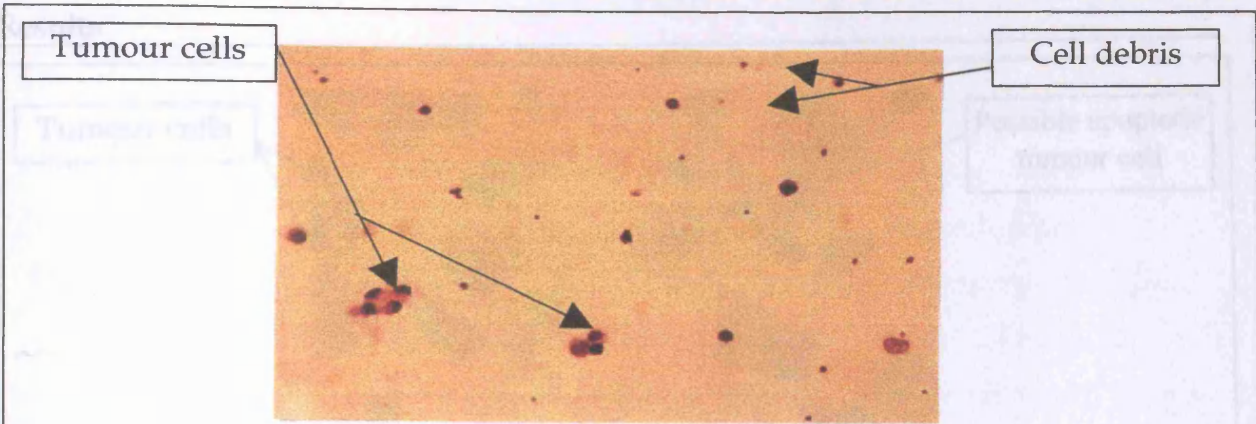


Figure 3.73

Enzymatic disaggregation of T5, cytocentrifuge preparation stained with HE, x40 magnification.

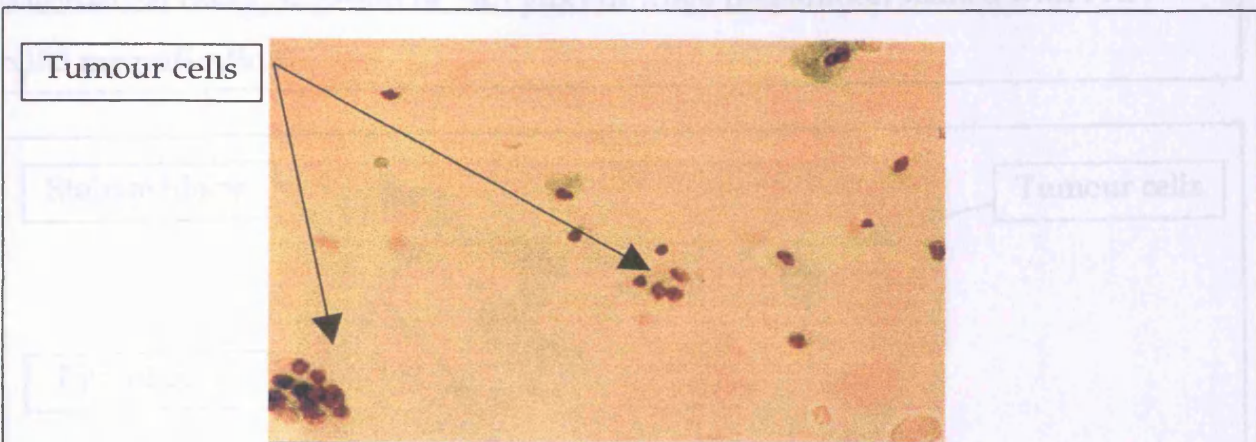


Figure 3.74

Enzymatic disaggregation of T5, cytocentrifuge preparation stained with PAP, x40 magnification

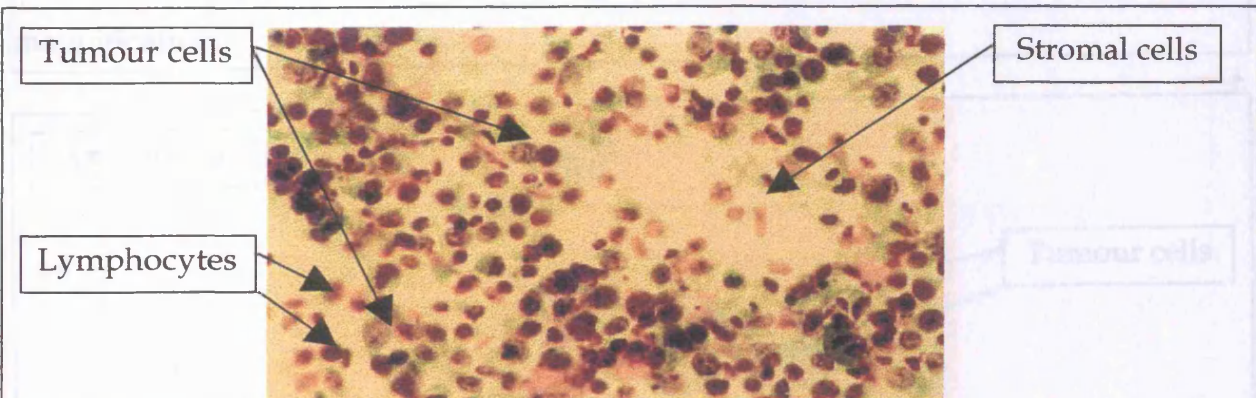


Figure 3.75

Mechanical disaggregation of T6, cytocentrifuge preparation stained with PAP, x40 magnification.

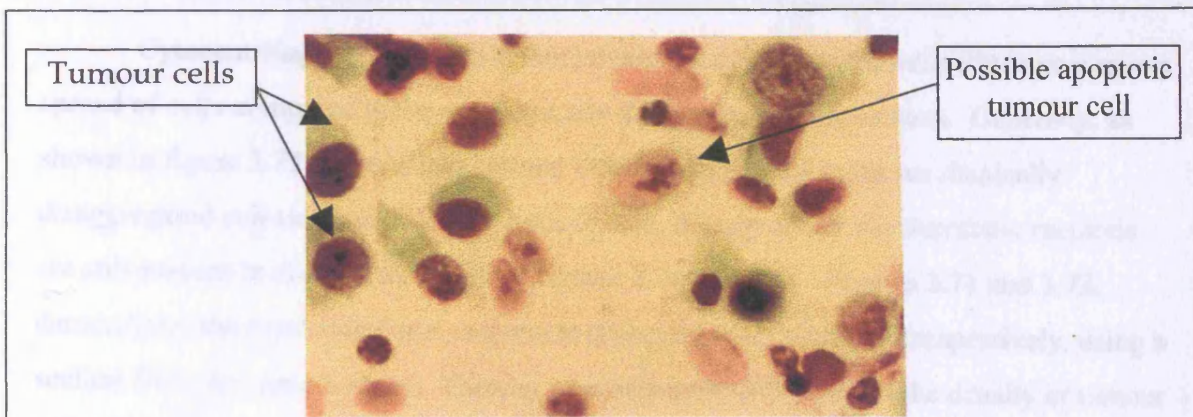


Figure 3.76

Mechanical disaggregation of T6, cyto centrifuge preparation stained with PAP, x100 magnification.

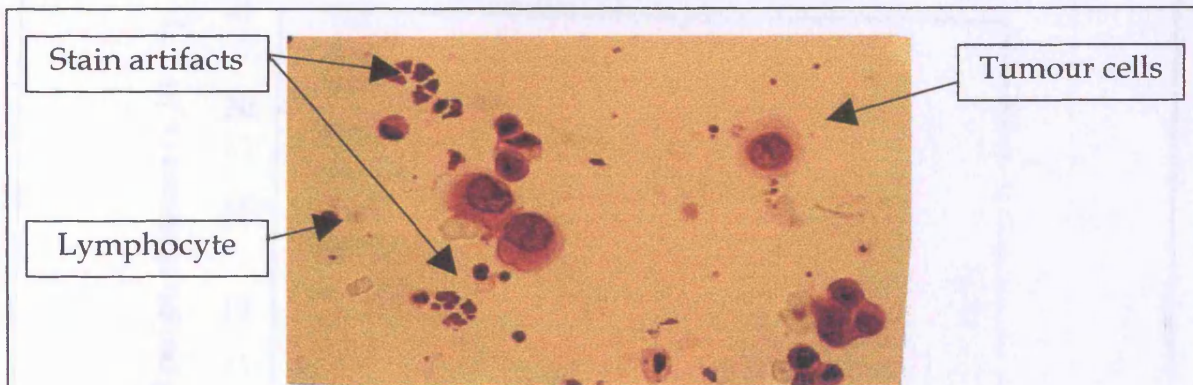


Figure 3.77

Enzymatic disaggregation of T7, cyto centrifuge preparation stained with HE, x40 magnification.

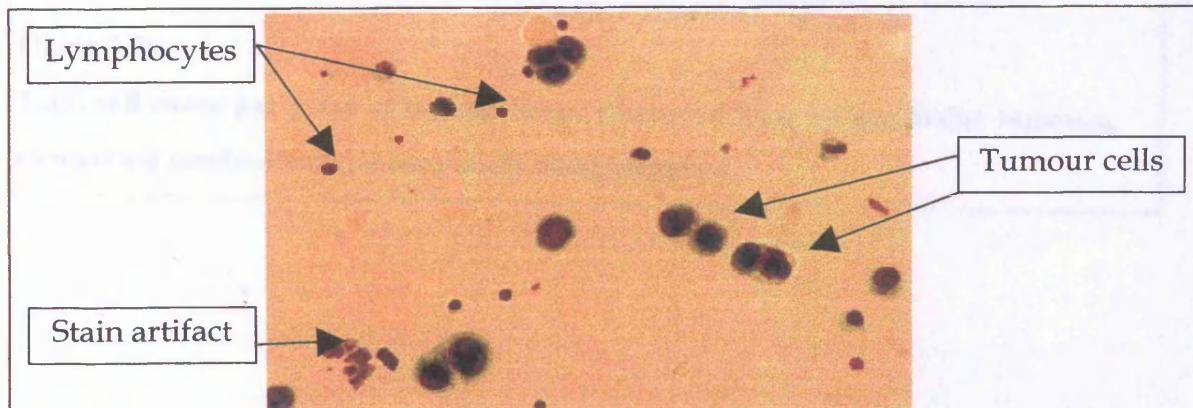


Figure 3.78

Enzymatic disaggregation of T7, cyto centrifuge preparation stained with PAP, x40 magnification.

Cyto-centrifuge preparations of enzymatically disaggregated cells illustrate a sparse spread of cells compared to the mechanically disaggregated suspensions. Generally, as shown in figure 3.72, there is less cellular debris than present in the mechanically disaggregated cell suspensions. The tumour cells disaggregated via enzymatic methods are still present in clumps, as shown in figures 3.74 and 3.78. Figures 3.71 and 3.72, demonstrate the mechanical and enzymatic disaggregation disruption respectively, using a section from the same tumour. There is a considerable difference in the density of tumour cells, the mechanical disruption producing more, coupled with a large amount of debris, figure 3.72 shows a cleaner cyto-centrifuge preparation, but with less cells.

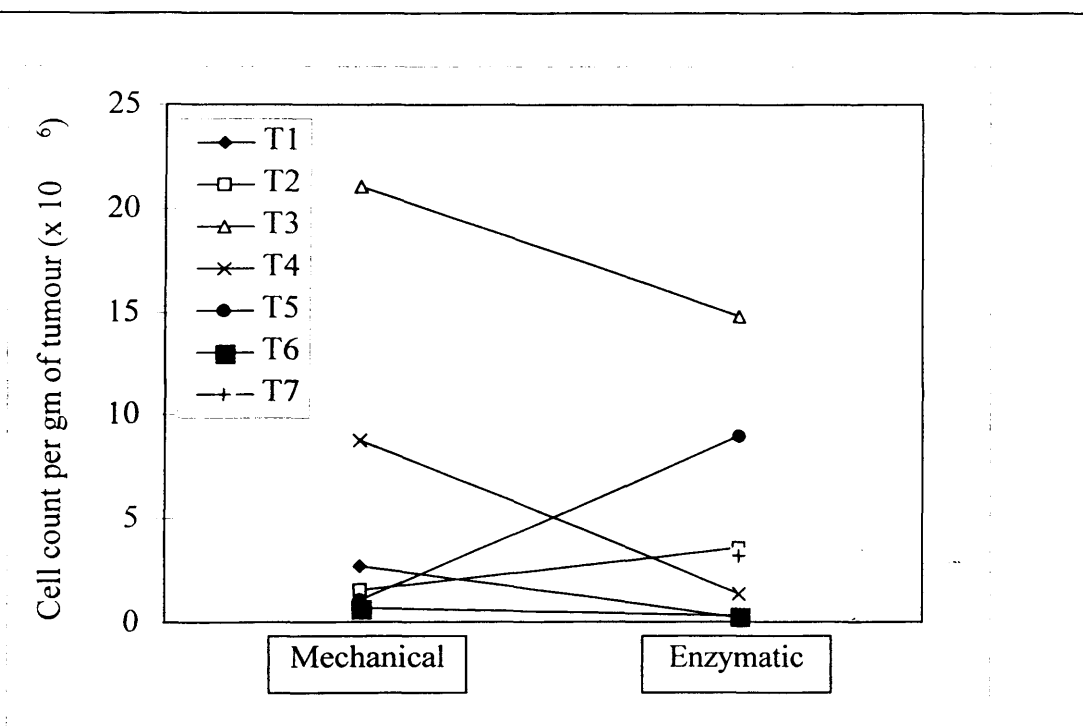
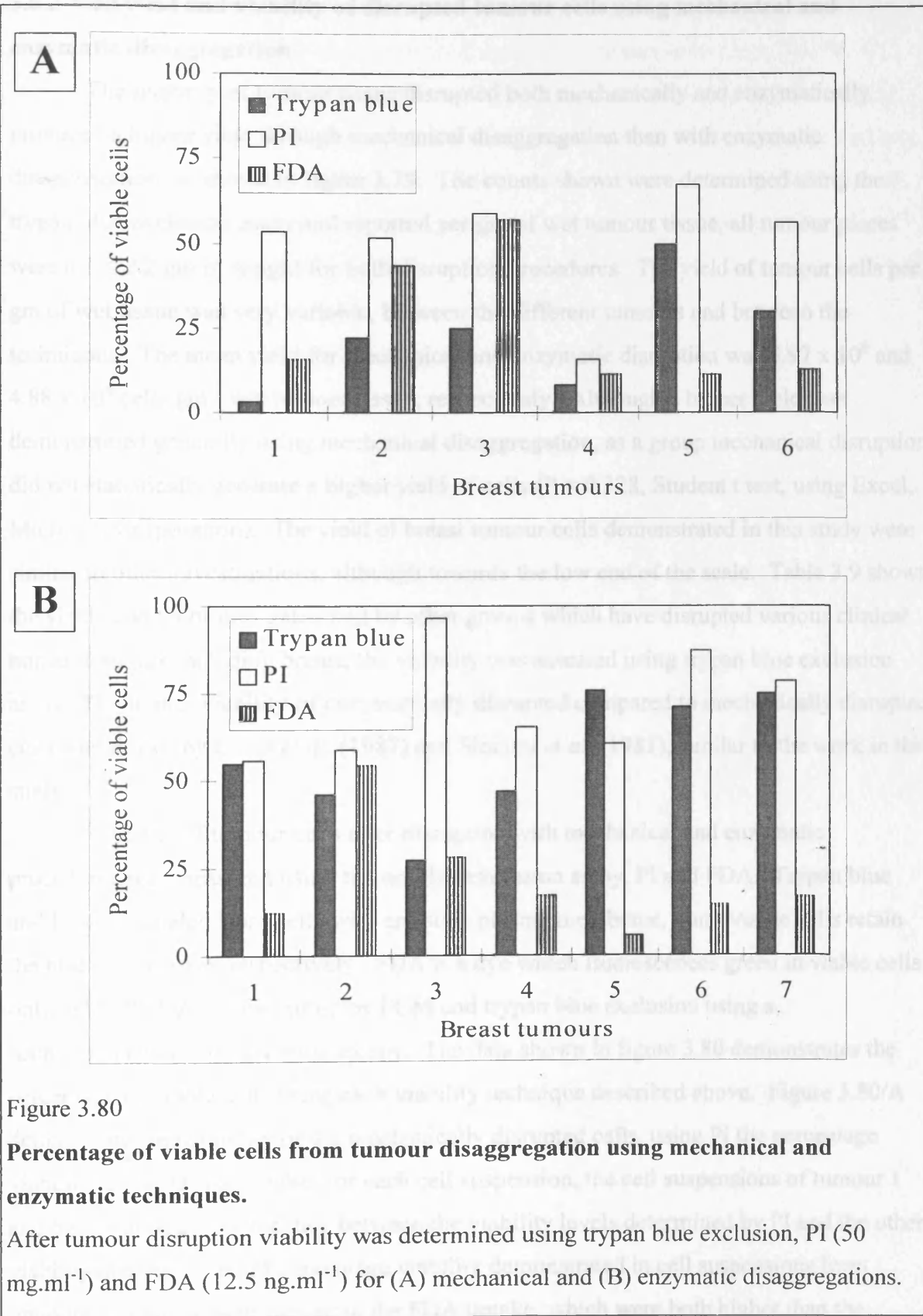


Figure 3.79

Total cell count per gram of tumour tissue disrupted from human breast tumours, comparing mechanical and enzymatic disaggregation.



3.6.2 Cell yield and viability of disrupted tumour cells using mechanical and enzymatic disaggregation

The majority of tumour tissue disrupted both mechanically and enzymatically produced a higher yield through mechanical disaggregation than with enzymatic disaggregation, as shown in figure 3.79. The counts shown were determined using the trypan blue exclusion assay and reported per gm of wet tumour tissue, all tumour pieces were $0.1 \leq 2.2$ gm in weight for both disruption procedures. The yield of tumour cells per gm of wet tissue was very variable, between the different tumours and between the techniques. The mean yield for mechanical and enzymatic disruption was 5.97×10^6 and 4.88×10^6 cells.gm⁻¹ wet tumour tissue, respectively. Although a higher yield was demonstrated generally using mechanical disaggregation, as a group mechanical disruption did not statistically generate a higher yield of cells ($P = 0.328$, Student t test, using Excel, Microsoft Corporation). The yield of breast tumour cells demonstrated in this study were similar to other investigations, although towards the low end of the scale. Table 3.9 shows the yields and viabilities generated by other groups which have disrupted various clinical human tumours including breast, the viability was assessed using trypan blue exclusion assay. The higher viability of enzymatically disrupted compared to mechanically disrupted cells was shown by Costa *et al.* (1987) and Slocum *et al.* (1981), similar to the work in this study.

Viability of tumour cells after disruption with mechanical and enzymatic procedures was measured using trypan blue exclusion assay, PI and FDA. Trypan blue and PI are excluded from cells with an intact plasma membrane, non - viable cells retain the blue and red dye, respectively. FDA is a dye which fluorescences green in viable cells only. PI and FDA are measured by FCM and trypan blue exclusion using a haemocytometer and light microscopy. The data shown in figure 3.80 demonstrates the percentage of viable cells using each viability technique described above. Figure 3.80/A demonstrates the viability of the mechanically disrupted cells, using PI the percentage viability is consistently higher for each cell suspension, the cell suspensions of tumour 1 and 6 show a large discrepancy between the viability levels determined by PI and the other viability markers. The PI percentage viability demonstrated in cell suspensions from tumours 2, 3 and 4 were similar to the FDA uptake, which were both higher than the trypan blue measurements. Using trypan blue measurements the viability of mechanically disrupted cells is $\leq 50\%$ with a range of 3 - 50%.

The viability of the cell suspensions generated from enzymatic disruption were measured with trypan blue, PI and FDA, and these data are shown in figure 3.80/B. Generally the PI percentage viability for each cell suspension, similar to the mechanical disruption, was the highest, with the exception of tumours 3 and 4, PI percentage viability was comparable to the trypan blue counts. The FDA uptake for the majority of tumours was low. Using trypan blue counts the viability of enzymatically disrupted cells was \leq 76% with a range of 27 - 76%.

3.6.3 Fine needle aspirate (FNA) samples

3.6.3.1 Presentation of cell suspensions to the LSC

Three slide designs were tested for their suitability of using small cell samples and LSC analysis. A range of cell concentrations were used from 0.1 - 100 x 10⁴ cells/ml. The slide and cell preparations were initially analysed using light and fluorescent microscopy.

Tumour Type	Investigating group	Disruption technique	Range of yield (x 10 ⁶ cells.gm ⁻¹)	Viability (percentage)
Breast	This study	mechanical	0.675 - 8.75	3 - 50
		enzymatical	0.24 - 14.8	27 - 76
Breast	Costa <i>et al.</i> , 1987	mechanical	4 - 76	5 - 28
		enzymatical	1 - 128	24 - 84
Ovarian		mechanical	0.2 - 47	7 - 32
		enzymatical	9 - 53	45 - 89
Melanoma		mechanical	6 - 143	5 - 46
		enzymatical	3.7 - 74	49 - 82
Scirrhou breast adenocarcinomas	Torres <i>et al.</i> , 1995	mincing (mechanical)	7 - 117	0 - 23
		scraping (mechanical)	9 - 100	0 - 23
Melanoma	Slocum <i>et al.</i> , 1981	mechanical	2.3 - 314	0 - 83
		enzymatical	8.5 - 284	2 - 98
Sarcoma		mechanical	0.4 - 211	1 - 51
		enzymatical	7.9 - 217	45 - 99
Lung carcinoma		mechanical	1.8 - 500	1 - 65
		enzymatical	2.2 - 262	9 - 98

Table 3.9

Total cell yield and viability of various human tumours using mechanical or enzymatic disruption techniques.

These results were those carried out in this study and other investigating groups from literature.

Between the 16 well glass chamber slide, 8 well Permanox chamber slide and a 12 well PTFE coated slide, the PTFE was the most suitable. The 16 well glass slide was difficult to use, the removal of the rubber gasket which held the chambers to the slide was problematic, it was not removed without disruption of the cells. The 8 well chamber slide also incorporated a rubber gasket, but this was removed easily. Using light microscopy the majority of cells were moving around between the individual chambers, this may have been because the rubber gasket was not completely removed and channels of fluid were able to flow between wells. The glue from the chambers appeared to demonstrate a bright

green fluorescence. The third slide of 12 wells seemed to be the most ideal system to use, the slide had been coated in PTFE apart from 12 circular wells (0.5 mm in diameter). A 50 μl cell suspension pipetted into each well was held within the well by surface tension, the media was easily removed by washing in PBS and once coverslipped the wells were sealed and the cells remained round enough for them to be detectable on the LSC using light scatter. The cells which were incubated with $100 \mu\text{mol.L}^{-1}$ and 1 mmol.L^{-1} doxorubicin both demonstrated a detectable red fluorescence using fluorescence microscopy. Those cells which had been incubated with $100 \mu\text{mol.L}^{-1}$ adhered better to the slide than those incubated with 1 mmol.L^{-1} . The PTFE slide was also scanned using the LSC to establish that the cells were detectable using light scatter and that the red fluorescence was quantifiable, the light scatter detected was similar to MCF-7/S cells when scanned using chamber slides. Two wells were quantified, one with control cells and the second with cells which had been incubated for 1 hour with $100 \mu\text{mol.L}^{-1}$ doxorubicin. Red integral and red max peak fluorescence were measured using control and test ($100 \mu\text{mol.L}^{-1}$) cells from the control and positive cells, then overlaid as shown in figure 3.81. This figure demonstrates the typical overlapping peaks of the control and the cells positive for doxorubicin.

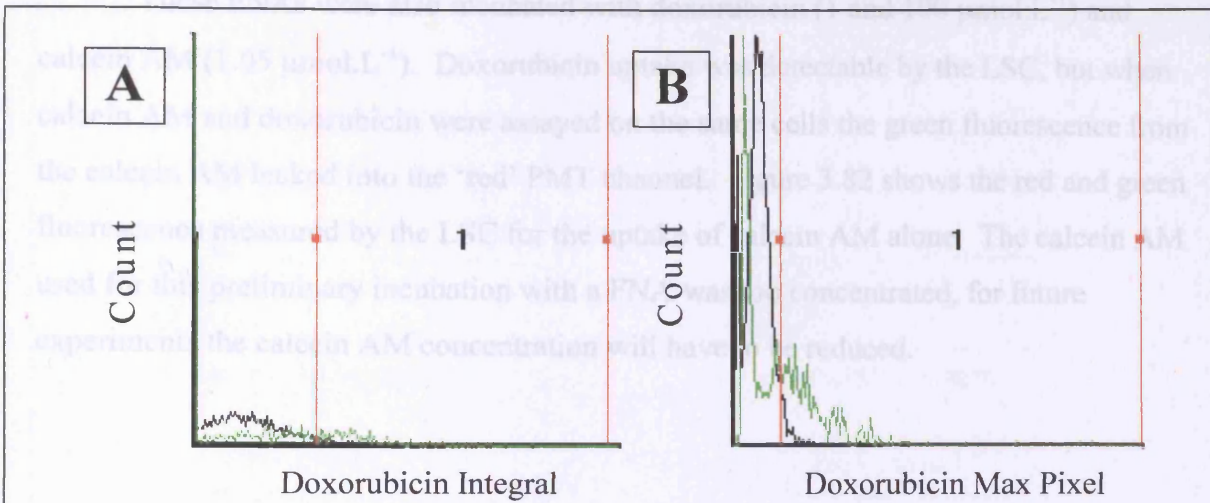


Figure 3.81

Illustration of MCF-7/S cells incubated with doxorubicin and analysed using the LSC and 12 well PTFE coated slide.

MCF-7/S cells were incubated with 0 or 100 $\mu\text{mol.L}^{-1}$ doxorubicin and prepared for the LSC using a PTFE coated slide. Cell detection was performed using light scatter.

Fluorescence is presented as (A) Red Integral and (B) Red max peak. Control cells are represented as a black histogram and positive cells (100 $\mu\text{mol.L}^{-1}$) cells the red histogram.

3.6.3.2 Human breast tumour FNA assay

Two breast tumour sections have been used to produce FNAs. The total cell count and viability as determined using trypan blue exclusion are shown in table 3.10.

FNA	Total cell count	Trypan blue percentage viability
1	4.5×10^6	9
2	6.8×10^6	5

Table 3.10

Total cell count and viability using trypan blue exclusion of FNAs taken from two human breast tumours.

These FNAs were also incubated with doxorubicin (1 and 100 $\mu\text{mol.L}^{-1}$) and calcein AM (1.05 $\mu\text{mol.L}^{-1}$). Doxorubicin uptake was detectable by the LSC, but when calcein AM and doxorubicin were assayed on the same cells the green fluorescence from the calcein AM leaked into the 'red' PMT channel. Figure 3.82 shows the red and green fluorescence measured by the LSC for the uptake of calcein AM alone. The calcein AM used for this preliminary incubation with a FNA was too concentrated, for future experiments the calcein AM concentration will have to be reduced.

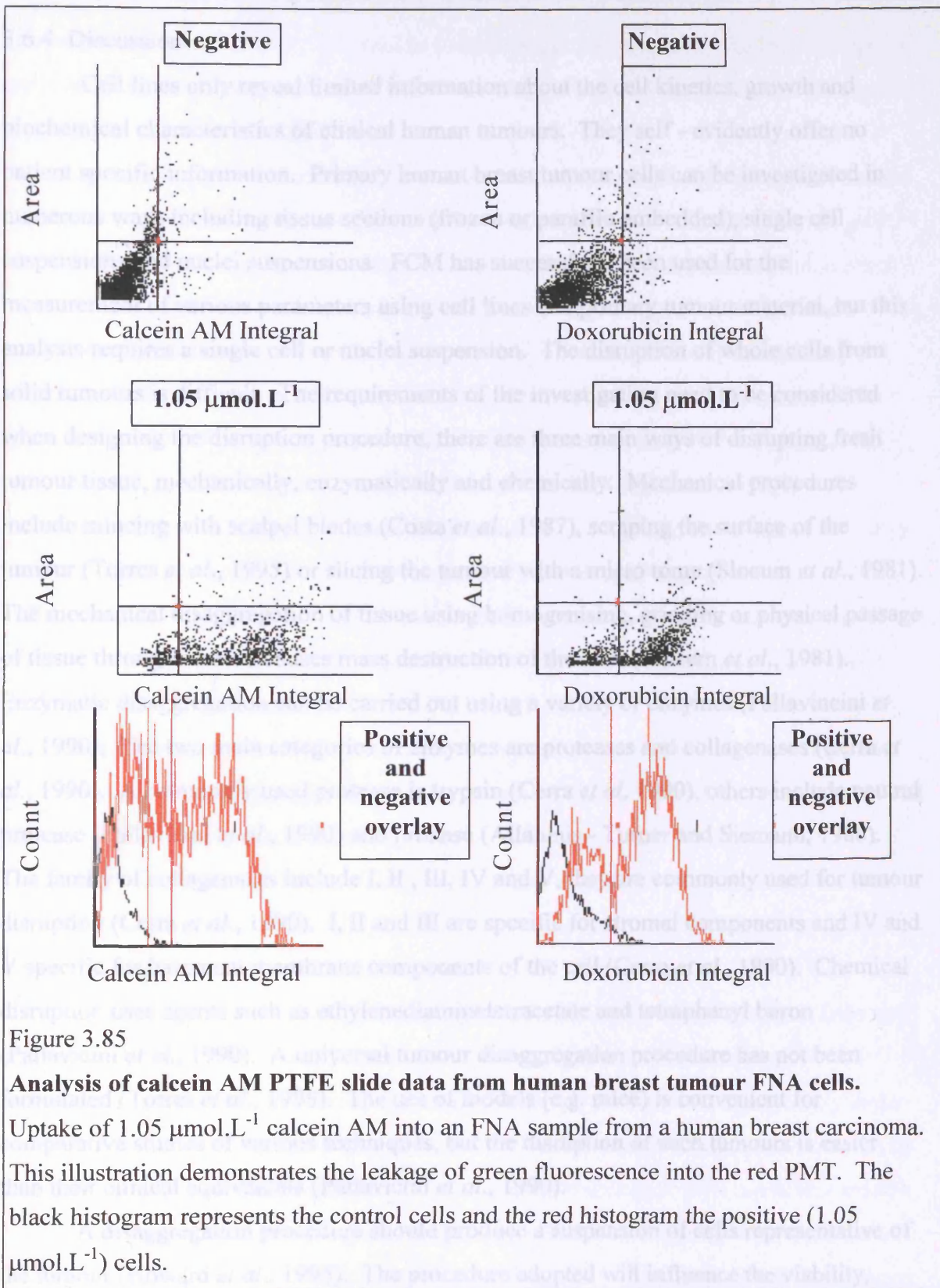


Figure 3.85

Analysis of calcein AM PTFE slide data from human breast tumour FNA cells.

Uptake of $1.05 \mu\text{mol.L}^{-1}$ calcein AM into an FNA sample from a human breast carcinoma. This illustration demonstrates the leakage of green fluorescence into the red PMT. The black histogram represents the control cells and the red histogram the positive ($1.05 \mu\text{mol.L}^{-1}$) cells.

3.6.4 Discussion

Cell lines only reveal limited information about the cell kinetics, growth and biochemical characteristics of clinical human tumours. They self - evidently offer no patient specific information. Primary human breast tumour cells can be investigated in numerous ways including tissue sections (frozen or paraffin embedded), single cell suspensions and nuclei suspensions. FCM has successfully been used for the measurement of various parameters using cell lines and primary tumour material, but this analysis requires a single cell or nuclei suspension. The disruption of whole cells from solid tumours is difficult. The requirements of the investigation need to be considered when designing the disruption procedure, there are three main ways of disrupting fresh tumour tissue, mechanically, enzymatically and chemically. Mechanical procedures include mincing with scalpel blades (Costa *et al.*, 1987), scraping the surface of the tumour (Torres *et al.*, 1995) or slicing the tumour with a micro tome (Slocum *et al.*, 1981). The mechanical disaggregation of tissue using homogenising, grinding or physical passage of tissue through screens causes mass destruction of the cells (Slocum *et al.*, 1981). Enzymatic disaggregation can be carried out using a variety of enzymes (Pallavicini *et al.*, 1990). The two main categories of enzymes are proteases and collagenases (Cerra *et al.*, 1990). A commonly used protease is trypsin (Cerra *et al.* 1990), others include neutral protease (Pallavicini *et al.*, 1990) and pronase (Allalunis - Turner and Siemann, 1986). The family of collagenases include I, II , III, IV and V, they are commonly used for tumour disruption (Cerra *et al.*, 1990). I, II and III are specific for stromal components and IV and V specific for basement membrane components of the cell (Cerra *et al.*, 1990). Chemical disruption uses agents such as ethylenediaminetetracetate and tetraphenyl boron (Pallavicini *et al.*, 1990). A universal tumour disaggregation procedure has not been formulated (Torres *et al.*, 1995). The use of models (e.g. mice) is convenient for comparative studies of various techniques, but the disruption of such tumours is easier than their clinical equivalents (Pallavicini *et al.*, 1990).

A disaggregation procedure should produce a suspension of cells representative of the tumour (Howard *et al.*, 1995). The procedure adopted will influence the viability, yield, preservation of cell types and membrane antigens of the cells (Allalunis - Turner and Siemann, 1986). For this study a procedure was required which gave high viability, high yield and metabolically active cells. Mechanical procedures are quick and easy (Slocum *et al.*, 1981) but they lead to low viability, probably through the tearing of desmosomes from

the cells (Cerra *et al.*, 1990). Enzymatic procedures cause less acute physical damage to cells, but can alter cell surface markers (Cerra *et al.*, 1990) and cause the loss of aneuploid populations (Costa *et al.*, 1987).

Generally, a combination of mechanical and enzymatic disaggregation is required (Howard *et al.*, 1995) to extract tumour cells. Mincing (Rong *et al.*, 1985) the tumour tissue before enzymatic incubation increases the surface area of the tumour for enzyme attack. Studies have investigated a selection of enzymatic cocktails (Howard *et al.*, 1995), most investigators utilize a protease, collagenase and DNase. Various cocktails of enzymes show measurable differences in cell viability and yield with different tumour types (Howard *et al.*, 1995; Slocum *et al.*, 1981 and Costa *et al.*, 1987). The enzyme cocktail used for this study was the same as described by Rong *et al.* (1985), 0.1% collagenase I, 0.01% hyaluronidase and 0.02% DNase. DNase is used to cleave the sticky ends of DNA strands which have been released from damaged cells (Cerra *et al.*, 1990), collagenase and hyaluronidase are to breakdown the stroma and extracellular matrix, the support tissue around the cells. Rong *et al.* (1985) agitated tumour tissue in enzyme solutions for 12 - 18 hours at room temperature, for this study the enzyme disaggregation was agitated on a roller for 3.5 hours at 37°C. A short incubation time of 1 - 2 hours at 37°C was used by other groups (Allalunis - Turner and Siemann, 1986; Costa *et al.*, 1987; Slocum *et al.*, 1981 and Howard *et al.*, 1995), this was more manageable than an incubation time of 12 - 18 hours, without a definitive investigation into various incubation times of enzymatic disruption using human breast tumours, it was difficult to conclude from the literature which would be most suitable.

Figures 3.67 - 3.78, demonstrate a significant difference in the spread of cells and cell debris between the mechanically and enzymatically disrupted cells. The cytocentrifuge preparations from mechanically disrupted cells show a significantly larger amount of debris and extracellular matrix tissue. The increased viability demonstrated by enzymatically disrupted cells compared to mechanically disrupted cells could be caused by the selective elimination of damaged and non - viable cells as suggested by Howard *et al.* (1995), this theory could be substantiated by these images. The decrease in cell and tissue material between the mechanical and enzymatic tumour disruptions is caused by the digestion of this material by the enzyme cocktail. Although the cocktail of enzymes used for this study should not have specific activity for the plasma membrane of cells, a damaged cell as it breaks up will expose DNA to the DNase in solution, which will lead to

the destruction of DNA. The further break up of damaged cells can be caused by the agitation of the cell suspension for 3.5 hours, but also the enzyme preparations maybe contaminated with proteases (Cerra *et al.*, 1990) which could contribute to the break down of damaged cells.

In the investigations of tumour disruption, numerous end points were measured, many highlighted the percentage of cell types, viability and yield (Howard *et al.*, 1995 and Costa *et al.*, 1987), it has been shown that the use of enzymes could lead to a loss of aneuploid cells (Costa *et al.*, 1987). The ideal disruption procedure would yield all the cells from a tissue sample therefore generating a truly representative suspension of the cells present within the tissue. The percentages of cell types between host lymphoid cells and tumour cells have been shown to be similar for both mechanical and enzymatic disaggregation (Slocum *et al.*, 1981). The measurement of different cell types within the cell suspensions from mechanical and enzymatic disruption was not performed for this study, the viability studies of the cell suspensions were measured using all cells, the distinction between infiltrating lymphocytes and other non - tumour cells was not made. A higher magnification should have been used for the analysis of the trypan blue exclusion assay so that cell types could be distinguished and a viability count of tumour cells only could have been determined. The viability assay using PI and FDA on the flow cytometer was single colour labelling using consecutive cell samples. The discrepancy found with the viability results analysed for this study between the various techniques has also been shown by Carpentier *et al.* (1992). This group used various solid tumours for daunorubicin uptake studies and the viability of the tumour cells disrupted from 7 human primary breast tumours using an FNA technique are shown in table 3.11. The difference in the PI and trypan blue results do not show a trend and highlight the difficulties with these assays that were found within this study, that human breast tumour cells are unpredictable.

Trypan blue - light microscopy (Percentage)	PI - Flow cytometry (Percentage)
3.5	4.5
30	12
8	8
8	2
17	27
13	3
25	19

Table 3.11

Viability of human breast primary tumour cells disrupted using fine needle aspiration.

Each tumour sample was analysed for viability using trypan blue exclusion using light microscopy and PI uptake measured by flow cytometry. These results were adapted produced by Carpentier *et al.* (1992).

The FCM viability staining, used in this study, could have been coupled with a epithelial cell marker, such as epithelial membrane antigen (Dako Ltd., Ely, England). Cytokeratin labelling has been adopted by many investigating groups (Brotherick *et al.*, 1995 and Nagle *et al.*, 1986) to isolate epithelial cells, but antibodies such as NCL - 5D3 against cytokeratin 8 and 18 and CAM 5.2 against cytokeratin 8, 18 and 19, are intermediate filament proteins, therefore intracellular targets which require permeabilisation of the cells. The permeabilisation of the cells would not be possible in this study, unless it was shown that the procedure did not change the uptake and fluorescence of doxorubicin, from within the tumour cells. The determination of viability is also an integral part of this study and this could not easily be determined in conjunction with permeabilisation. O'Brien and Bolton (1995) have investigated flow cytometry based viability assays which would be compatible with 1% paraformaldehyde and -20°C methanol fixation. This group established that antibody labelling of tubulin and cytokeratin were suitable probes for detecting non - viable cells which withstood the fixation procedure. This technique was used with the MDA - MB - 175 VII human breast

carcinoma cell line. The use of cytokeratin - FITC would be particularly interesting for this study as it is specific for epithelial cells.

The disaggregation of solid tumours to yield a representative cell suspension has limitations. Breast tumours are heterogeneous, a very large number of the tumour cells would be necessary to be truly representative. The identification of metabolically active and viable cells is most important, because, the doxorubicin uptake solely of viable cells is pertinent to this study. The use of an enzymatic technique would seem to yield a higher viability than a mechanical procedure, although enzyme treatment may prevent the use of surface markers and the accurate determination of a DNA histogram. The addition of an epithelial cell marker might identify the tumour cells, within the cell suspension. The subsequent determination of the cell types within a tumour cell suspension would be important to exclude the misidentification of contaminating cell types, such as the infiltrating lymphoid cells. The use of light scatter on the flow cytometer can not be used to disregard all lymphoid cells as the tumour cells have a wide range of sizes which include the larger lymphoid cells.

The use of an FNA, would allow the determination of patient specific information about doxorubicin uptake. The resistance of a tumour could be assessed using doxorubicin uptake before surgery. This might then influence the treatment strategy of the consequential chemotherapy. Cells from an FNA might thus be used for diagnostic purposes. The FNA sampling technique would be ideal for use with the LSC, although the FCM could have problems with the low cell yield of FNAs (Brotherick *et al.*, 1995). The LSC is capable of analysing low numbers of cells as they are retained on a cell slide, with minimal cell loss. An informative FNA would provide tumour cells, contaminated with other cell types, principally blood cells (Maas *et al.*, 1995), and normal epithelial.

The FNAs performed for this study however, generated cells with a very low viability (5 and 9%). This may have been because of the trauma of the sampling technique, the surgery or because the cells were non-viable before removal. Improvement in FNA sampling technique may lead to an increase in viability. Low viability was reported by Carpentier *et al.* (1992) who used FNAs of human primary breast tumours and compared them with cells obtained from solid tumour disruption (table 3.11). They measured DNA histograms using cytokeratin gating, to assess ploidy. There was a discrepancy in 3/20 patients analysed, 3 patients demonstrating aneuploid peaks using cells disrupted from the solid tumour sections which were lost with the use of FNAs. The

comparison of FNA and tumour tissue analysis using ploidy by Greenbaum *et al.* (1984) demonstrated a significant enrichment of non-diploid nuclei with the use of FNA rather than the disrupted tumour sections, this group described their findings as being caused by the selective aspiration of tumour cells, as the tumour cells were less adhesive as the surrounding normal tissue cells. If information about the resistance of tumour cells to doxorubicin is only required after surgery then the disruption of tumour sections could be performed which would provide a larger number of cells and possibly a more representative profile of tumour cells. The use of chemotherapy prior to surgery can be used for tumour demonstrating nodal involvement presenting in young patients.

The physical separation of tumour cells using epithelial cell markers such as EMA may be possible. Physical separation could be performed using density gradients, such as histopaque and ficoll which are routinely used for lymphoid cell separations, but these methods utilise the size and buoyancy of each cell type and the tumour cells may include a wide range of sizes and densities which may hinder their separation from lymphoid cells. Immunomagnetic bead separation would be a possibility, using a bead targeted at epithelial cells. There are immuno magnetic beads available which can be detached, after cell isolation, which is preferable for viability and drug uptake studies. This procedure has been used to isolate tumour cells from FNAs for RT - PCR of mRNA of the MDR1 gene (Maas *et al.*, 1995), therefore the small cellular samples should be sufficient for immunomagnetic separations. This system would need investigation as to the percentage return of epithelial cells, the sensitivity, precision and influence on the viability of the cells.

HUMAN TUMOUR PROLIFERATION

3.7 Human tumour proliferation

3.7.1 Comparison of flow and laser scanning cytometry for a bivariate assay using cell proliferation in human solid tumours as a model

A direct comparison was made of proliferation data measured using flow and laser scanning cytometry of identical aliquots of human tumor nuclei labelled *in vivo* with bromodeoxyuridine (BrdUrd). The LSC was used to measure parameters in its flow cytometry derived data collection mode, its additional capabilities for visualization and relocation of cells were not used. The determination of a slow or fast proliferating tumour would enable the targetting of chemotherapy, namely doxorubicin. Doxorubicin acts most effectively on cells that are in S phase and those which are rapidly proliferating as cell death may only occur after doxorubicin treatment if the cell tries to proceed through the cell cycle. Slowly proliferating tumours may require lower treatment courses of low dose chemotherapy to allow time for the maximum number of cells to be at a stage in their cell cycle to be susceptible to this treatment.

3.7.1.1 Flow and laser scanning cytometry

The human tumour dissociated nuclei suspensions were analysed using the FCM and LSC. The data generated by both techniques was analysed in a similar way as described in section 2.3.5. The typical cytometric dotplots and histograms analysed are shown in figure 3.83.

3.7.2 Statistical analysis

Flow and laser scanning cytometry data were compared statistically using the paired Student t - test and Spearman's rank order correlation. The paired t- test was used to determine whether there was a significant statistical difference between the two techniques, the rank order correlation determines whether the two data sets are related. Statistical analyses were carried out using JMP (SAS Institute Inc., Cary, NC).

The comparison of the measured parameters by flow and laser scanning cytometry are shown in table 3.12. The median values shown demonstrate a similarity for most parameters. The greatest differences were seen for the number of cells analysed and the coefficient of variation (CV) of the G1/G0 population. Using

Results

flow cytometry a greater number of cells were analysed and a superior CV of the G1/G0 population was generated.

Parameter	LSC	FCM	Paired t - test
Aneuploid tumours per No. analysed	14/31	13/31	
LI (%)	8.8 (0.9 - 36.5)	8.5 (0.7 - 42.9)	0.0134
RM	0.77 (0.58 - 0.96)	0.74 (0.61 - 0.99)	0.205
Ts (hours)	12.0 (6.5 - 37.5)	12.0 (6.1 - 27.3)	0.985
Tpot (days)	4.8 (1.1 - 111.1)	4.72 (0.8 - 130.0)	0.43
CV of G1/G0	8.4 (3.6 - 23.7)	4.0 (2.3 - 12.8)	<0.0001
G2/G1 ratio	2.07 (1.94 - 2.32)	2.03 (1.89 - 2.35)	0.057
No. of cells analysed	1473 (206 - 4676)	5000 (1075 - 20000)	<0.0001

Table 3.12

Median values of each parameter assessed by LSC and FCM and paired t - test results comparing the two analysis techniques.

The numbers in parentheses represent the range of values.

3.7.3 Correlation between LSC and FCM

The correlation between LSC and FCM for DNA index, labelling index (LI), duration of S - phase (Ts) and potential doubling time (Tpot) are shown in table 3.13. The correlation between LSC and FCM varied depending upon the parameter. DNA index, LI and Tpot (table 3.13) demonstrated an excellent correlation, but parameters such as Ts (table 3.13), relative movement (RM) ($R = 0.464$, $p = 0.0169$) and CV of G1/G0 peak ($R = 0.464$, $p = 0.0085$), the correlation was considerably poorer. A perfect correlation as determined by Spearman's rank would produce an outcome of 1 and no correlation 0. The only parameter tested that did not demonstrate correlation was G2/G1 ratio ($R = 0.255$, $p = 0.166$).

Parameter	Spearman's Rank value	p - value
DNA index	0.98	<0.0001
LI	0.92	<0.0001
RM	0.43	0.0169
Ts	0.45	0.015
Tpot	0.85	<0.0001
CV of G1/G0	0.46	0.0085
G2/G1 ratio	0.26	0.166
No. of cells analysed	0.39	0.038

Table 3.13

Rank correlation analysis of each measured parameter, comparing LSC and FCM.

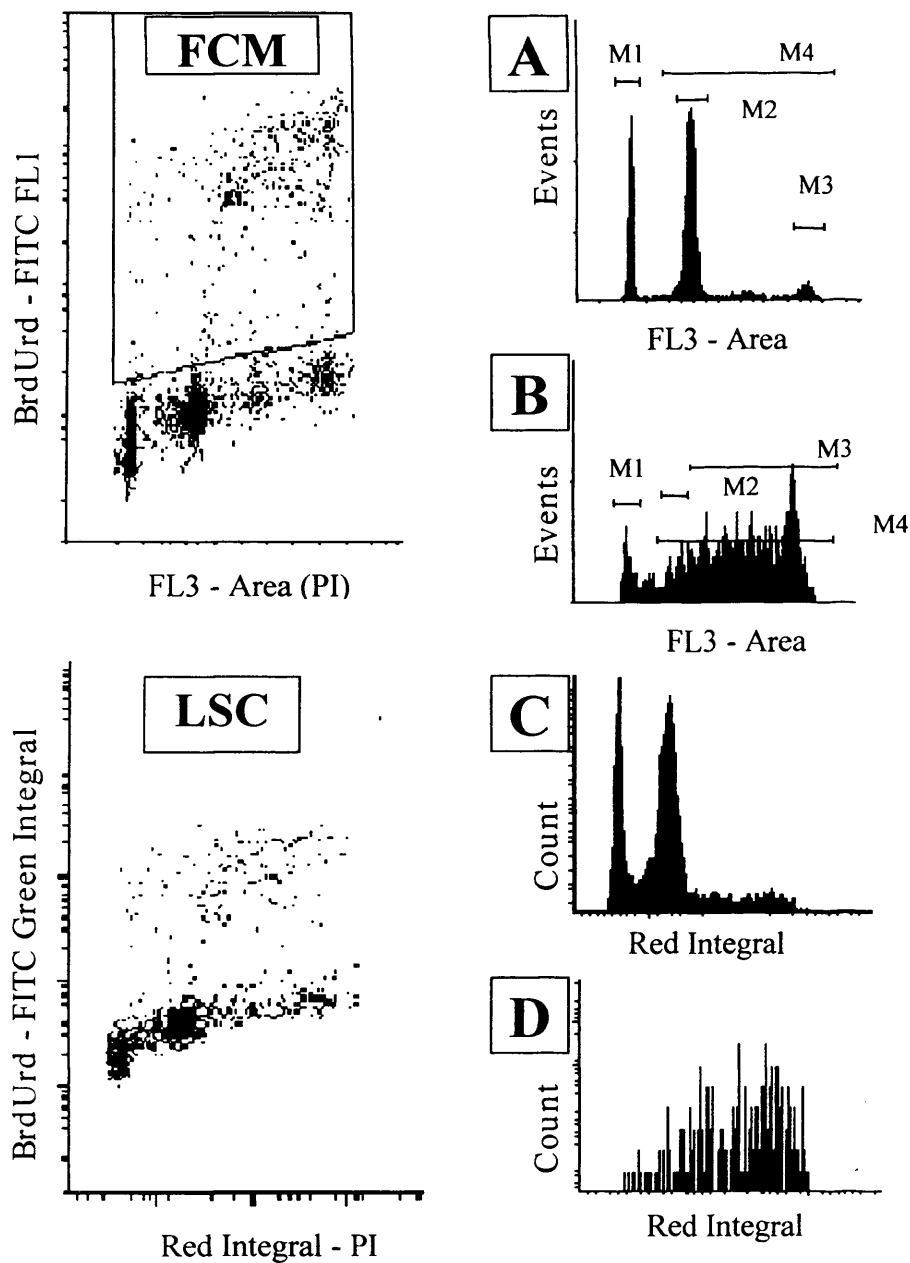


Figure 3.83

FCM and LSC analysis of human nuclei labelled with PI and BrdUrd - FITC.

After a BrdUrd injection prior to surgery, nuclei from a gastric tumour were disrupted. The nuclei have been stained with FITC labelled anti - BrdUrd antibody and PI. Histograms (A) and (C) show total DNA histograms measured by FCM and LSC, respectively. The DNA histograms of those cells positive for BrdUrd uptake only are shown measured by FCM (B) and LSC (D).

3.7.4 Discussion

The data analysis presented from FCM and LSC demonstrate excellent concordance in the interpretation of the DNA profile. Using the initial classification of DNA ploidy only one tumour was classified differently by FCM compared with LSC. By FCM this tumour was hyperdiploid and diploid by LSC. This was mainly due to the larger CV of the G1/G0 populations as analysed by LSC, which obscured the peaks that were side by side. The CVs of the G1/G0 populations tended to be greater by LSC, but did not compromise the agreement of the absolute value of DNA index between FCM and LSC. The statistical comparison between FCM and LSC for this study was 97% which was similar to the 96% quoted by Martin-Reay *et al.* (1994), 92% quoted by Clatch *et al.* (1997) and 91.7% quoted by Sasaki *et al.* (1996). In the Sasaki study, correlation analysis also revealed very similar agreement, $r^2 = 0.97$, compared to 0.983 in this present study.

Other studies have shown inferior LSC derived CVs for DNA profiles in comparison with FCM (Martin - Reay *et al.*, 1994; Sasaki *et al.*, 1996 and Clatch *et al.*, 1997). In our study the mean CVs were 8.8% and 4.8% respectively for LSC and FCM: Sasaki reported ~4.5% for LSC and between 2.5 and 3.5% for FCM. The trend is similar in both studies, although the CVs reported here were larger. This can mainly be attributed to the preparation of tumour nuclei and staining procedures. The nuclei for this study were digested from archival ethanol-fixed tumour material containing partially denatured DNA whilst Sasaki used fresh material and stained only for DNA. It is encouraging that agreement in DNA index measurement was still evident at these higher CV values.

The assessment of the proliferation parameters labelling index (LI), T_s (duration of S phase) and T_{pot} (potential doubling time) represents another degree of complexity not yet attempted by LSC. S-phase fractions (SPF) were compared previously (Martin - Reay *et al.*, 1994) and showed good correlation ($r = 0.83$) between LSC and FCM. Analysis of BrdUrd incorporation by LSC has been reported in cell lines (Gorczyca *et al.*, 1996) and has shown that cell kinetic information can be derived using a fraction labelled mitosis method. This study is the first to apply the LSC to dynamic proliferation measurements in solid tumours. The analysis revealed that measurement of the LI was in good agreement between the two methods. This has previously been shown in intercomparison studies of T_{pot} (Wilson *et al.*, 1993 and

Haustermans *et al.*, 1995) in which the LI has proven a robust parameter that relies on relatively simple region setting. In contrast, the calculation of Ts has proven problematical in FCM analysis. Previous comparisons (Wilson *et al.*, 1993 and Haustermans *et al.*, 1995) have failed to reach agreement in Ts and this has been attributed to complexities of the DNA profile, systematic interobserver differences, sample preparation and tumour heterogeneity. No single parameter emerged from this study to explain the disagreements between LSC and FCM. Some of the greatest discrepancies in Ts were found when fewer than 1000 cells were analysed in aneuploid tumours but other specimens with these characteristics showed good agreement. The inference from this and previous FCM studies is that Ts is intrinsically difficult to measure and will remain a problem in the determination of Tpot.

The comparison of Tpot showed acceptable agreement between the two methods as the LI dominated the calculation, the correlation coefficient reaching 0.85. This raises the question as to whether calculation of Tpot, through estimation of the unreliable Ts, adds or detracts from the information provided by LI. The results generated in this study have previously been published by Rew *et al.*, (1998).

The *in vivo* labelling of S-phase cells with BrdUrd allows the determination of the length of time involved with the traverse of a cell through different phases of the cycle. The assessment of cells in one particular phase of the cycle can be assessed using other methods but these often only give an indication of the proportion of cells involved in each phase. This straight forward procedure performed in parallel with an assay which could determine the resistance status of a patient prior to chemotherapy, could provide invaluable information to the clinicians about the most appropriate way to treat each individual. It would have been interesting to have performed BrdUrd uptake into the sensitive and resistant MCF-7 cells in parallel with the doxorubicin uptake treatment. Other techniques to determine cell phase lengths include S-phase fraction, tritiated thymidine labelling index and mitotic index. The measurements outlined in this study are incorporated into an unpublished study as part of a multi-centre clinical trial into the use of radiotherapy of head and neck cancers. Pretreatment cell kinetic analysis is performed and correlated with the outcome of the radiotherapy, with the hope of predicting which patients would respond badly to the treatment and determine which patients should be considered for a more regime of radiotherapy (Wilson, 1994).

The conclusion is that, although its rate of scanning and data acquisition is significantly slower than the FCM, the LSC can provide comparable information on smaller numbers of cells. A number of variables, including the magnification of the objective lens (x10, x20 or x40) and the density and quality of the cytospin preparation influence the quality of data collection. Optimisation of these parameters and the potential to record precise location in time and space, and constructing an image of up to several hundred pixels per cell or nucleus, open up greater possibilities for solid tumour research.

LSC analysis offers the ability to determine the same parameters as the FCM. Whilst each sample is fixed on the slide additional information could also be gained. The detection of apoptosis could also be carried out, TUNEL based detection kits are widely available (e.g. R & D systems, Abingdon, England). The analysis of apoptosis using this system would be to label 3' OH ends of DNA fragments. These DNA fragments being a hallmark of apoptosis. Terminal deoxynucleotidyl transferase (TdT) polymerizes labeled nucleotides to the 3' OH ends of DNA (1999/2000 Apoptosis catalog, R & D systems). The detection system used could be fluorescence or chromogenic. Subsequent analysis of the DNA to determine apoptotic status of the nuclei would be preferential as a chromogenic label, for this study. The apoptotic status of the nuclei would be quantitative but it could be correlated with the DNA histograms of the individual cells using the relocation facility of the LSC. Qualitative apoptosis detection has been performed successfully on the LSC using *in situ* DNA strand break labelling methods, which was comparable to FCM analysis (Li and Darzynkiewicz, 1995).

Accurate analysis of aneuploid and especially diploid DNA histograms is hindered by the probability of the present of normal structural tissue cells such as stromal or infiltrating cells. DNA analysis using flow cytometry has often been coupled with cell identification labels, such a cytokeratin. The isolation of tumour cells with a cytokeratin marker would enable a possible diploid peak in an aneuploid tumour to be identified as being normal host cells. Antigen markers such as cytokeratin are inappropriate for disrupted nuclei as these epitopes have been removed, but this cell proliferation analysis could be carried out on cell suspensions instead of cell nuclei. Analysis of cell suspensions would introduce possible unspecific antibody binding to the cytoplasm. To create the minimum of cell loss,

protein loss and morphological change is to use a restriction endonuclease and exonuclease, to break down the DNA to allow the incorporation of the BrdUrd. The use of these agents is expensive and different cell types may require different endonucleases (Wilson, 1994).

Tumour nuclei offer an accessible source of patient specific information as an alternative to intact tumour cells. A functional multidrug resistant assay could not be performed using nuclei although MDR protein expression could be identified using fluorescently labelled antibodies. A nuclei preparation could be utilised in parallel to a whole cell assay. Using disaggregation techniques nuclei within the cell debris could be used for a proliferation assay based upon the one described in this study. Ideally tissue removed from a patient using a FNA or biopsy could be assayed for their multidrug resistance and proliferation status. The resistance and proliferation status of the tumour would offer information about the regime of chemotherapy that would be most effective.

DISCUSSION

4.1 **Technical discussion**

4.1.1 **The investigation of the mechanisms of the binding of drug to DNA.**

The preliminary work was designed to study the basic properties of doxorubicin, mitoxantrone and ethidium bromide. Ethidium bromide as a classical intercalator and was used as a positive control for the investigation of the interaction of drug - DNA. Preliminary experiments demonstrated doxorubicin intercalated into DNA and illustrated the fluorescent characteristics which makes it a suitable drug for detection using fluorescent microscopy and cytometry techniques. The drug/DNA binding studies have demonstrated that doxorubicin and mitoxantrone intercalate with DNA, although experimentally the binding affinities calculated were lower than those determined by other groups.

4.1.2 **Cell lines: MCF-7/S and MCF-7/R**

The investigation of drug interaction with mammalian DNA in a model 'test - tube' system can categorise the theoretical processes, but these experimental conditions do not reflect the complications of the chemical and structural interactions within a cell.

The MCF-7 cell lines used for this study are frequently used for human breast cancer research, they are an accepted model for breast tumours. They originate from a metastatic tumour of the breast rather than a primary tumour, but cell lines from primary breast tumours are rare. In the literature they demonstrate considerable variability in their oestrogen receptor expression and their ability to proceed down the apoptotic pathway. These two cell lines compliment each other, offering investigation of doxorubicin sensitive and resistant cells. The MCF-7/R resistant cell line over expresses P – gp which is present on many resistant breast tumour cells. These cells demonstrate the extreme phenotypes of doxorubicin sensitive and resistant tumour cells, but they are the best human model which is available. The use of cell lines offer advantages and disadvantages for therapeutic research. The advantages include a continuous source of cells of standardised phenotype which any research group can cultivate, without the need to have access to human tissue. Once removed from the original primary tumour growth site, the metastatic cells, which give rise to these cells lines, will dedifferentiate to exhibit their own unique characteristics. Metastatic tumour cells will be phenotypically different from primary tumour cells, and again different from the cells which are grown as cell lines.

These differences are accepted compromises for the ability to manipulate an accessible source of human tumour cells.

Growth medium which is used for cell lines is a mixture of soluble proteins and amino acids which allow the cells to grow, but the balance of growth factors do not accurately reflect the milieu of the cells *in vivo*. Cell culture medium contains one tenth of the protein content of plasma (Bennis *et al.*, 1997), therefore the different protein levels could affect the interactions of chemical agents and cell structures, especially as many analytes within the body are protein bound.

The model of drug incubation of cells in suspension is an oversimplification of the interaction of chemotherapy within breast tumours *in vivo*. A tumour is a heterogeneous structure with various degrees of vascularization, a complex cell mixture, with areas of actively growing and necrotic cells. Although the cell line/drug interaction which was used for this study was inaccurate, it represented a system to investigate the ideal interaction between cells and drug *in vivo* within the tumour. The use of animal models would not have been suitable for this project. Many tumour disaggregation procedures have used animal models for breast cancers, but these tumours were found to have different properties to human tumours.

The cell lines were used exclusively while in exponential growth (S – phase). The growth characteristics of MCF-7/S cells were investigated using the MTT assay. This assay was used with 96 well plates and the most suitable cell seeding concentration and exponential growth time was determined. Although this assay measured cell viability it was not suitable for the simultaneous detection of doxorubicin on individual cells. The MTT assay measures the viability of a whole population in a single colourimetric reading, with no facility to measure individual cellular doxorubicin fluorescence.

For the ultimate goal of quantifying doxorubicin uptake on human aspirated tumour cells, a viable and non-viable cell discriminator is required. Doxorubicin has been shown in this study to enter non-viable cells as prolifically as it enters viable cells. To eliminate non-viable cells from this assay a fluorescent marker which could be used simultaneously with doxorubicin was sort. The two most suited probes were calcein AM and sytox. In the literature, calcein AM has been used both as a viability tool and multidrug resistance assay. Using cell lines from this study calcein AM has shown to be a sensitive multidrug resistant marker, which could not separate viable and non-viable

MCF-7/R cells. Sytox although was not as bright as calcein AM was the most suitable viability probe investigated.

In parallel to the doxorubicin incubations of the MCF-7/S and MCF-7/R cell lines, a cell proliferation assay using BrdUrd pulse labelling could have been used to determine the cell cycle phase of the cells and the relationship between cycle phase and consequent cytostatic influences of doxorubicin.

4.1.3 Instrumentation – FCM and LSC

The naturally fluorescent anthracyclines have been studied using flow cytometry, with the aim of correlating intracellular uptake with cell proliferation and resistance (Krishan and Ganapathi, 1979 and 1980). FCM has been used for many years as the standard for quantitative fluorescent measurements on individual cells of a large population. The use of FCM has provided the base for the development of the clinical assay for this study, but it has its limitations. For this study a number of parameters were under investigation (a) doxorubicin uptake (red fluorescence), (b) viability (green fluorescence) and (c) tumour cell identification. Tumour cells could be labelled using a fluorescent external epithelial cell marker.

The LSC can quantify the doxorubicin uptake and viability probes in a similar way to FCM, but enables cell identification to be performed visually, using light microscopy. Using conventional techniques the cells positive for doxorubicin fluorescence and viability can be gated. The cells within this region can then be analysed using the LSCs unique relocation facility that would enable each cell of this region to be visualised and its cell type determined. If light microscopy was not providing enough contrast to identify the cells, the slide could be histologically stained to make cell identification easier. After FCM analysis the cells are lost to 'waste', therefore there would not be a visual check to guarantee the cells which appear in the analysis, to eliminate artefact. Using visualisation the location of fluorescent markers can be seen and quantified within the cell.

Although not used for this study, the movement and location of 'free' doxorubicin and specifically the albumin conjugated CytocapsTM could be analysed. Quantitative measurements of fluorescent events within the nucleus and cytoplasm can be assessed separately using 'peripheral' contours, this technique has been described by Deptala *et al.* (1998), investigating the movement of nuclear factor kappa B (NF – κ B). The analysis of CytocapsTM can be carried out very efficiently by the LSC. This technique offers the

capabilities of following the location of the CytocapsTM, in real time, as they enter the cell. The LSC was only used qualitatively in this study to demonstrate the movement of the CytocapsTM using images, but with the use of peripheral contouring their movement could be quantified over time.

The LSC is a useful tool for the detection of two fluorescent markers and cell identification using its relocation facility. Quantifying only fluorescence FCM and LSC, have been shown to be comparable for many assays, such as the cell nuclei proliferation assay. The FCM has the advantage of a vast quantity and quality of knowledge, which has been accumulated over the last two decades. It is quick and the data generated is familiar to many. The LSC is generally slower and its use has not been as extensively defined or investigated. The ability that the LSC has over the FCM is its relocation facility, it enables fluorescence signals to be confirmed and artefact to be eliminated.

The clinical FNA samples required for the assessment of doxorubicin uptake into viable tumour cells are heterogeneous and contain low numbers of viable tumour cells as demonstrated in this study. The FCM is a sensitive instrument, but the requirement to positively identify doxorubicin, cell identification and viability on a small population of cells maybe difficult to resolve from artefact. The nature of FCM flow system also introduces an opportunity for cells to be lost. The static fixing of LSC samples on microscope slides reduces loss, and enables repeated scanning and visual determination of any cell population.

4.1.4 Sample preparation for the LSC

Two approaches have been used in this study to analyse cells on the LSC, cytocentrifuge preparation and chamber slides. Cytocentrifuge preparations have been used successfully for BrdUrd and PI detection and analysis of tumour nuclei, but for the titrations of doxorubicin and calcein AM the results did not demonstrate a dose response. The computation or triggering signal used by cytocentrifuge preparation was fluorescence, i.e. red fluorescence for doxorubicin titrations and green fluorescence for calcein AM. The analysis of each cell is determined by the cells ability to produce a quantity of fluorescence which triggers the LSC. At low concentrations of doxorubicin and calcein AM the fluorescence was dim and the LSC was unable to detect any cells. The events detected for these samples were probably erroneous, possibly caused by dust. At higher concentrations, the cells could be detected and fluorescence quantified but the results

could still contain errors. As discussed previously (section 3.3.5) the data contour is a function of the threshold contour, therefore the area of the cell which is analysed will be a similar shape to the initial threshold contour. Figure 4.1 illustrates two extreme examples of fluorescence and light scatter contouring.

For this study the use of chamber slides using whole viable cells was the most suitable procedure. The cells analysed using the chamber slides were detected using light scatter. Using this procedure all cells, regardless of the levels of fluorescence would be analysed. This type of contouring enables the whole cell to be encapsulated within the data contour, enabling all fluorescence to be quantified. Contouring on the nucleus using fluorescence computation could reduce the area of the cell which is analysed, depending upon the shape of the cell, this is illustrated in figure 4.1. This phenomenon is also possible using light scatter contouring although, not so pronounced.

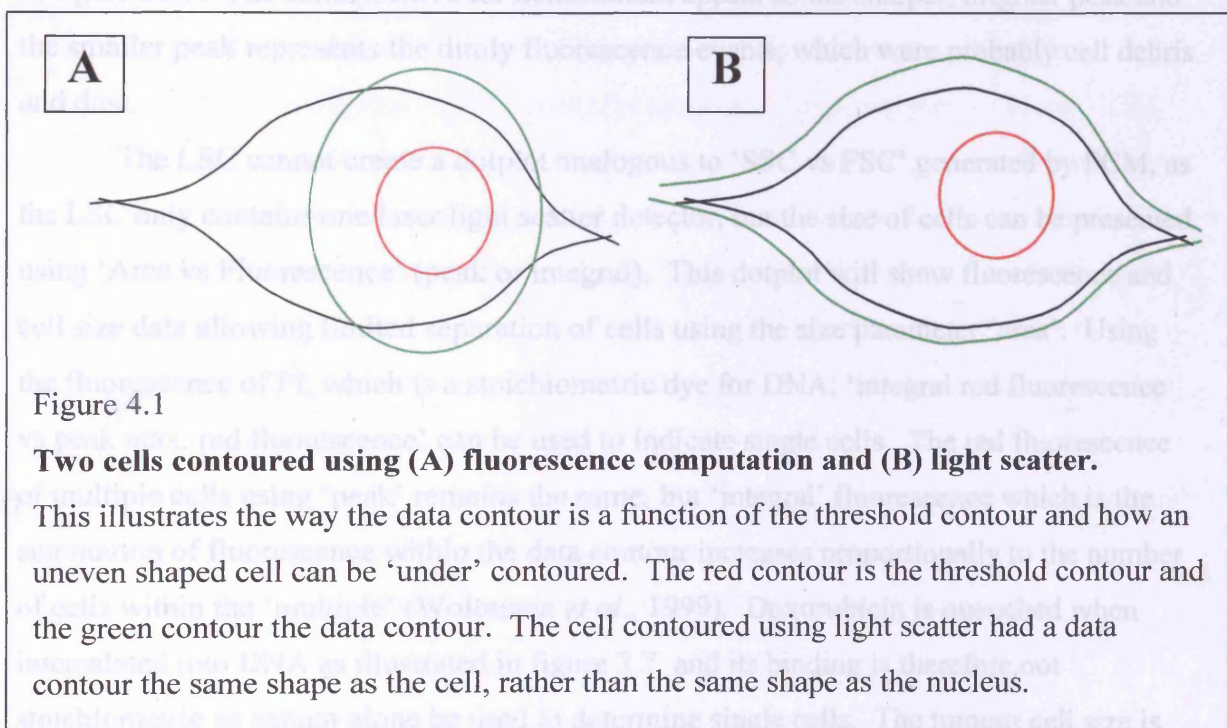


Figure 4.1

Two cells contoured using (A) fluorescence computation and (B) light scatter.

This illustrates the way the data contour is a function of the threshold contour and how an uneven shaped cell can be 'under' contoured. The red contour is the threshold contour and the green contour the data contour. The cell contoured using light scatter had a data contour the same shape as the cell, rather than the same shape as the nucleus.

4.1.5 Colour compensation

The colour compensation mechanisms for FCM and LSC are different. For the LSC colour compensation is carried out after data has been collected and it is a function of the software. Using two colour analysis the concentration of viability probe (sytox) and doxorubicin may need adjusting to get the best resolution of the two signals, while still

using an optimal concentration of each agent. Infact the FACScan used for this study could not compensate between FL1 (green) and FL3 (red),

4.1.6 Gates/regions

For FCM analysis, in this study, gating was used to eliminate cell debris and allow only single cells to be analysed. Gating for FCM was set using cell lines. The common use of FCM in the literature with knowledge spanning three decades, has enabled the user to gate 'single cells' only, using forward and side scatter parameters.

The determination of single cells on the LSC should also have been carried out, whereas in this study all events were detected using the LSC and analysed for fluorescence. This resulted in the detection of two fluorescent peaks instead of one that was usually seen with parallel FCM analysis. An example of 'double peaks' can be seen in figure 3.37. The cells positive for doxorubicin appear as the sharper, brighter peak and the smaller peak represents the dimly fluorescence events, which were probably cell debris and dust.

The LSC cannot create a dotplot analogous to 'SSC vs FSC' generated by FCM, as the LSC only contains one laser light scatter detector, but the size of cells can be presented using 'Area vs Fluorescence' (peak or integral). This dotplot will show fluorescence and cell size data allowing limited separation of cells using the size parameter 'area'. Using the fluorescence of PI, which is a stoichiometric dye for DNA, 'integral red fluorescence vs peak max. red fluorescence' can be used to indicate single cells. The red fluorescence of multiple cells using 'peak' remains the same, but 'integral' fluorescence which is the summation of fluorescence within the data contour increases proportionally to the number of cells within the 'multiple' (Woltmann *et al.*, 1999). Doxorubicin is quenched when intercalated into DNA as illustrated in figure 3.7, and its binding is therefore not stoichiometric so cannot alone be used to determine single cells. The tumour cell size is variable so the 'area' parameter of cells would be unreliable to definitively gate single cells. An alternative technique for the detection of single cells performed could be using a combination of 'area vs red fluorescence (peak or integral)' and relocation. Once cells have been identified a gate can be created to incorporate the majority of single cells. From the gated 'single cells' histograms and dotplots would subsequently be produced from those cells negative for sytox staining, which were therefore viable. Sytox staining only

offers an exclusion criteria, which is not as preferable as an inclusion criteria which would exclude more cell debris and artefact.

The LSC data was self gated by the software which calculated all parameters using 'no multiple cells'. WinCyte software (Compucyte, Mass., USA) gives you the option to electronically remove all events which it understands to be 'multiple'. MCF-7/S cells labelled with calcein AM were analysed with and without 'multiple' cells and the difference in the mean fluorescence of the positive population was not significant (data not shown). Woltmann *et al.* (1999) demonstrated the use of this software parameter to analyse single cells only, incorporated with a broad nuclear size gate. Although multiple cells were discounted from this analysis the cell debris was not efficiently excluded.

4.1.4 Human tumour studies

Extraction of nuclei from archival tumour samples has demonstrated valuable information on the proliferation status of tumour cells, this information can then be utilised to determine the most appropriate chemotherapy drugs and regime to use. This proliferation assay allowed the rates and cell cycle status of the cells within the tumour to be assessed. This study has demonstrated that the LSC is a comparable technique to FCM for measurements of Tpot and similar analysis. The parallel detection of the BrdUrd - FITC and PI using FCM and LSC demonstrated a good correlation of results for the majority of the parameters which can be calculated from this labelling. This reflects the relative ease of detecting isolated nuclei by LSC compared to whole cells. Information about proliferation would be complementary to the measurement of doxorubicin resistance status in the clinical setting, it would allow the targeting of drugs to particular phases of the cell cycle, or initiate therapy designed for fast or slow proliferating tumours.

4.2 Biological discussion

4.2.1 Response of MCF-7/S and MCF-7/R cells to doxorubicin treatment.

The effect of incubating the cells incubated with 'free' and albumin conjugated doxorubicin (CytocapsTM) was investigated using time course studies. These studies were designed to establish how long it took a sensitive cell to die following doxorubicin treatment in comparison with the uptake of the drug measured by fluorescence, and to compare drug sensitive and resistant cells.

The sensitive and resistant MCF-7/S and MCF-7/R cells were incubated with 0, 1, 10 and 100 $\mu\text{mol.L}^{-1}$ doxorubicin for one hour and then grown for 4 – 144 hours. Growth of the sensitive MCF-7/S cells was not affected until 72 hours, yet apoptosis and viability remained at the same level as in the controls. The reason for the loss of cells at 72 hours is unclear as viability was not lower despite a 50% loss of cells. Extra time points would be needed between 48 and 72 hours to determine the cause of this loss. By 72 hours doxorubicin at all concentrations had exerted a cytostatic effect upon the cells. Although the FCM results suggest that the cells responded similarly to 10 and 100 $\mu\text{mol.L}^{-1}$ doxorubicin, using light microscopy (figure 3.38), the cells which were incubated with 100 $\mu\text{mol.L}^{-1}$ appeared to be considerably more ‘stressed’ than the cells incubated with 10 $\mu\text{mol.L}^{-1}$.

At the high concentrations of doxorubicin used for this study the cells are unlikely to have been removed from the population via an apoptotic pathway. Intercalation of doxorubicin between DNA base pairs inhibits the cell’s ability to allow transcription of mRNA, therefore preventing protein synthesis, and the apoptotic pathway. Muller *et al.* (1997) has shown in MOLT - ALL cells (a T cell line) that apoptosis is only possible at concentrations of doxorubicin below 1 $\mu\text{mol.L}^{-1}$. It was presumed that the cells initiated apoptosis through stress caused by a mechanism other than intercalation, for example the trapping of topoisomerase II. At high doxorubicin concentrations Muller *et al.* (1997) showed similar cytotoxic effects, than were seen using low concentrations, but caused by oxidative damage to the cellular DNA, not apoptosis. Using this model, if the cells removed from the cell population, in this study, have died they probably did so as a result of oxidative damage to the cells, rather than apoptosis. Even at low doxorubicin concentrations there have been conflicting reports about the ability of MCF-7/S cells to die via apoptosis. MCF-7/S cells have been found to undergo apoptosis (Kyprianou *et al.*, 1991 and Wang *et al.*, 1995), but acute (1 $\mu\text{mol.L}^{-1}$) and chronic (50 nmol.L^{-1}) doxorubicin treatment have been used by Fornari *et al.* (1994 and 1996) and shown to caused decreased viability without inducing apoptosis, similar to that demonstrated in this study. Fornari *et al.* (1996) correlated the lack of apoptosis with a decrease in the mRNA levels of *c - myc*, high levels of *c - myc* oncogene which is documented to contribute to apoptosis (White, 1993).

Doxorubicin can kill cells at all stages of the cell cycle but the sensitivity of the cells varies, and is dependent on the cell line and the concentration of doxorubicin

(Barranco, 1984). The human B - cell lymphoma cell line DoHH2 was investigated by Smith *et al.* (1994) using low and high concentrations of doxorubicin and idarubicin. Both agents halted the cells in early S - phase at low concentrations, and at G2/M using high concentrations. Synchronised CHO cells were used to demonstrate that at low concentrations of doxorubicin (0.01 - 0.5 $\mu\text{g}\cdot\text{ml}^{-1}$) 30 - 90% cells were killed, the remaining viable cells had their cell cycle progression delayed, which was reversible within 2 - 4 hours. The cells then progressed through the cell cycle at least once more. Using higher doses of doxorubicin irreversible and immediate blocks were created in the cell cycle preventing further progression. Cells within an exponentially growing population could be at various stages of the cell cycle, therefore the death of cells would be unlikely to take place at the same time. A delay between drug action and cell death could be produced as the cells try to move through the cell cycle. The cell may be stopped naturally via the cell cycle checkpoints at G1/S or G2/M but some neoplastic cells may have the ability to avoid these checkpoints (Smith *et al.*, 1994). Cells would eventually cease to cycle when exogenous doxorubicin action such as DNA intercalation, inhibition of topoisomerase II and/or inhibition of DNA polymerase, had functionally prevented the cells' progression. The cell will eventually break down and collapse once the cell was unable to maintain its house keeping functions. It is possible that this is the pathway which MCF-7/S took in this study, leading to their demise.

The uptake experiments using the MCF-7/R cells, in this study, have shown that doxorubicin had very little effect on these cells, even at the high concentration of 100 $\mu\text{mol}\cdot\text{L}^{-1}$. The ability of these cells to evade the effects of doxorubicin was through a combination of mechanisms. The high expression of P - gp present in these cells (Davies *et al.*, 1996) would have reduced and/or altered the distribution of the doxorubicin within the cell, preventing doxorubicin interacting with DNA. In addition ROS, which contribute to doxorubicin cytotoxicity, would have been reduced to normal levels by increased levels of glutathione peroxidase in the resistant cell line (Sinha *et al.*, 1987 and Akman *et al.*, 1990).

4.2.2 Optimisation and limitations

The primary objective of this study was to detect anthracycline resistant cells within a clinical FNA sample using the reduced retention of doxorubicin, such an analysis requires the investigation of the sensitivity and specificity of FCM and LSC methods. The

difference in doxorubicin retention, between a sensitive and resistant cell is dependent upon the cell type (Frankfurt, 1987; Luk and Tannock, 1989; Herweijer *et al.*, 1989 and Carpentier *et al.*, 1992). The specificity of FCM and LSC to detect resistant cells by fluorescence would be high if the sensitive cells were several fold brighter than the resistant cells, but increasingly difficult if the populations overlap, as shown in figure 4.2. The isolation of resistant MCF-7/R cells among a population of MCF-7/S cells has not been carried out in this study but FCM and LSC should be able to detect a difference in the fluorescence demonstrated by MCF-7/S and MCF-7/R cells using $100 \mu\text{mol.L}^{-1}$ doxorubicin incubation. Creating regions to capture 'resistant' cells would be efficient if cells of defined fluorescence could be easily categorised as 'sensitive' or 'resistant'.

The sensitivity of the LSC and FCM to separate a small percentage of resistant cells from sensitive cells using doxorubicin uptake should be demonstrated, using a mixture of MCF-7/S and MCF-7/R cells. The percentage of resistant cells which have been analytically separated from a sensitive population of cells by FCM has previously been reported at 0.5% (Frankfurt, 1987), 13 % (Carpentier *et al.*, 1992) and 2.5% (Herweijer *et al.*, 1989). For both specificity and sensitivity investigations one population of cells could be labelled with an external green fluorescent tag e.g. epithelial membrane antigen which would enable the identification of both populations by a second method, other than doxorubicin uptake. Inevitably the distinction between sensitive and resistant cells will be unclear if there is overlap between the two populations, as shown in figure 4.2. To determine whether these cells are sensitive or resistant using doxorubicin uptake alone would be subjective.

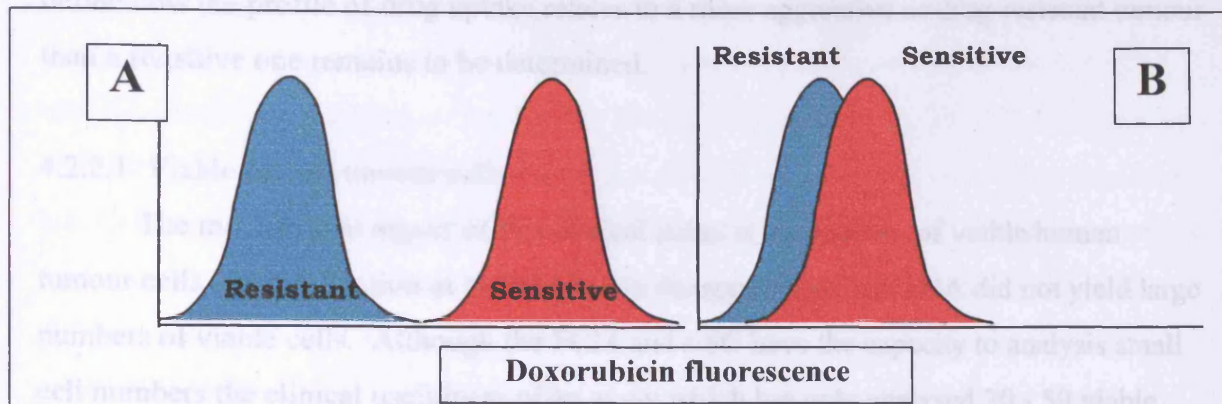


Figure 4.2

A specific and non – specific assay for determining the a resistant cell from a sensitive cell, using doxorubicin fluorescence.

- (A) A specific assay showing excellent separation between the fluorescence of sensitive and resistant cells.
- (B) A non – specific assay showing poor separation between the fluorescence of sensitive and resistant cells.

Colony formation has been used in the past to determine the sensitivity of tumour cells to drugs. It was found that there was a continuous correlation of anthracycline uptake and surviving fraction of clonogenicity (Luk and Tannock, 1989) demonstrating that there is not a clear 'cut off' point between 'sensitive' and 'resistant' cells using these techniques. These studies comparing colony formation and anthracycline FCM fluorescence have mainly used cell lines, therefore the heterogeneity of cells within tumours has not been investigated for interferences and range of results, within a single population. Studies evaluating anthracycline uptake into primary tumour cells by FCM have not explained how they determined which cells were 'sensitive' and which 'resistant' (Carpentier *et al.*, 1992). A reference range or 'cut off' point of anthracycline retention would need to be established if extensive work is to be carried out to determine the outcome of primary tumour cells with defined levels of doxorubicin uptake. The assay that has been developed for this study can determine cells that have reduced doxorubicin uptake but, whether this could be discriminated in a clinical sample was not possible to determine. This was in part due to the inherent difficulties associated with isolation of viable tumour cells from either FNAs or solid tumours. How this assay could be used to

define how the profile of drug uptake relates to a more aggressive or drug resistant tumour than a sensitive one remains to be determined.

4.2.2.1 Viable human tumour cells

The most critical aspect of this clinical assay is the analysis of viable human tumour cells. The extraction of these cells via disaggregation and FNA did not yield large numbers of viable cells. Although the FCM and LSC have the capacity to analysis small cell numbers the clinical usefulness of an assay which has only analysed 20 - 50 viable tumour cell from each patient, is debatable. By contrast the use of the LSC for the analysis of the cell proliferation assay based on PI and BrdUrd - FITC labelling has shown the ease and convenience of analysing tumour nuclei suspensions. Nuclei would offer a large population for analysis, the extraction technique is more robust than those for extraction of viable whole cells and once removed from the tumour they do not need to be incubated to keep them viable.

4.2.2.2 Drug uptake and cell killing

In this study, although doxorubicin exerted a cytostatic effect and consequent cell loss, only small rises in detectable cell death and apoptosis were found in either MCF-7/S but not MCF-7/R cells. The uptake of doxorubicin measured in MCF-7/S does not necessarily indicate that the cells will die, or at least not using the time course used in this study. Previous work comparing the uptake of doxorubicin by FCM with clonogenic studies has reported that there is a good correlation, between drug uptake and cell function and in this study there was correlation between drug uptake and cytostatic effect. From this study and from descriptions of the use of MCF-7/S in the literature, free doxorubicin does not consistently induce apoptosis. However, the CytocapsTM did induce apoptosis by 72 hours.

4.2.2.3 CytocapsTM

The detection and cytostatic effects of the CytocapsTM were studied using both FCM and LSC. The CytocapsTM allow delivery of a concentrated capsule of doxorubicin, at considerably lower concentrations than 'free' doxorubicin, therefore perhaps enabling the use of this form of doxorubicin, with theoretically lower side effects. Although the capsules which are incubated with cells have a lower total doxorubicin concentration, than

an equivalently active 'free' doxorubicin concentration, the contact between the cell and capsule may involve a greater concentration of doxorubicin to one area of the cell. The specific interactions of these capsules with the MCF-7/S and MCF-7/R cells could reveal additional information about the action of doxorubicin with tumour cells, there may be a specific target upon the cell which the capsule targets. CytocapsTM and other encapsulated type delivery systems can offer an increased accumulation within a tumour (Lim *et al.*, 1997 and Kratz *et al.*, 1998b) than free doxorubicin, as the particles get trapped within the capillaries of the tumour. An obstruction in the ability of these drug delivery systems to destroy tumour cells is that they can be rapidly taken up by the reticuloendothelial system of the liver (Nam *et al.*, 1998). A site specific delivery system offers a route for drug delivery to metastatic liver tumours and is being investigated by many groups to improve the specificity of the particles to reach their target and for the drug to remain 'bound' and generally inactive until the target has been reached.

If the behaviour of the CytocapsTM could be determined and there was a significant difference in the location of the CytocapsTM within 'sensitive' and 'resistant' cells, then they could be used as an ideal fluorescent label as they have bright intense fluorescence which can be easily detected and visualised by the LSC.

4.2.3 Future work

This study has established a foundation of information for the use of the LSC and FCM to analyse intact, viable, disaggregated tumour cells and extracted nuclei. To use the uptake and retention of doxorubicin as a patient specific assay to determine the resistance status of a neoplasm, intact disaggregated tumour are required. This assay has been developed and could be performed using the LSC, but the extraction of viable tumour cells remains to be resolved.

This study has focused on the analysis of tumour cells from primary breast tumours. The primary tumour is generally cured by a surgical procedure but the circulating and metastatic tumour cells remain. These cells are phenotypically different from the primary tumour cells (Marx, 1993 and Zhang *et al.*, 1989). To continue this work it would be clinically relevant to analyse the tumour cells or nuclei from the systemic circulation, separated out from peripheral blood. It is the resistance of these cells to chemotherapy that is most clinically relevant. Analysis of circulating tumour cells of doxorubicin uptake could be performed in conjunction with a panel of potentially

prognostic parameters. Circulating epithelial cells could be removed from whole blood using a magnetic bead separation or density gradient system. Magnetic beads could be labelled with epithelial membrane antigen, this would provide a positive population of epithelial cells which could be assayed using the developed viable cell doxorubicin assay. Epithelial cell nuclei could be analysed for ER status, DNA ploidy, S - phase fraction and multidrug resistance phenotype. This panel of parameters might provide further prognostic and therapy targeting information. The multidrug resistance phenotype has been measured with S - phase fraction by Chevillard *et al.* (1996) who found that the slowly proliferating tumours were most resistant and these tumour cells demonstrated a higher MDR1 gene expression. This approach could be combined with measurements of ER to determine whether the patient will respond to anti - oestrogen therapy such as tamoxifen. The use of tamoxifen concurrently with doxorubicin would be interesting to monitor as tamoxifen has been shown to be a P - gp inhibitor.

In parallel to developing a routine assay which can predict resistance of metastasis, a tumour marker which could be used to follow the response and progression of treatment. A blood borne tumour marker could allow the adjustment of treatment without waiting for a change in clinical symptoms, a marker equivalent to CEA perhaps could be assayed in parallel with these other parameters before, during and after treatment to establish if there is any feasible correlation.

Reagent recipes

Modified Essential Medium (MEM)

50 ml MEM 10x concentrate, mixed with 450ml sterile PBS, 12 ml 1 mol.L⁻¹ Hepes and 1 ml 1M.L⁻¹ NaOH. This mixture constitutes the working MEM.

Phosphate buffered saline (PBS)

NaCl (40g), K₂HPO₄·3H₂O (7.925g) and KH₂PO₄ (1.7g) were dissolved in 500 ml of double distilled water to form a 10x stock solution. When required 25 ml of stock solution was mixed with 475 ml of double distilled water, which was adjusted to pH 7.4 with 5 mol.L⁻¹ NaOH or 5 mol.L⁻¹ HCl, and autoclaved.

Tris buffer

Trizma hydrochloride mixed with distilled water at 8 mmol.L⁻¹ adjusted to pH 7.4 with 5 mol.L⁻¹ NaOH or 5 mol.L⁻¹ HCl.

0.9% (w/v) saline

9g NaCl dissolved in 100 ml of distilled water.

0.1% Trypsin / 0.02% EDTA

10 ml of 1 M.L⁻¹ Hepes, 20 ml 2.5% trypsin and 10 ml 1% EDTA were mixed with 460 ml PBS under sterile conditions.

RPMI

To 500 ml RPMI 1640 were added 5 ml L- glutamine (200 mmol.L⁻¹) and 10 ml 1mol.L⁻¹ Hepes.

DMEM complete medium

To 500 ml DMEM were added 5 ml L- glutamine (200 mmol.L⁻¹), 10 ml 1 mol.L⁻¹ Hepes and 10 ml Pen/Strep. (1 x 10⁵ IU.L⁻¹).

Abbreviations

ABC - ATP - Binding Cassette

AD 32 - N - trifluoroacetyl - adriamycin - 14 - valerate

ALL - acute lymphoblastic leukaemia

ATP - adenosine - triphosphate

BCECF - AM - 2', 7' - bis - (2 - carboxyethyl) - 5 - (and - 6) - carboxyfluorescein
acetoxymethyl ester

BrdUrd - 5' - bromo - 2' - deoxyuridine

B/W - black and white

c - concentration of drug

¹⁴C - carbon with a RMM of 14 gram

°C - temperature in degrees centigrade

CAF - chemotherapy regime containing cyclophosphamide, doxorubicin and 5 -
fluorouracil

Calcein AM - calcein acetoxymethyl

Carboxy FDA - carboxy fluorescein diacetate

CCD - closed circuit digital

CD - circular dichroism

CMF - chemotherapy regime containing cyclophosphamide, methotrexate and 5 -
fluorouracil

CO₂ - Carbon dioxide

COSHH - control of substances hazardous to health

CV - Coefficient of variation

DCIS - ductal *in situ* carcinoma

DiO - dioctadecyloxacarbocyanine

DNA - Deoxyribonucleic acid

DMSO - dimethyl sulphoxide

Doxorubicin - (1S, 3S) - 3- glycoloyl - 1, 2, 3, 4, 6, 11 - hexahydro - 3, 5, 12 -
trihydroxy - 10 - methoxy - 6, 11 - dioxonaphthacen - 1 - yl 3 - amino - 2, 3,
6 - trideoxy - α - L - lyxopyranoside hydrochloride

DPX - 'Distrene - 80', 'Plasticizer', 'Xylene'

EA50 - eosin - azure

ECACC - European Collection of Animal Cell Culture

Appendices

ECG - electrocardiogram

EDTA - ethylenediaminetetraacetic acid

e.g. - for example

ER - Oestrogen receptor

Ethidium bromide - 2, 7 - diamino - ethyl - 9 - phenyl - phenanthridium bromide

FCM - Flow cytometry

FCS - fetal calf serum

FDA - fluorescein diacetate

FL1 - green PMT of the FACScan

FL2 - orange PMT of the FACScan

FL3 - red PMT of the FACScan

Fluoro - 3AM - Fluoro - 3 acetomethoxy ester

FNA - fine needle aspirate

FSC - forward light scatter

g - g force

G0 - phase of the cell cycle which contains cells which are not actively cycling

G1 - first resting phase of the cell cycle

G2 - second resting phase of the cell cycle or premitotic phase

G - C - guanine - cytosine

gm - gram

HCl - hydrogen chloride

H & E - haematoxylin and eosin

H₂O₂ - hydrogen peroxide

HPLC - high performance liquid chromatography

HSA - human serum albumin

³H - TdR - tritiated thymidine

IC₅₀ - 50% inhibitory concentration

IMS - industrial methylated spirit

ISEL - *in situ* end labelling

i. v. - intravenous

K - affinity constant (for Scatchard plot)

LI - Labelling index

λ max. - absorbance maximum

Appendices

log - logarithm

LRP - lung resistance protein

LSC - laser scanning cytometer

Ltd - limited

M - mitosis

M1 - marker 1 or region 1

M2 - marker 2 or region 2

M3 - marker 3 or region 3

M4 - marker 4 or region 4

Mass. - Massachusetts

max. - maximum

MCF-7/S - Parental MCF-7 human breast adenocarcinoma cell line

MCF-7/R - MCF-7 cells resistant to doxorubicin

MDA MB 231 - human breast adenocarcinoma cell line

MDR - multidrug resistance

MEM - minimal essential medium

MFI - Mean fluorescence intensity

min - minutes

Mitoxantrone -

MMM - chemotherapy regime containing mitoxantrone, methotrexate and mitomycin C

MRC - medical research council

MRP - multidrug resistance associated protein

MTT - 3 - [4, 5 - dimethylthiazol - 2 - yl] - 2, 5 - diphenyltetrazolium bromide

MTT formazan - 1 - [4, 5 - dimethyl thiazol - 2 - yl] - 3, 5 - diphenylformazan

mV - millivolts

n - number of binding sites available per DNA phosphate group

NADH - reduced form of nicotinamide adenine dinucleotide

NADPH - reduced form of nicotinamide adenine dinucleotide phosphate

No. - Number

NST - no special type

OG6 - orange G

PAP - Papanicolaou cytology stain

PBS - phosphate buffered saline

Appendices

PC - personal computer

Pearson r - Pearson rank

Pen/Strep. - penicillin and streptomycin solution

P - gp - P - glycoprotein

pH - negative logarithm of H^+ concentration expressed in molarity

PI - propidium iodide

PMT - photomultiplier tube

ppm - parts per million

PS - phosphatidylserine

PTFE -

r - the number of binding sites occupied per DNA phosphate group

Rh 123 - rhodamine 123

RM - Relative movement

ROS - reactive oxygen species

rpm - revolutions per minute

RPMI - RPMI 1640 medium without phenol red indicator, buffered with 0.04 mol.L⁻¹
Hepes and supplemented with 2 mmol.L⁻¹

RPMI - FCS - RPMI 1640 medium without phenol red indicator, buffered with 0.04
mol.L⁻¹ Hepes and supplemented with 2 mmol.L⁻¹ plus 10% FCS

RNA - ribonucleic acid

S - phase of the cell cycle when the synthesis of DNA takes place

SAM - sheep - α - mouse

+/- 1 SD - plus or minus 1 standard deviation

sec - second

SPF - S phase fractions

SOD - superoxide dismutase

SSC - side light scatter

T1 - tumour 1

T2 - tumour 2

T3 - tumour 3

T4 - tumour 4

T5 - tumour 5

T6 - tumour 6

Appendices

T7 - tumour 7

Tpot - Potential doubling time

TUNEL - terminal deoxynucleotide transferase - mediated dUTP - biotin nick - end
labelling

Ts - duration of S - phase

UK - United Kingdom

USA - United States of America

UV/Visible - ultraviolet/visible

v/v - volume/volume

w/v - weight/volume

REFERENCES

References

Aas T, Borresen AL, Geisler S, Smith - Sorensen B, Johnsen H, Varhaug JE, Akslen LA and Lonning PE. (1996) Specific P53 mutations are associated with *de novo* resistance to doxorubicin in breast cancer patients. *Nature Medicine*, **2**; 811 - 814.

Abrams J, Jacobovitz D, Dumont P, Semal P, Mommen P, Klastersky J and Atassi G. (1986) Subrenal capsule assay of fresh tumors: problems and pitfalls. *European Journal of Clinical Oncology*, **22**; 1387 - 1394.

Akman SA, Forrest G, Chu FF, Esworthy RS and Doroshow JH. (1990) Antioxidant and xenobiotic enzyme gene expression in doxorubicin - resistant MCF-7 breast cancer cells. *Cancer Research*, **50**; 1397 - 1402.

Allalunis - Turner MJ and Siemann DW. (1986) Recovery of cell subpopulations from human tumour xenografts following dissociation with different enzymes. *British Journal of Cancer*, **54**; 615 - 622.

Alley MC, Scudiero DA, Monks A, Hursey ML, Czerwinski MJ, Fine DL, Abbot BJ, Mayo JG, Shoemaker RK and Boyd MR. (1988) Feasibility of drug screening with panels of human tumour cell lines using a microculture tetrazolium assay. *Cancer Research*, **48**; 589 - 601.

Altmann SA, Randers L and Rao G. (1993) Comparison of trypan blue dye exclusion and fluorometric assays for mammalian cell viability determinations. *Biotechnology Progress*, **9**; 671 - 674.

Alton PA. (1993) The role of DNA topoisomerase II in drug resistance. *British Journal of Haematology*, **85**; 241 - 245.

Arancia G, Calcabrini A, Meschinin S and Molinari A. (1998) Intracellular distribution of anthracyclines in drug resistant cells. *Cytotechnology*, **27**; 95 - 111.

References

- Arcamore F. (1978) Daunomycin and related antibiotics *in* Topics in antibiotic chemistry, (Sammes PG ed.) John Wiley & sons, p99 - 229.
- Bachur NR, Yu F, Johnson R, Hickey R, Wu Y and Malkas L. (1993) Anthracycline interference with helicase action. Abstracts of papers of the American Chemical Society, **205**; 49.
- Baldini N, Scotlandi K, Serra M, Kusuzaki K, Shikita T, Manara MC, Maurici D and Campanacci M. (1992) Adriamycin binding assay: a valuable chemosensitivity test in human osteosarcoma. *Journal of Cancer Research and Clinical Oncology*, **119**; 121 - 126.
- Bargou RC, Jurchott K, Wagener C, Bergmann S, Metzner S, Bommert K, Mapara MY, Winzer KJ, Dietel M, Dorken B and Royer HD. (1997) Nuclear localization and increased levels of transcription factor YB - 1 in primary human breast cancers are associated with intrinsic MDR1 gene expression. *Nature Medicine*, **3**; 447 - 450.
- Barranco SC. (1984) Cellular and molecular effects of adriamycin on dividing and non-dividing cells. *Pharmacological Therapy*, **24**; 303 - 319.
- Baum M, Saunders C and Meredith S. (1995) *Breast cancer - A guide for every woman*. Oxford medical publications.
- Bech - Hanser NT, Sarangi F, Sutherland DJA and Ling V. (1977) Rapid assays for evaluating the drug sensitivity of tumor cells. *Journal of the National Cancer Institute*, **59**; 21 - 27.
- Beck WT. (1987) The cell biology of multidrug resistance. *Biochemical Pharmacology*, **36**; 2879 - 2887.
- Beck WT, Cirtain MC, Danks MK, Felsted RL, Safa AR, Wolverton JS, Suttle DP and Trent JM. (1987) Pharmacological, molecular, and cytogenetic analysis of 'atypical' multidrug - resistant human leukemic cells. *Cancer Research*, **47**; 5455 - 5460.

References

- Bedner E, Burfeind P, Gorczyca W, Melamed MR and Darzynkiewicz Z. (1997) Laser scanning cytometry distinguishes lymphocytes, monocytes, and granulocytes by differences in their chromatin structure. *Cytometry*, **29**; 191 - 196.
- Bedner E, Burfeind P, Hsieh TC, Wu JM, Aguero - Rosenfeld ME, Melamed MR, Horowitz HW, Wormser GP and Darzynkiewicz Z. (1998) Cell cycle effects and induction of apoptosis caused by infection of HL - 60 cells with human granulocytic ehrlichiosis pathogen measured by and laser scanning cytometry. *Cytometry*, **33**; 47 - 55.
- Bedner E, Halicka HD, Cheng W, Salomon T, Deptala A, Gorczyca W, Melamed MR and Darzynkiewicz Z. (1999) High affinity binding of fluorescein isothiocyanate to eosinophils detected by laser scanning cytometry: a potential source of error in analysis of blood samples utilizing fluorescein - conjugated reagents in flow cytometry. *Cytometry*, **36**; 77 - 82.
- Beerman H, Smit VTHBM, Kluin PM, Bonsing BA, Hermans J and Cornelisse CJ. (1991) Flow cytometric analysis of DNA stemline heterogeneity in primary and metastatic breast cancer. *Cytometry*, **12**; 147 - 154.
- Begg AC, McNally NJ, Shrieve DC and Karcher H. (1985) A method to measure the duration of DNA synthesis and the potential doubling time from a single sample. *Cytometry*, **6**; 620 - 626.
- Benjamin RS, Riggs CE and Bachur NR. (1973) Pharmacokinetics and metabolism of adriamycin. *Clinical Pharmacology and Therapeutics*, **14**; 592 - 600.
- Bennis S, Ichas F and Robert J. (1995) Differential effects of verapamil and quinine on the reversal of doxorubicin resistance in a human leukemia cell line. *International Journal of Cancer*, **62**; 283 - 290.
- Bennis S, Faure P, Chapey C, Hu YP, Fourche J, El Yamani J, and Robert J. (1997) Cellular pharmacology of lipophilic anthracyclines in human tumour cells in culture selected for resistance to doxorubicin. *Anti - Cancer Drugs*, **8**; 610 - 617.

Billingham ME. (1991) Role of endomyocardial biopsy in diagnosis and treatment of heart disease *in* Cardiovascular pathology, (Silver MD ed.) Second edition, Churchill Livingstone, p1465 - 1486.

Bordbar AK, Saboury AA and Moosavi - Movahedi AA. (1996) The shapes of Scatchard plots for systems with sets of binding sites. *Biochemical Education*, **24**; 172 - 175.

Brotherick I, Lennard TWJ, Cook S, Johnstone R, Angus B, Winthereik MP and Shenton BK. (1995) Use of biotinylated antibody DAKO - ER 1D5 to measure oestrogen receptor on cytokeratin positive cells obtained from primary breast cancer cells. *Cytometry* **20**; 74 - 80.

Broxterman HJ, Pinedo HM, Kuiper CM, Schuurhuis GJ and Lankelma J. (1989) Glycolysis in P - glycoprotein - overexpressing human tumor cell lines, effects of resistance - modifying agents. *FEBS Letters*, **247**; 405 - 410.

Bustamante J, Galleano M, Medrano EE and Boveris A. (1990) Adriamycin effects on hyperperoxide metabolism and growth of human breast tumour cells. *Breast Cancer Research and Treatment* **17**; 145 - 153.

Cabanes A, Tzemach D, Goren D, Horowitz AT and Gabizon A. (1998) Comparative study of the antitumour activity of free doxorubicin and polyethylene glycol - coated liposomal doxorubicin in a mouse lymphoma model. *Clinical Cancer Research*, **4**; 499 - 505.

Capranico G, de Isabella P, Penco S, Tinelli S and Zunino. (1989) Role of DNA breakage in cytotoxicity of doxorubicin, 9 - deoxydoxorubicin, and 4 - demethyl - 6 - deoxydoxorubicin in murine leukemia P388 cells. *Cancer Research*, **49**; 2022 - 2027.

Carpentier Y, Gorisse MC and Desoize B. (1992) Evaluation of a method for detection of cells with reduced drug retention in solid tumours. *Cytometry*, **13**; 630 - 637.

References

Carter SK. (1975) Adriamycin - a review. *Journal of the National Cancer Institute*, **6**; 1265 - 1274.

Cerra R, Zarbo RJ and Crissman JD. (1990) Dissociation of cells from solid tumours. *Methods in Cell Biology*, **33**; 1 -12.

Chaires JB, Dattagupta N and Crothers DM. (1982) Studies on interaction of anthracycline antibiotics and DNA : equilibrium binding studies on interaction of daunomycin with DNA. *Biochemistry*, **21**; 3933 - 3940.

Chaires JB, Dattagupta N and Crothers DM. (1985) Kinetics of the daunomycin - DNA interaction. *Biochemistry*, **24**; 260 - 267.

Chevillard S, Pouillart P, Beldjord C, Asselain B, Beuzeboc P, Magdelenat H and Vielh P. (1996) Sequential assessment of multidrug resistance phenotype and measurement of S - phase fraction as predictive markers of breast cancer response to neoadjuvant chemotherapy. *Cancer*, **77**; 292 - 300.

Clatch RJ, Walloch JL, Zutter MM and Kamentsky LA. (1996) Immunophenotypic analysis of hematological malignancy by laser scanning cytometry. *American Journal of Clinical Pathology*, **105**; 744 - 755.

Clatch RJ, Walloch JL, Foremand JR and Kamentsky LA. (1997) Multiparameter analysis of DNA content and cytokeratin expression in breast carcinoma by laser scanning cytometry. *Archives of Pathology and Laboratory Medicine*, **121**; 585 - 592.

Coates A, GebSKI V, Stat M, Bishop JF, Jeal PN, Woods RL, Snyder R, Tattersall MHN, Byrne M, Harvey V, Gill G, Simpson J, Drummond R, Browne J, van Cotten R and Forbes JF. (1987) Improving the quality of life during chemotherapy for advanced breast cancer - a comparison of intermittent and continuous treatment strategies. *The New England Journal of Medicine*, **317**; 1490 - 1495.

References

- Coley HM, Amos WB, Twentyman PR and Workman P. (1993) Examination by laser scanning confocal fluorescence imaging microscopy of anthracyclines in parent and multidrug resistant cell lines. *British Journal of Cancer*, **67**; 1316 - 1323.
- Cooper AJ, Hayes MC, Duffy PM, Davies CL and Smart CJ. (1996) Multidrug resistance evaluation by confocal microscopy in primary urothelial cancer explant colonies. *Cytotechnology*, **18**;1 - 6.
- Cornbleet MA, Stuart - Harris RC, Smith IE, Coleman RE, Rubens RD, M^cDonald M, Mouridsen HT, Rainer H, van Oosterom AT and Smyth JF. (1984) Mitoxantrone for the treatment of advanced breast cancer : single - agent therapy in previously untreated patients. *European Journal of Clinical Oncology*, **20**; 1141- 1146.
- Costa A, Silvestrini R, Del Bino G and Motta R. (1987) Implications of disaggregation procedures on biological representation of human solid tumours. *Cell Tissue Kinetics*, **20**; 171 - 180.
- Crabbe J. (1990) Correct use of Scatchard plots. *Trends in Biochemical Science*, **15**; 12 - 13.
- Cummings J, Anderson L, Willmott N and Smyth JF. (1991) The molecular pharmacology of doxorubicin *in vivo*. *European Journal of Cancer*, **27**; 532 - 535.
- Cummings J and Gardiner J. (1997) The multi - role application of HPLC to the analysis of anticancer drugs - 4. *Chromatography and Analysis*, **8**; 5 - 7.
- Davidson BR, Sams VR, Styles J, Dean C and Boulos PB. (1989) Comparative study of carcinoembryonic antigen and epithelial membrane antigen expression in normal colon, adenomas and adenocarcinomas of the colon and rectum. *Gut*, **30**; 1260 - 1265.
- Davies R, Budworth J, Riley J, Snowden R, Gescher A and Gant TW. (1996) Regulation of p - glycoprotein 1 and 2 gene expression and protein activity in two MCF-7/dox cell line subclones. *British Journal of Cancer* **73**; 307 - 315.

- De Bruijn P, Verweij J, Loos WJ, Kolker HJ, Planting AST, Nooter K, Stoter G and Sparreboom A. (1999) Determination of doxorubicin and doxorubicinol in plasma of cancer patients by high - performance liquid chromatography. *Analytical Biochemistry*, **266**; 216 - 221.
- De Clerck LS, Bridts CH, Mertens AM, Moens MM and Stevens WJ. (1994) Use of fluorescent dyes in the determination of adherence of human leucocytes to endothelial cells and the effect of fluorochromes on cellular function. *Journal of Immunological Methods*, **172**; 115 - 124.
- Dengler WA, Schulte J, Berger DP, Mertelsmann R and Fiebig HH. (1995) Development of a propidium iodide fluorescence assay for proliferation and cytotoxicity assays. *Anti - Cancer Drugs*, **6**; 522 - 532.
- Denizot F and Lang R. (1986) Rapid colorimetric assay for cell growth and survival. *Journal of Immunological Methods*, **89**, 271 - 277.
- Deptala A, Bedner E, Gorczyca W and Darzynkiewicz. (1998) Activation of nuclear factor kappa B (NF - κ B) assayed by laser scanning cytometry (LSC). *Cytometry*, **33**; 376 - 382.
- Dieterich B, Albe X, Vassilakos P, Wieser S, Friedrich R and Krauer F. (1995) The prognostic value of DNA ploidy and S - phase estimate in primary breast cancer : prospective study. *International Journal of Cancer*, **63**; 49 - 54.
- Dive C, Gregory CD, Phipps DJ, Evans DL, Milner AE and Wyllie AH. (1992) Analysis and discrimination of necrosis and apoptosis (programmed cell death) by multiparameter flow cytometry. *Biochimica et Biophysica Acta*, **1133**; 275 - 285.
- Dolbeare F. (1995) Bromodeoxyuridine: a diagnostic tool in biology and medicine, Part II: Oncology, chemotherapy and carcinogenesis. *Histochemical Journal*, **27**; 923 - 964.

References

- Dombi GW. (1984) Constructing nonlinear Scatchard plots. *Journal of Chemical Education*, **61**, 527 - 528.
- Doroshaw JH. (1986) Prevention of doxorubicin - induced killing of MCF-7/S human breast cancer cells by oxygen radical scavengers and iron chelating agents. *Biochemical and Biophysical Research Communications*, **135**; 330 - 335.
- Doroshaw JH, Akman S, Chu FF and Esworthy S. (1990) Role of the glutathione peroxidase cycle in the cytotoxicity of the anticancer quinones. *Pharmacological Therapy*, **47**; 359 - 370.
- Durand RE and Olive PL. (1981) Flow cytometry studies of intracellular adriamycin in single cells *in vitro*. *Cancer research*, **41**; 3489 - 3494.
- Drori S, Eytan GD and Assaraf YG. (1995) Potentiation of anticancer - drug cytotoxicity by multidrug - resistance chemosensitizers involves alterations in membrane fluidity leading to increased membrane permeability. *European Journal of Biochemistry*, **228**; 1020 - 1029.
- Durr FE. (1988) Biochemical pharmacology and tumour biology of mitoxantrone and ametantrone. *Bioactive molecules*, **6**; 163 - 200.
- Eksborg S, Strandler HS, Edsmyr F, Naslund I and Tahvanainen P. (1985) Pharmacokinetic study of IV infusions of adriamycin. *European Journal of Clinical Pharmacology*, **28**; 205 - 212.
- Endicott JA and Ling V. (1989) The biochemistry of P - glycoprotein - mediated multidrug resistance. *The Annual Review of Biochemistry*, **58**; 137 - 171.
- Engelholm SA, Spang - Thomsen M, Brunner N, Nohr I and Vindelov LL. (1985) Disaggregation of human solid tumours by combined mechanical and enzymatic methods. *British Journal of Cancer*, **51**; 93 - 98.

References

- Epstein RJ and Smith PJ. (1988) Estrogen - induced potentiation of DNA damage and cytotoxicity in human breast cancer cells treated with topoisomerase II - interactive antitumor drugs. *Cancer Research*, **48**; 297 - 303.
- Erttmann R, Erb N, Steinhoff A and Landbeck G. (1988) Pharmacokinetics of doxorubicin in man: dose and schedule dependence. *Journal of Cancer Research in Clinical Oncology* **114**; 509 - 513.
- Eytan GD, Regev R, Oren G and Assaraf YG. (1996) The role of passive transbilayer drug movement in multidrug resistance and its modulation. *The Journal of Biological Chemistry*, **271**; 12897 - 12902.
- Feller N, Kuiper CM, Lankelma J, Ruhdal JK, Scheper RJ, Pinedo HM and Broxterman HJ. (1995) Functional detection of MDR1/P170 and MRP/P190 - mediated multidrug resistance in tumour cells by flow cytometry. *British Journal of Cancer*, **72**; 543 - 549.
- Fenoglio JJ & Silver MD. (1991) Effects of drugs on cardiovascular system *in Cardiovascular pathology* (Silver MD ed) Second edition Churchill Livingstone, p1205 - 1229.
- Ferrand VL, Montero Julian FA, Chauvet MM, Hirn MH and Bourdeaux N. (1996) Quantitative determination of the MDR - related P - glycoprotein, Pgp 170, by a rapid flow cytometric technique. *Cytometry*, **23**; 120 - 125.
- Fisher GR and Patterson LH. (1992) Lack of involvement of reactive oxygen in the cytotoxicity of mitoxantrone, CI941 and amentantrone in MCF-7 cells: comparison with doxorubicin. *Cancer Chemotherapy and Pharmacology*, **30**; 451 - 458.
- Flens MJ, Izquierdo MA, Scheffer GL, Fritz JM, Meijer CJLM, Scheper RJ and Zaman GJR. (1994) Immunochemical detection of the multidrug resistance - associated protein MRP in human multidrug - resistant tumor cells by monoclonal antibodies. *Cancer Research*, **54**; 4557 - 4563.

References

- Fornari FA, Randolph JK, Yalowich JC, Ritke MK and Gewirtz DA. (1994) Interference by doxorubicin with DNA unwinding in MCF-7 breast tumour cells. *Molecular Pharmacology* **45**; 649 - 656.
- Fornari FA, Jarvis WD, Grant S, Orr MS, Randolph JK, White FKH and Gewirtz DA. (1996) Growth arrest and non - apoptotic cell death associated with the suppression of c - myc expression in MCF-7 breast tumour cells following acute exposure to doxorubicin. *Biochemical Pharmacology* **51**; 931 - 940.
- Forsyth IA. (1991) The mammary gland. *Bailliere's Clinical Endocrinology and Metabolism*, **5**; 809 - 832.
- Fox ME and Smith PJ. (1990) Long - term inhibition of DNA synthesis and the persistence of trapped topoisomerase II complexes in determining the toxicity of antitumor DNA intercalators mAMSA and mitoxantrone. *Cancer Research*, **50**; 5813 - 5818.
- Fox ME and Smith PJ. (1995) Subcellular localisation of the antitumour drug mitoxantrone and the induction of DNA damage in resistant and sensitive human colon carcinoma cells. *Cancer Chemotherapeutic Pharmacology*, **35**; 403 - 410.
- Frankfurt OS. (1987) Flow cytometric screening for selective toxicity to multidrug - resistant cells. *Journal of the National Institute of Cancer*, **79**; 831 - 836.
- Frey T, Yue S and Haughland RP. (1995) Dyes providing sensitivity in flow - cytometric dye - efflux assays for multidrug resistance. *Cytometry*, **20**; 218 - 227.
- Gaber MH, Ghannam MM, Ali SA and Khalil WA. (1998) Interaction of doxorubicin with phospholipid monolayer and liposomes. *Biophysical Chemistry*, **70**; 223 - 229.
- Gandecha BM. (1985) Development of potential antitumour agents based on considerations of the mode of action and pharmacokinetics of daunomycin and doxorubicin. PhD thesis, De Montfort Univerisity.

References

- Gebhardt MC, Kusuzaki K, Mankin HJ and Springfield DS. (1994) An assay to measure adriamycin binding in osteosarcoma cells. *Journal of Orthopaedic Research*, **12**; 621 - 627.
- Graham MD, Lakhani S and Gazet J-C. (1991) Breast conserving surgery in the management of *in situ* breast carcinoma. *European Journal of Surgical Oncology*, **17**: 258 - 264.
- Greenall M. (1996) Advanced disease *in* Surgical oncology (Allen - Mersh TG ed.), Chapman & Hall Medical, p 383 - 392.
- Greenbaum E, Koss LG, Sherman AB and Elequin F. (1984) Comparison of needle aspiration and solid biopsy technics in the flow cytometric study of DNA distributions of surgically resected tumors. *American Journal of Clinical Pathology*, **82**; 559 - 564.
- Goldstein LJ, Pastan I and Gottesman MM. (1992) Multidrug resistance in human cancer. *Critical Reviews in Oncology/Hematology*, **12**; 243 - 253.
- Gorczyca W, Melamed MR and Darzynkiewicz Z. (1996) Laser scanning cytometer (LSC) analysis of fraction of labelled mitoses (FLM). *Cell Proliferation*, **29**; 539 - 547.
- Gorczyca W, Darzynkiewicz Z and Melamed MR. (1997) Laser scanning cytometry in pathology of solid tumors. *Acta Cytologica*, **41**; 98 - 108.
- Gorczyca W, Davidian M, Gherson J, Ashikari R, Darzynkiewicz Z and Melamed MR. (1998) Laser scanning cytometry quantification of estrogen receptors in breast cancer. *Analytical and Quantitative Cytology and Histology*, **20**; 470 - 476.
- Grogan T, Dalton W, Rybski J, Spier C, Meltzer P, Richter L, Gleason M, Pindur J, Cline A, Scheper R, Tsuruo T and Salmon S. (1990) Optimization of immunocytochemical P - glycoprotein assessment in multidrug - resistant plasma cell myeloma using three antibodies. *Laboratory Investigation*, **63**; 815 - 824.

References

- Halliwell B and Bomford A. (1989) ICRF - 187 and doxorubicin - induced cardiac toxicity. *The New England Journal of Medicine* **320**; 399 - 400.
- Hartley JA, Reszka K, Zuo ET, Wilson WD, Morgan AR and Lown JW. (1988) Characteristics of the interaction of anthrapyrazole anticancer agents with deoxyribonucleic acids: structural requirements for DNA binding, intercalation, and photosensitization. *Molecular Pharmacology*, **33**; 265 - 271.
- Haughland RP. (1996) *Handbook of Fluorescent Probes and Research Chemicals*. Sixth edition, Molecular Probes.
- Haustermans K, Vanuytsel L, Geboes K, Lerut T, Van Thillo J, Leysen J, Coosemans W and van der Schueren E. (1994) *In vivo* cell kinetic measurements in human oesophageal cancer: what can be learned from multiple biopsies. *European Journal of Cancer*, **30A**; 1787 - 1791.
- Hedley DW. (1993) Flow cytometric assays of anticancer drug resistance. *Annals of the New York Academy of Sciences*, **677**; 341 - 353.
- Heppner GH. (1984) Tumor heterogeneity. *Cancer Research*, **44**; 2259 - 2265.
- Herweijer H, van den Engh G and Nooter K. (1989) A rapid and sensitive flow cytometric method for the detection of multidrug - resistant cells. *Cytometry*, **10**; 463 - 486.
- Hickman JA. (1992) Apoptosis induced by anticancer drugs. *Cancer and Metastasis Reviews*, **11**; 121 - 139.
- Higgins CF and Gottesman MM. (1992) Is the multidrug transporter a flippase? *Trends in Biochemical Science*, **17**; 18 - 21.

References

- Hollo Z, Homolya L, Davis CW and Sarkadi B. (1994) Calcein accumulation as a fluorometric functional assay of the multidrug transporter. *Biochimica et Biophysica Acta*, **1191**; 384 - 388.
- Homolya L, Hollo Z, Germann UA, Pastan I, Gottesman MM and Sarkadi B. (1993) Fluorescent cellular indicators are extruded by the multidrug resistant protein. *The Journal of Biological Chemistry*, **268**; 21493 - 21496.
- Homolya L, Hollo Z, Muller M, Mechetner EB and Sarkadi B. (1996) A new method for quantitative assessment of P - glycoprotein - related multidrug resistance in tumour cells. *British Journal of Cancer*, **73**; 849 - 855.
- Hortobagyi GN. (1997) Anthracyclines in the treatment of cancer, an overview. *Drugs*, **54**; 1 - 7.
- Howard RB, Shroyer KR, Marcell T, Swanson, Pagura ME, Mulvin DW, Cowen MT and Johnston MR. (1995) Time - related effects of enzymatic disaggregation on model human lung carcinomas. *Cytometry*, **19**; 146 - 153.
- Huschtsha LI, Bartier WA, Ross CEA and Tattersall MHN. (1996) Characteristics of cancer cell death after exposure to cytotoxic drugs *in vitro*. *British Journal of Cancer*, **73**; 54 - 60.
- Inaba M, Kobayashi H, Sakurai Y and Johnson RK. (1979) Active efflux of daunorubicin and adriamycin in sensitive and resistant sublines of P388 leukaemia. *Cancer Research*, **39**; 2200 - 2203.
- Johnson RK, Zee - Cheng RKY, Lee WW, Acton EM, Henry DW and Cheng CC. (1979) *Cancer Treatment Reports*, **63**; 425 - 439.
- Jones KH and Senft JA. (1985) An improved method to determine cell viability by simultaneous staining with fluorescein diacetate - propidium iodide. *The Journal of Histochemistry and Cytochemistry*, **33**; 77 - 79.

Kamada T, Sasaki K, Tsuji T, Todoroki T, Takahashi M and Kurose A. (1997) Sample preparation from paraffin - embedded tissue specimens for laser scanning cytometry DNA analysis. *Cytometry*, **27**; 290 - 294.

Kamentsky LA and Kamentsky LD. (1991) Microscope based multiparameter laser scanning cytometer yielding data comparable to flow cytometry data. *Cytometry*, **12**; 381 - 387.

Kamentsky LA, Kamentsky LD, Fletcher JA, Kurose A and Sasaki K. (1997) Methods for automatic multiparameter analysis of fluorescence *in situ* hybridized specimens with laser scanning cytometer. *Cytometry*, **27**; 117 - 125.

Kapuscinski J, Darzynkiewicz Z, Traganos F and Melamed MR. (1981) Biochemical Pharmacology 30, 231 - 240. Interactions of a new antitumour agent, 1, 4 - dihydroxy - 5, 8 - bis [[2 - [(2 - hydroxyethyl) amino] - ethyl] amino] - 9, 10 - anthranedione, with nucleic acids. *Biochemical Pharmacology*, **30**; 231 - 250.

Kawasaki M, Sasaki K, Satoh T, Kurose A, Kamada T, Furuya T, Murakami T and Todoroki T. (1997) Laser scanning cytometry (LSC) allows detailed analysis of the cell cycle in PI stained human fibroblasts (TIG - 7). *Cell Proliferation*, **30**; 139 - 147.

Kedar E, Ikejiri BL, Bonnard GD and Herberman RB. (1982) A rapid technique for isolation of viable tumor cells from solid tumors : use of the tumor cells for induction and measurement of cell - mediated cytotoxic responses. *European Journal of Clinical Oncology*, **18**; 991 - 1000.

Keizer HG, Schuurhuis GJ, Broxtermann HJ, Lankelma J, Schoonen WGEJ, van Rijn J, Pinedo HM and Joenje H. (1989) Correlation of multidrug resistance with decreased drug accumulation, altered subcellular drug distribution, and increased P - glycoprotein expression in cultured SW - 1573 human tumour cells. *Cancer Research*, **49**; 2988 - 2993.

References

Keizer HG, Pinedo HM, Schuurhuis GJ and Joenje H. (1990) Doxorubicin (adriamycin) : A critical review of free radical - dependent mechanisms of cytotoxicity. *Pharmacological Therapy*, **47**; 219 - 231.

Kerr JFR, Winterford CM and Harmon BV. (1993) Apoptosis. *Cancer*, **73**; 2013 - 2026.

Kessel D, Beck WT, Kukuruga and Schulz V. (1991) Characterization of multidrug resistance by fluorescent dyes. *Cancer Research*, **51**; 4665 - 4670.

Klumper E, Pieters R, Kaspers GJL, Huismans DR, Loonen AH, Rottier MMM, van Wering, van der Does - van der Berg A, Hahlen K, Creutzig U and Veerman AJP. (1991) *In vitro* chemosensitivity assessed with the MTT assay in childhood acute non - lymphoblastic leukemia. *Leukemia*, **9**; 1864 - 1869.

Konen PL, Currier SJ, Rutherford AV, Gottesman MM, Pastan I and Willingham C. (1989) The multidrug transporter : rapid modulation of efflux activity monitored in single cells by the morphologic effects of vinblastine and daunomycin. *The Journal of Histochemistry and Cytochemistry*, **37**; 1141 - 1145.

(a) Kratz F, Beyer U, Roth T, Tarasova N, Collery P, Lechenault F, Cazabat A, Schumacher P, Unger C and Falken U. (1998) Transferrin conjugates of doxorubicin : synthesis, characterization, cellular uptake, and *in vitro* efficacy. *Journal of Pharmaceutical Sciences*, **87**; 338 - 346.

(b) Kratz F, Beyer U, Collery P, Lechenault F, Cazabat A, Schumacher P, Falken U and Unger C. (1998) Preparation, characterization and *in vitro* efficacy of albumin conjugates of doxorubicin. *Biology and Pharmacy Bulletin*, **21**; 56 - 61.

Krishan A. (1975) Rapid flow cytofluorometric analysis of mammalian cell cycle by propidium iodide. *The Journal of Cell Biology*, **66**; 188 - 193.

References

Krishan A and Ganapathi R. (1979) Laser flow cytometry and cancer chemotherapy : detection of intracellular anthracyclines by flow cytometry. *Journal of Histochemistry and Cytochemistry*, **12**; 1655 - 1656.

Krishan A and Ganapathi R. (1980) Laser flow cytometric studies on the intracellular fluorescence of anthracyclines. *Cancer Research*, **40**; 3895 - 3900.

Krishan A, Sridhar KS, Davila E, Vogel C and Sterheim W. (1987) Patterns of anthracycline retention modulation in human tumour cells. *Cytometry*, **8**; 306 - 314.

Krishan A. (1994) Rapid determination of cellular resistance - related drug efflux in tumour cells. *Methods in Cell Biology*, **42**; 21 - 30.

Krishan A, Fitx CM and Andritsch I. (1997) Drug retention, efflux, and resistance in tumor cells. *Cytometry*, **29**; 279 - 285.

Kyprianou N, English HF, Davidson NE and Issacs JT. (1991) Programmed cell death during regression of the MCF-7 human breast cancer following oestrogen ablation. *Cancer Research* **51**; 162 - 166.

Labroille G, Belloc F, Bilhou - Nabera C, Bonnefille S, Bascans E, Boisseau MR, Bernard P and Lacombe F. (1998) Cytometric study of intracellular P - gp expression and reversal of drug resistance. *Cytometry*, **32**; 86 - 94.

Langer R. (1998) Drug delivery and targeting. *Nature*, **392**; 5 - 10.

Lau DHM, Duran GE and Sikic BI. (1994) Analysis of intracellular retention of morpholinyl anthracyclines in multidrug resistant cancer cells by interactive laser cytometry. *International Journal of Oncology*, **5**; 1273 - 1277.

Lehne G, De Angelis P, Clausen OPF, Egeland T, Tsuruo T and Rugstad HE. (1995) Binding diversity of antibodies against external and internal epitopes of the multidrug resistance gene product P - glycoprotein. *Cytometry*, **20**; 228 - 237.

- Li X and Darzynkiewicz Z. (1995) Labelling DNA strand breaks with BrdUTP. Detection of apoptosis and cell proliferation. *Cell Proliferation*, **28**; 571 - 579.
- Liminga G, Nygren P, Dhar S, Nilsson K, and Larsson R. (1996) Cytotoxic effect of calcein acetoxymethyl ester on human tumor cell lines : drug delivery by intracellular trapping. *Anti-Cancer Drugs*, **6**; 578 - 585.
- Lim HJ, Masin D, Madden TD and Bally MB. (1997) influence of drug releases characteristics on the therapeutic activity of liposomal mitoxantrone. *The Journal of Pharmacology and Experimental Therapeutics*, **281**; 566 - 573.
- Ling H, Priebe W and Perez - Soler R. (1993) Apoptosis induced by anthracycline antibiotics in P388 parent and multidrug - resistant cells. *Cancer Research*, **53**; 1845 - 1852.
- Lipshultz SE, Grenier MA and Colan SD. (1999) Doxorubicin - induced cardiomyopathy. *The New England Journal of Medicine*, **340**; 653 - 654.
- Liu Y, Peterson DA, Kimura H and Schubert D. (1997) Mechanism of cellular 3 - (4, 5 - dimethylthiazol - 2 - yl) - 2, 5 - diphenyltetrazolium bromide (MTT) reduction. *Journal of Neurochemistry*, **69**; 581 - 593.
- Lown JW, Morgan AR, Yen SF, Wang YH and Wilson WD. (1985) Characteristics of the binding of the anticancer agents mitoxantrone and ametantrone and related structures of deoxyribonucleic acids. *Biochemistry*, **24**; 4028 - 4035.
- Luk CK and Tannock IF. (1989) Flow cytometry analysis of doxorubicin accumulation in cells from human and rodent cell lines. *Journal of the National Cancer Institute*, **81**; 55 - 59.
- Luther E and Kametsky LA. (1996) Resolution of mitotic cells using laser scanning cytometry. *Cytometry*, **23**; 272 - 278.

References

Maas RA, Bruning PF, Breedijk AJ, Top B and Peterse HL. (1995) Methods in laboratory investigation. Immunomagnetic purification of human breast carcinoma cells allows tumor - specific detection of multidrug resistance gene 1 - mRNA by reverse transcriptase polymerase chain reaction in fine - needle aspirates. *Laboratory Investigation*, **72**; 760 - 764.

Martin SJ, Reutelingsperger CPM, M^cGahon AJ, Rader JA, van Schie RCAA, LaFace DM and Green DR. (1995) Early redistribution of plasma membrane phosphatidylserine is a general feature of apoptosis regardless of the initiating stimulus : inhibition by overexpression of Bcl - 2 and Abl. *Journal of Experimental Medicine*, **182**; 1545 - 1556.

Martin SJ, Reutelingsperger CPM and Green DR. (1996) Annexin V : a specific probe for apoptotic cells *in* *Techniques in Apoptosis : A users guide* (Cotter TG and Martin SJ ed.) Portland Press Ltd, p107 - 120.

Martin - Reay DG, Kamensky LA, Weinberg DS, Hollister KA and Cibas ES. Evaluation of a new slide - based laser scanning cytometer for DNA analysis of tumours. *American Journal of Clinical Pathology*, **102**; 432 - 438.

Marx J. (1993) Cellular changes on the route to metastasis. *Science*, **259**; 626 - 629.

Matsuzaki T, Suzuki T, Fujikura K, Takata K. (1997) Nuclear staining for laser confocal microscopy. *Acta Histochemistry and Cytochemistry*, **30**; 309 - 314.

M^cGown AT, Ward TH and Fox BW. (1983) Comparative studies of the uptake of daunorubicin in sensitive and resistant P388 cell lines by flow cytometry and biochemical extraction procedures. *Cancer Chemotherapy and Pharmacology*, **11**; 113 - 116.

Molinari A, Cianfriglia M, Meschini S, Calcabrini A and Arancia G. (1994) P - glycoprotein expression in the golgi apparatus of multidrug resistant cells. *International Journal of Cancer*, **59**; 789 - 795.

References

Moore PL, Mac Coubrey IC and Haugland RP. (1990) A rapid, pH insensitive, two color fluorescence viability (cytotoxicity) assay. *Journal of Cell Biology*, **111**;A304.

Mosmann T. (1983) Rapid colorimetric assay for cellular growth and survival: application to proliferation and cytotoxicity assays. *Journal of Immunological Methods*, **65**; 55 - 63.

Muggia FM. (1997) Clinical efficacy and prospects for use of pegulated liposomal doxorubicin in the treatment of ovarian and breast cancers. *Drugs*, **54**; 22 - 29.

Muller I, Jenner A, Bruchelt G, Niethammer D and Halliwell B. (1997) Effect of concentration of the cytotoxic mechanism of doxorubicin - apoptosis and oxidative DNA damage. *Biochemical and Biophysical Research Communications*, **230**; 254 - 257.

Musco ML, Cui S, Small D, Nodelman M, Sugarman B and Grace M. (1998) Comparison of flow cytometry and laser scanning cytometry for the intracellular evaluation of adenoviral infectivity for the intracellular evaluation of adenoviral infectivity and p53 protein expression in gene therapy. *Cytometry*, **33**; 290 - 296.

Nagle RB, Bocker W, Davis JR, Heid HW, Kaufmann M, Lucas DO and Jarasch ED. (1986) Characterization of breast carcinomas by two monoclonal antibodies distinguishing myoepithelial from luminal epithelial cells. *The Journal of Histochemistry and Cytochemistry*, **34**; 869 - 881.

Nam SM, Cho JE, Son BS and Park YS. (1998) Convenient preparation of tumour - specific immunoliposomes containing doxorubicin. *Journal of Biochemistry and Molecular Biology*, **31**; 95 - 100.

Neidle S. (1978) Interactions of daunomycin and related antibiotics with biological receptors *in* Topics in antibiotic chemistry (Sammes PG ed.) John Wiley & sons, p242 - 278.

References

- Neyfakh AA. (1988) Use of fluorescent dyes as molecular probes for the study of multidrug resistance. *Experimental Cell Research*, **174**; 168 - 176.
- Nygren P, Fridborg H, Csoka K, Sundstrom C, De la Torre M, Kristensen J, Bergh J, Hagberg H, Glimelius B, Rastad J, Tholander B and Larsson. (1994) Detection of tumor - specific cytotoxic drug activity *in vitro* using the fluorometric microculture cytotoxicity assay and primary cultures of tumour cells from patients. *International Journal of Cancer*, **56**; 715 - 720.
- O'Brien M and Bolton WE. (1995) Comparison of cell viability probes compatible with fixation and permeabilization for combined surface and intracellular staining in flow cytometry. *Cytometry*, **19**; 243 - 255.
- Ormerod MG, Sun XM, Brown D, Snowden RT and Cohen GM. (1993) Quantification of apoptosis and necrosis by flow cytometry. *Acta Oncologica*, **32**; 417 - 424.
- Papadopoulos NG, Dedoussis GVZ, Spanakos G, Gritzapis AD, Baxevanis CN and Papamichail M. (1994) An improved fluorescence assay for the determination of lymphocyte - mediated cytotoxicity using flow cytometry. *Journal of Immunological Methods*, **177**; 101 - 111.
- Pallavicini MG, Taylor IW and Vindelov LL. (1990) Preparation of cell/nuclei suspensions from solid tumors for flow cytometry *in* *Flow Cytometry and Sorting*, Second edition, Wiley - Liss, Inc. p187 - 194.
- Palmeira CM, Serrano J, Kuehl DW and Wallace KB. Preferential oxidation of cardiac mitochondrial DNA following acute intoxication with doxorubicin. *Biochimica et Biophysica Acta*, **1321**; 101 - 106.
- Pandis N, Teixeira MR, Gerdes AM, Limon J, Bardi G, Andersen JA, Idvall I, Mandahl n, Mitelman F and Heim S. (1995) Chromosome abnormalities in bilateral breast carcinomas. *Cancer*, **76**; 250 - 258.

References

- Petty RD, Sutherland LA, Hunter EH and Cree IA. (1995) Comparison of MTT and ATP - based assays for the measurement of viable cell number. *Journal of Bioluminescence and Chemiluminescence*, **10**; 29 - 34.
- Pommier Y. (1993) Interaction of anthracyclines with mammalian DNA topoisomerases. *Abstracts of Papers of the American Chemical Society*, **205**; 47.
- Poot M, Gibson LL and Singer VL. (1997) Detection of apoptosis in live cells by MitoTracker™ red CMXRos and SYTO dye flow cytometry. *Cytometry*, **27**; 358 - 364.
- Powles TJ, Jones AL, Judson IR, Hardy JR and Ashley SE. (1991) A randomised trial comparing combination chemotherapy using mitomycin C, mitozantrone and methotrexate (3M) with vincristine, anthracycline and cyclophosphamide (VAC) in advanced breast cancer. *British Journal of Cancer*, **64**; 406 - 410.
- Quigley GJ, Wang AHJ, Ughetto G, van der Marel, van Boom JH and Rich A. (1980) Molecular structure of an anticancer drug - DNA complex : daunomycin plus d(CpGpTpApCpG). *Proceedings of the National Academy of Sciences of the USA*, **77**; 7204 - 7208.
- Ravid A, Rocher D, Machlenkin A, Rotem C, Hochman A, Kessler - Icekson G, Liberman UA and Koren R. (1999) 1, 25 - Dihydroxyvitamin D₃ enhances the susceptibility of breast cancer cells to doxorubicin - induced oxidative damage. *Cancer Research*, **59**; 862 - 867.
- Reeve L and Rew DA. (1997) New technology in the analytical cell sciences : the laser scanning cytometer. *European Journal of Surgical Oncology*, **23**; 445 - 449.
- Regev R and Eytan GD. (1997) Flip - flop of doxorubicin across erythrocyte and lipid membranes. *Biochemical Pharmacology*, **54**; 1151 - 1158.
- Resnicoff M, Medrano EE, Podhajcer OL, Bravo AI, Bover L and Mordoh J. (1987) Subpopulations of MCF7 cells separated by Percoll gradient centrifugation : A model to

References

analyze the heterogeneity of human breast cancer. Proceedings of the National Academy of Sciences of the USA, **84**; 7295 - 7299.

Rew DA, Wilson GD and Weaver PC. (1991) Proliferation characteristics of human colorectal carcinomas measured *in vivo*. British Journal of Surgery, **78**; 60 - 66.

Rew DA, Campbell ID, Taylor I and Wilson GD. (1992) Proliferation indices of invasive breast carcinomas after *in vivo* 5 - bromo - 2' - deoxyriding labelling: a flow cytometric study of 75 tumours. British Journal of Surgery, **79**; 335 - 339.

Rew DA, Reeve LJ and Wilson GD. (1998) Comparison of flow and laser scanning cytometry for the assay of cell proliferation in human solid tumours. Cytometry, **33**; 355 - 361.

Rew DA, Woltmann G and Wardlaw AJ. (1999) Laser - scanning cytometer. The Lancet, **353**; 255- 256.

Rigg KM, Shenton BK, Murray IA, Givan AL, Taylor RMR and Lennard TWJ. (1989) A flow cytometric technique for simultaneous analysis of human mononuclear surface antigens and DNA. Journal of Immunological Methods, **123**; 177 - 184.

Rizzo V, Penco S, Menozzi M, Geroni C, Vigevani A and Arcamone. (1988) Studies of anthracycline - DNA complexes by circular dichroism. Anti - Cancer Drug Design, **3**; 103 - 115.

Rong GH, Grimm EA and Sindelar WF. (1985) An enzymatic method for the consistent production of monodispersed viable cell suspensions from solid tumours. Journal of Surgical Oncology, **28**; 131 - 133.

Ross DD, Thompson BW, Ordonez JV and Joneckis CC. (1989) Improvement of flow - cytometric detection of multi - drug resistant cells by cell - volume normalization of intracellular daunorubicin content. Cytometry, **10**; 185 - 191.

References

Rotman B and Papermaster BW. (1966) Membrane properties of living mammalian cells as studied by enzymatic hydrolysis of fluorogenic esters. *Proceeding of the Academy of Sciences of the USA*, **55**; 134 - 141.

Sacks NPM and Baum M. (1996) Treatment *in* Surgical oncology (Allen - Mersh TG ed.) Chapman & Hall Medical, p 351 - 372.

Salmon SE, Hamburger AW, Soehnlen B, Duris BGM, Alberts DS and Moon TE. (1978) Quantitation of differential sensitivity of human - tumor stem cells to anticancer drugs. *The New England Journal of Medicine*, **298**; 1321 - 1327.

Sasaki K, Kurose A, Miura Y, Sato T and Ikeda E. (1996) DNA ploidy analysis by laser scanning cytometry (LSC) in colorectal cancers and comparison with flow cytometry. *Cytometry*, **23**; 106 - 109.

Satoh T, Yamamoto K, Miura KF, Saskai K and Ishidate M. (1999) Application of laser scanning cytometry to the analysis of chromosomal aberrations induced by benzo[a]ptrene in CHO - WBLT cells. *Cytometry*, **35**; 363 - 368.

Scatchard G. (1949) The attractions of proteins for small molecules and ions. *Annals of the New York Academy of Sciences*, **51**; 660 - 672.

Schnipper LE. (1986) Clinical implications of tumor - cell heterogeneity. *The New England Journal of Medicine*, **314**; 1423 - 1431.

Schoenbach EB, Colsky J and Greenspan EM. (1952) Observations on the effects of the folic acid antagonists, aminopterin and amethopterin, in patients with advanced neoplasms. *Cancer*, **6**; 1201 - 1220.

Schuurhuis GJ, Broxterman HJ, van der Hoeven, Pinedo HM and Lankelma J. (1987) Potentiation of doxorubicin cytotoxicity by the calcium antagonist bepridil in anthracycline - resistant and - sensitive cell lines. *Cancer Chemotherapy and Pharmacology*, **20**; 285 - 290.

Schuurhuis GJ, van Heijningen THM, Cervantes A, Pinedo HM, de Lange JHM, Keizer HG, Broxterman HJ, Baak JPA and Lankelma J. (1993) Changes in subcellular doxorubicin distribution and cellular accumulation alone can largely account for doxorubicin resistance in SW - 1573 lung cancer and MCF-7 breast cancer multidrug resistant tumour cells. *British Journal of Cancer*, **68**; 898 - 908.

Shapiro HM. (1995) *Practical flow cytometry*. Wiley - Liss Inc. Third edition.

Shi T, Wrin J, Reeder J, Liu D and Ring DB. (1995) High - affinity monoclonal antibodies against P - glycoprotein. *Clinical Immunology and Immunopathology*, **76**; 44 - 51.

Siegfried JA, Kennedy KA, Sartorelli and Tritton TR. (1983) The role of membranes in the mechanism of action of antineoplastic agent adriamycin. *The Journal of Biological Chemistry*, **258**; 339 - 343.

Sieuwerts AM, Klijn JGM, Peters HA and Foekens JA. (1995) The MTT tetrazolium assay scrutinized: how to use this assay reliably to measure metabolic activity of cell cultures *in vitro* for the assessment of growth characteristics, IC₅₀ - values and cell survival. *European Journal of Clinical Chemistry and Clinical Biochemistry*, **33**, 813 - 823.

Sinha BK, Katki AG, Batist G, Cowan KH and Myers CE. (1987) Adriamycin - stimulated hydroxyl radical formation in human breast tumour cells. *Biochemical Pharmacology*, **36**; 793 - 796.

Slocum HK, Pavelic ZP, Rustrum YM, Creaven PJ, Karakousis, Takita H and Greco WR. (1981) Characterization of cells obtained by mechanical and enzymatic means from human melanoma, sarcoma and lung tumors. *Cancer Research*, **41**; 1428 - 1434.

Sluysers M. (1995) Mutations in the estrogen receptor gene. *Human Mutation*, **6**; 97 - 103.

References

- Smith IE & Powles TJ. (1991) Chemotherapy: general principles *in* Medical management of breast cancer (Powles TJ and Smith IE ed.) Martin Dunitz, p125 - 132.
- Smith PJ, Rackshaw C and Cotter F. (1994) DNA fragmentation as a consequence of cell cycle traverse in doxorubicin - and idarubicin - treated human lymphoma cells. *Annals of Hematology*, **69**; S7 - S11.
- Smyth JF, Macpherson JS, Warrington PS, Leonard RCF and Wolf CR. (1986) The clinical pharmacology of mitoxantrone, **17**; 149 - 152.
- Soule HD, Vazquez J, long A, Albert A and Brennan M. (1973) A human cell line from a pleural effusion derived from a breast carcinoma. *Journal of the National Cancer Institute*, **51**; 1409 - 1416.
- Steller H. (1995) Mechanisms and genes of cellular suicide. *Science*, **267**; 1445 - 1455.
- Steward DJ, Evans WK, Shepherd FA, Wilson KS, Pritchard KI, Trudeau ME, Wilson JJ and Martz K. (1997) Cyclophosphamide and fluorouracil combined with mitoxantrone versus doxorubicin from breast cancer : superiority of doxorubicin. *Journal of Clinical Oncology*, **15**; 1897 - 1905.
- Stokke T, Solberg K, DeAngelis P and Steen HB. (1998) Propidium iodide quenches the fluorescence of TdT - incorporated FITC - labeled dUTP in apoptotic cells. *Cytometry*, **33**; 428 - 434.
- Taylor - Papadimitriou J, Stampfer M, Bartek J, Lewis A, Boshell M, Lane EB and Leigh IM. (1989) Keratin expression in human mammary epithelial cells cultures from normal and malignant tissue: relation to *in vivo* phenotypes and influence of medium. *Journal of Cell Science*, **94**; 403 - 413.
- Tennant JR. (1964) Evaluation of the trypan blue technique for determination of cell viability. *Transplantation*, **2**; 685 - 694.

References

- Terry NHA, Meistrich ML, Rouben LD, Lynch PM, Dubrow RA and Rich TA. (1995) Cellular kinetics in rectal cancer. *British Journal of Cancer*, **72**; 435 - 441.
- Tewey KM, Rowy TC, Yang L, Halligan BD and Liu LF. (1984) Adriamycin - induced DNA damage mediated by mammalian DNA topoisomerase II. *Science*, **226**; 466 - 468.
- Tiberghien F and Loo F. (1996) Ranking of P - glycoprotein substrates and inhibitors by a calcein - AM fluorometry screening assay. *Anti - Cancer Drugs*, **7**; 568 - 578.
- Tidefelt U, Prenekert M and Paul C. (1996) Comparison of idarubicin and daunorubicin and their main metabolites regarding intracellular uptake and effect on sensitive and multidrug - resistant HL60 cells. *Cancer Chemotherapy and Pharmacology*, **38**; 476 - 480.
- Toikkanen S, Helin H, Isola J and Joensuu H. (1992) Prognostic significance of HER-2 oncoprotein expression in breast cancer: a 30 year follow up. *Journal of Clinical Oncology*, **7**; 1044 - 1048.
- Tomita K, Chikumi H, Tokuyasu H, Yajima H, Hitsuda Y, Matsumoto Y and Sasaki T. (1999) Functional assay of NF - κ B translocation into nuclei by laser scanning cytometry; inhibitory effect by dexamethasone or theophylline. *Naunyn - Schmiedeberg's Archives of Pharmacology*, **359**; 249 - 255.
- Torres FX, Mackowiak PG, Brown RD, Linden MD and Zarbo RJ. (1995) Comparison of two methods of mechanical disaggregation of scirrhous breast adenocarcinomas for DNA flow cytometric analysis of whole cells. *American Journal of Clinical Pathology*, **103**; 8 - 13.
- Tounekti O, Belehradek J and Mir LM. (1995) Relationships between DNA fragmentation, chromatin condensation, and changes in flow cytometry profiles detected during apoptosis. *Experimental Cell Research*, **217**; 505 - 516.

References

- Traganos F. (1990) Single - and multiparameter analysis of the effects of chemotherapeutic agents on cell proliferation *in vitro* in Flow cytometry and Sorting, second edition, p773 - 801, Wiley - Liss.
- Trail PA, Willner D and Hellstrom KE. (1995) Site - directed delivery of anthracyclines for treatment of cancer. *Drug Development Research*, **34**; 196 - 206.
- Tritton TR and Yee G. (1982) The anticancer agent adriamycin can be actively cytotoxic without entering cells. *Science*, **217**; 248 - 250.
- Trotter PJ, Orchard MA and Walker JH. (1997) Relocation of annexin V to platelet membranes is a phosphorylation - dependent process. *Biochemical Journal*, **328**; 447 - 452.
- Twentyman PR, Rhodes T and Rayner S. (1994) A comparison of rhodamine 123 accumulation and efflux in cells with P - glycoprotein - mediated and MRP - associated multidrug resistance phenotypes. *European Journal of Cancer*, **30A**; 1360 - 1369.
- Vigevani A and Williamson MJ. (1980) Doxorubicin. *Analytical Profiles of Drug Substances*, **9**; 245 - 274.
- Vilallonga FA and Phillips EW. (1978) Interaction of doxorubicin with phospholipid monolayers. *Pharmaceutical Science*, **67**; 773 - 775.
- Visscher DW, Zarbo RJ, Jacobsen G, Kambouris A, Talpos G, Sakr W and Crissman JD. (1990) Multiparametric deoxyribonucleic acid and cell cycle analysis of breast carcinomas by flow cytometry. *Laboratory Investigation*, **62**; 370 - 378.
- Walker RA, Jones L, Chappell S, Walsh T and Shaw JA. (1997) Molecular pathology of breast cancer and its application to clinical management. *Cancer and Metastasis Reviews*, **16**; 5 - 27.
- Wall DM, Sparrow R, Hu XF, Nadalin G, Zalberg JR, Marschner IC, van der Weyden M and Parkin JD. *European Journal of Cancer*, **29A**; 1024 - 1027.

- Wang TTY and Phang JM. (1995) Effects of estrogen on apoptotic pathways in human breast cancer cell line MCF-7. *Cancer Research*, **55**; 2487 - 2489.
- Wang XM, Terasaki PI, Rankin GW, Chia D, Zhong HP and Hardy S. (1993) A new microcellular cytotoxicity test based on calcein AM release. *Human Immunology*, **37**; 264 - 270.
- Waring MJ. (1970) Variation of the supercoils in closed circular DNA by binding of antibiotics and drugs: evidence for molecular models involving intercalation. *Journal of Molecular Biology*, **54**; 247 - 279.
- White E. (1993) Death - defying acts : a meting review on apoptosis. *Genes and Development*, **7**; 2277 - 2284.
- Whiteside TL, Miescher S, Hurlimann J, Moretta Land von Flidner V. (1986) Clonal analysis and in situ characterization of lymphocytes infiltrating human breast carcinomas. *Cancer Immunology and Immunotherapy*, **23**; 169 - 178.
- Wilson GD. (1991) Assessment of human tumour proliferation using bromodeoxyuridine - current status. *Acta Oncologica*, **30**; 903 - 910.
- Wilson GD. (1994) Analysis of DNA - measurement of cell kinetics by the bromodeoxyuridine / anti - bromodeoxyuridine method *in* *Flow cytometry - A practical approach*, (Ormerod MG ed.), second edition, p137 - 156, IRL Press, Oxford.
- Wilson MS, West CML, Wilson GD, Roberts SA, James RD and Schofield PF. (1993) An assessment of the reliability and reproducibility of measurement of potential doubling times (Tpot) in human colorectal cancers. *British Journal of Cancer*, **67**, 754 - 759.
- Woltmann G, Ward RJ, Symon FA, Rew DA, Pavord ID and Wardlaw AJ. (1999) Objective quantitative analysis of eosinophils and bronchial epithelial cells in induced sputum by laser scanning cytometry. *Thorax*, **54**; 124 - 130.

References

Yamaue H, Tanimura H, Nakamori M, Noguchi K, Iwahashi M, Tani M, Hotta T, Murakami K and Ishimoto K. (1996) Clinical evaluation of chemosensitivity testing for patients with colorectal cancer using MTT assay. *Dis Colon Rectum* **39**; 416 - 422.

Young RC, Ozols RF and Myers CE. (1981) The anthracycline antineoplastic drugs. *The New England Journal of Medicine*, **305**; 139 - 153.

Zhang G, Gurtu V, Kain SR and Yan G. (1997) Early detection of apoptosis using a fluorescence conjugate of annexin V. *Biotechniques*, **23**; 525 - 531.

Zhang R, Wiley J, Howard SP, Meisner LF and Gould MN. (1989) Rare clonal karyotypic in primary cultures of human breast carcinoma cells. *Cancer Research*, **49**; 444 - 449.

Zunino F, Gambetta R, Di Marco A and Zaccara A. (1972) Interaction of daunomycin and its derivatives with DNA. *Biochimica Biophysica Acta*, **277**, 489 - 498.